THE UNIVERSITY *of* EDINBURGH

Quantifying climate-dependent ammonia emissions from global agriculture: from development of the AMmonia–CLIMate (AMCLIM) model to its application and implications

Jize Jiang

Submitted for the Doctor of Philosophy

School of GeoSciences

The University of Edinburgh

2023

Declaration

I declare that this thesis has been composed solely by myself and that it has not been submitted, in whole or in part, in any previous application for a degree. Except where states otherwise by reference or acknowledgment, the work presented is entirely my own.

Jize Jiang

September 2023

Abstract

Ammonia (NH_3) is one of the primary forms of reactive nitrogen and can negatively affect the environment and human health. It has adverse impacts on air, water, soil quality and ecosystems. Emissions of NH_3 mainly originate from agricultural activities and are found to be strongly dependent on environmental conditions. Current emission inventories often consider the effects of environmental factors in a limited way. To address this deficiency in existing estimates, a dynamic, process-based emission model, AMmonia–CLIMate (AMCLIM) has been developed to quantify agricultural NH_3 emissions.

AMCLIM simulates important physical, chemical and biological processes that are sensitive to climatic conditions in agricultural systems, and focuses on major livestock farming and synthetic fertilizer use. The model has been applied to different scales, with modelled results evaluated by comparison with site-measurements, showing close agreement. When applied at the global scale, AMCLIM operates at high spatial and temporal resolution, and AMCLIM is thought to be the first model that simulates NH_3 emissions from all individual sectors using a consistent process-based modelling approach, with high levels of detail.

For the year 2010, global agricultural NH_3 emissions estimated by AMCLIM are 44.9±4.4 Tg N yr^{-1}, equivalent to 22±2 % of agricultural nitrogen input (synthetic fertilizer and livestock excreta) being lost through NH_3 volatilization. The global estimates of AMCLIM are consistent with other models and studies. Around 1/3 of the NH_3 emissions result from synthetic fertilizer use, with 2/3 associated with livestock farming (including housing,

manure management, land application of manure and grazing). China, India, US, Brazil and Pakistan result in the largest estimated emissions, together accounting for nearly 60 % of global NH_3 emissions. Cattle are the largest emitter group among livestock, followed by pigs, chicken, sheep and goats. Emissions of NH_3 not only show large spatial variations but also exhibit significant seasonal variation. The highest estimated NH_3 emissions are found in July, mainly driven by the planting season and high temperatures in the northern hemisphere.

The impacts of temperature, wind speed and water availability on NH_3 volatilization have been investigated. Increasing temperature and wind speed facilitates volatilization to cause more NH_3 emissions, with temperature normally being the most critical factor especially under cold conditions. A global sensitivity test to temperature indicates that annual NH_3 emissions may increase by around 7 % due to a (uniform) 2 °C warming, compared to the base value of year 2010. Ammonia emissions tend to be larger under drier conditions, but wetter soils can either result in higher or lower emissions, depending on complex interactions with other variables. Soil pH is also a critical factor as alkaline soils typically lead to more intense volatilization. Mitigation measures have been simulated and have been found to be effective in reducing NH_3 emissions. These include decreasing nitrogen application rates and improving livestock feeding materials, covering stored manure and better land application techniques (e.g., incorporation and deep placement). It is estimated that a potential 40 % abatement of global NH_3 emissions can be achieved when applying a suite of the tested measures.

Using AMCLIM, it is estimated that NH_3 emissions have increased from 39.8 Tg N yr^{-1} in 2000 to 45.2 Tg N yr^{-1} in 2018, and future emissions by 2100 are projected to go up to 51

to 55 Tg N yr^{-1} due to warming alone (with 2018 activity) and can reach 59 to 102 Tg N yr^{-1} when also combined with growing livestock numbers and synthetic fertilizer usage. It is suggested that climate change and food production pose risks for future agricultural NH_3 emissions at different spatial scales. Regional and local environment and agricultural systems may suffer the consequences of the warming effect, while the globe may face challenges due to increased food production.

Lay summary

Ammonia (NH_3) is a gas containing nitrogen, which has significant impacts on the environment. It affects the air we breathe, the quality of our water and soil, and the functioning of ecosystems. The main sources of NH_3 emissions are agriculture, such as livestock rearing and fertilizer use. The amount of NH_3 released into the air can be very different in places with different environmental conditions, but current studies often lack consideration of these effects. A special model called AMmonia–CLIMate (AMCLIM) has been developed to understand and calculate NH_3 emissions from agriculture, whilst taking into account how the environment influences these NH_3 emissions.

The AMCLIM model includes various factors and processes to estimate how much NH_3 originates from the breakdown of livestock excreta and chemical fertilizers. AMCLIM can be used for simulations with different spatial coverage: it can estimate the NH_3 gas from a farm, a piece of cropland and the whole planet. When focusing on small scales, AMCLIM provides good results as evaluated by comparison with measurements. For global simulations, the calculations of the model are done at a high frequency and resolution, with high levels of detail.

For the year 2010, it is estimated by AMCLIM that around 22±2 % of the nitrogen used in agriculture is lost as NH_3 emissions, which adds up to about 44.9±4.4 million tons of nitrogen. Most of these emissions come from livestock agriculture (such as housing, dealing with manure and grazing) and the use of fertilizers. Countries including China, India, the US, Brazil and Pakistan have the highest levels of NH_3 emissions. Among

different types of livestock, cattle rearing causes the largest NH_3 emissions. These emissions are different across the globe and change throughout the year. The highest NH_3 emissions are estimated to occur in July due to the timing of planting and high temperatures.

Ammonia emissions are affected by both the environmental conditions and how farming is managed. Factors like temperature, wind speed and water availability are important in affecting the NH_3 emissions. Simply speaking, hotter and windy conditions make NH_3 emissions bigger. Dry conditions typically tend to increase emissions, but more complicated interactions are also found as sometimes there is less NH_3 emitting. Applying fertilizers to more alkaline soils can also result in more NH_3 volatilized from the field. Various measures have been tested to learn how much NH_3 emissions can be reduced, such as by applying less nitrogen fertilizers, mixing or burying the fertilizer into soils and covering stored manure etc. By applying a group of these effective measures, it is possible to cut down about 2/5 of NH_3 emissions.

Using the AMCLIM model, the NH_3 emissions are estimated to have increased over the past 20 years, as a result of both global environmental change and food production. Future NH_3 emissions are expected to keep rising because of warming temperatures and increasing livestock and fertilizer use, and the emissions may more than double the present values by the end of this century. Such a consequence can worsen environmental problems and cause harm from the nutrient use for both the local community and the whole world. Therefore, managing NH_3 emissions will be crucial to protect our environment and ensure sustainable agriculture in the future.

Acknowledgements

Doing a PhD is not an easy thing (maybe not that difficult, but the final stretch of my PhD life proved to be quite stressful and much harder than expected). Throughout this journey, you met many people. These people are like sculptors, leaving a mark on you, whether profound or shallow, happy or painful, unforgettable or insignificant. They exert an influence on you, some of which can be so substantial that they shape your life. Some broaden your horizons and point out new routes for you, others help you make good decisions, and some are just people with whom you enjoy staying and chatting. Well, it is a big world, so inevitably there are people who make your life hard. Even worse, some people punch you hard with no good reasons, driven solely by their own interests. Luckily, most of the people I have encountered are kind and considerate, which sometimes leads me to have a delusion as if I were the blessed one. I have been surrounded by these people throughout my PhD, which I feel flattered.

When I started writing my acknowledgements, I am in my family's new home in Guangzhou, China, about 9400 km (note this estimate has uncertainty) away from Edinburgh, where two of my PhD's most vital people are located (more precisely, "Edinburgh is the working place"). In light of this, I want to convey my deepest gratitude to my supervisors, mentors, colleagues (hmm this is arrogant) and friends (this is true), Prof David Stevenson (University of Edinburgh) and Prof Mark Sutton (UK Centre for Hydrology & Ecology). Our bonds spans over six years (I know David for even longer, ~seven years as David gave us undergraduate lectures in 2016). Six years of time is long, providing enough time for me to complete my Master's project, develop a lot of interesting

ideas and useful skills, to build up my confidence, and now approach the final phase of my doctoral studies. But six years are also short, as our journey should not conclude here. I feel you have taken care of me so well that I am hesitant to leave this comfort zone like a "coddled child". It has always been a great pleasure to work with you and be at your side.

David! Our paths crossed for the first time during the Environmental Pollution course. You lectured a theme on global scale atmospheric pollution. I found your stuff very interesting, so I did your practical and then opted for the assignment from your section. You kindly answered all my bothering questions with patience. Perhaps it was during that moment that the notion of "this is the researcher who I want to work with" began to take root. I still remember the last question, where I needed to provide an answer within 150 words. You gave me a quite harsh comment: "this is correct, but the sentence is awkwardly structured" (very straightforward, good job David!). That was the very first impression you left on me: friendly, patient, kind but rigorous. In my 4th year, I approached you and expressed my willingness to work on my undergraduate project under your supervision. You helped formulate a project, but we ended up with realizing that our ambitions went far beyond feasibility (still very "naive" now)! *All roads lead to Rome*, it just took me an additional year to have the privilege of working with you as a Master's student. Then you know all the stories in the next six years! We have had a lot of long conversations about probably everything one can imagine, which then adds another "wise" tag on you in my heart. We have shared many wonderful moments, like the pristine sky and quiet nights at the Bothy Cottage. I must say you made very good veggie haggis and pizza, and the tasty pastries (as a "professional chef", I seldom give peer-recognition). It has been really delightful over these years working with you. Thank you so much David for your company and mentorship. Thanks for your support, patience and wisdom.

Hey Mark! Now it is time to revisit our journey! Clock ticks back to six years ago when David brought up your name in discussions about a potential Master's project (see ~7 lines above; but I know you will read through this section). Back then, I knew nothing about ammonia and nitrogen, so I became quite confused after reading your famous 2013 paper (you know what I mean). I needed some explanations and guidance! I sent you a carefully-crafted email. Surprisingly, your swift reply came, and you asked me if I want to have a chat at CEH. Absolutely! Our first meeting was both enjoyable and enlightening. You educated me and gave many insightful ideas, which suddenly illuminated the paths ahead, making me see all the possibilities that are in front of me. I believe our "nitrogen adventure" officially started when you said: "I am happy to be a co-supervisor" (also it was the time when the "best team on ammonia emission modelling" established – this is pretty arrogant but is very likely to be true, and you see I build up my confidence)! Your consistent support, optimism and encouragement have been instrumental. If David represents the Earth that provides me a habitant to thrive, then you are the Sun that radiates warmth and shines above my head. Your example is one that people want to follow (not your travelling duty!) Sometimes when I came across obstacles and challenges, I'd pause and think "what would Mark do in this situation". You give me the direction and inspire me all the time, and that is why I never want to disappoint you (then you know the 90 % goal thing…). We have developed numerous interesting ideas, and our three-hour meetings usually passed by in the blink of an eye. You've imparted valuable knowledge, both in science and life (not to forget "diplomatic" skills as well, haha) I am grateful to have you as my supervisor and life-long mentor, and thanks for making everything possible (and really apologize for the "upsetting decision" afterwards). Okay, I could easily write another chapter (probably an entire book) talking about the stories and shared experiences between the three of us.

However, I think I have to constrain myself otherwise emotions overflow and I find myself crying like a baby.

I want to thank the National Environmental Research Council (NERC) and the UK Research Innovation Global Challenge Research Fund South Asian Nitrogen Hub (UKRI GCRF SANH) for giving me this opportunity.

I want to thank Dr Aimable Uwizeye and Dr Giuseppe Tempio from the UN FAO for providing data and substantial help for this project. Thanks to Dr Alessandra Falcucci (UN FAO) for providing data and technical support. Thank you very much. This work is not possible without all of you.

I want to thank Prof Mat Heal and all members (past and present) from the MACAQUE group for having interesting discussion (although I sometimes did not show up …). I have benefited quite a lot from your questions and ideas.

I want to thank Prof Paul Palmer who was my supervisor of my undergraduate dissertation. Thank you, Paul, for guiding me into the world of science. Working with you has helped me develop a strong interest in research and become more determined. I want to thank Dr Alex Thomas for being my personal tutor during undergraduate. Thank you, Alex, for giving me many useful suggestions. I want to thank Dr Simon Jung. Thank you, Simon, for being my advisor (also my undergraduate lecturer; you recognized me after two years!). I want to thank Prof Dave Reay for all the help. I also want to express my gratitude to all the people in Crew building, in particular, Dr Massimo Bollasina and Prof Simon Tett.

I want to thank Dr Eiko Nemitz, Dr Massimo Vieno, Dr Ulli Dragosits, Dr Claudia Steadman, Prof Ute Skiba, Ed Carnell, Sam Tomlinson and Dr Ajinkya Deshpande from the UK CEH. Thank you all for the interesting and inspiring conversations and the help for my PhD. I want to thank Kate Mason for endless help and support for coordination. I want to thank Dr Bill Bealey and the SANH coordination team. Thank you for making such a fantastic annual hub meeting in Maldives! Also thanks to all the friends and colleagues I met in Maldives.

I want to thank Sophie Ramette (and the PGR office), Dr Mike Mineter and Justin MacNeil (and the geos IT team) for all the logistical and technical help, which makes the PhD life easier. I also want to thank the UK ARCHER2 and JASMIN computing team.

I want to thank my all my friends throughout this journey. In particular, to Dr Fei Yao and Dr Alcide Zhao, thanks for kind help and advice during this PhD.

I want to thank Dr Fiona McGibbon. We have had many pleasant conversations and shared wonderful times. You are the person who let me know about a lot of interesting things of the world. Thank you and David for encouraging me throughout the last couple of years! Thanks to Dr Antje Branding (and Mark) for inviting me for dinner (tasty dishes but unable to rate as a “professional chef” because I only had once, so limited “data availability” and perhaps should visit more!). The cider as a gift is also worth a mention.

I want to thank Ajinkya and Dr Benjamin Loubet for reviewing this thesis and being the examiners. Thank you both for giving lots of insightful and valuable comments and for having a very interesting and relaxed viva! Benjamin, I hope that you enjoyed the trip to Edinburgh from Paris! Also thanks Dave for being the chair of the viva.

I have tried to include everyone who I am grateful for, but just in case I use Alcide's "dodgy" way of expressing my gratitude "please allow me to extend my deep appreciation to all of you".

A special thanks to Prof Lenny Winkel and Prof Johan Six for inviting me to Zurich and offering me a job at ETH Zurich (Apologize again to Eiko, Massimo and Mark for not taking the offered position at CEH). Thanks to Dr Andrea Stenke, Dr Moritz Laub and team members from IEG and SAE for a warm welcome in Zurich. I enjoyed the trip. It was a very pleasant visit!

Lastly, I want to express my gratitude to my family. To my parents and my maternal grandmother, the life of this PhD sometimes is a bit weird because of the covid-19, but I manage to sail through with no big problems with your unconditional love and support. Time flows like water, silently yet relentlessly. It is difficult and sad to see you all getting old. I hope that you are proud of me (though it feels a bit embarrassing to say this in front of you, so I am writing it down here; I know that none of you can barely understand English, so I feel more at ease expressing it in this way). This thesis is also dedicated to my maternal grandfather who passed away in December 2021, and my paternal grandmother who passed away in September 2022. Hope both of you can watch over and witness this completion from heaven. Thanks to all my family members, including Yuzhi Lin and Yifeng Xu, for your support. To Linqi (Lynne) Xu, much appreciated for your company, understanding and love. We have each other's back for the rest of our lives.

Contents

List of Figures

List of Tables

List of Abbreviations

AFOs	Aminal Feeding Operations
AGM	Aerodynamic Gradient Method
AMCLIM	AMmonia-CLIMate model
AR6	IPCC's sixth Assessment Report on Climate Change
BNF	Biological nitrogen fixation
CLRTAP	Convention on Long-Range Transboundary Air Pollution
CTM	Chemistry and Transport Models
DJF	December-January-February
DM	Dry matter
ECMWF	European Centre for Medium-Range Weather Forecasts
EDGAR	Emissions Database for Global Atmospheric Research
EFs	Emission factors
ENA	The European Nitrogen Assessment
ERA5	European Centre for Medium-Range Weather Forcasts Reanalysis v5
EU	European Union
FAO	Food and Agriculture Organization
FTP2	Farming the Planet 2
GGCMI3	Global Gridded Crop Model Intercomparison Phase 3

GLEAM	Global Livestock Environmental Assessment Model
GRAMINAE	GRassland AMmonia INteractions Across Europe
HWSD	Regridded Harmonized World Soil Database
IFA	International Fertilizer Association
IPCC	Intergovernmental Panel on Climate Change
JJA	June-July-August
MAM	March-April-May
MMS	Manure Management Systems
NCP	North China Plain
NH	Northern Hemisphere
NRMSE	Normalized root mean square error
OM	Organic matter
PM	Particulate matter
REA	Relaxed Eddy Accumulation
RH	Relative humidity
SH	Southern Hemisphere
SON	September-October-November
SSPs	Shared Socioeconomic Pathways
TAN	Total ammoniacal nitrogen
TFRN	Task Force on Reactive Nitrogen
UN	United Nations

UNECE	United Nations Economic Commision for Europe
UNEP	Unite Nations Environment Programme
USEPA	US Enviornmental Protection Agency
VOCs	Volatile organic compounds
WB	World Bank

Chapter 1
Introduction

1.1 Motivation and research aims

Ammonia (NH_3) is the one of the most critical species in the nitrogen cycle. It is the primary form of reduced reactive nitrogen (N_r) and also the principle alkaline gas in the atmosphere, which can have significant impacts on the environment. Excessive NH_3 emissions affect air, soil, water quality and local ecosystems, and can pose serious threats to human society. The largest NH_3-emitting sector is agriculture, via the volatilization of NH_3 from fertilizer and animal excreta. Estimated agricultural NH_3 emissions have increased rapidly from over 20 Tg N yr^{-1} in the 1970s to over 45 Tg N yr^{-1} in the 2010s (EDGAR, 2023) as a result of agricultural intensification.

Environmental conditions, such as temperature, water availability and many other meteorological factors can greatly influence NH_3 emissions. A warmer climate tends to cause higher NH_3 emissions, with one projection indicating NH_3 emissions increasing to 93 Tg N yr^{-1} in 2100 due to increases in temperature (Sutton et al., 2013). As synthetic fertilizer use and livestock farming are expected to increase with growing population, it has been estimated that projected NH_3 emissions could reach 135 Tg N yr^{-1} (89-179) by the end of this century (Sutton et al., 2013), nearly trebling the present values. Such large increases,

if realised, are likely to significantly exacerbate existing environmental problems associated with excessive N_r.

Current emission inventories and future projections for NH_3 are largely based on emission factors (EFs) and models that only consider the impacts of environmental factors in relatively limited ways. This may result in not only less reliable estimates of NH_3 emission, but also uncertainty in atmospheric chemistry simulations by chemistry and transport models (CTMs), which require representative NH_3 emissions that capture the spatial and temporal variability. So the questions arise: how to improve the quantification of NH_3 emissions that are sensitive to environmental conditions? How do NH_3 emissions vary in a changing climate? Moreover, local management practices can also have huge impacts on NH_3, and improvements in agricultural practices are found to be effective in NH_3 abatement. Therefore, it is also worth investigating the influences of management practices on NH_3 emissions and the potential measures that can effectively mitigate NH_3 emissions, including consideration of their environmental dependencies.

The overarching goals of this thesis and the research questions that this thesis aims to answer include

1. **Presenting the development and evaluation of a dynamic, process-based NH_3 emission model.**

a) How can a model be developed for quantifying climate-dependent NH_3 emissions based on knowledge at the process-based level?

b) How well does the model agree with measurements for NH_3 emissions from different agricultural activities?

2. Applying the model at the global scale to estimate agricultural NH_3 emissions.

a) What is the magnitude of global agricultural NH_3 emission?

b) What are the sectoral NH_3 emissions (e.g., from synthetic fertilizer use and different livestock types) and what is the contribution of each major agricultural activity?

c) What is the spatial distribution of agricultural NH_3 emissions and the corresponding volatilization rates (i.e., the percentage of agricultural N that is volatilized as NH_3)?

d) What are the daily/seasonal temporal profiles of agricultural NH_3 emissions?

e) What are the major N flows and pathways in the agricultural systems?

3. Enhancing understanding of the impacts of environmental factors and management practices on NH_3 emissions.

a) How do environmental conditions/factors affect NH_3 emissions from agriculture?

b) How to improve agricultural practices to reduce NH_3 emissions?

4. Estimating present and future NH_3 emissions.

a) How have NH_3 emissions changed over the past two decades in this century?

b) What could future NH_3 emissions from agriculture look like (emission totals and spatial patterns)?

1.2 Reactive nitrogen in the environment

1.2.1 Background

Nitrogen is the most abundant element in the air, making up 78% of the Earth's atmosphere in the form of di-nitrogen (N_2), and N plays a key role in the Earth System. Nitrogen is essential for the growth of vegetation and crops and is tightly coupled with the carbon cycle that shapes the functioning and structure of ecosystems. The unreactive nature of N_2 means that it cannot be assimilated by most organisms. In natural systems, to convert the highly stable N_2 to biologically available resources for life, a process called biological nitrogen fixation (BNF) is achieved by symbiotic bacteria, or by reactions in lightning to form nitrogen oxides (NO_x). Nitrogen compounds that are accessible to organisms are defined as reactive nitrogen (N_r), which includes inorganic reduced nitrogen (e.g., NH_3, NH_4^+), inorganic oxidised nitrogen (e.g., NO_x, N_2O, NO_3^-) and organic forms of nitrogen (e.g., amino acids, proteins). In natural environments, N_r is normally scarce, often limiting the productivity of ecosystems. Meanwhile, in early human's society, agricultural and industrial productivity was also largely constrained by the limiting supply of N_r. With the increasing demand for food in the late nineteenth century, BNF became insufficient to feed the world's growing population. This challenge was only overcome in the early twentieth century with the development of Haber-Bosch process, an industrial process that produces NH_3 using di-nitrogen and hydrogen by a high-pressure reaction. Since the 1950s, N_r production in Europe has increased exponentially due to the Haber-Bosch process, which not only satisfied the agricultural needs, but also supplied a vital feedstock for industrial processes (Sutton et al., 2011b).

The dramatic increasing of anthropogenic N_r production has greatly benefited human society through its largest use: agricultural fertilizers. Without anthropogenic N_r, a hectare of good agricultural land produces about two tonnes of cereal annually, a yield of which is only about a quarter of the yield compared to the same land with additional chemical fertilizer (Sutton et al., 2011b). According to Erisman et al. (2008), synthetic fertilizers have supported 48% of the global population, 100 years after the invention of the Haber-Bosch process to synthesize NH_3 directly from its elements. There is no doubt that N_r manufacturing has greatly facilitated human productivity. However, unintended leaks of N_r into the environment in various forms have led to numerous adverse effects on the environment and human health. The European Nitrogen Assessment (ENA) highlighted that the overall costs of N_r losses to the environment in Europe outweigh the direct economic benefits of N_r in agriculture. Thus the ENA estimated that excess N_r in the environment costs the European Union (EU) between 70–320 billion euros annually, while the direct benefits of N_r for farmers are only between 25–130 billion euros per year (Sutton et al., 2011b, c). It is reported that the largest societal costs are associated with the harmful impacts on human health and ecosystems resulting from air and water pollution, with a smaller fraction from the effect of nitrous oxide (N_2O) emission on climate warming (Sutton et al., 2011b, c).

1.2.2 Ammonia and the Nitrogen Cycle

The nitrogen cycle describes the movement of N between the Earth's various reservoirs (such as atmosphere, hydrosphere, biosphere and lithosphere) within a repeating cycle,

which plays a key role in the biogeochemistry of the Earth. Figure 1.1 illustrates the major natural processes involved in the nitrogen cycle.

Under natural conditions, atmospheric N_2 is mostly reduced to NH_3 and ammonium (NH_4^+) through BNF. This process transfers large natural nitrogen flows from the atmosphere to terrestrial and marine ecosystems. Bacteria then assimilate NH_3/NH_4^+ as organic forms of nitrogen, which can be used by other organisms. After organisms die, organic nitrogen is mineralized back into NH_3/NH_4^+. With oxygen, NH_3/NH_4^+ can be oxidised to nitrite (NO_2^-) and nitrate (NO_3^-) by a process called nitrification. If oxygen is limited, denitrifying bacteria may use NO_2^- and NO_3^- as an oxidant to convert organic carbon to carbon dioxide. This process, called denitrification, converts the NO_2^- and NO_3^- to N_2, thus returning the nitrogen from the biosphere to the atmosphere. It is also worth mentioning that nitrous oxide (N_2O), which is a greenhouse gas with a strong global warming potential, can also be generated through denitrification (not shown in Figure 1.1).

As noted, lightning is another pathway for fixing atmospheric N_2, which introduces nitrogen oxides (NO_x : the combination of NO + NO_2) to remote regions of the troposphere. Nitrogen oxides are then oxidised to nitric acid (HNO_3), which is scavenged by rain. The nitrogen cycle also involves exchange between the lithosphere and other reservoirs. Burial of dead organisms in the bottom of the ocean can bring nitrogen to the lithosphere, and these dead organisms are then incorporated into sedimentary rock. The stored nitrogen is eventually released by weathering of the sedimentary rocks. This process closes the nitrogen cycle in the surface reservoirs.

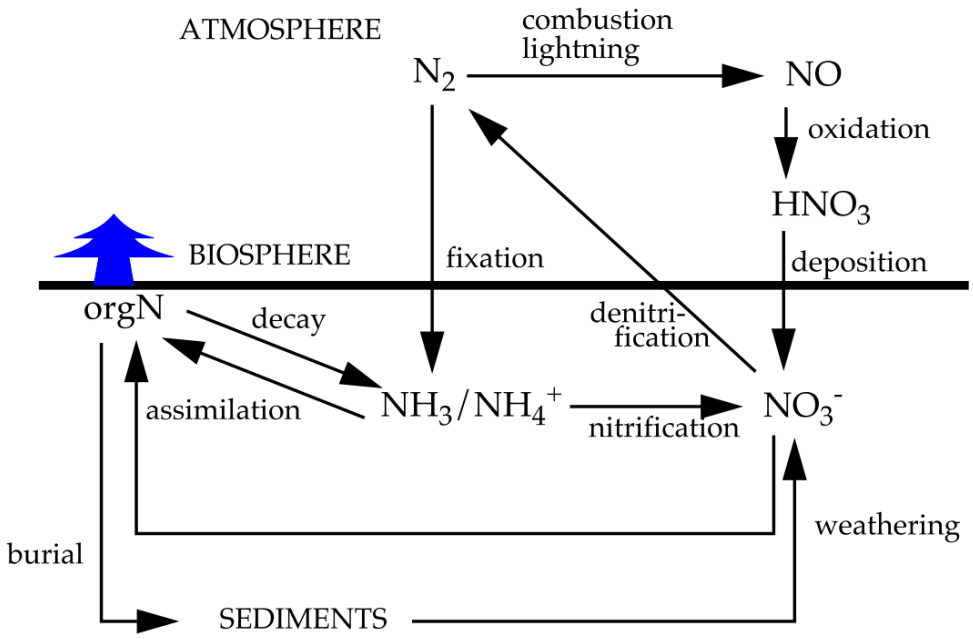

Figure 1.1. Major natural processes in the nitrogen cycle (figure from Jacob, 2000).

Humans have substantially altered the nitrogen cycle by increasing the production of N_r through three processes (Fowler et al., 2013). The first process is the combustion of fossil fuels for transportation and energy production, which generates NO_x from the oxidation of N_2 under high temperature. The second process is the creation of NH_3 from industrial production of fertilizer and chemicals through the Haber-Bosch process. And the third process is the planting of nitrogen-fixing crops that convert N_2 to NH_3, which contributes substantial quantities of N_r to soils.

Anthropogenic activities have had a profound impact on the nitrogen cycle, very likely doubling its turnover rates (Gruber and Galloway, 2008; Sutton et al., 2011b; Fowler et al.,

2013). While natural processes such as BNF and lightning contribute about 203 Tg N yr^{-1} of N_r to the terrestrial and marine ecosystems annually, human activities add a comparable amount of 210 Tg N yr^{-1} in the 21st century (Fowler et al., 2013). The main anthropogenic sources of fixed N include fertilizer production, agricultural BNF and combustion. Among these sources, 180 Tg N yr^{-1} is in the reduced form of NH_3 from fertilizer production and agricultural BNF, while 30 Tg N yr^{-1} is in the oxidised form (NO_x) from combustion (Fig 1.2).

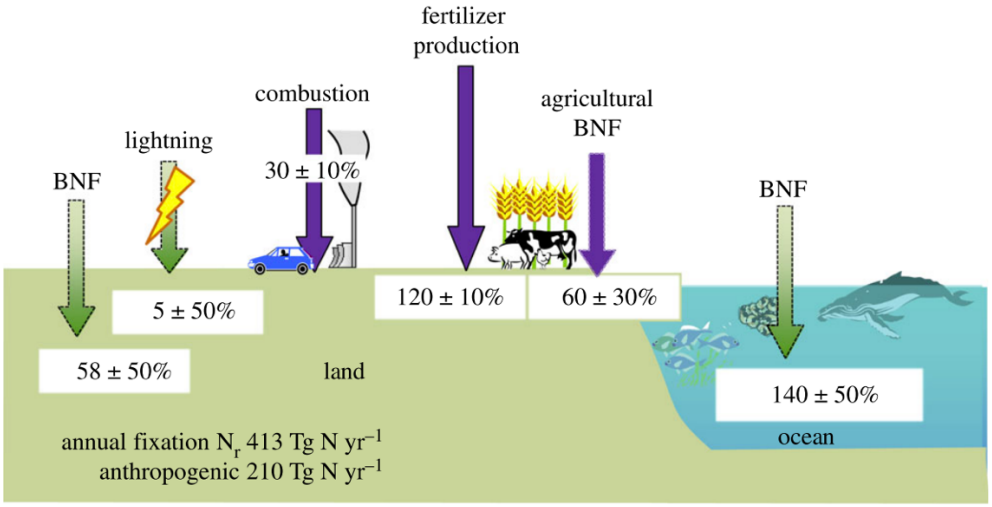

Figure 1.2. Global N fixation in both oxidised and reduced forms of N (units Tg N yr^{-1}, with percentage uncertainties). Arrows indicate transfers of N_2 from the atmosphere to terrestrial and marine ecosystems. Green arrows represent natural sources, and purple arrows represent anthropogenic sources (figure from Fowler et al., 2013).

These fixed N_r compounds undergo a variety of chemical processing in the atmosphere and microbial and plant biochemical processing in the terrestrial and marine systems. Figure

1.3 shows the relative magnitudes of N_r cycling within these environments, with the terrestrial environment processing the largest quantity of 240 Tg N yr^{-1}. Oceans process an estimated 230 Tg N yr^{-1}, and the remaining 100 Tg N yr^{-1} is estimated to be processed in the atmosphere.

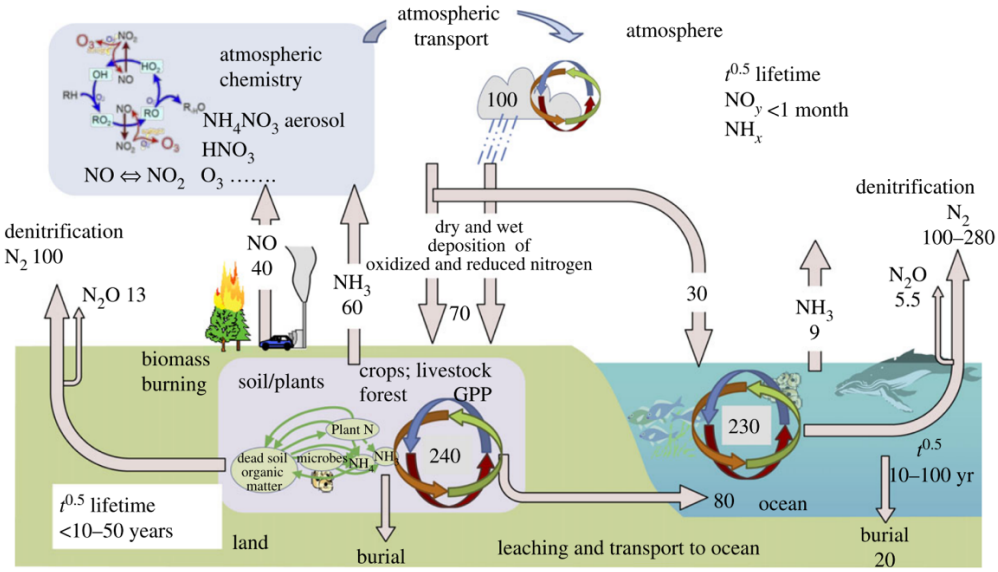

Figure 1.3. Processing and fluxes of N_r in terrestrial and marine systems and in the atmosphere (Tg N yr^{-1}) (figure from Fowler et al., 2013).

1.2.3 Environmental impacts of reactive nitrogen

Nature is normally very effective in conserving and recycling N_r components because of its limited availability. In contrast, anthropogenic N_r flows are less conservative. A

well-managed system is expected to fully recycle N_r within the system, but this is nearly impossible to achieve. As a result, there are unintended N_r losses into the environment.

Galloway et al. (2003) introduced the concept of the "N cascade" to illustrate how leakage of N_r through different media contributes to a range of environmental responses until it is denitrified back into N_2 (Fig 1.4). Taking NH_3 as an example, a freshly produced NH_3 molecule from the Haber-Bosch process is intended to enrich soil fertility and increased production of crops, subsequently feeding livestock and humans and enabling essential living activities. However, the NH_3 molecule can undergo many unintended transformations, leading to a cascade effect. For example, NH_3, NO_x and N_2O can be released to the atmosphere, causing aerosol formation, ozone production and enhancing the greenhouse effect. The leaching of NO_3^-/ NO_2^- to freshwater systems, catchment and open oceans results in eutrophication. Ecosystems are damaged due to N_r deposition, such as NH_3 and NO_x. These transformations and processes have a wide range of negative impacts on the environment.

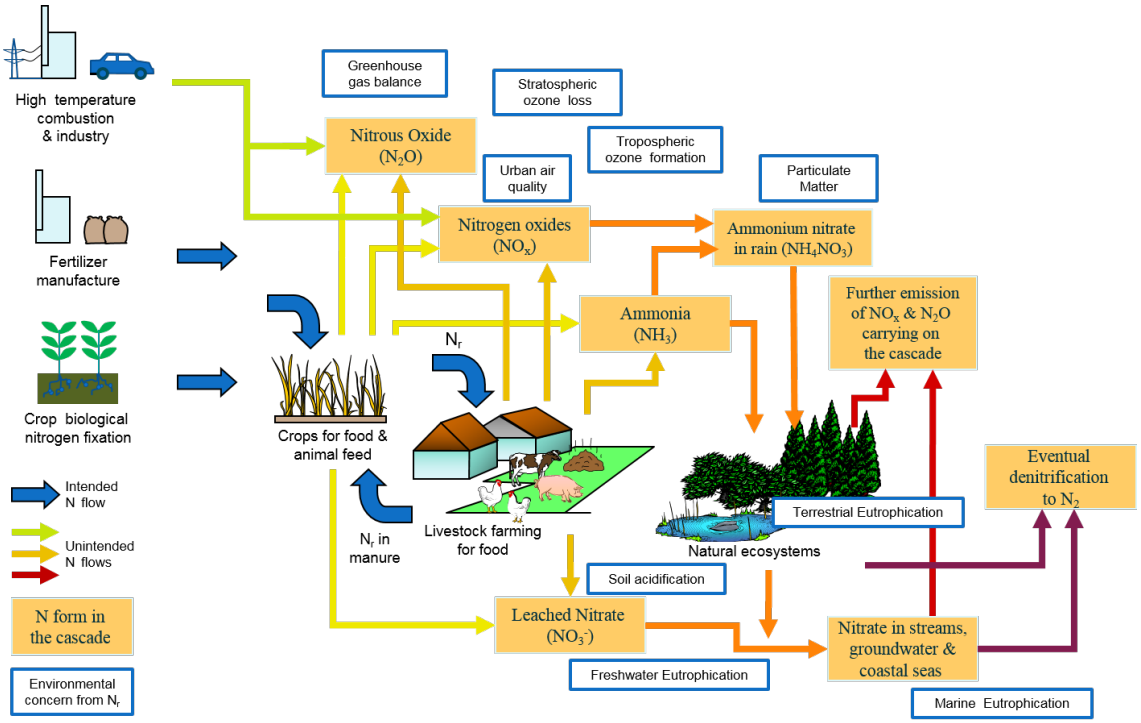

Figure 1.4. Schematic of N cascade. Unintentional losses of N_r to the environment from agricultural and industrial activities (taken from Sutton et al., 2011).

The significant environmental impacts of excess N_r can be summarized by an acronym "WAGES", which represents five major threats due to N_r: Water quality, Air quality, Greenhouse balance, Ecosystems and biodiversity, and Soil quality (Sutton et al., 2011a; Fig 1.5). The impacts on each of these aspects can be far-reaching and long-lasting.

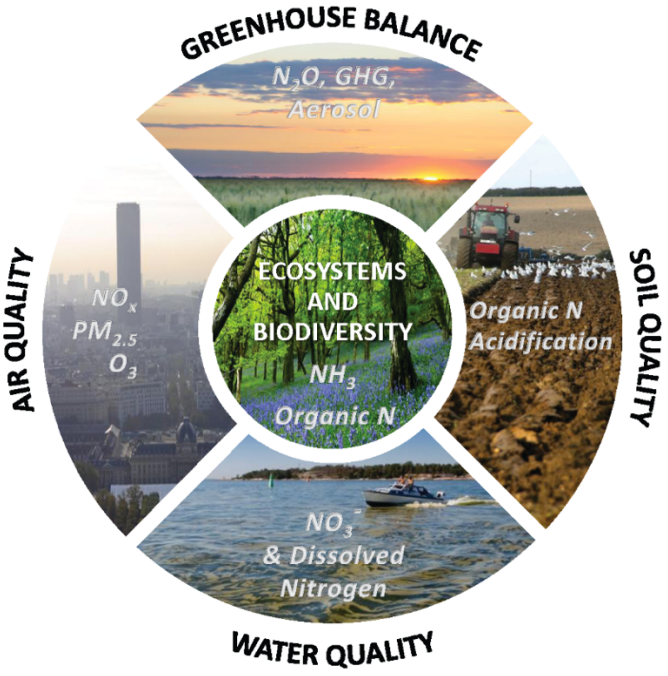

Figure 1.5. Summary of the five key environmental threats of excess reactive nitrogen by an acronym as the 'WAGES' (figure from Sutton et al., 2011a).

Water quality

Excess N_r causes acidification and eutrophication in water systems. Nitrogen is a key nutrient required to support primary production by plants and algae in water ecosystems (Durand et al., 2011). In undisturbed aquatic systems, organic N is the main form of nitrogen export, and concentrations of inorganic N are generally much lower compared to organic N. However, direct deposition of N_r or leached N_r (nitrate originated as NO_x or NH_3/NH_4) can introduce a net input of acidity to these systems, which can significantly influence their productivity and biodiversity. Research has shown that HNO_3 is the main

cause of acidification in many parts of Europe and North America (Murdoch and Stoddard, 1992; Allott et al., 1995; Wright et al., 2001). Eutrophication can occur in both marine and non-marine freshwater systems. Estuaries and their adjacent coastlines are particularly affected by eutrophication from N_r, which can be four times the natural background, resulting in biodiversity loss, toxic algal blooms and fish kill (Billen et al., 2011).

Air quality

Air quality is significantly affected by atmospheric releases of N_r. Both NH_3 and NO_x are precursor air pollutants and contribute to the formation of particulate matter (PM; as ammonium, NH_4^+ and nitrate, NO_3^- aerosol), which can reduce visibility of the atmosphere and pose threats to human health. Prolonged exposure to high levels of NH_3 and PM can cause respiratory and cardiovascular diseases (Brunekreef and Holgate, 2002; Pinder et al., 2007; Wyer et al., 2022). Ammonia is the most significant alkaline gas in the atmosphere, while NO_x plays a crucial role in the production of tropospheric ozone (also a major air pollutant). In addition, NO_x can affect other key oxidants and radical species, making it closely coupled to the oxidizing capacity of the atmosphere (Isaksen et al., 2009). It has been reported that N_r contributes 30% to 70% of the PM by mass (Sutton et al., 2011b). Globally, Gu et al. (2021) and Yao et al. (2023) have estimated that control of NH_3 emission is more cost-effective than further control of NO_x emissions.

Greenhouse gas balance

While N_2O is a potent greenhouse gas and an important contributor to radiative forcing because of its strong warming potential and relatively long lifetime in the atmosphere, N_r containing aerosols have a cooling effect by scattering radiation (the direct effect) and

influencing cloud formation (the indirect effect). According to the IPCC's sixth Assessment Report on Climate Change (AR6), N_2O is estimated to contribute approximately 0.21 W m^{-2} of radiative forcing (Intergovernmental Panel On Climate Change, 2023), while Xu and Penner (2012) estimated that the direct and indirect anthropogenic forcing from particulate nitrate and ammonium at the top of the atmosphere was –0.12 W m^{-2} and –0.09 W m^{-2}, respectively. European N_r emissions are estimated to have a net cooling effect on climate of –16 mW m^{-2}, with the uncertainty ranging between substantial cooling to a small net warming (– 47 to +15 mW m^{-2}) (Butterbach Bahl et al., 2011b; Sutton et al., 2011b).

Ecosystems and biodiversity

The lifetime of N_r in the atmosphere is relatively short (with the exception of N_2O), ranging from days to weeks (Jacob, 2000; Fowler et al., 2013; Seinfeld and Pandis, 2016). The removal of N_r from the atmosphere through deposition has huge impacts on biodiversity of the ecosystems, causing foliar damage to vegetation, eutrophication, acidification and susceptibility to secondary stress (Krupa, 2003; Dise et al., 2009). Atmospheric deposition of N_r encourages organisms to thrive that favour high nutrient supply or more acidic conditions, which outcompete other vulnerable species that are adapted to low nutrient levels and sensitive to elevated N_r deposition or are poorly buffered against acidification. Grassland, heathland, peatland and forest ecosystems are considered vulnerable habitats (Dise et al., 2011). Although the relative effects of different forms of N_r (e.g., NO_3^- versus NH_4^+) on ecosystems remain unclear for many habitats, gaseous NH_3 is recognised to be particularly harmful to vegetation, especially to lower plants, through direct foliar damage (Dise et al., 2011), and is thought to be at least partly related to the 'alkaline air' effect of NH_3 on sensitive vegetation (Sutton et al., 2020).

Soil quality

Additional N_r typically has a beneficial effect on soils, and typically enhances soil fertility and to stimulates the growth of plants. But when presenting in large amounts, excess N_r can have adverse impacts on both agricultural and natural soils, which includes soil acidification, changes in soil organic matter (OM) content and loss of soil biodiversity associated with eutrophication (Butterbach-Bahl et al., 2011a). Soil acidification is a common consequence of excess N_r, which results from the deposition of both NH_3 and NO_x emissions, as well as more directly from fertilizer and manure applications. Soil acidification negatively impacts crop yield and forest growth, and increases leaching of toxic components, such as heavy metals. The impact of N fertilization on agricultural soil OM content is varied, with some studies showing increases while others show decreases due to N from fertilization (Glendining et al., 1996; Sleutel et al., 2003). Increased N_r deposition has greatly altered C and N cycling and soil C/N ratios over the last decade (Vitousek et al., 1997; Gundersen et al., 1998; Corre et al., 2007). Eutrophication of natural soils caused by the high nitrogen input is often linked to low C/N ratios of organic matter, elevated nitrogen leaching and a reduction in biodiversity.

1.3 Ammonia emission: its sources and fates

1.3.1 Sources of ammonia emissions

The dominant source of NH_3 emission is from agriculture, often accounting for over 80 % of the total NH_3 emissions (Sutton et al., 2000; Hertel et al., 2011). Agricultural NH_3 emissions are mainly from NH_3 volatilization from synthetic fertilizer and livestock excreta, and the involved processes are very sensitive to the environmental conditions such as temperature.

The N loss from the agricultural systems through NH_3 emission can originate from various agricultural activities, as illustrated in Figure 1.6, including livestock housing and grazing, manure management, and the application of both manure and synthetic fertilizer to the land.

Nitrogen applied to arable land is taken up by crops (or grass), while livestock obtain N from feed and grazing and convert it into meat, milk, or eggs. Any surplus of N is then excreted, which is a by-product that can be used as manure fertilizer. Livestock manure can be managed in different ways depending on local needs, such as being stored for further use or burned as fuel. Although N is desired to be used by living organisms as much as possible, a significant portion of nitrogen is lost through volatilization unintentionally.

Compared with agriculture, non-agricultural sources of NH_3 emissions are much smaller, typically accounting for only 5 to 15 % of the total emissions, depending on the region (Sutton et al., 2000, 2013). These sources include biomass burning, transport, industry, residential and some natural sources such as soil and ocean emissions.

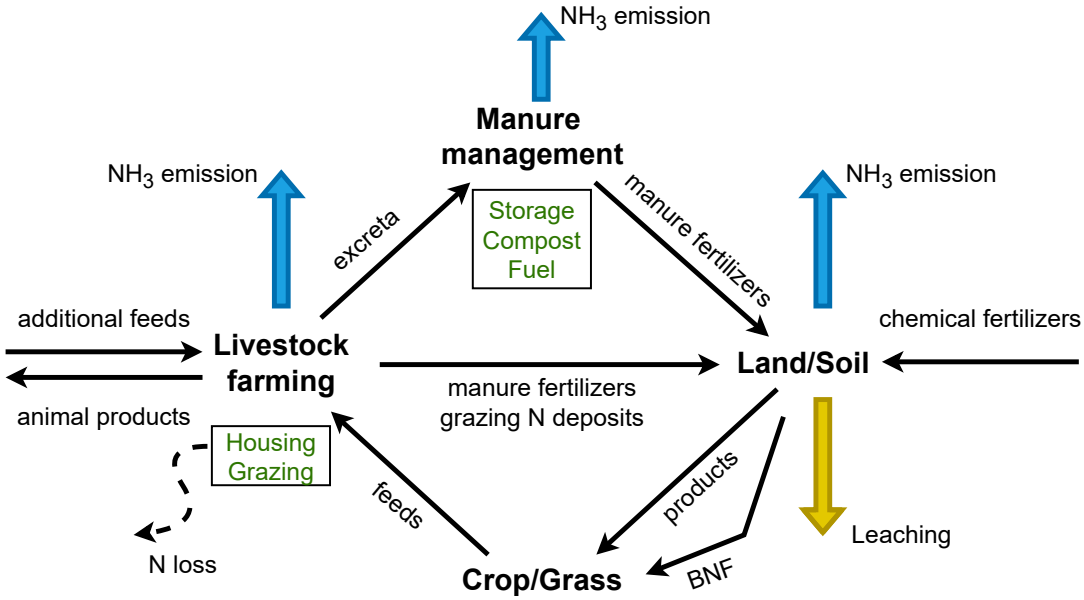

Figure 1.6. Schematic of NH_3 emissions that originate from livestock farming and crop agriculture following the N flows. Note the difference between this figure and Figure 1.4 that illustrates the N cascade. This figure focuses on the NH_3 emissions from various activities in the agricultural system.

1.3.2 Atmospheric processing of ammonia

Ammonia is released from the surface and undergoes a variety of processes once it enters the atmosphere. Ammonia is reactive and consequently relatively short-lived in the atmosphere, with a typical lifetime of hours to days (Bian et al., 2017; Ge et al., 2022). As introduced in Section 1.2.2, NH_3 emissions can lead to the formation of aerosols in the presence of gas phase acids, such as sulphuric acid (H_2SO_4, forming ammonium sulfate) and nitric acid (HNO_3, forming ammonium nitrate). Atmospheric NH_3 can be transported

away from the emission source and be removed from the atmosphere by dry or wet deposition. The efficiency of these processes depends on the prevailing meteorological and environmental conditions. Therefore, the atmospheric concentration of NH_3 shows significant spatial and temporal variation.

Gas phase NH_3 can either lead to aerosol formations or condense onto existing atmospheric particles. For aerosol formation, NH_3 readily reacts with gas phase H_2SO_4 and HNO_3, forming ammonium sulphate ($(NH_4)_2SO_4$) and ammonium nitrate (NH_4NO_3), respectively. The former reaction between NH_3 and H_2SO_4 is favourable over HNO_3, if H_2SO_4 is present. A two-step processes is used to describe the reaction:

$$NH_3 + H_2SO_4 \rightarrow NH_4HSO_4 \tag{1.1}$$

$$NH_3 + NH_4HSO_4 \rightarrow (NH_4)_2SO_4 \tag{1.2}$$

The reaction is considered irreversible and dependent on temperature and humidity. In contrast, when NH_3 reacts with HNO_3, it leads to an equilibrium between the gases and aerosol phase products, but it is a reversible process:

$$NH_3 + HNO_3 \rightleftharpoons NH_4NO_3 \tag{1.3}$$

The equilibrium depends on temperature and humidity (Stelson et al., 1979; Stelson and Seinfeld, 1982).

Besides undergoing chemical reactions to form aerosols, NH_3 can also be removed from the atmosphere effectively through dry and wet deposition. Dry deposition is the direct

transfer of NH_3 onto terrestrial or marine surfaces, while the wet deposition occurs when NH_3 is captured by rain droplets and subsequently deposited on surfaces. Given its high solubility, NH_3 is readily deposited on wet surfaces and scavenged by precipitation. As a result, NH_3 typically does not travel long distances from its source before being deposited or scavenged (Hertel et al., 2011; Fowler et al., 2013; Seinfeld and Pandis, 2016). By comparison, ammonium aerosols have a longer lifetime than NH_3 and can travel greater distances (Hertel et al., 2011; Fowler et al., 2013; Seinfeld and Pandis, 2016).

1.4 Estimating ammonia emissions

1.4.1 Emission factors and process-based models

The two most commonly used methods for estimating NH_3 emissions are EFs and process-based models. Emission factors are empirically derived or experimental values, which summarize NH_3 volatilization rates that vary by specific source sectors. The NH_3 emission is then calculated by combining statistical activity data with reference EFs. The simplicity in calculations is an advantage. However, these EFs may not provide an accurate representation of NH_3 volatilization because NH_3 emissions are highly sensitive to environmental conditions, such as temperature, that show large spatial and temporal variations. For example, it has been suggested that a 5 °C rise in temperature will lead NH3 volatilization potential to nearly double, as predicted by solubility and thermodynamics (Sutton et al., 2013). As EFs only consider the climatic effects to a limited extent, using

constant values to describe the fraction of N that volatilizes as NH_3 from different sources may not provide realistic estimates under all environmental conditions. Significant uncertainties may result from using EFs in large-scale assessment (e.g., global-scale calculations), and these also typically lack information in the temporal characteristics of NH_3 emissions. Due to increasing awareness of the climate sensitivity of NH_3 emissions, EFs have been improved by either applying corrections of environmental factors or temporal profiles, for example, in Ren et al. (2023).

Process-based models are another method used to estimate NH_3 emissions, which are developed based on the theoretical understanding of relevant processes and foundations developed for sources (Sutton et al., 1995; Nemitz et al., 2001; Flechard et al., 2013; Móring et al., 2016). Process-based models attempt to include the effects of environmental factors on NH_3 volatilization to address the deficiency of the EFs that are lack of response to environmental drivers. These models can have different levels of complexity, with different processes and factors emphasized.

Nemitz et al. (2001) developed a two-layer model (2LCCPM) to investigate the bi-directional exchange of NH_3 between the ground layer and the vegetation above. The 2LCCPM model incorporates the "compensation point" theory (Farquhar et al., 1980; Sutton et al., 1995), which introduces a theoretical equilibrium reached by the atmospheric NH_3 concentrations above a given source or sink of NH_3. This bi-directional exchange scheme has been adapted and modified for different purposes in later studies and models, such as estimating NH_3 emissions from fertilized agricultural land like CMAQ-EPIC (Bash et al., 2013; Fu et al., 2015; Chen et al., 2021) and DLEM (Xu et al., 2018, 2019a) and for investigating NH_3 volatilization from urine patches in the GAG model (Moring et al., 2016).

Pinder et al. (2004) constructed a model for simulating NH_3 emissions from dairy cattle with a range of activities included, such as housing, grazing, manure storage and application. The FAN model, which simulates global agricultural NH_3 emissions, includes response to climatic factors and has detailed soil processes (Riddick et al., 2016; Vira et al., 2020a).

Although process-based models are more sophisticated compared with EFs, they also have limitations. For example, the CMAQ-EPIC model (Bash et al., 2013) has limited representations for the soil processes, and the FAN model simulates manure management and livestock housing in a much simpler way relative to its land simulations. Due to the difficulties in covering all processes in a reasonable level of detail, each model has its own focus. It is critical to justify which processes are important and should be included because process-based models often require more detailed model inputs and higher computational resources than studies and inventories that use the EFs.

A further approach is the use of empirical models, which may be derived from regression relationships between measurements and driving parameters (Bouwman et al., 2002) or from simplification of more detailed process based models (Ramanantenasoa et al., 2019). In practice, such approaches may range from incorporation of empirical elements within largely process-based models to EF approaches with some additional effects considered.

1.4.2 Global assessment of ammonia emissions

Existing NH_3 emission inventories largely rely on the use of EFs due to the simplicity of this approach. As non-agricultural NH_3 emissions are primarily driven by activities and are

less dependent on climate, it is rational to use EFs for these sources. Table 1.1 summaries estimates of global NH_3 emission from inventories and several process-based models. Agriculture is the largest sector of NH_3 emissions, and inventories that focus on different years suggest comparable total emissions. In particular, Emissions Database for Global Atmospheric Research (EDGAR) emphasizes the larger contribution of agricultural NH_3 (including manure management and agricultural soils) than other studies. As shown in Figure 1.7, EDGAR estimates that global NH_3 emissions have substantially increased over the past 50 years, and agricultural NH_3 emissions are estimated to have nearly doubled. Meanwhile, models mainly focus on assessing agricultural NH_3 and provide broadly consistent estimates with inventories.

Table 1.1. Estimates of global NH_3 emissions.

Inventory/Model		Year	Agricultural NH_3 (Tg N yr^{-1})	Total NH_3 (Tg N yr^{-1})
Inventory	EDGAR v6.1[a]	2010	44.2	50.7
		2018	46.4	53.1
	Dentener&Crutzen1994[b]	1990	28.4	45.0
	Bouwman1997[c]	1990	34.2	53.6
	Van Aardenne2001[d]	2000	33.7	43.0
	Beusen2008[e]	2000	32	
	MASSAGE_NH_3[f]	2005-2008	34	54
Model	CAMEO[g]	2005-2015	44	
	FANv1[h]	2000	33	
	FANv2[i]	2010	48	

[a] EDGAR, 2023 [b] Dentener and Crutzen, (1994) [c] Bouwman et al. (1997) [d] Van Aardenne et al. (2001) [e] Beusen et al. (2008) [f] Paulot et al. (2014) [g] Beaudor et al. (2023) [h] Riddick et al. (2016) [i] Vira et al. (2020)

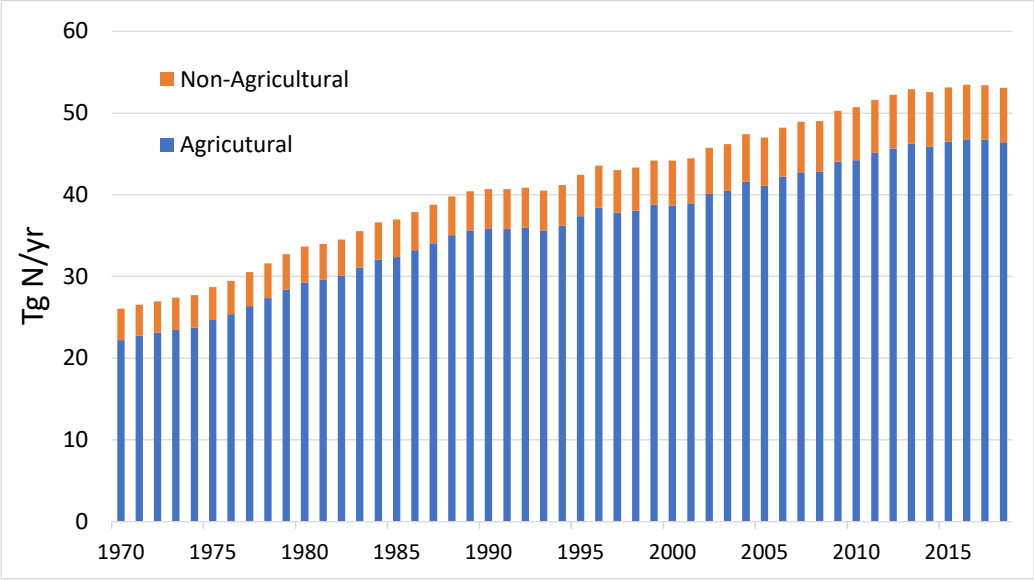

Figure 1.7. Global NH_3 emission from agricultural and non-agricultural sources between year 1970 and 2018 (based on data from EDGAR, 2023).

1.5 Existing guidance and policies on ammonia emission control

As discussed, NH_3 emissions have significant environmental and human health implications. Plenty of studies have demonstrated the benefits and importance of NH_3 control on the sustainable development and human well-being. For example, recent studies have shown that abating NH_3 is a cost-effective measure in addressing air pollution (Gu et al., 2021; Xu et al., 2022; Liu et al., 2023). Such scientific evidence needs to be translated into policies, regulations and economic incentives to have real-world impacts. Over the past decades, there have been great achievements in reducing sulphur dioxide (SO_2) and NO_x

for improving the air quality due to the success of policies. By comparison, less attention has been given to NH_3, which remains a key challenge for the future.

The Gothenburg Protocol, established under the United Nations Economic Commission for Europe (UNECE) as part of the Convention on Long-Range Transboundary Air Pollution (CLRTAP), is the first international protocol that addressed the needs of reducing NH_3 emissions for the benefit in human health and environment, along with SO_2, NO_x and volatile organic compounds (VOCs) (UNECE, 2012). The protocol set emission mitigation targets for countries and included national emissions reduction commitments. However, under revision of the UNECE Gothenburg Protocol in 2012, the EU projected decrease in the NH_3 emissions was only 2 per cent compared with 30 per cent for SO_2 and 29 per cent for NO_x, with NH_3 being the least ambitious of all pollutants considered (UNECE, 2012).

The *UNECE Guidance Document on preventing and abating ammonia from agricultural sources* (Ammonia Guidance Document, ECE/EB.AIR/120; Bittman et al., 2014) provided supporting material to the Gothenburg Protocol and has encouraged the use of best available techniques to reduce NH_3 from various agricultural sectors, along with the scientific background, economic cost and limitations of the techniques (Bittman et al., 2014). Similarly, the *UNECE Framework Code for Good Agricultural Practice for Reducing Ammonia Emissions* (Ammonia Framework Code, ECE/EB.AIR/129) is designed to support Parties in establishing or updating their national advisory codes of good agricultural practice to control ammonia emissions (UNECE, 2015). Although these documents are for guidance only and is not a prescriptive set of measures for full adoption, they present potential effective low NH_3 emission systems in agricultural practices.

These two documents further facilitated the establishment of the *UNECE Guidance Document on Integrated Sustainable Nitrogen Management* (ECE/EB.AIR/149) prepared by the Task Force on Reactive Nitrogen (TFRN), which focuses on broader perspectives to guide Parties and other stakeholders in tackling multiple forms of nitrogen loss simultaneously (Sutton et al., 2022). A further important milestone is the Colombo Declaration, where 14 United Nations (UN) members states agreed the ambition to halve nitrogen waste by 2030. This follows up the first ever UN Resolution on Sustainable Nitrogen Management (UNEP/EA.4/14), and itself informed adoption of the subsequent resolution at the 5th UN Environment Assembly (UNEP/EA.5/2; UNEP, 2019, 2022).

In addition to the international frameworks, national policies also play a crucial role in regulating domestic NH_3 emissions. Notable examples include the Netherland's Nitrogen Emission Action Programme (Programmatische Aanpak Stikstof), which both addresses NH_3 and NO_x emissions within the country. Denmark's Action Plans have been implemented to reduce NH_3 emissions whilst also improving water quality (Danish Ministry of Climate, Energy and Utilities, 2019). The United Kingdom's Clean Air Strategy (DEFRA, 2019) and United States Clean Air Act (USEPA, 2021) highlighted the significance of controlling farming NH_3 for better air quality. These national policy actions have demonstrated the ambitions and comprehensive efforts in mitigating NH_3 emissions. However, there are still gaps between developed countries and some developing countries regarding monitoring and reducing NH_3 emissions due to limited resources and knowledge or lack of awareness.

While significant progress has been made, challenges remain, and continuous efforts are required to achieve substantial NH_3 emission reductions and to develop integrated

approaches to N management. Furthermore, future research should also focus on evaluating the effectiveness of implemented policies, identifying cost-effective strategies and enhancing international collaboration.

1.6 Thesis layout

The motivation and aims of this study, along with background and introduction of the topic are presented in this chapter (Chapter 1). The main chapters presenting methods and results of the research are Chapters 2 to 6. Chapter 2 is a methodology chapter that describes the development of the emission model AMmonia–CLIMate (AMCLIM), which presents the overall model structure, simulated processes and input data required for running the model. Chapters 3 to 5 are written in the format of scientific papers that consist of introduction, methods and materials, results, discussion and conclusions. These chapters present the quantification of NH_3 emissions from synthetic fertilizer use (Chapter 3), pig and poultry farming (Chapter 4) and ruminant farming (Chapter 5) by using the AMCLIM model, with complementary and detailed descriptions of the model development for individual sectors. Chapter 6 is a synthesis chapter that provides a comprehensive outlook on agricultural NH_3 emissions simulated by the model, including analysis for impacts of environmental factors and management practices on NH_3 volatilization, potential mitigation measures and present and future NH_3 emissions in the 21st century. Chapter 7 contains the conclusions and key research findings, as well as limitations and future outlook.

Chapter 2
Development of AMmonia–CLIMate (AMCLIM) model

2.1 Overview

AMmonia–CLIMate (AMCLIM) is a dynamical emission model that quantifies climate-dependent NH_3 emissions from agriculture. It incorporates the effects of environmental conditions on the formation and transport of N compounds to simulate the temporal evolution of each N species, especially NH_3. There are three modules in AMCLIM: a) Housing, b) Manure Management and c) Land. The model focuses on synthetic fertilizer application and livestock farming, simulating relevant physical, chemical and biological processes that govern the N flows in agricultural systems, whilst also considering agricultural management practices.

The AMCLIM model can be operated at multiple scales; it is calibrated and validated at the site scale by comparing with measurements and experimental studies and then is applied on a global scale to provide estimates of global NH_3 emissions. For site-scale simulations, the AMCLIM model explores various source sectors and can be run with different length

time-step, depending on inputs given in the measurement datasets. For global simulations, the AMCLIM model covers all major agricultural sectors and aims to provide a comprehensive assessment of agricultural NH_3 emissions. Livestock sectors include pigs, poultry, cattle, sheep and goats, which together dominate the livestock NH_3 emissions. The AMCLIM model also simulates NH_3 emission from global synthetic fertilizer use on crops.

2.2 Model structure and components

The design of the AMCLIM model is closely associated with human activities in agriculture. The model structure and components are shown in Figure 2.1. Three main modules in AMCLIM cover essential agricultural activities and practices, and the connections between modules reflect the typical N flows in the livestock production systems (as introduced in Section 1.3.1), from animal housing to manure storage and then to the ultimate land spreading. As NH_3 emissions can be released at all stages, all modules need to provide robust estimates as previous components can have substantial influences on the following ones, i.e., less emission from housing leaves higher N content in the animal excreta and possibly cause larger emissions in the succeeding practices.

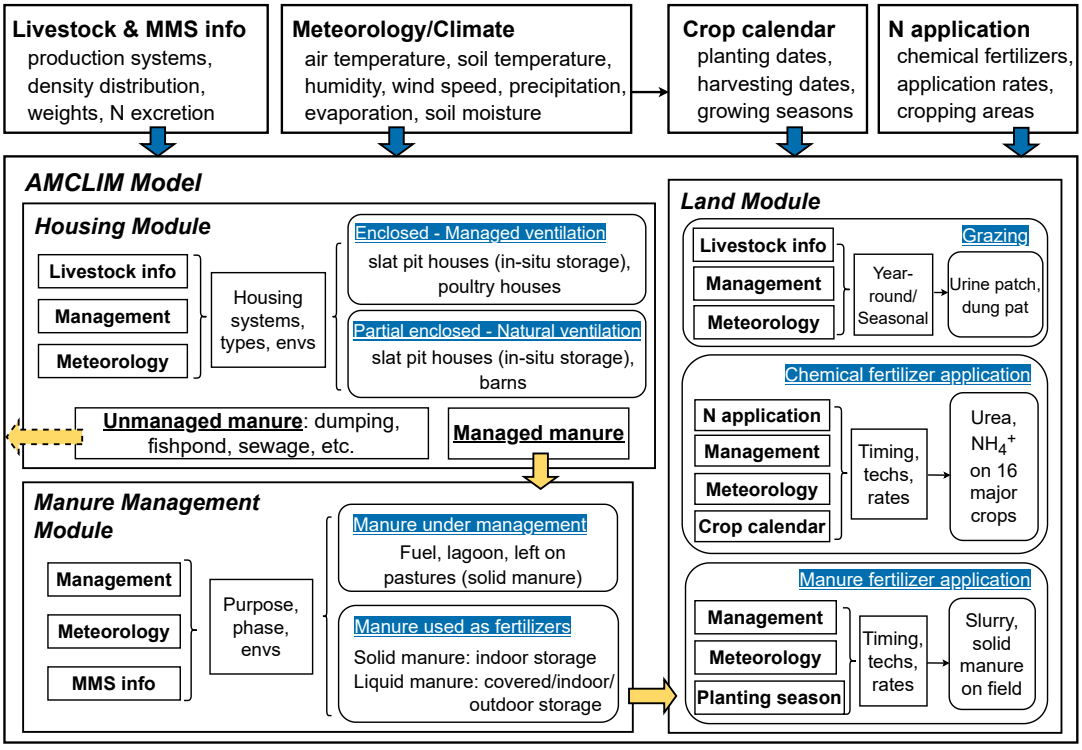

Figure 2.1. Components and structure of the AMCLIM model and inputs (blue arrows) used for simulations. The dashed yellow arrows represent a fraction of unmanaged N from housing that is not simulated in the Manure Management Module (AMCLIM–MMS). Solid yellow arrows represent the N flows between modules. (MMS: Manure Management Systems. Envs: Environments. Techs: Techniques.)

2.2.1 Housing Module

A Housing Module in AMCLIM (AMCLIM–Housing) was designed to estimate the NH_3 emission from livestock housing. Pigs and poultry are mostly kept in buildings, and

ruminants like cattle and sheep may also spend a considerable amount of time in barns or stalls depending on weather and local management. In animal houses, nitrogen in animal excretion can decompose and potentially leads to NH_3 emission. Ventilation in the house causes turbulence and mixing of indoor air. Indoor NH_3 increases as NH_3 is quickly released from the surface through mixing under turbulent conditions. But indoor NH_3 must be controlled below a certain level for eliminating odour and maintaining a healthy environment for the animals. Meanwhile, ventilation continuously removes NH_3 from the house to the outside free atmosphere and brings in fresh air, which results in a decline of indoor NH_3 concentrations. In AMCLIM–Housing, NH_3 removed from the animal house to the free atmosphere is assumed to equal the amount of NH_3 released from the surface to the indoor atmosphere, which is considered to be true under most conditions when there are no filters that absorb NH_3. Released NH_3 may get deposited on "clean" wet surfaces in the animal house, e.g., walls. This flux is considered to be negligible due to NH_3 saturation in small amount of water so is not included in the model.

AMCLIM–Housing includes two housing systems and three house types, depending on the production system of the livestock and management. Two housing systems are distinguished: enclosed housing and partially enclosed housing, which are reflected by different indoor environmental conditions. Enclosed housing is assumed to have forced heating and managed ventilation, which is commonly used for commercial pig and poultry production systems in order to improve livestock performance (Gyldenkærne, 2005; FAO, 2018). Partially enclosed housing refers to barns or houses that are naturally ventilated, of which the indoor environment is assumed to be close to the natural environment. These two systems are employed to differing degrees by different livestock sectors and production

systems. For example, cattle have a higher tolerance to cold weather than pigs and poultry so are typically kept in naturally ventilated barns (Seedorf et al., 1998a).

Three house types are included in AMCLIM–Housing: 1) houses with slatted floors and storage pits, 2) normal barns (without slatted floors and pits) and 3) poultry houses. The first house type allows animal excreta to be removed quickly and effectively, so the house can be easily cleaned. The slatted floor is usually concrete or iron, and there are partially slatted compartments. The gap area of the slatted floor usually accounts for approximately 20 % and no more than 50 % of the total floor area (Aarnink et al., 1997). The excreta fall to the pit underneath through the gaps and is stored in-situ for a period. Emission of NH_3 can be from both the slatted floor area and the storage pit. Such slatted-pit houses are prevalent in pig farming, especially for industrial production system. This house type is simulated by a two-reservoir emission scheme in AMCLIM–Housing, with details given in Chapter 4.

The second house type is barns. Barns are commonly used facilities in livestock housing because they can be easily set up and requires less capital input compared to animal houses with slatted floor and pit storage. Barns are normally naturally ventilated and are not fully enclosed. During cold days, mechanical blocking may be applied to open barns to reduce ventilation (Gyldenkærne, 2005a). Excreta and bedding are frequently removed to a separate storage unit to keep the barn clean. In most cases, daily cleaning of barns is necessary. Barn modelling is described and discussed in Chapter 4 and 5.

The third house type is poultry houses. Poultry houses for broiler and layer production systems are mainly enclosed with forced heating and ventilation except for some regions.

Commonly, poultry excreta accumulate and remains in the houses for a long time, e.g., months to years until it is removed. Bedding materials such as straw are added to absorb moisture as well as to reduce emissions, which is typically for breeders and meat-type poultry (FAO, 2018a). Details of poultry house modelling are presented in Chapter 4.

2.2.2 Manure Management Module

Properly dealing with animal excreta is crucial because poorly managed animal excreta cause large unintentional NH_3 emissions, which results in a series of environmental issues. Under adequate management, livestock excreta become a valuable N source and can be spread on land as fertilizers. Manure is a mixture of animal excreta (including urine and faeces), bedding, feeds, drinking water and water used for cleaning from the housing. Collected manure is usually stored for a period until it is applied to fields at an appropriate time, and manure can also be used as fuel. In AMCLIM, a Manure Management Module (AMCLIM–MMS) was developed to simulate the NH_3 emission from the stage when manure is removed from the housing systems and before it is spread on land. According to the Global Livestock Environmental Assessment Model 2 (GLEAM2) (FAO, 2018a), there are over 20 manure management systems (MMS), and these MMS are in either liquid or solid phase based on the water content (see Appendix B4,). The main divisions identified for AMCLIM and regrouped from the GLEAM-defined MMS are based on the similarities existing in the general practices, as follows:

A) Indoor storage: manure is stored and managed in stables/barns/enclosed or partially enclosed facilities.

B) Outdoor storage: manure is stored in open environments, i.e., an earthen basin or pond.
C) Covered storage: manure is stored in tanks or containers with a cover/crust on top.
D) Left on land: manure is left on pastures soon after it is removed from housing, or there is daily spreading of collected manure on fields.

The above divisions of MMS were implemented in AMCLIM–MMS for simulating NH_3 emissions, and each division may include two phases or only include one phase. It worth mentioning that the types of manure storage included in AMCLIM is a simplification. The current level of complexity is justified as adequate for global modelling. It is impossible to simulate every specific practice in manure management given the computational costs and the extra uncertainty entailed from more assumptions on data and processes. Divisions A, B and C represent manure storage in different manners. Subsequent land spreading of manure N from these three divisions will be simulated by the Land Module (see Section 2.2.3). In contrast, manure N from division D which has already been spread or left on land will not go into the Land Module of AMCLIM, and the NH_3 emission is counted as manure management emission. As described in Table B3 (see Appendix B7), manure can be used as fuel (burned) or converted to fuel (digester), which may cause significant NH_3 emissions but is not included in the AMCLIM model due to the uncertainty (limited studies) and scope of this study. Meanwhile, these types of management are only a small fraction across the globe. The amount of manure N used as fuel will be presented but will not be simulated further here. In addition, there is unmanaged manure N from housing. Although it is not an MMS according to the definitions used in GLEAM2, it is still critical because this fraction reflects a direct N loss from the agricultural system to the environment. Unmanaged N is quite common in a few regions and nations for some particular livestock production

systems according to the UN Food and Agriculture Organization (FAO, 2018a). These unregulated systems include “discharge”, “dumping”, “fishpond” and “public sewage”, which have adverse impacts on local aquatic systems and ecosystems. Nitrogenous manure discharged to water bodies does not cause large NH_3 emissions but has other environmental implications. The amount of nitrogen that is not managed at this stage is reported but not simulated further in AMCLIM. This is treated as a loss or an untraceable term in AMCLIM–MMS.

2.2.3 Land Module

Agricultural soils have been estimated to contribute to 60 to 80 % of the NH_3 emission from the whole agricultural sector (Beusen et al., 2008; Crippa et al., 2018; Vira et al., 2020b). The Land Module of the AMCLIM (AMCLIM–Land) model consists of three submodules that quantify the NH_3 emission from animal grazing, land spreading of manure and synthetic fertilizer application, respectively. The submodules for simulating grazing and manure application are closely linked to AMCLIM–Housing and AMCLIM–MMS.

There are two types of grazing in the Grazing Submodule: year-round grazing and seasonal grazing. The former practice indicates that ruminants freely roam around on pastures throughout the year, while the latter addresses the fact that ruminants graze seasonally depending on the climate/weather (e.g., ruminants are gathered in and housed for winter), and excreted N from the seasonal grazing livestock is split into two parts: housing and grazing. Emission of NH_3 from grazing fields is dominated by urine patch emissions, and dung pat is found to contribute to only a tiny fraction (Saarijärvi et al., 2006; Laubach et

al., 2013). Schemes for both urine patches and dung pats are included in the Grazing Submodule, with details presented in Chapter 5.

As mentioned in Section 2.2.2, manure is applied to land after storage. Applied manure is assumed to have generally identical features as the stored manure, i.e., the liquid phase storage leads to application of slurry which is a type of manure that has relatively low dry matter (DM) content, and the solid phase storage leads to solid manure application in AMCLIM–Land. It is assumed in AMCLIM that the manure from each livestock sector is spread on fields independently and there is no use of a mixture of manure.

Synthetic fertilizer application is an independent component in AMCLIM–Land as it is not directly associated with the livestock farming that is simulated by the other modules. The Synthetic Fertilizer Application Submodule simulates the flows of N applied on crops with an emphasis on the estimation of NH_3 emission, from the application of urea N and ammonium N. Nitrogen application rates and planting calendars for individual crops were incorporated into the model to simulate the spatial and temporal variability of NH_3 emission which is influenced by human management.

Three typical techniques in fertilizer application were implemented, namely: a) broadcasting, b) incorporation and c) deep placement. Each technique has advantages and disadvantages in practice from the aspects of nutrient use efficiency, costs and environmental impacts, which are presented and discussed in Chapter 3. In AMCLIM–Land, all of the above three techniques are used for synthetic fertilizer application, while manure is assumed to be applied only at the surface by broadcasting. Contrary to housing and manure management, land simulations are driven by the natural climatic conditions

under local management. Practices that can affect the environmental variables, i.e., irrigation events and slurry application which temporarily alter the soil moisture, are evaluated in the AMCLIM–Land with details given in later chapters.

2.3 Modelled N processes

The AMCLIM model was developed based on the understanding of physical and chemical processes. The model simulates atmospheric, soils and interfacial processes which are associated with the N flows in agricultural practices, as shown in Figure 2.2. These processes govern the formation of NH_3 emissions and are strongly dependent on environmental factors. Simulated processes differ in each module because of the different systems and practices and different environmental conditions (i.e., indoor conditions for housing vs. outdoor/open conditions for fertilizer application and grazing) and may vary between livestock sectors because of different forms of N in the animal excreta (i.e., uric acid in poultry excreta vs. urea in pig excreta). This section provides a brief general introduction to these processes, and detailed descriptions and parameterizations, as well as more specific processes, are presented in the following chapters.

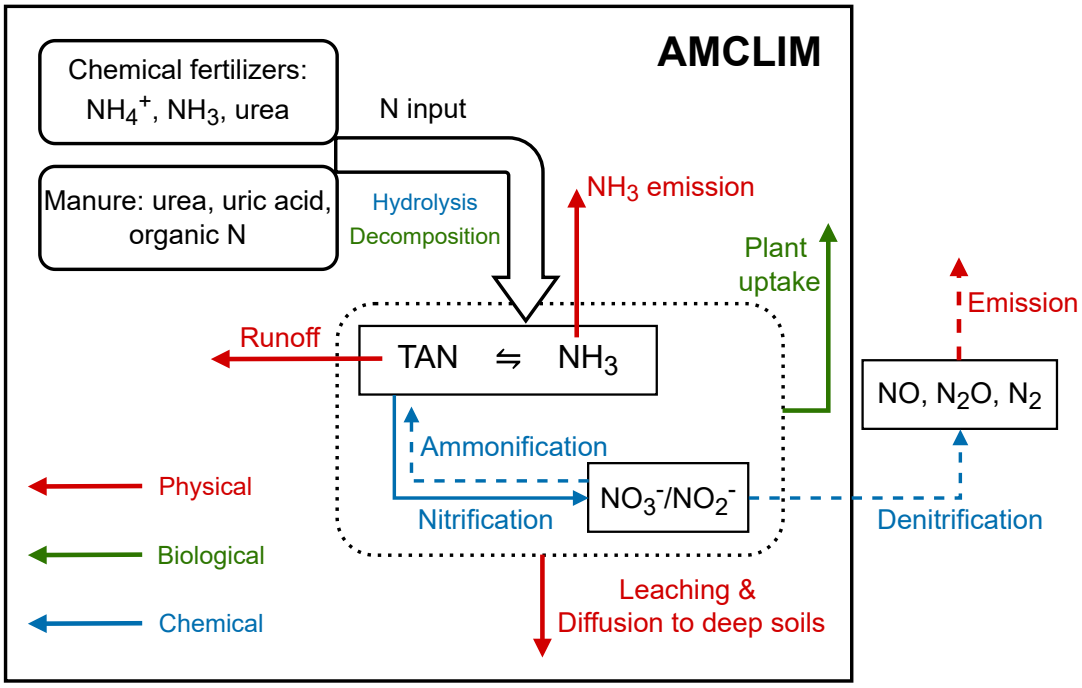

Figure 2.2. Simulated N processes in the AMCLIM model (shown in the solid black box). Ammonification, denitrification, and emission of NO, N_2O and N_2 are not included in this study but are shown (dashed arrows; or outside the black box) to provide the comprehensive concept. The dotted black box indicates soil N processes. Red arrows represent physical processes, including NH_3 volatilization, surface runoff, leaching and diffusion of nitrogen to deep soils. Green arrows represent biological processes, such as plant uptake of N and decomposition of organic N. Blue arrows represent chemical transformations, including hydrolysis of urea and uric acid in animal excreta and nitrification.

2.3.1 Masses of nitrogen pools and concentrations

In the AMCLIM model, pools of N compounds are determined by the sources and losses. Flows between the pools are simulated, termed fluxes. Masses of pools are calculated at every time step. The general expression for the time-dependent N pools can be simply written as:

$$\frac{\mathrm{d}M_{\mathrm{N}}}{\mathrm{d}t} = F_{\mathrm{P_N}} - F_{\mathrm{L_N}} \tag{2.1}$$

where M_{N} is the mass of a N species (g N m^{-2}, given in per unit area; all masses have units of g m^{-2} if not specifically explained). $F_{\mathrm{P_N}}$ and $F_{\mathrm{L_N}}$ (g N m^{-2} s^{-1}; all N flows have units of g N m^{-2} s^{-1} if not specifically explained) represent the sum of production (including inputs) and losses of the N compound, respectively.

AMCLIM uses the same mass balance approach to calculate the water pool and then solve the concentrations in the aqueous phase of each N species by dividing the mass by the volume of water, as follows:

$$[\mathrm{N}] = \frac{M_{\mathrm{N}}}{V_{\mathrm{H_2O}}}, \tag{2.2}$$

where [N] (g mL^{-1}) is the concentration of the N species, and $V_{\mathrm{H_2O}}$ (mL m^{-2}) is the volume of water. It must be noted that the sources and losses terms of each N pool and the water pool in different modules are not the same, and Equation 2.2 is a general representation for the concentration calculations, which is modified when considering multi-phase equilibria. Details are given in the following chapters.

2.3.2 Volatilization of ammonia

The most important N species simulated in the AMCLIM model is the total ammoniacal nitrogen (TAN, TAN = NH_3+ NH_4^+), which can either be partitioned into gaseous or aqueous NH_3 and aqueous or adsorbed NH_4^+ (as shown in Equation 2.3).

$$M_{\mathrm{TAN}} = M_{\mathrm{NH_3,g}} + M_{\mathrm{TAN,aq}} + M_{\mathrm{TAN,s}}\ , \tag{2.3}$$

Livestock excreta and synthetic fertilizers are major sources of N inputs to the environment that cause NH_3 emissions (Fig. 2.2). The physical and biochemical processes involved in these anthropogenic activities influence the transformations between various N forms and the transport of N species, in which the abundance of TAN is the key component that governs the NH_3 emission potential (Γ) of a system.

Ammonia emission is a physiochemical process that typically takes place from wet or drying surfaces. Gas phase NH_3, held within the excreta and soil pore spaces, or at the surface in the slurry, is in dynamic equilibrium with aqueous ammonium depending on the substrate pH and temperature response of combined Henry and dissociation equilibria as follows (Nemitz et al., 2000):

$$\chi = \frac{161500}{T}\exp\left(\frac{-10378}{T}\right)\Gamma, \tag{2.4}$$

$$\Gamma = \frac{[\mathrm{NH_4^+}]}{[\mathrm{H^+}]} = \frac{[\mathrm{TAN}]}{K_{\mathrm{NH_4^+}}+[\mathrm{H^+}]} \tag{2.5}$$

where K_{NH4+} is the dissociation constant of NH_4^+.

The flux of NH_3 (F_{NH_3}) volatilized to the atmosphere from the surface is then determined by assuming a resistance model (developed from the electrical resistance analogy). The model uses gas concentrations at two vertical levels constrained by a set of resistances (Sutton et al., 2013), which is calculated from:

$$F_{NH_3} = \frac{[\chi_{sfc} - \chi(z)]}{R}, \quad (2.6)$$

where χ_{sfc} represents the concentration at the surface, and $\chi(z)$ represents the concentration at a reference height. Equation 2.6 represents a general formula as the resistance term needs to be parameterized for different environments, e.g., inside an animal house, or on cropland, which is influenced by turbulent conditions, specific to each setting. The magnitude of concentrations at two heights used in Equation 2.6 determines the direction of the NH_3 flux, i.e., emission takes place when surface concentration is higher, and deposition takes place if surface concentration is lower. A bi-directional air-land exchange scheme incorporating vegetation interactions is more sophisticated in simulating NH_3 fluxes (emissions and depositions) as proposed by Sutton et al. (2013). Given the complexity and computational expense of bi-directional exchange, the AMCLIM model focuses on a uni-directional transport in this study. This is considered to be appropriate in most cases as agricultural activities usually lead to big emission source at the surface, e.g., animal houses, fertilizer applications. The implementation of the bi-directional exchange scheme can be a potential future work.

2.3.3 Chemical transformations of nitrogen compounds and biological processes

There are various N compounds that are included in AMCLIM, and the model simulates the chemical transformations between these species. There are two important chemical pathways that can influence the source and loss of the TAN pool. The **first one** is the hydrolysis of ureic N (uric acid and urea) and the mineralization of organic N, which leads to TAN formation, expressed as follows:

$$F_{\mathrm{TAN}} = \sum K_{\mathrm{N}_i} M_{\mathrm{N}_i} = K_{\mathrm{Urea}} M_{\mathrm{Urea}} + K_{\mathrm{UA}} M_{\mathrm{UA}} + K_{\mathrm{OrgN}} M_{\mathrm{OrgN}}, \qquad (2.7)$$

where K_{N} is the conversion rate (s^{-1}) at which a N compound, e.g., urea, UA and organic N, decomposes to form TAN. All decomposition processes are assumed to be first-order reactions so that the production of TAN is dependent on the mass of the reactants. The conversion rates expressed as the general term K_{N} used in Equation 2.7 are strongly dependent on environmental factors, such as temperature, RH and the substrate pH.

In contrast to the decomposition that leads to TAN production, the **second pathway** is through nitrification which is a TAN removal process where NH_4^+ and NH_3 are oxidised into nitrite (NO_2^-) or nitrate (NO_3^-). Nitrification is a key process in ecosystem N cycling because of its relevance for nutrient loss in ecosystems (Butterbach-Bahl et al., 2011b), i.e., readily leaching of NO_2^- and NO_3^- from soils. Nitrification is generally an aerobic process and is considered to take place in soils and solid manure systems due to exposure to oxygen. Conversely, for liquid systems, such as the slurry system or lagoons, nitrification is absent or negligible due to high water content that reduces oxygen availability. In AMCLIM, nitrification is calculated when solving the losses of the TAN pool in the following

practices: solid phase manure management and land simulations, including fertilizer application and grazing. A simple first-order reaction is used to estimate nitrification (F_{nitrif}) as shown in Equation 2.8.

$$F_{\text{nitrif}} = K_{\text{nitrif}} M_{\text{TAN}}, \tag{2.8}$$

where K_{nitrif} (s^{-1}) is the nitrification rate which is influenced by temperature, substrate pH and water availability. The amount of nitrified N is subtracted from the TAN pool and is added to the nitrate (including nitrite) pool.

Plant uptake of N, which mainly occurs throughout the crop growing season, also influences the TAN pool (and nitrate/nitrite pool) in soils and is an important N pathway for NH_3 emissions as it depletes NH_4^+ concentrations in soil. However, existing studies argue that plant uptake is likely to have only a small effect on the TAN pool considering its timescales (Vira et al., 2020b). Although the importance of plant uptake in affecting volatilization relative to other processes remains unclear, the amount of N taken up by crops is a critical indicator for evaluating fertilizer use efficiency and provides implications for reducing NH_3 emissions and other N losses. Therefore, the AMCLIM model incorporated a plant uptake scheme to quantify plant N uptake. Details are given in Chapter 3.

2.3.4 Physical transport of nitrogen species

There are two basic types of physical transport of N species in the AMCLIM model: diffusion and mass movement of N in water. Diffusion is driven by concentration gradients

and can be either gaseous or aqueous. The diffusive fluxes ($F_{\text{diffusion(aq/gas)}}$) are estimated by a general equation as follows:

$$F_{\text{diffusion(aq/gas)}} = \frac{[\text{N}_1]-[\text{N}_2]}{R_{\text{aq/gas}}}, \tag{2.9}$$

where $R_{\text{aq/gas}}$ (s/m) is the resistance that constrains the aqueous or gaseous diffusion processes.

The transport of N compounds by the movement of water includes two critical loss processes: leaching and surface runoff. Both processes are evaluated by multiplying the corresponding concentrations by the movement fluxes. For leaching (F_{leaching}), a percolation flux of water (q_{p}, m/s) is used for the calculation, as follows

$$F_{\text{leaching}} = q_{\text{p}} \cdot [\text{N(soil)}], \tag{2.10}$$

where [N(soil)] is the concentration of the N species in the soil. The loss via surface runoff ($F_{\text{N runoff}}$) is calculated similarly by the following equation:

$$F_{\text{N runoff}} = q_{\text{r}} \cdot [\text{N(sfc)}], \tag{2.11}$$

where q_{r} (m/s) is the surface runoff flux of water, and [N(sfc)] is the surface concentration of the N species. It is worth noting that the surface runoff of N is assumed to ultimately enter water bodies and not to contribute to further emissions.

2.4 Model global applications

2.4.1 Model inputs and setup for global applications

The AMCLIM model is driven by meteorological reanalysis data and uses a variety of external data resources as model inputs. As shown in Figure 2.1, there are four primary inputs to AMCLIM: meteorology, livestock and MMS information, nitrogen application data and crop calendars. The meteorological fields required by AMCLIM include hourly air temperature, humidity, wind speed, precipitation, evaporation, soil temperature and soil moisture. These variables are taken from the European Centre for Medium-Range Weather Forecasts Reanalysis v5 (ERA5) collection (Hersbach et al., 2018). In addition to the meteorological variables, hourly surface runoff and subsurface runoff fluxes are also ERA5 reanalysis data. The ERA5 data have a resolution of 0.25° × 0.25° in longitude-latitude grid.

The primary input to AMCLIM–Housing, livestock data, is provided by the GLEAM2 model, which includes annual average animal density distribution, animal live body weights and annual total N excretion rates, with a spatial resolution of 0.083° × 0.083° in longitude-latitude grid. Data for each type of livestock are categorised into production systems, e.g., broiler and layer chicken, industrial and backyard pigs. Global MMS data by livestock sectors are also from the GLEAM2 model. Additional livestock information is N content and forms in urine and faeces, urinary N concentration and excretion pH, which is obtained from the literature. More details are given in Chapters 4 and 5.

For modelling synthetic fertilizer application, the AMCLIM model uses N application rates for 16 crops and corresponding crop calendars from the Global Gridded Crop Model

Intercomparison Phase 3 (GGCMI3) dataset, with a spatial resolution of 0.5° × 0.5° (Mueller et al., 2012; Hurtt et al., 2020; Jägermeyr et al., 2021). Other data requirements include soil physical properties and soil chemical characteristics such as soil sand and clay content, soil pH and soil organic matter content, which are presented in the following chapters.

The AMCLIM model is run at a 0.5° × 0.5° resolution on a global latitude-longitude grid (360 × 720). The time step for all global simulations in AMCLIM is an hour, and the model outputs hourly NH_3 emission and other N fluxes and pathways. The simulations were mainly carried out for the year 2010 and 2018 with one year as spin-up and covered a longer period over the past two decades to study the interannual variations and long-term trend of NH_3 emissions. The AMCLIM model was also used to simulate several N scenarios that influences the NH_3 emissions under a changing climate and tested the effectiveness of mitigation measures for NH_3 abatement. Details are presented in Chapter 6.

2.4.2 Global upscaling for livestock housing, manure management and grazing

The AMCLIM model quantifies the NH_3 emissions from global livestock farming of pigs, poultry, cattle, sheep and goats. Simulated practices include housing, manure storage and management, and manure application on fields. Practices differ between livestock sectors, i.e., ruminants vs. pigs and poultry. Practice can also vary in different production systems within the same livestock sector. For example, industrial-scale pig factories that are fully market-oriented often have relatively high stocking density and use modernised housing

systems with slatted floors and storage pits which require more capital input. In comparison, backyard-scale and family-run farms use simpler settings and cheaper materials to build animal houses, e.g., barns with solid concrete or pavement floor, and the herd performance is normally lower than commercial systems.

One challenge for global modelling is that there are enormously different management systems across the globe varying with regions, policies and climate. The AMCLIM model aims to have a comprehensive inclusion of influential management factors whilst also carrying out reasonable simplifications for providing general and universal schemes and reducing the computational burden. The geographical distribution of livestock and production systems information determine the housing systems and house types. The indoor environment of the animal houses is affected by the weather and is related to the housing systems. AMCLIM–Housing uses a series of generalized equations that reflect the relationship between indoor conditions and outdoor conditions to derive the indoor temperature, RH and ventilation for the animal houses. The house types affect the source areas of NH_3 volatilization and the N exchange between housing and manure storage. As both floor and storage pit are sources of NH_3 emissions, animal houses with pit storage tend to have larger source areas of emission compared to houses without pit storage. In houses with in-situ storage (e.g., a pit), the manure is less frequently removed. But in normal animal barns, manure can be collected on a daily basis. This results in a more frequent transfer of smaller amounts of manure from a more often cleaned housing system to the stores and may possibly lead to a larger emission potential.

AMCLIM–MMS takes the nitrogen that is from AMCLIM–Housing as inputs, from which the nitrogen is then used by the Manure Application Submodule in AMCLIM–Land. The

environmental conditions of indoor manure storage are assumed to be the same as the open animal barns. The natural environments drive the simulations for outdoor manure management. Manure storage is assumed to be long-term, and stored manure is assumed to be spread on land twice a year. Short-term manure storage is included as a subdivision under the Manure Management Division D, that manure is applied or left on pastures (in Section 2.2.2).

2.4.3 Global upscaling for grazing and application of manure and synthetic fertilizer

Concerning the global simulations for livestock grazing and the land application of manure and synthetic fertilizer, it is assumed that practices take place under natural environmental conditions, so the simulations are directly driven by meteorological reanalysis data.

For grazing, the local practices of whether it is year-round grazing or seasonal grazing are based on the production systems. Timing of the seasonal grazing practices varies in different regions due to the climate, for which the air temperature is used as a decisive indicator (see Section 5.2.2). In the Grazing Submodule, all excretion is assumed to be deposited on pastures for year-round grazing, and only a fraction of excretion is deposited while grazing seasonally. It should be noted that there is a distinction between the grazing area and the source area of NH_3 emissions. The grazing field can be very large, but only a fraction of the area has livestock excretion. According to Saarijärvi et al. (2006), around 1/5 of grazed pasture is deposited with excreta. This source area is split into urine patches and dung pats based on values provided by Saarijärvi et al. (2006), which allows the NH_3

emission to be simulated separately to investigate the relative importance of both schemes (see Section 5.2.2).

Land application of manure is assumed to take place throughout the spring and winter planting seasons, respectively. All stored manure is applied on fields without explicitly simulating a vegetation cover in the Manure Application Submodule. The manure application rates are determined by the stored manure mass at the beginning of planting, and the N application rates are calculated accordingly from the amount of N remaining in the stored manure that is ready for land application.

The AMCLIM simulations for synthetic fertilizer application incorporate crop calendar and N application rates. Synthetic fertilizers are assumed to be solely applied on croplands for crop growing in the Synthetic Fertilizer Application Submodule. Applied nitrogen in synthetic fertilizers is split into three main types, urea N, ammonium N and nitrate N. Nitrate application contributes to a negligible amount of NH_3 emission so is not specifically simulated in AMCLIM. Urea N and ammonium N are applied by three techniques (as introduced in Section 2.2.3). It is assumed that there is no use of a mixture of multiple types of fertilizers or techniques. All three techniques used for application are simulated independently on the global scale, and the geographic distribution of techniques is determined for all the countries based on national income level (see Appendix B3). The total NH_3 emission from synthetic fertilizers use is a weighted sum of the compound emissions simulated by using each technique. Details are presented in Chapter 3. The application of urea causes a temporary increase in soil pH because the hydrolysis of urea consumes hydrogen ions in the soil. Therefore, the AMCLIM model uses an empirical relationship to represent the soil pH dynamic and does not explicitly simulate this

complicated process. The same empirical formula is also applied in the grazing simulations (see Section 5.2.2).

Chapter 3
Ammonia emissions from synthetic fertilizer applications

3.1 Introduction

The invention of synthetic fertilizer revolutionized agriculture by significantly increasing crop yields with additional nitrogen input. Since the development of the famous Haber-Bosch process, it is estimated that about half of the global population has been supported by this innovation (Erisman et al., 2008). However, while synthetic fertilizers have brought immense benefits to humanity, the use of synthetic fertilizers also causes significant environmental impacts. A large portion of applied N is lost to the environment instead of being absorbed by the crops, through processes such as runoff, leaching, and in particular, volatilization of NH_3 to the air. These processes greatly disturb the N cycle and cause a wide range of environmental problems.

Fertilizer use is a major source of agricultural NH_3 emissions. Since the mid-20^{th} century, the exponential increase in synthetic fertilizer use has led to a drastic rise in NH_3 emissions (Lu and Tian, 2017; Xu et al., 2019b). Improving our understanding of the NH_3 emissions from synthetic fertilizers is critical not only for evaluating their environmental impacts and

resource distributions, but also for developing effective mitigation measures, especially in the face of a changing climate and growing population. Although studies have been conducted to quantify NH_3 emissions from synthetic fertilizers, most of these estimates rely on emission factors (EFs) that are not climate-dependent or only take climate effects into account to a limited extent.

In this chapter, the LAND Module of AMCLIM (AMCLIM–Land) is described, which can dynamically simulate NH_3 emissions based on local management whilst also considering the impacts of environmental factors on NH_3 volatilization. The chapter presents applications of AMCLIM–Land for simulating fertilizer related NH_3 emissions and evaluations against measurement at the site scale and its global applications, as well as the results and implications. The extension of the model to address NH_3 emissions from manure is described in Chapters 4 and 5.

3.2 Methods and Materials

AMCLIM–Land simulates N flows following the applications of various types of nitrogen fertilizers (this chapter focuses on synthetic fertilizer), with an emphasis on the NH_3 volatilization to the air. It simulates key processes related to fertilizer applications, taking into account management practices specific to fertilizer applications. This section provides a detailed description of the simulated processes in AMCLIM–Land and highlights the representation of critical management practices. Applications of AMCLIM–Land at site and global scale are also introduced.

3.2.1 Simulated processes and soil layers in AMCLIM–Land

AMCLIM–Land simulates NH_3 volatilization at the land surface and the soil processes involved in the evolution of N species. AMCLIM–Land models the physical, chemical and biological processes associated with fertilizer applications, including NH_3 volatilization to the atmosphere, surface runoff, nitrogen diffusion and leaching into deep soil, nitrification, hydrolysis of urea and plant N uptake, as illustrated in Figure 2.2.

To simulate these processes, AMCLIM–Land defines four soil layers with a total depth of 28 cm, each with a specific thickness of 2 cm, 5 cm, 7 cm and 14 cm, respectively (Fig 3.1a). The upper two layers (0–2 cm, 2–7 cm) correspond to the first soil layer defined by ERA5 reanalysis data, while the lower two layers (7–14 cm, 14–28 cm) correspond to the second soil layer in ERA5 (Hersbach et al., 2020). By integrating these soil layers into its model, AMCLIM–Land can simulate the soil processes related to fertilizer applications at various depths.

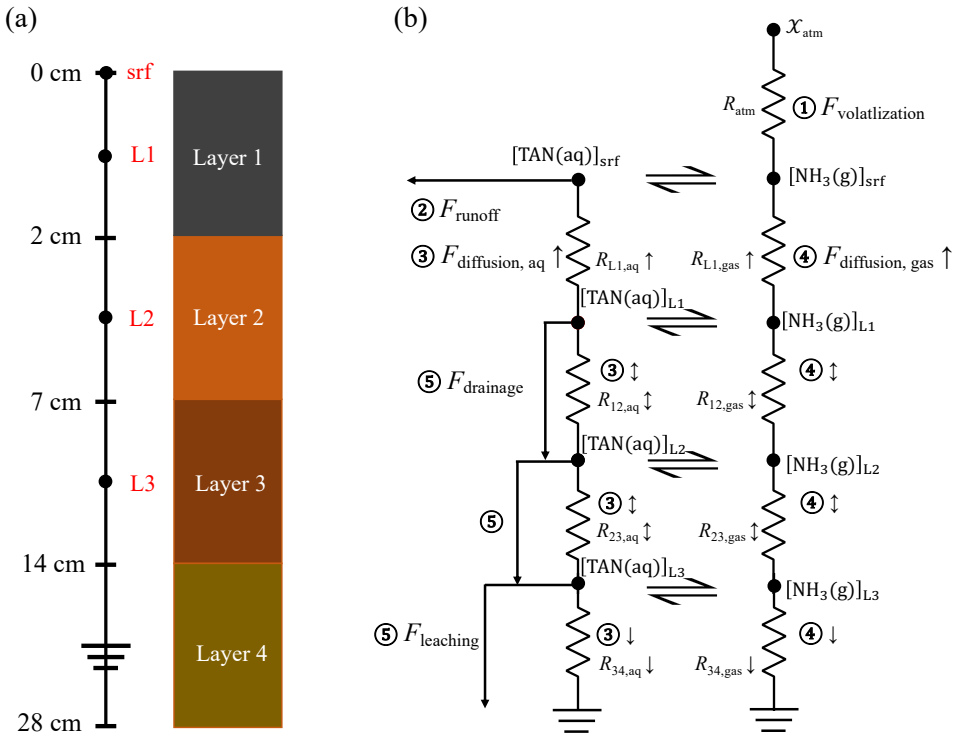

Figure 3.1. Sketch of vertical soil layers and physical transport scheme for N species (showing TAN as an example) in AMCLIM–Land (a) Four soil layers in the soil column from the surface (0 cm) to a depth of 28 cm. (Not scaled); (b) Physical transport of N species in soils and atmosphere. Processes include 1) NH_3 volatilization, 2) surface runoff, 3) aqueous diffusion, 4) gaseous diffusion and 5) drainage/leaching. The concentrations of aqueous TAN and gaseous NH_3 are the mean concentrations of each soil layer, represented by black dots. Soil resistances are shown between two black dots, with the numbering representing the soil layers, i.e., R_{12} is the soil resistance for diffusion from soil layer 1 to layer 2. Arrows represent the direction of diffusion which can be upwards, downwards or bi-directional. Transport distances for diffusion are the distance between the midpoints of two adjacent soil layers, e.g., 3.5 cm from soil layer 1 to layer 2, and 6 cm from soil layer 2 to layer 3. The

concentrations of N species in the bottom soil layer are assumed to be 0, and downward fluxes take place from the above layer 3 to this layer.

3.2.1.1 Calculation of soil TAN pool and partition

In AMCLIM, the most critical N species that is simulated is TAN, which is the core N pool that governs NH_3 emission. In managed arable lands, the primary sources of the TAN pool are the application of N fertilizers, where ammonium acts as a direct source, while urea is an input of TAN via hydrolysis. The TAN pool in soils can be depleted through multiple processes, such as NH_3 volatilization, diffusion and nitrification etc., as introduced previously. The time-dependent TAN pool (M_{TAN}; given in per unit area; all masses have units of g m^{-2} if not specifically explained) is determined by the following equation, which includes the inputs and the depleting processes:

$$\frac{\mathrm{d}M_{\mathrm{TAN}}}{\mathrm{d}t} = I_{\mathrm{TAN}} + F_{\mathrm{TAN}} - F_{\mathrm{NH_3}} - F_{\mathrm{TAN\,runoff}} - F_{\mathrm{diffusion}} - F_{\mathrm{leaching}} - F_{\mathrm{nitrif}} - F_{\mathrm{uptake}} \quad , \tag{3.1}$$

where I_{TAN} (g N m^{-2} s^{-1}) represents direct input of TAN species, such as ammonium or ammonia, and F_{TAN} is the TAN production, i.e., through urea hydrolysis for synthetic fertilizer application (together with other processes are presented in Appendix A1). The remaining fluxes are removal processes explained in Section 2.3 ($F_{\mathrm{NH_3}}$ – flux of NH_3 volatilization; $F_{\mathrm{TAN\,runoff}}$ – flux of surface TAN runoff; $F_{\mathrm{diffusion}}$ – diffusive fluxes; F_{leaching} – flux of leaching; F_{nitrif} – nitrification; F_{uptake} – flux of N uptake by plants/crops; all N fluxes/flows have units of g N m^{-2} s^{-1} if not specifically explained).

It should be noted that each soil layer may have different modelled processes. Equation 3.1 provides a general expression for the TAN budget of the entire soil column. Nitrogen losses through volatilization and runoff occur at the land surface in the top soil layer. These losses are not included in deeper soil layers, where volatilization and surface runoff are absent. Furthermore, it is assumed that there is no N uptake in the top soil layer. In addition, diffusive and drainage fluxes considered as losses in the soil layer above become sources of nitrogen for the layer underneath. Fluxes are modified accordingly in each simulated soil layer, and detailed equations are presented in Appendix A2.

Equation 3.2 describes the partitioning of the soil TAN pool into three phases: gaseous NH_3 that exists in the air-filled porous space of soil, aqueous TAN dissolved in the soil water, and solid exchangeable TAN adsorbed onto solid particles (Riedo et al., 2002; Vira et al., 2020b):

$$M_{\mathrm{TAN}} = z\,((\varepsilon - \theta)[\mathrm{NH_3(g)}] + \theta[\mathrm{TAN(aq)}] + (1-\varepsilon)[\mathrm{TAN(s)}]), \qquad (3.2)$$

where θ is the soil volumetric water content ($m^3\ m^{-3}$ or $m\ m^{-1}$) and ε is the porosity of soil (or the soil volumetric water content at saturation). The thickness of the soil layer is represented by z (m). Gaseous NH_3 is in equilibrium with aqueous TAN. The gaseous concentration of NH_3 ($[NH_3(g)]$) can be expressed as follows:

$$[\mathrm{NH_3(g)}] = K_{\mathrm{NH_3}} \cdot [\mathrm{TAN(aq)}], \qquad (3.3)$$

where $K_{\mathrm{NH_3}}$ is a combined coefficient of Henry and dissociation equilibria as shown in Equations 2.4 and 2.5. Similarly, the concentration of solid exchangeable TAN can be expressed by the following equation:

$$[\mathrm{TAN(s)}] = K_\mathrm{d} \cdot [\mathrm{TAN(aq)}], \tag{3.4}$$

where K_d ($\mathrm{m^3\ m^{-3}}$) is the partition coefficient that represents soil adsorbed of TAN, which is dependent on soil properties (see Appendix A3). By combining Equations 3.2 – 3.4, the concentration of aqueous TAN is given by:

$$[\mathrm{TAN(aq)}] = \frac{M_\mathrm{TAN}}{z(\theta + K_{\mathrm{NH_3}}(\varepsilon - \theta) + K_\mathrm{d}(1-\varepsilon))}. \tag{3.5}$$

AMCLIM–Land also simulates other N species, including urea and nitrate, which have their own equations and processes that are detailed in Appendix A2.

3.2.1.2 Chemical transformations and biological processes of nitrogen in soils

Nitrogen in soils occurs in several forms which are controlled by a range of chemical and biological processes. Nitrification and plant N uptake are crucial processes in AMCLIM–Land for simulating N dynamics in soils. Nitrification is the process by which NH_4^+ is converted to NO_3^-, which leads to depletion of the soil TAN pool. Nitrification is dependent on the abundance of NH_4^+ (as shown in Equation 2.8), and its rate is influenced by various environmental factors, such as temperature, oxygen availability and substrate pH (Parton et al., 1996b, 2001b; Malhi and McGill, 1982; Bateman and Baggs, 2005; Gilmour, 1984; Norton and Stark, 2011). In AMCLIM–Land, the nitrification rate is calculated by scaling the optimum nitrification rate ($K_\mathrm{nitrif,opt}$) by normalising factors that depend on temperature ($k_\mathrm{nitrif,T}$), water-filled pore space ($k_\mathrm{nitrif,WFPS}$) and pH ($k_\mathrm{nitrif,pH}$) as follows:

$$K_\mathrm{nitrif} = K_\mathrm{nitrif,opt}\, k_\mathrm{nitrif,T}\, k_\mathrm{nitrif,WFPS}\, k_\mathrm{nitrif,pH}. \tag{3.6}$$

The optimum nitrification rate and the representation of each dependence is presented in Appendix A4.

The uptake of N by crops is a key biological process in AMCLIM–Land and is a critical indicator for evaluating the fertilizer N use efficiency. However, simulating plant N uptake is complex and can be challenging; AMCLIM–Land uses a root uptake scheme derived from several studies (Riedo et al., 1998; Thornley, 1991; Thornley and Cannell, 1992a; Thornley and Verberne, 1989). The scheme uses an integrated root activity parameter for N uptake (α_{root}, g N m^{-2} s^{-1}), the combined response factor for substrate C and N level ($J_{C,N}$), the effective available N pool for the plant, including NH_4^+ and NO_3^- (M_{Neff}, g N m^{-2}), and the correction constant for root activity (K_{Neff}, g N m^{-2}), which is expressed by the following equation:

$$F_{\mathrm{uptake}} = \frac{\alpha_{\mathrm{root}}}{J_{C,N}} \frac{M_{\mathrm{Neff}}}{M_{\mathrm{Neff}} + K_{\mathrm{Neff}}}, \tag{3.7}$$

The uptake of N by crops in AMCLIM–Land is mainly affected by temperature, and it is assumed to take place in soil layers beneath the top soil layer (as explained in Section 3.2.1.1). The growth of crops is represented by a set of empirical parameters reflecting the maturing state of roots. The C and N dynamics of crop growth are not modelled; constant values suggested by literature are used in this study as the model focuses on the NH_3 emission process. Details are presented in Appendix A5.

3.2.1.3 Physical transport of nitrogen in soils

The physical transport scheme of TAN and other N compounds (e.g., nitrate), is shown in Figure 3.1b. General descriptions of these transport processes have been presented in Section 2.3.4. The volatilization of NH_3 from the land surface to the atmosphere is driven by the concentration difference at two heights and is constrained by the atmospheric resistances, which is calculated as:

$$F_{\mathrm{NH_3}} = \frac{[\mathrm{NH_3(g)}]_{\mathrm{srf}} - \chi_{\mathrm{atm}}}{R_{\mathrm{a}} + R_{\mathrm{b}}}, \tag{3.8}$$

where $[\mathrm{NH_3(g)}]_{\mathrm{srf}}$ and χ_{atm} are NH_3 concentrations at the surface and atmospheric NH_3 concentration at a reference height consistent with atmospheric resistances (typically 2 m). R_a and R_b are aerodynamic and boundary layer resistance, respectively (see Appendix A6). AMCLIM–Land simulates NH_3 volatilization as a uni-directional process, i.e., NH_3 flux is an emission only, and deposition is not simulated. There is no interaction with surface vegetation as explained in Section 2.3.2 so that there is no surface resistance in Equation 3.8.

Diffusion processes in soils are similar to volatilization and are also driven by concentration gradients. AMCLIM simulates diffusion in both the aqueous and gaseous phases. Each phase is limited by soil resistances, which are functions of transport distance, molecular diffusivities and soil tortuosity factors (Móring et al., 2016; Vira et al., 2020a). Detailed calculations are given in Appendix A7. Diffusion is treated as a bi-directional process between soil layers 1 to 3, while diffusion is assumed to take place downward only from soil layer 3 to the bottom soil layer and upward only from soil layer 1 to the soil surface

(Fig 3.1b). It is worth noting that the surface concentrations used to calculate fluxes from the surface are solved variables by assuming an equilibrium state. Upward diffusion from the first soil layer to the surface ($F_{\text{diffusion to surface}}$) is equal to the sum of NH_3 emission and runoff from the land surface to satisfy mass conservation (details given in Appendix A8), as follows:

$$F_{\text{diffusion to surface}} = F_{\text{NH}_3} + F_{\text{N runoff}}. \quad (3.9)$$

The transport of N by movement of water includes leaching and runoff (Equation 2.10 and 2.11). Leaching of NO_3^- occurs more frequently because NO_3^- is highly mobile in soils compared with NH_4^+, while NH_4^+ is absorbed on the soil cation exchange complex so is less mobile (Butterbach-Bahl et al., 2011b). Annual NH_4^+ leaching is usually less than 5 % of the total dissolved N in soil but may have larger contributions in soils with heavy NH_4^+ loads (Dise et al., 2009; de Vries et al., 2007). Nitrogen flows out from the simulated soil column is termed as "leaching", while N fluxes that are transport between soil layers by water movement are termed as "drainage", as shown in Figure 3.1b. The percolation flux of water (q_p, in Equation 2.10) is the minimum between soil hydraulic conductivity (K_s, m s^{-1}) and water drainage potential of a soil layer (D_{pot}, m s^{-1}), as expressed by the following equation:

$$q_p = \min(K_s, D_{pot}). \quad (3.10)$$

The soil hydraulic conductivity is related to the soil textures and soil water content. The water drainage potential is defined as the excess amount of water beyond soil field capacity draining out from the soil layer. The calculation of q_p is given in Appendix A9. In contrast,

the surface runoff flux of water (q_r, in Equation 2.11) is not explicitly modelled in AMCLIM–Land but is taken from the reanalysis meteorological dataset as described in Section 2.4.1.

3.2.1.4 Soil pH scheme in AMCLIM–Land

Soil pH can greatly affect NH_3 emissions from fertilizer. Urea application is found to have strong impacts on soil pH as urea hydrolysis consumes hydrogen ions (H^+) ($CO(NH_2)_2 + 2H_2O + H^+ \xrightarrow{\text{urease}} 2NH_4^+ + HCO_3^-$). Experimental studies found that soil pH increased dramatically after urea application (including urine deposition), resulting in a peak in NH_3 emissions (Chantigny et al., 2004; Curtin et al., 2020; Cabrera et al., 1991; Móring et al., 2016). Móring et al (2016) developed a detailed chemistry scheme for soil pH dynamics in a urine patch and suggested that it is nevertheless suitable to use a fixed pH for larger scale modelling as it is extremely difficult to explicitly simulate soil pH change on a larger scale, e.g., global scale (Móring et al., 2017). AMCLIM–Land therefore uses an empirical relationship describing the soil pH after urea application. Soil pH is assumed to reach a peak value of 8.5 within 24 to 48 hours after application, and then gradually recovers back to the original values in the next 120 hours, as shown in Figure 3.2 (Chantigny et al., 2004; Móring et al., 2016). Due to limited experimental knowledge, for soils with higher pH than 8.5, pH values are assumed to remain unchanged in AMCLIM–Land. Meanwhile, soil pH also does not change for fertilizer applications other than urea, e.g., NH_4^+, for which a database of soil pH is used in AMCLIM–Land (see Section 3.2.3.2)

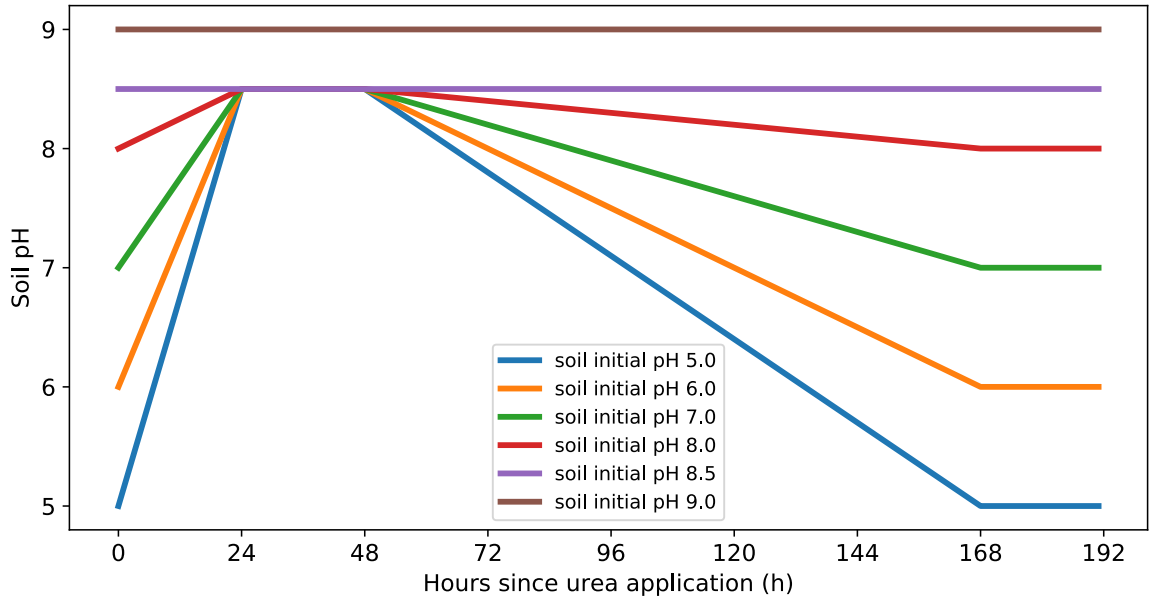

Figure 3.2. Soil pH scheme used in AMCLIM–Land. Changes of soil pH for 192 hours (8 d) after urea application for soils with initial pH of six different values.

3.2.2 Representations of human management in AMCLIM–Land

Local agronomic practices can significantly impact the environment and the distribution of resources. Therefore, it is crucial to ensure that numerical models adequately represent human management in agricultural systems. However, given the vast diversity of management and practices across the globe, simplifications are often necessary. AMCLIM–Land addresses this challenge by focusing on some of key activities in crop farming: the timing and techniques of fertilizer applications, as well as irrigation.

3.2.2.1 Fertilizer application timing and techniques

Nitrogen fertilizers are applied on cropland within a specific time period of the year depending on the climatic conditions, crop types and other environmental factors. AMCLIM–Land incorporates a static crop calendar dataset which specifies the planting and harvesting seasons for major crops in both rain-fed and irrigated croplands (Jägermeyr et al., 2021). AMCLIM assumes a simple scheme for synthetic fertilizer application, where half the fertilizer is applied at the beginning of the planting season and the other half in the middle of the growing period, i.e., midway between the dates of planting start and harvesting start.

AMCLIM–Land includes three techniques for fertilizer application: broadcasting, incorporation and deep placement (as introduced in Section 2.2.3). Different techniques refer to different locations where fertilizer N is applied, which can be reflected in AMCLIM–Land by distributing N input to the corresponding soil layer(s). "**Broadcasting**" is the easiest method and involves spreading fertilizers broadly at the land surface, with N input added only to the first soil layer. "**Incorporation**" requires additional work to mix fertilizer deeper into the soil, and AMCLIM–Land assumes that applied N is well-mixed in the top two soil layers as a representation of immediate incorporation after fertilizer application. "**Deep placement**" is a less commonly used technique that involves burying fertilizer under the soil surface to mitigate nutrient loss to the air, and the model reflects this by adding N input to the third soil layer in simulations. By including this range of application techniques, the AMCLIM model can simulate NH_3 emissions under different management that more closely reflect real-world situations and allows testing of potential

mitigation measures. AMCLIM–Land does not simulate the impacts of fertilizer application on changing soil characteristics.

3.2.2.2 Irrigation events

Water availability is a crucial factor that influences crop performance and determines local agricultural practices. In areas with adequate rainfall, natural precipitation is sufficient for crop growth, while in arid or semi-arid regions, additional water inputs are necessary for crop production. AMCLIM–Land classifies croplands into two categories: rain–fed and irrigated. For rain–fed croplands, it is assumed that there are no irrigation events, so soil moisture is represented using reanalysis soil moisture data and the percolation flux (in Equations 2.10 and 3.10) is represented by reanalysis subsurface runoff data. For irrigated croplands, irrigation is assumed to occur after fertilizer application and when necessary. Consequently, the soil moisture of irrigated croplands needs to be re-estimated, as expressed by the following equation:

$$\theta_{\mathrm{irr,t}} = \theta_{\mathrm{rea,t}} + \Delta\theta, \tag{3.11}$$

where $\theta_{\mathrm{irr,t}}$ and $\theta_{\mathrm{rea,t}}$ represent the soil water content of irrigated croplands and the reanalysis soil water content data at time t, respectively. The reanalysis soil moisture data provide a reference value for "unperturbed" conditions, i.e., no irrigation. The term $\Delta\theta$ represents an incremental change in soil moisture due to various to processes and activities, including irrigation (w_{irr}, m), percolation flux of water (q_{p}, m s^{-1}) and water uptake by crops (W_{uptake}, m s^{-1}):

$$\Delta\theta = \frac{w_{\mathrm{irr}} - (q_{\mathrm{p}} + W_{\mathrm{uptake}})\Delta t}{z}, \tag{3.12}$$

where Δt is the model time step. The amount of water applied during a single irrigation event equals the soil water content when the top two soil layers reach field capacity (θ_{fc}). The water uptake by crops is described in Appendix A5. As mentioned, irrigation also takes place when necessary. Water is applied when the soil is too dry for crop growth. The threshold for initiating irrigation is when soil water content falls below the soil wilting point (θ_{wp}), as expressed by the following equation:

$$w_{\mathrm{irr}} = \begin{cases} \theta_{\mathrm{fc}} \sum_{i=1}^{2} z_{\mathrm{i}}, & \text{if } \theta_{\mathrm{irr,t}} \leq \theta_{\mathrm{wp}} \\ 0, & \text{if } \theta_{\mathrm{irr,t}} > \theta_{\mathrm{wp}} \end{cases}. \tag{3.13}$$

Irrigation is considered to have impacts on NH_3 emissions by influencing the leaching and altering the soil moisture. There are other processes affecting soil moisture such as evapotranspiration, which are considered to be implicitly included in the reanalysis data. It is worth noting that Equation 3.11 is a simplified approximation for the soil moisture of irrigated croplands, and water uptake by plants is only simulated under this condition. A systematic simulation of soil moisture based on the underlying physics is beyond the scope of this study and is not considered in AMCLIM–Land.

3.2.3 Modelling NH_3 emissions from fertilizer application at site and global scale

3.2.3.1 Application of AMCLIM–Land at site scale

AMCLIM–Land was applied at site scale to simulate NH_3 emissions from a fertilized grassland. To evaluate the model, modelled emissions were compared with measurements from the GRAMINAE (GRassland AMmonia INteractions Across Europe) experiment on NH_3 biosphere-atmosphere exchange conducted over intensively managed grassland in Braunschweig (52º 18´N, 10º 26´E), Germany (Sutton et al., 2009a; Sutton et al., 2009b). The GRAMINAE project measured NH_3 fluxes from managed grassland at three different stages: prior to cutting, post-cutting, and after fertilization using a combination of aerodynamic gradient method (AGM) and relaxed eddy accumulation (REA). AMCLIM–Land was applied to simulate the NH_3 emissions during the third stage, in which ammonium nitrate fertilizer was broadcast onto the grassland at a rate of 100 kg N per hectare on 5 June 2000. The N input to AMCLIM–Land was then set to be 5 g ammonium N per meter square which is equivalent to 50 kg NH_4^+–N per hectare for the simulation (because nitrate is assumed not to contribute to NH_3 emissions in the model). AMCLIM–Land was driven by meteorological variables such as air temperature, relative humidity, wind speed, precipitation and ground temperature. Soil properties and characteristics, including soil moisture, soil pH and soil textures, were also used as model input, all measured at the site by the GRAMINAE project. Measured atmospheric NH_3 concentrations interpolated to a reference height of 1 m were used to determine the emissions, with atmospheric resistances calculated from the meteorology. AMCLIM–Land was operated with a 15-min time step to

match the frequency of meteorological inputs and the integrated NH_3 fluxes measured by AGM. The GRAMINAE project provided the necessary level of detail for running AMCLIM–Land to simulate NH_3 emissions from fertilizer application, and additional information can be found in Sutton et al. (2009). No irrigation event occurred after fertilizer application, so AMCLIM–Land used measured soil moisture data documented by the GRAMINAE dataset.

3.2.3.2 Global application of AMCLIM–Land: input and model set up

AMCLIM–Land was also applied at the global scale to quantify NH_3 emissions from global synthetic fertilizer application. There were three major types of inputs: nitrogen application information, crop calendars and meteorological variables, as illustrated in Figure 2.1. Nitrogen application data were obtained from the GGCMI3 dataset for 16 major crops, including synthetic fertilizer N application rates and total synthetic fertilizer N applied to crops (Mueller et al., 2012; Hurtt et al., 2020). The GGCMI3 datasets reported data for years from 1850 to 2015. Data for years after 2015 were then extended by a linear interpolation. Data for the year 2010 and 2018 were used in this Chapter, and a timeseries for global fertilizer use of the 21st century is given by Figure C6 in Appendix C3. The crops simulated are listed in Appendix B1. The areas of croplands that use synthetic fertilizers were derived from GGCMI3, which have incorporated the harvested area from the Farming the Planet 2 (FTP2) dataset (Monfreda et al., 2008).

Nitrogen fertilizers include several types, such as urea, ammonium nitrate and ammonium phosphate etc. AMCLIM–Land considers three groups of applied N: ammonium N, urea N and nitrate N. Ammonium N directly enters the soil TAN pool and has little immediate

impact on the soil pH, while urea hydrolysis results in a temporary rise of soil pH after application. In contrast, nitrate use causes little NH_3 emission compared to ammonium and urea. AMCLIM–Land combines the GGCMI3 nitrogen application data with country-level synthetic fertilizer consumption statistical data provided by the International Fertilizer Association (IFA, 2021) to split the application rates into fractions of the three groups of applied N (see Appendix B2). The area of cropland that uses a specific type of fertilizer is proportional to the fraction of the fertilizer used.

The crop calendars used in AMCLIM–Land were also obtained from the GGCMI3 dataset, which distinguish the planting and harvesting seasons of crops in rain-fed and irrigated systems. These calendars were used to determine the timing of fertilizer application, and each crop has a specific calendar that varies geographically. It should be noted that these crop calendars are static modelling results based on climatology and therefore do not vary with years.

The meteorological inputs for AMCLIM were from the ERA5 reanalysis meteorology as introduced in Section 2.4.1 and include air temperature, relative humidity (derived from dew point temperature), wind speed, rainfall, soil temperature and water content at 2 levels (0–7 cm, 7–28 cm) and runoff fluxes. Soil data inputs such as soil pH, soil texture (sand, clay and silt fraction) and soil organic matter content were obtained from the Regridded Harmonized World Soil Database (HWSD) v1.2 (FAO and IIASA, 2012; Wieder et al., 2014). The GRIPC dataset was used to classify cropland into rain–fed and irrigated systems and to determine the irrigation events and corresponding crop calendars.

AMCLIM–Land uses a longitude-latitude grid at a resolution of 0.5° × 0.5°, with an hourly time step. All model inputs were regridded to the model resolution if necessary. AMCLIM–Land was set up to use a one-year spin-up in order to keep an annual cycle of simulation period for each grid (as fertilization that takes place in November or December may result in NH_3 emissions in the following year), and was run for three rounds in which three application techniques were simulated independently and were assumed not to interact with each other. Each round was comprised of 32 full-year simulations, with urea and ammonium N run separately for the 16 major crops. The total NH_3 emission from fertilizer application is calculated using the following equation:

$$F_{\mathrm{NH_3}} = \sum_{\mathrm{i=1}}^{3} f_{\mathrm{tech(i)}} \sum_{\mathrm{j=1}}^{2} f_{\mathrm{fert(j)}} \sum_{\mathrm{n=1}}^{16} F_{\mathrm{NH_3(i,j,n)}}, \tag{3.14}$$

where $F_{\mathrm{NH_3(i,j,n)}}$ is the component NH_3 emission from *n* crop with fertilizer type *j* by using application technique *i*, and $f_{\mathrm{tech(i)}}$ and $f_{\mathrm{fert(j)}}$ are the fraction of the application technique and fertilizer type used in a grid, respectively. The assumption in AMCLIM–Land is that the fraction of a specific fertilizer application technique used is related to the country income level, with higher income countries assumed to use more incorporation and deep placement compared with lower income countries. The income classification is provided by World Bank statistics (WB, 2022). The details are presented in Appendix B3.

3.3 Results

3.3.1 Site simulations for NH_3 emissions from synthetic fertilizer application

Figures 3.3 and 3.4 show the results of simulated NH_3 emissions over 10 days from the fertilized post-cutting grassland (the GRAMINAE campaign site), along with comparisons with measurements. Meteorological conditions are given in Figure 3.3, which shows that the ground temperature at the study site varied between 10 and 25 °C, with three particularly hot days on 9, 10 and 13 June. It is notable that ground temperature, relative humidity (RH) and friction velocity (which is dependent on wind speed and atmospheric stability) showed large diurnal variations. During the daytime, ground temperature and friction velocity were high while RH was low, with the opposite occurring at night time. Atmospheric resistances (including aerodynamic and boundary layer resistance) are inversely related to the friction velocity, of which values were small during the day and much larger at night. A few precipitation events occurred during the study period, with the largest rainfall occurring on 10 June (Fig 3.3c). Soil water content was measured every two days at two depths of 0.15 and 0.30 m. The grassland was watered prior to the fertilization on 15 to 17 May, and there was no irrigation between 5 to 15 June. Therefore, subsurface runoff fluxes retrieved from the ERA5 reanalysis data were used as the percolation fluxes to determine drainage and leaching, ranging from 0.60 to 0.75 mm d^{-1} in the simulated days. The shallower layer had lower soil water content than deeper soils, and moisture levels at both depths decreased from 12 % to 10 % in the 10 days following fertilizer application.

The extent to which rainfall affected soil water content was uncertain based on the available measurements.

Ammonium nitrate fertilizer was applied on the grassland by broadcasting at 5:00 – 6:00 am on 5 June, 2000. Emissions of NH_3 occurred immediately after the fertilization, with maximum values of over 3000 ng m^{-2} s^{-1} observed on the same day. The measured emissions then gradually decreased over the following days, but showed strong diurnal variability, peaking around the midday, when temperature and friction velocity were high, and declining to a minimum at night when these variables were low. By 7 June, the third day after fertilization, the highest emission was 1500 ng m^{-2} s^{-1}, which was only half of the peak value observed on the first day. The NH_3 emissions increased substantially on 8 June relative to the previous day (7 June) and declined again. From 12 June, the measured emissions were generally less than 500 ng m^{-2} s^{-1}, which was significantly lower compared with the first week.

Figure 3.3d demonstrates that the AMCLIM model is capable of capturing the predominant features of the measured NH_3 emissions throughout the simulated period and producing estimates for daily NH_3 emissions and sub-hourly fluctuations comparable to the measurements. However, there are some differences between modelled and measured NH_3 fluxes, particularly on the first day and during night time simulations. Simulated emissions are higher than measurements in the afternoon and evening of the first day and night time on 6, 7, 9 and 10 June. Meanwhile, the highest measured emissions on 8 June are over 2500 ng m^{-2} s^{-1}, but AMCLIM is unable to replicate these values and underestimates the peak emissions by about 40 %. It should be noted that particularly large standard errors (shown as shaded grey area) also exist in measured NH_3 fluxes during 8–10 June, which is mostly

due to instrument uncertainties when reading concentrations in these hot days (Sutton et al., 2009b). Overall, AMCLIM overestimates cumulative NH_3 emissions by 50 % from 5 June to 15 June (when there are available measurements). The modelled cumulative NH_3 is 0.49 g m^{-2} compared to 0.32±0.07 g m^{-2} by the measurements (Sutton et al., 2009b).

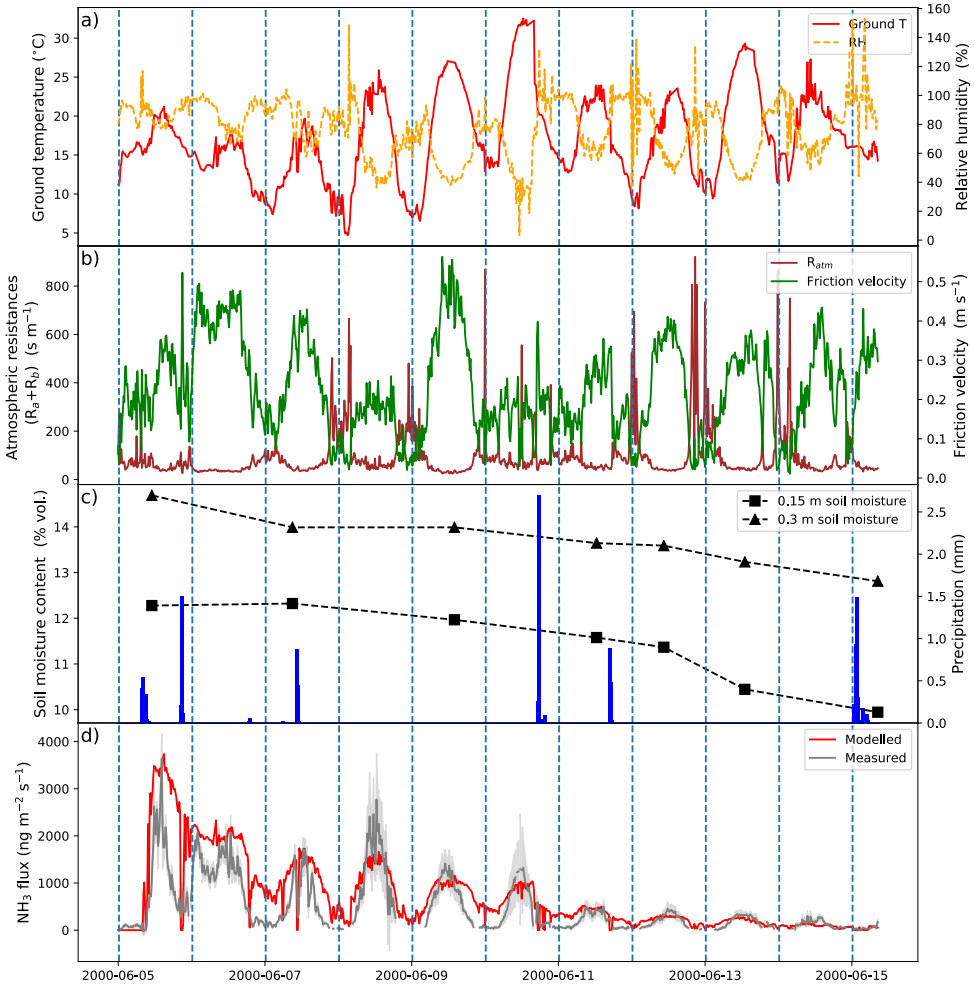

Figure 3.3. Meteorological variables measured by GRAMINAE and site simulations for NH_3 emissions from a post-cutting grassland after fertilization in Braunschweig, Germany, from 5 June 2000 to 15 June 2000 by AMCLIM–Land. (a) Surface temperature and relative humidity. (b) Atmospheric resistances and friction velocity. (c) Soil volumetric water content at 0.15 m and 0.30 m depth and precipitation. (d) Modelled and measured NH_3 emissions.

Figure 3.4 shows the modelled concentrations of N species (aqueous TAN and gaseous NH_3; in this paragraph, TAN refers to aqueous TAN only excluding solid exchangeable TAN) in soils, as well as soil resistances and the NH_3 emissions. The solved concentrations of surface NH_3 are found to be much higher than the atmospheric NH_3 concentration at 1 m. Surface NH_3 concentrations range between 100 and 150 μg m^{-3} on the first day, and between 50 to 100 μg m^{-3} for the rest of the week, while the atmospheric concentrations of NH_3 are mostly within the range between 0 to 25 μg m^{-3}. Two evident peaks in surface NH_3 concentrations that are larger than 200 μg m^{-3} on 10 June can be seen. In comparison to NH_3 concentrations, surface TAN concentration shows greater variation within a day, and its trends are opposite to the emissions, with higher values at night and lower values in the day. In the top soil layer (0–2 cm), TAN concentrations show a smooth declining curve from 1750 g m^{-3} to less than 250 g m^{-3} throughout the simulated period (Fig 3.4c), indicating depletion of the TAN pool due to N losses through multiple pathways, which together act as a 1^{st} order loss process. The NH_3 concentrations of this soil layer show large variations due to the diurnal cycle in the temperature.

Soil resistance that constrains aqueous diffusion are found to be much larger than the resistance for gaseous diffusion (Fig 3.4c). It is found that soil resistances are larger at night than day time due to low temperature, which slows down diffusion fluxes through the soil. Surface TAN concentrations are higher at night when atmospheric resistances and corresponding soil resistances are larger. When there are no runoff fluxes (i.e., no precipitation), upward soil diffusion fluxes are only balanced by the volatilization. As a solved variable by assuming an equilibrium state, surface TAN concentrations therefore tend to be high, leading to low concentration gradients. Meanwhile, since the resistances

are large, upwards diffusive fluxes become smaller, which limits the surface fluxes (i.e., volatilization).

An averaged value of measured soil pH of ~6.3 was used for the simulations (Fig 3.4d). As a result, the gamma value (($[NH_4^+]/[H^+]$) of the top soil layer derived from the TAN concentration is shown as a smooth decaying curve. The modelled gamma values of the top soil layer were between 50000 and 25000, which are the same order of magnitude as the estimated measured values (exact measured values of gamma are not available; crude values are estimated from Figure 3 in Personne et al. (2009); Sutton et al. (2009b) by vision) and are comparable with the simulated gamma of the litter layer by Personne et al. (2009). Surface runoff was directly represented by the precipitation, and the modelled NH_3 emissions show sharp declines immediately after rain (e.g., 5 June evening) because the surface runoff is a competing pathway to the volatilization, which together deplete the TAN pool of the soil (Fig 3.3). For the entire simulated period of 5 to 15 June, 10.4 % of the applied ammonium N is estimated to be lost due to NH_3 emissions to the air, 1.1 % is washed off by rainfall (runoff), 13.4 % is converted to NO_3^- through nitrification, and the remaining 75.1 % of N is retained in the soil.

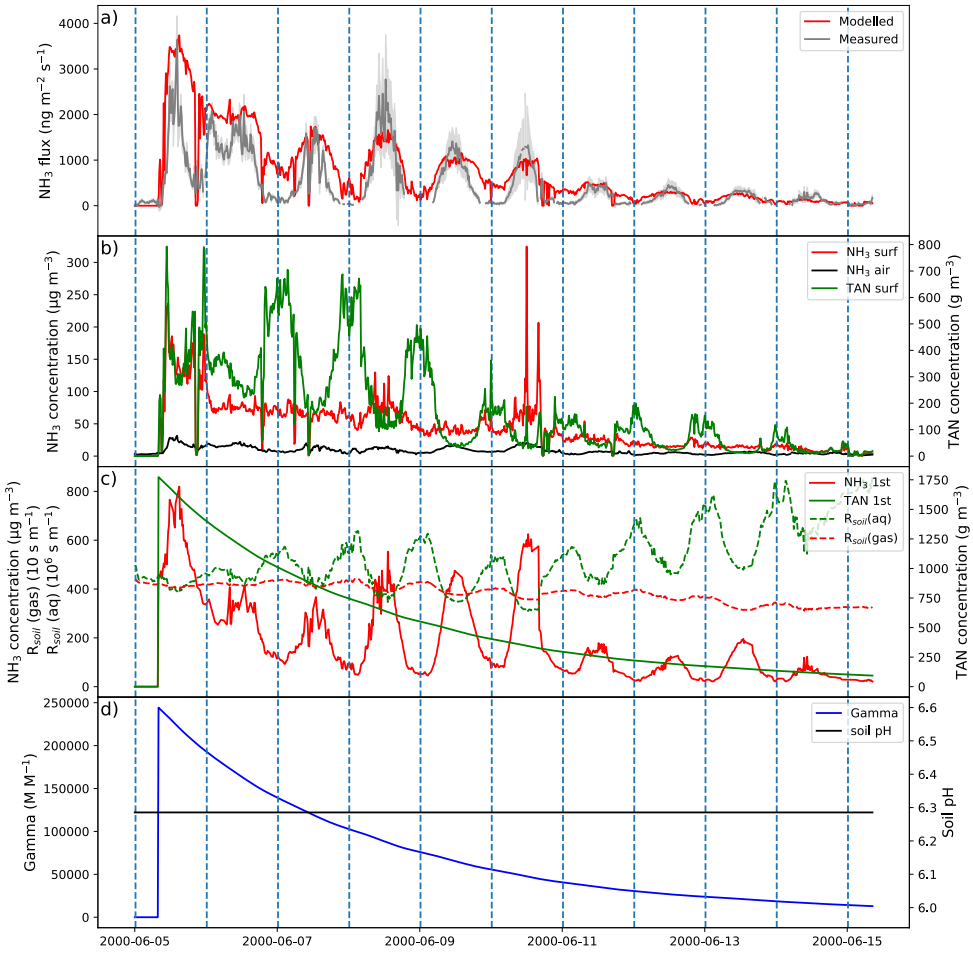

Figure 3.4. Modelled variables in the site simulations for NH_3 emissions from a post-cutting grassland after fertilization in Braunschweig, Germany, from 5 June 2000 to 15 June 2000 by AMCLIM–Land. (a) Modelled and measured NH_3 emissions. (b) Solved concentrations of TAN and NH_3 at the surface and the atmospheric concentration of NH_3. (c) Concentrations of TAN and NH_3 of the 1st (top) soil layer, and soil resistances for aqueous and gaseous diffusions. (d) Gamma value ($[NH_4^+]/[H^+]$) of the 1st (top) soil layer and soil pH used in AMCLIM–Land.

To evaluate the performance of the model against the measurements, AMCLIM–Land operated 12 runs with varying model parameters, variables and processes. In general, there were four groups of simulations, with correlation coefficients ("r" value) of each run and measurements, standard deviations normalized to measurements and normalized root mean square error (NRMSE) showing in Figure 3.5. The base run exhibits the "best" fitting as it is the closest point to the measurement. All runs show similar correlation coefficients, ranging between 0.7 to 0.85, which demonstrates the model's robustness as over 50 % of the variability in the measured NH_3 flux can be explained by the model. Varying the thickness of the top soil layer leads to the largest changes in standard deviation and the NRMSE (circles in Fig 3.5). Changing z1 to 1 cm results in much larger NRMSE than the base value of 2 cm, and also overestimates the variability of the measurement. In contrast, simulations using different atmospheric NH_3 concentrations at 1 m does not show significant changes in NRMSE (triangles in Fig 3.5), and the standard deviations of these simulations are close to those of the measurement. A range of tortuosity correction was tested (stars in Fig 3.5). Lowering tortuosity (no tortuosity and j=6) results in large increase in NRMSE compared with the base run using j of 8.5, with an overestimation of the variations of measured fluxes. By comparison, higher tortuosity (j=10) leads to comparable NRMSE but much smaller standard deviations. AMCLIM–Land was also run by switching off several N processes, including drainage flux to the soil layer underneath, surface runoff and nitrification ("P"s in Fig 3.5). Excluding the drainage of N in the model results in larger NRMSE than the base run, while excluding runoff or nitrification only leads to small changes.

Based on the comparison with the GRAMINAE measurements, AMCLIM–Land provided an overall reasonable estimate for the NH_3 emission from a fertilized field and generally captured the variations of NH_3 at a high temporal resolution. The Taylor plot shows that current model set up have produced the best fitting to the measurement compared with several model runs with varying parameters. Moreover, assuming a zero background NH_3 concentration for global simulations is justified as only limited impacts were found on the overall model performance. AMCLIM–Land was then applied at the global scale and the results are presented in the following sections.

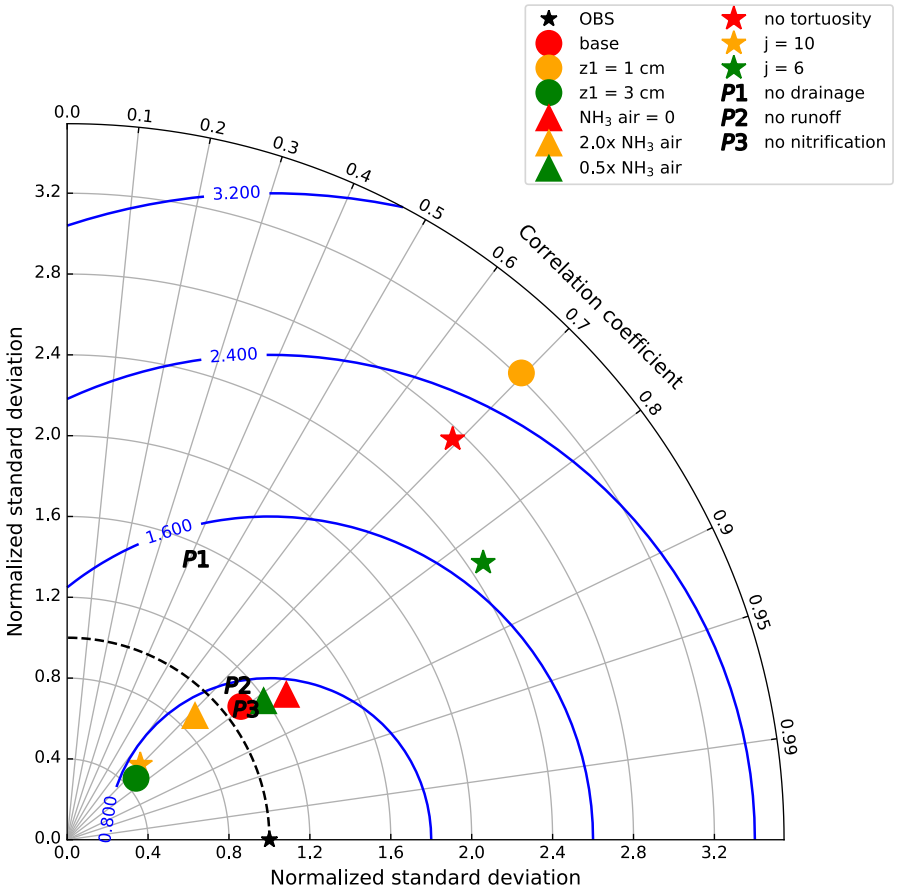

Figure 3.5. A Taylor plot of correlation of simulated and measured NH_3 emissions by GRAMINAE, and normalized standard deviation of the model and measurements for four groups of model runs. Circles: base run (red); top soil layer thickness z1 = 1 cm (orange); z1 = 3 cm (green). Triangles: atmospheric NH_3 concentration set to 0 (red); 2.0x measured NH_3 concentration (orange); 0.5x measured NH_3 concentration (green). Stars: no soil tortuosity correction for diffusion (red); tortuosity correction factor *j*=1.0 (orange); *j*=0.65 (green). P1–P3 represent simulations without drainage, surface runoff and nitrification, respectively. The blue contours represent the root mean square error normalized by measurements (NRMSE).

3.3.2 Global NH_3 emissions from synthetic fertilizer use

According to simulations using AMCLIM–Land, the global NH_3 emissions from synthetic fertilizer use are 15.0 Tg N yr^{-1} in 2010 and 16.8 Tg N yr^{-1} in 2018. The use of synthetic fertilizer increases from 102.3 Tg N yr^{-1} to 120.5 Tg N yr^{-1} during this period. The volatilization rates, which represent the percentage of applied N in ammonium and urea fertilizer that volatilizes as NH_3, are 17.2 % in 2010 and 16.7 % in 2018, respectively. Additional details about the use of three types of fertilizer are summarised in Table 3.1.

Table 3.1. Use of three types of synthetic fertilizers, corresponding NH_3 emissions and percentage of volatilization (P_V) simulated by AMCLIM–Land in 2010 and 2018. Data for synthetic fertilizer use are derived from GGCMI3 and IFA. [a]Nitrate fertilizer is assumed not to contribute to NH_3 emissions in AMCLIM–Land. [b]Percentage of volatilization when not including nitrate fertilizers. [c]Percentage of volatilization when including nitrate fertilizers.

Year		Ammonium	Urea	Nitrate[a]	Total
2010	Fertilizer use (Tg N yr^{-1})	31.9	55.2	15.1	102.3
	NH_3 emission (Tg N yr^{-1})	6.2	8.9	--	15.0
	P_v (%)	19.3	16.1	--	17.2[b] (14.6[c])
2018	Fertilizer use (Tg N yr^{-1})	39.8	61.3	19.5	120.5
	NH_3 emission (Tg N yr^{-1})	7.2	9.6	--	16.8
	P_v (%)	18.1	15.7	--	16.7[b] (13.9[c])

The geographical distributions of NH_3 emissions and the volatilization rates for 2010 and 2018 are shown in Figures 3.6 and 3.7. The spatial patterns are similar for both years, with the highest emissions occurring in some parts of South Asia (mainly India and Pakistan), the Northern China Plain (NCP) and northeastern China, and mid US and southern Canada.

Regions including Europe, the Middle East and South America also had high emissions in some countries such as France, Spain, Turkey, and Argentina.

For the volatilization rates (P_V), the highest rates are found in eastern Africa (e.g., Kenya, Ethiopia and Somalia), southern Africa (e.g., Namibia), part of East Asia (e.g., Mongolia and northern China), exceeding 50 %. High P_V values of over 36 % are also found in several regions in western US, the southern part of South America, the Sahel region, Ukraine, southwestern Russia and western Australia. It should be noted that regions with high volatilization rates do not always coincide with high emissions. Countries with high emissions often have moderate P_V rates. In particular, the NCP and northeastern China show P_V values of around 20 %, with high volatilization hot spots. The estimated volatilization rates of India are approximately 24 %, while some regions in the middle part of India and southern India show higher P_V values. In most parts of Europe, estimated P_V rates range from low to moderate (6 % to 18 %). However, both relatively high emissions and high volatilization rates are observed in mid US and Argentina.

Simulated NH_3 emissions from individual crops are shown in Figures C2 and C3. Among the 16 major crops, wheat, maize and rice are the top three emitter crops. The NH_3 emissions associated with wheat are the largest, with NH_3 increasing from 4.6 Tg N yr^{-1} 2010 to 5.3 Tg N yr^{-1} in 2018. Maize contributes to 2.9 and 3.2 Tg N yr^{-1} in 2010 and 2018, respectively, and emissions from rice increase from 2.4 Tg N yr^{-1} in 2010 to 2.5 Tg N yr^{-1} in 2018. For the other crops, emissions range from 41.9 (rye) to 843.4 (cotton) Gg N yr^{-1} in 2010, and from 45.4 (rye) to 1116.3 (cotton) Gg N yr^{-1} in 2018.

The total global NH_3 emissions from synthetic fertilizer use in 2018 are generally higher than 2010 as a result of increasing synthetic fertilizer, and most of crops have higher emissions in 2018 compared to 2010. Cotton and groundnut, in particular, have a 32 % increase in NH_3 emissions, which are the topmost increase over time among these crops. By comparison, rapeseed is the only crop of which emissions decreased, with around 3 % less NH_3 emitted in 2018 than in 2010.

In terms of volatilization rates (Fig.C4 and C5), sunflower has the highest estimated volatilization rates in 2010, with 28.5 % of applied N lost through NH_3 emissions. Sorghum (26.2 %) and millet (25.9 %) also have relatively high volatilization rates compared to other crops that had P_V values ranging from 10 % to 20 %. Cassava (10.6 %) and rye (9.6 %) have the smallest estimated volatilization rates in 2010, and rice has a smaller P_V of 11.3 % compared to maize (17.0 %) and wheat. In 2018, most crops have lower volatilization rates compared with 2010. In contrast, cotton, groundnuts and sorghum show slightly higher volatilization rate. Rye has the lowest P_V rates of 8.9 % in 2018, which is the only crop with P_V less than 10 % in both simulated years.

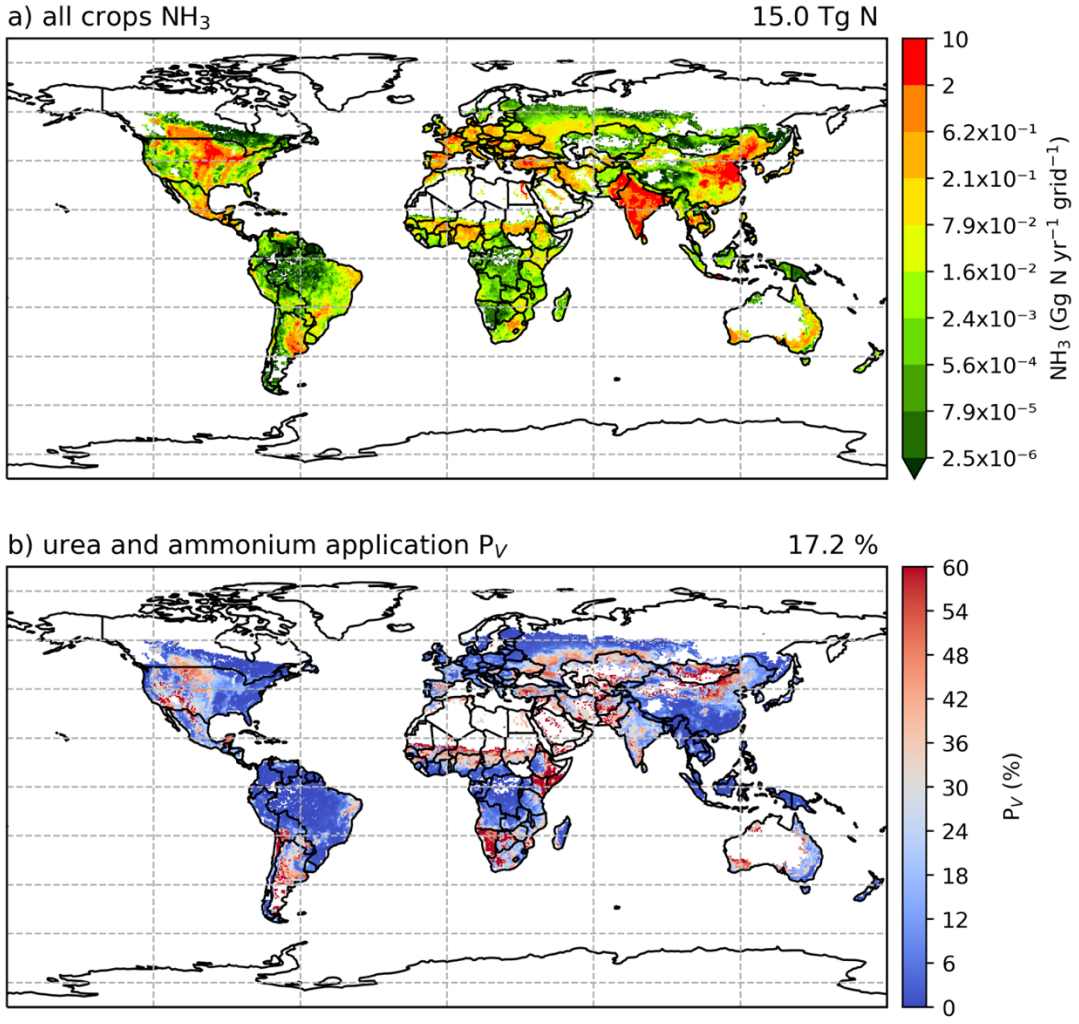

Figure 3.6. Simulated (a) annual global NH_3 emissions (Gg N yr^{-1} $grid^{-1}$) from synthetic fertilizer use in 2010. The colour bar represents 5th, 15th, 25th, 35th, 50th, 65th, 75th, 85th, 95th and 99th percentile of NH_3 emissions from synthetic fertilizer application in 2010. (b) Percentage of applied N in synthetic fertilizers (urea and ammonium fertilizers) that volatilizes (P_V) as NH_3 in 2010. The resolution is 0.5° × 0.5°. Maps of global fertilizer use in 2010 are shown in Figure B1.

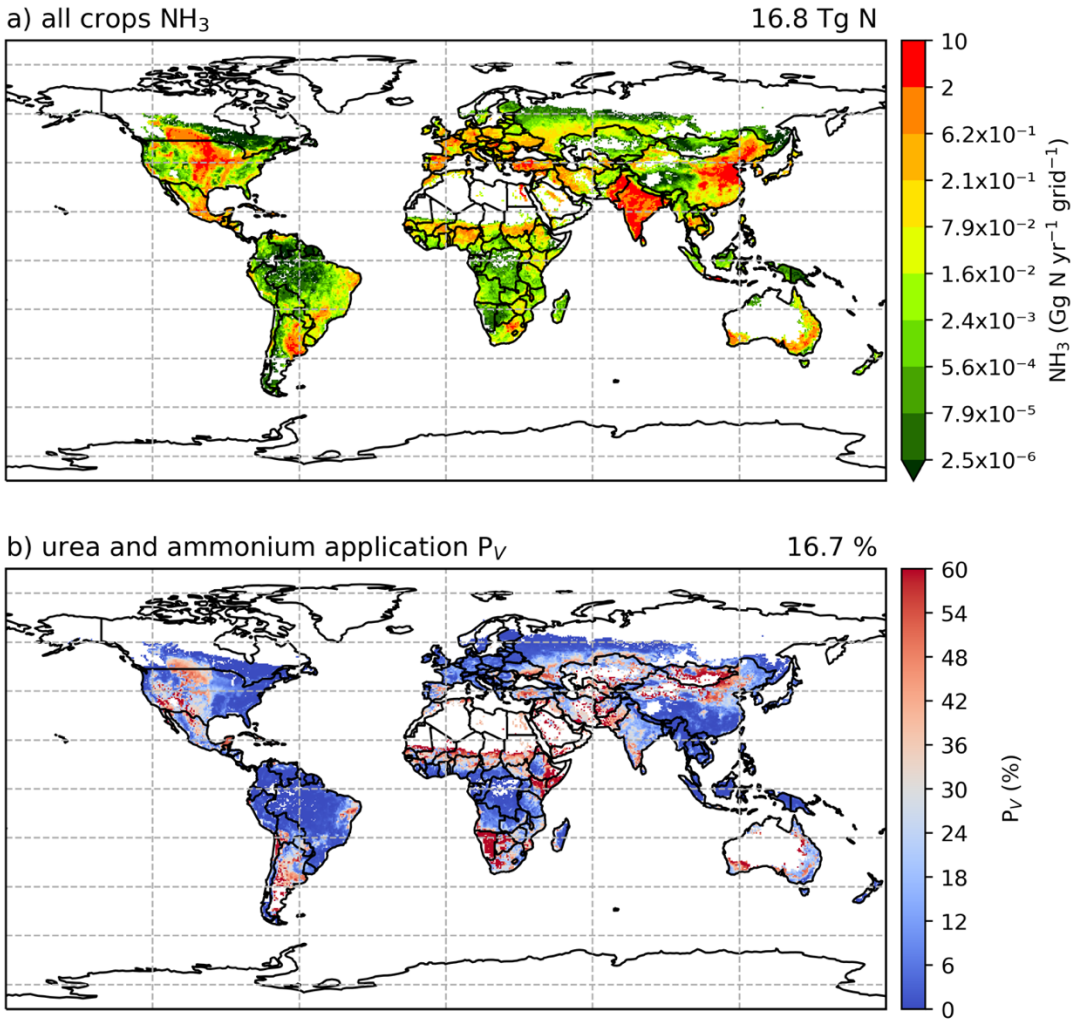

Figure 3.7. Same as Figure 3.6 but for 2018. Maps of global fertilizer use in 2018 are shown in Figure B2.

Figures 3.8 and 3.9 show the component NH_3 emissions from fertilization by different techniques for the two years. Broadcasting is responsible for more than 90 % of NH_3,

whereas incorporation and deep placement together contribute less than 10 % of the estimated global emissions. The geographical distributions of the volatilization rates for broadcasting are consistent with the global totals, given that broadcasting is the primary method used in fertilizer applications (Riddick et al., 2016). By comparison, incorporation and deep placement result in lower volatilization rates. Specifically, incorporation reduces simulated emissions by more than 50 % based on the P_V rates, while deep placement could potentially reduce emissions by almost 98 %, although this reduction needs to be further investigated as it may be an overestimation. Regions with high volatilization rates for broadcasting also have high rates even when fertilizers were assumed to be incorporated into the soils in the simulations, such as Argentina, northern China, Mongolia, Namibia and mid US (Fig 3.8b and Fig 3.8d; Fig 3.9b and Fig 3.9d).

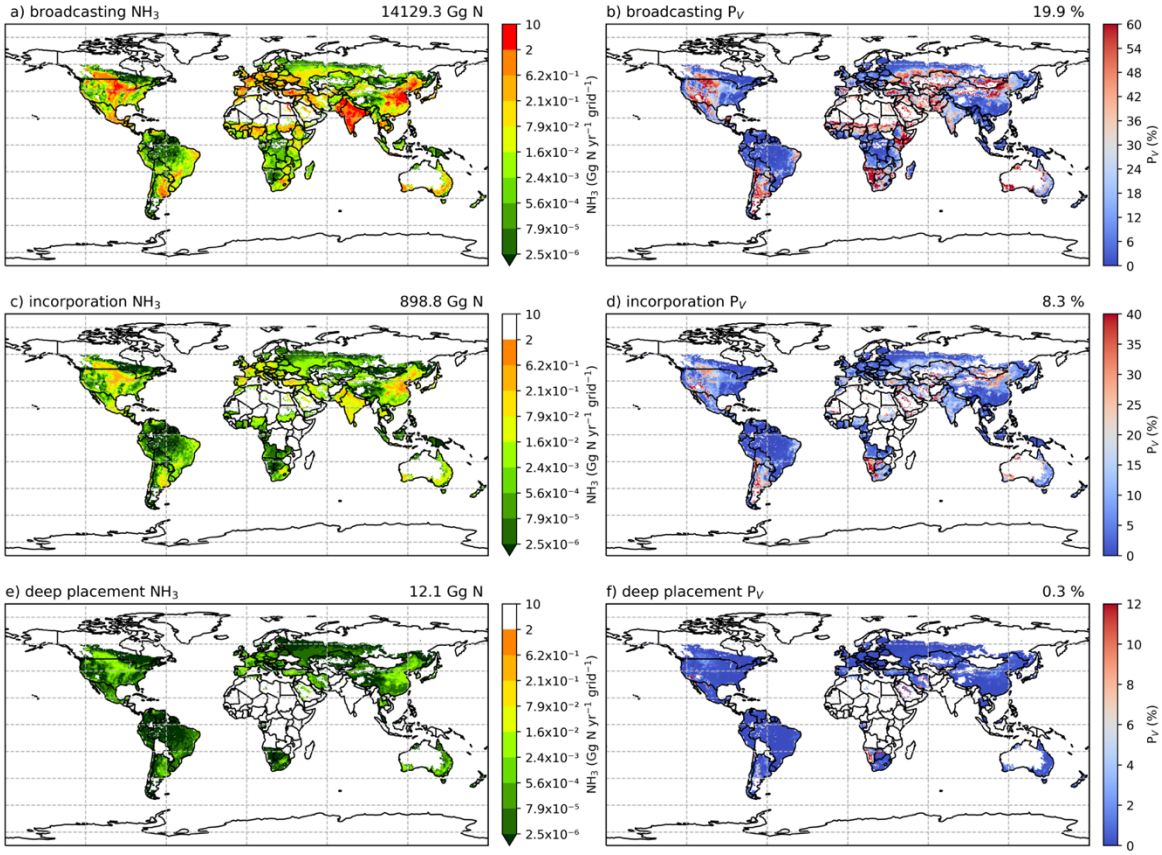

Figure 3.8. Simulated NH_3 emissions (Gg N yr^{-1}) from synthetic fertilizer application by three techniques and the corresponding volatilization rates (P_V) in 2010. NH_3 emissions from (a) broadcasting, (c) incorporation and (e) deep placement. Percentage of applied N that volatilizes as NH_3 by (b) broadcasting, (d) incorporation and (f) deep placement.

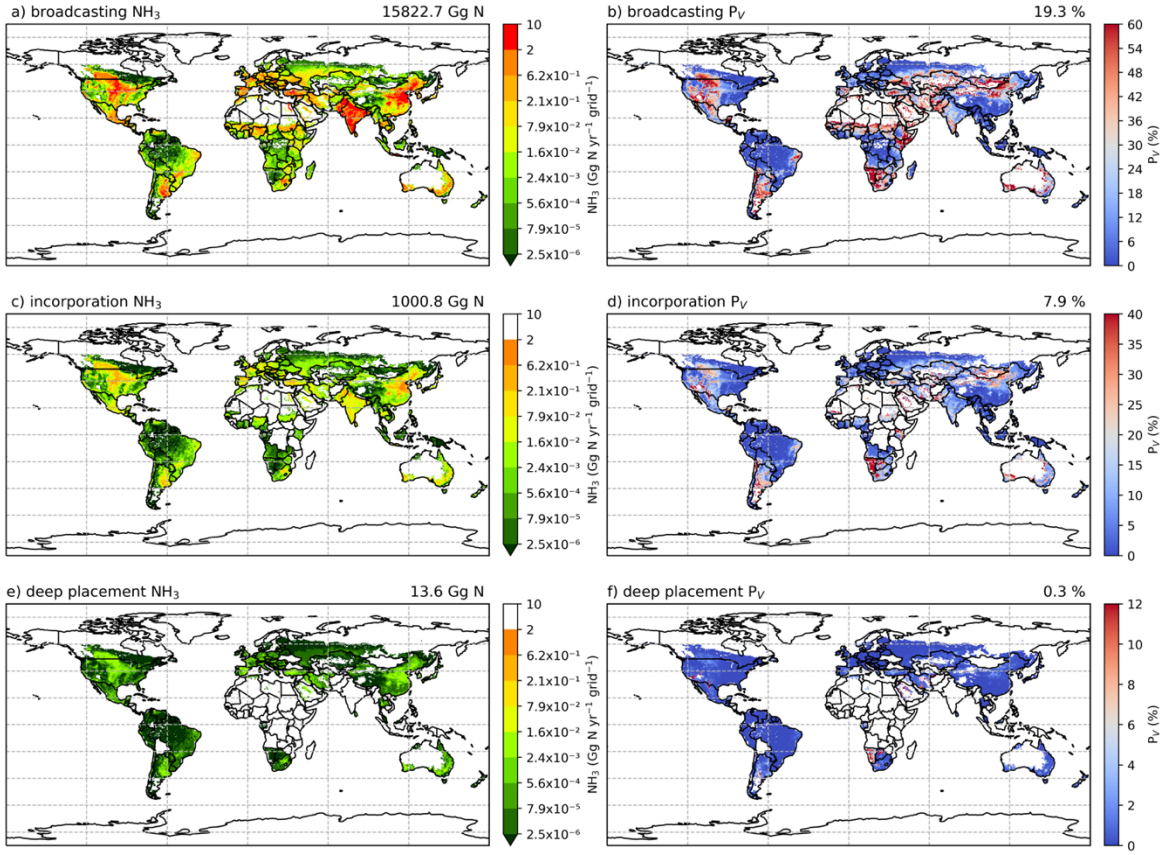

Figure 3.9. Same as Figure 3.8 but for 2018.

Figures 3.10 and 3.11 show the NH_3 emission from ammonium and urea fertilizer and the corresponding volatilization rates. In both 2010 and 2018, urea application results in more emissions than ammonium application due to its widespread use, although the emissions from each type of fertilizer are comparable. In 2010, about 40 % of emissions are from the use of ammonium and 60 % are from urea, and the relative contribution of ammonium to NH_3 emissions increases to 43 % in 2018. The volatilization rates of both fertilizers are

similar, with ammonium application resulting in slightly higher volatilization rates. The overall volatilization rate from ammonium application decreases from 19.3 % in 2010 to 18.1 % in 2018, while the rate for urea also decreases from 16.1 % in 2010 to 15.7 % in 2018.

As shown in Figure 3.10, ammonium application in 2010 shows higher volatilization rates than urea application in most of the regions, especially in Argentina, mid US, the Middle East (Iran and Turkey), South Asia (Pakistan, note that there was no urea application in Pakistan in 2010 according to IFA), while urea application shows higher volatilization than ammonium in northern China, Mongolia and Ukraine (Fig 3.10b and Fig 3.10d). In 2018, the spatial variations of the volatilization rates for both fertilizers are very similar (Fig 3.11b and Fig 3.11d).

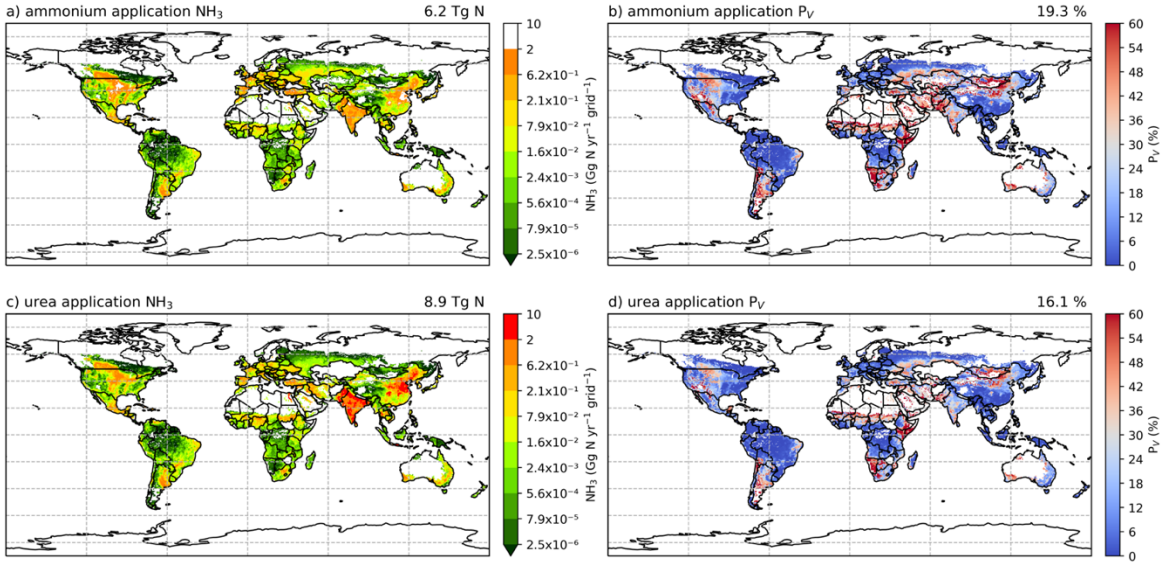

Figure 3.10. Simulated NH_3 emissions (Gg N yr^{-1}) from two main types of fertilizers and the corresponding volatilization rates (P_V) in 2010. Ammonia emissions from (a) ammonium application and (c) urea application. Percentage of applied N that volatilizes as NH_3 from (b) ammonium application and (d) urea.

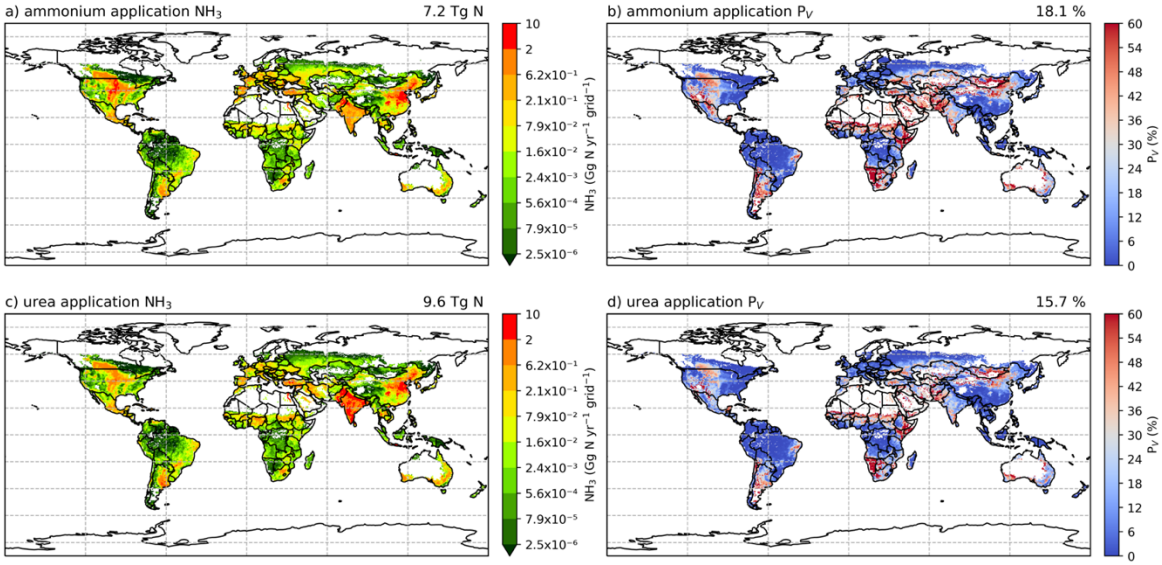

Figure 3.11. Same as Figure 3.10 but for 2018.

The fate of applied N in ammonium and urea fertilizers for 2010 and 2018 are shown in Figure 3.12. For both years, N uptake by crops is the largest among all processes, equivalent to 46.6 % (40.6 Tg N yr^{-1}) and 45.1 % (45.6 Tg N yr^{-1}) of fertilizer N applied in 2010 and 2018, respectively. Surface runoff is responsible for the smallest N loss, which is only 3.6 % (3.1 Tg N yr^{-1}) in 2010 and 2.4 % (2.4 Tg N yr^{-1}) in 2018. The amounts of N losses (in the form of ammonium and urea) due to volatilization, nitrification and dissolved in soils through diffusion and leaching are comparable. In 2010, around 16.8 % (14.6 Tg N yr^{-1}) of N undergoes nitrification and 14.5 % (12.6 Tg N yr^{-1}) is transferred to deeper soils. Nitrification is 16.2 Tg N yr^{-1} in 2018, accounting for 16.2 % of the total pathways, which is similar to 2010. The diffusive fluxes and leaching in 2018 are approximately 50 % higher

than the 2010 values (12.6 Tg N yr^{-1}), which together account for 11.0 % (18.5 Tg N yr^{-1}) of the N in synthetic fertilizers.

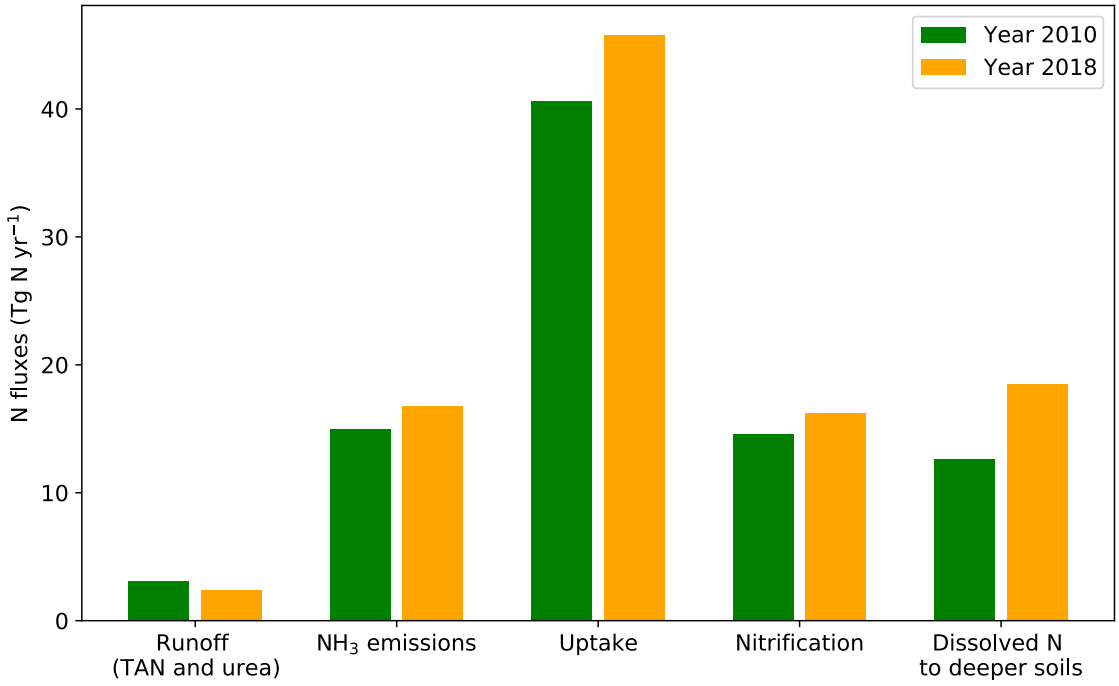

Figure 3.12. The fate of N of ammonium and urea application in 2010 and 2018 simulated by AMCLIM–Land. Note that the runoff only includes surface runoff of TAN and urea, while nitrate runoff is excluded.

3.3.3 Seasonal and regional NH_3 emissions from synthetic fertilizer use

As NH_3 emissions are greatly influenced by climatic conditions and local management, NH_3 emissions exhibit strong seasonality that varies across the globe. Figures 3.13 and 3.14 show the seasonal NH_3 emissions from fertilizer applications for 2010 and 2018,

respectively. The seasonal emissions in both years are similar, with over 50 % of NH_3 occurring in the Northern Hemisphere (NH) summer months and about 25 % in spring (all seasons refer to the NH seasons). Autumn and winter both contribute slightly over 10 % of the annual emissions. In the NH, more than 70 % of annual emissions are from JJA, while emissions in SON and DJF are significant in the Southern Hemisphere (SH). For example, Brazil and central African countries have predominantly SON emissions, while Argentina and southern Africa have the emissions largely occurred in JJA. Countries with high annual NH_3 emissions such as China, India and US generally show similar seasonal patterns, with the highest emissions occurring in JJA and lower emissions in other months.

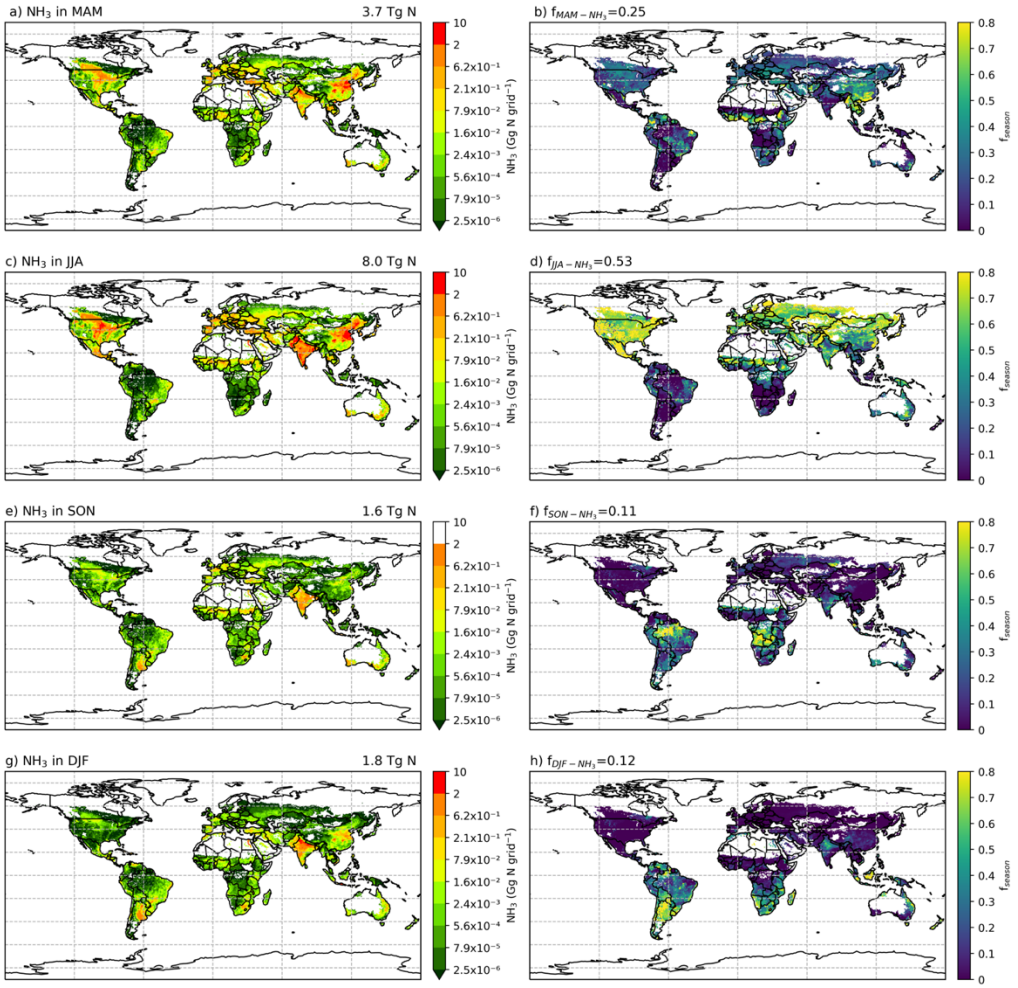

Figure 3.13. Seasonal NH_3 emissions (Gg N) from ammonium and urea fertilizer application and the relative percentage of annual emissions that are from the corresponding season (P_{season}, %) in 2010 simulated by AMCLIM–Land. Ammonia emissions in (a) March, April and May (MAM), (c) June, July and August (JJA), (e) September, October and November (SON), and (g) December, January and February (DJF). Percentage of annual emissions in the season of (b) MAM, (d) JJA, (f) SON and (h) DJF.

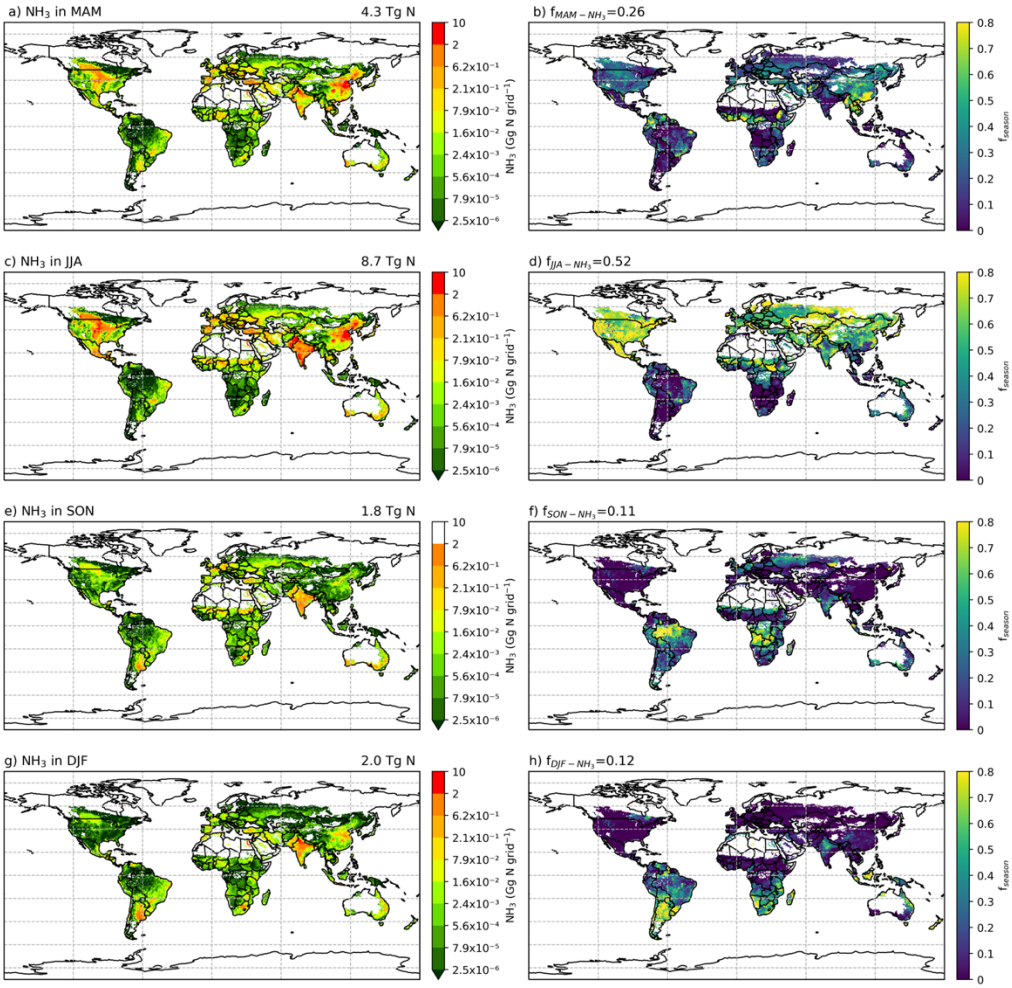

Figure 3.14. Same as Figure 3.13 but for 2018.

Global monthly emissions of NH_3 from synthetic fertilizer use categorized between the 16 crops are shown in Figure 3.15 and Figure 3.16. The trends for both 2010 and 2018 are generally the same. The highest emission of around 4.0 Tg N $month^{-1}$ occurs in July, and

August shows the second highest emission of around 2.5 Tg N month^{-1}. Large emissions take place in between April and August. The first emission peak is in May, which is the first month of the year when NH_3 emissions reach 2.0 Tg N month^{-1} in both years. Emissions slightly decrease in June, but then reach the maximum in July. Wheat-related emissions are seen throughout the year and are the most significant emissions in most months, expect for August, September, and October, in which rice contributes to the largest emissions. Maize is also one of the most important crops that result in NH_3 emissions from May to August.

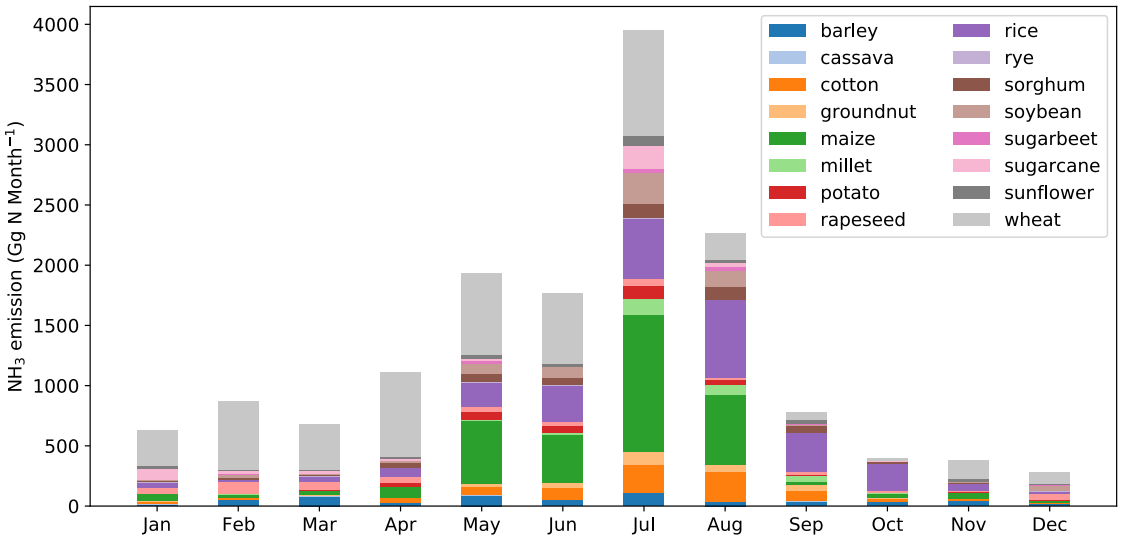

Figure 3.15. Global monthly NH_3 emissions (Gg N month^{-1}) from ammonium and urea fertilizer applications for 16 major crops in 2010 simulated by AMCLIM–Land.

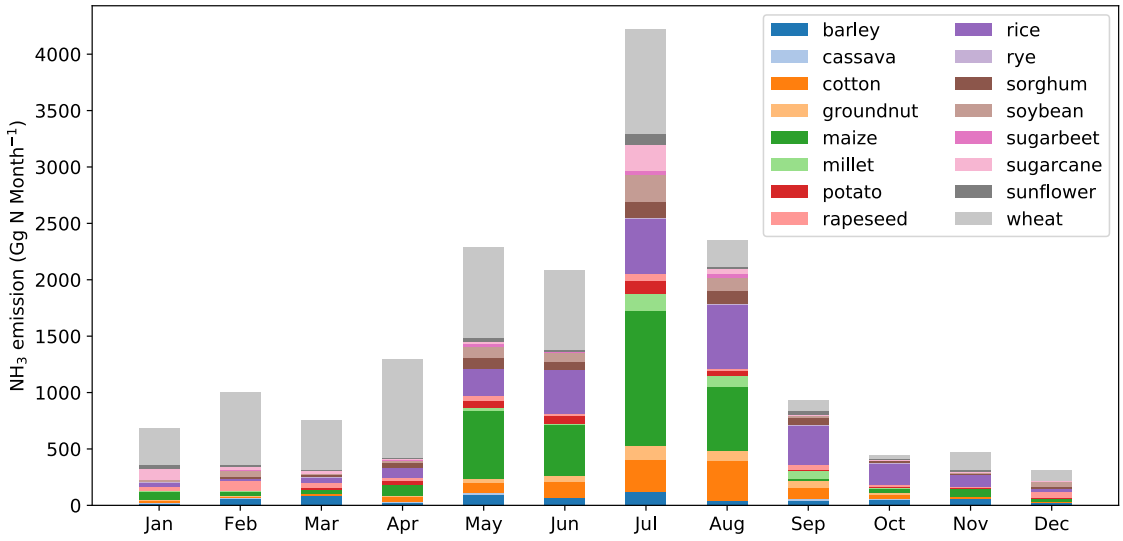

Figure 3.16. Same as Figure 3.15 but for 2018.

The seasonality of NH_3 emissions differs across the globe and varies between regions. Figure 3.17 and Figure 3.18 present monthly NH_3 emissions from 12 different geographical regions and the percentage of global monthly emissions that each region contributes. The map of the geographical regions is given in Appendix B4. The highest emissions are from East Asia and South Asia, with both regions responsible for roughly a quarter of global emissions. For year 2010, South Asia shows the highest emissions of over 3.8 Tg N yr^{-1}, while East Asia has the highest emissions of around 4.2 Tg N yr^{-1} for year 2018. North America has the third highest emissions, accounting for over 17 % of global emissions. Southern Africa has the lowest emissions, which only accounts for about 1 % of the global total. In terms of country-level statistics, China results in the largest emissions of 3.7 Tg N yr^{-1} in 2010 and 4.1 Tg N yr^{-1} in 2018, followed by India which contributes to 3.4 Tg N yr^{-1}

and 3.5 Tg N yr^{-1} in 2010 and 2018, respectively. US is the third largest emitter country with emissions of 1.9 Tg N yr^{-1} in 2010 and 2.0 Tg N yr^{-1} in 2018.

Regions in the NH, including East Asia, South Asia, North and Central Asia, Northern Europe and the Mediterranean, North America and the Middle East, generally show high emissions in JJA and MAM, as shown in Figures 3.17 and 3.18. In particular, East Asia, Northern Europe and North America exhibit very similar monthly variations, with high NH_3 emissions firstly occurring in May and reaching the maximum in July. North and Central Asia and South Asia show similar monthly trends, with summer (July or August) peaks of NH_3 emissions, and emissions in February are also high in these regions. The NH_3 emissions in the Mediterranean region are high in spring and summer emissions but much lower in autumn and winter. In contrast, South America and South Africa show higher winter emissions and lower emissions in other seasons. Oceania has distinct seasonal emission patterns. The emission in Oceania peaks in May and is high in August and September. Southeast Asia and Central Africa, two tropical regions, show different seasonal trends as Central Africa displays Northern Hemispheric characteristics and Southeast Asia shows similar trends to the SH. Figure 3.17 and Figure 3.18 show that different regions dominate NH_3 emissions in different seasons, with East Asia and South Asia being the largest contributors to spring and summer emissions, while South Asia and South America dominate autumn and winter emissions. North America also contributes significantly to summer emissions.

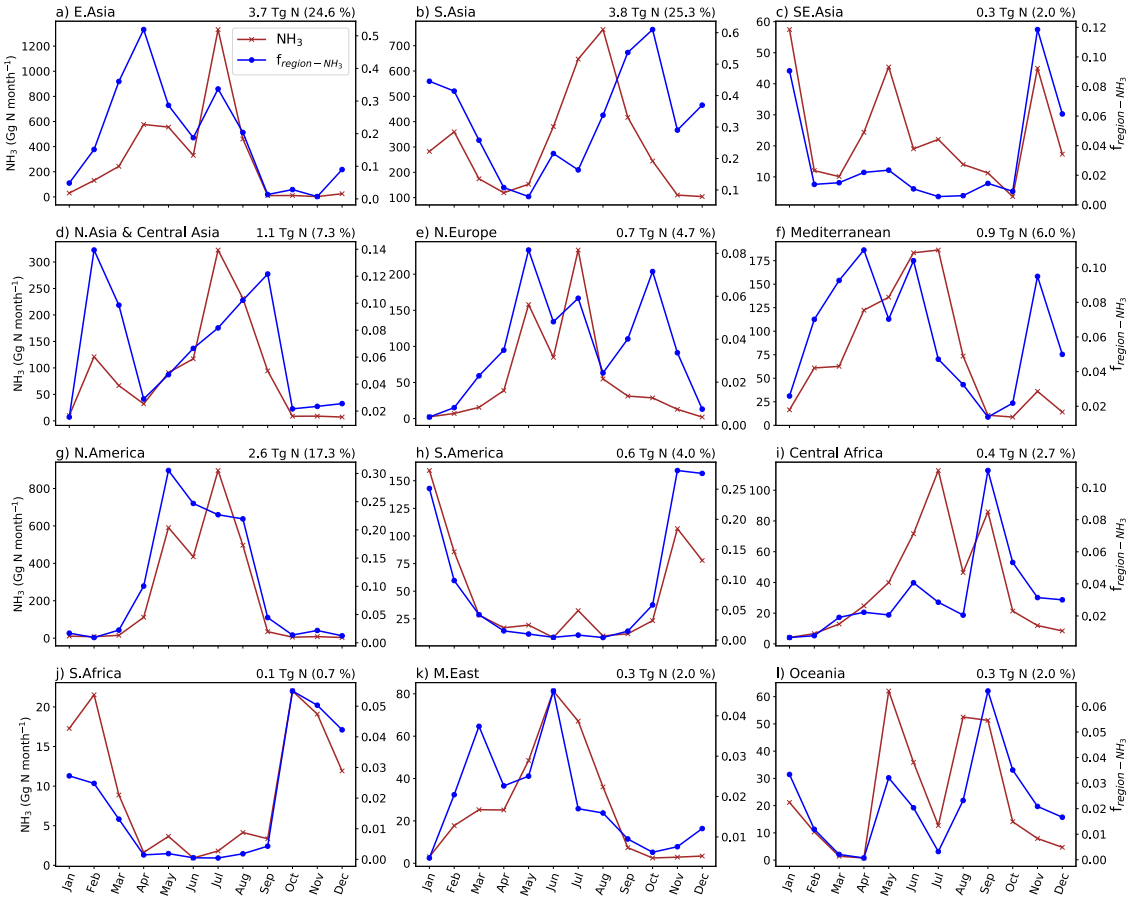

Figure 3.17. Monthly NH_3 emissions from ammonium and urea fertilizer application in different regions of the world and the relative percentage of the global monthly emissions that are from the corresponding regions (P_{region}). Annual total NH_3 emissions of the region are given at the top right corner of each plot, with the percentage of emissions from this region. The figure is for 2010.

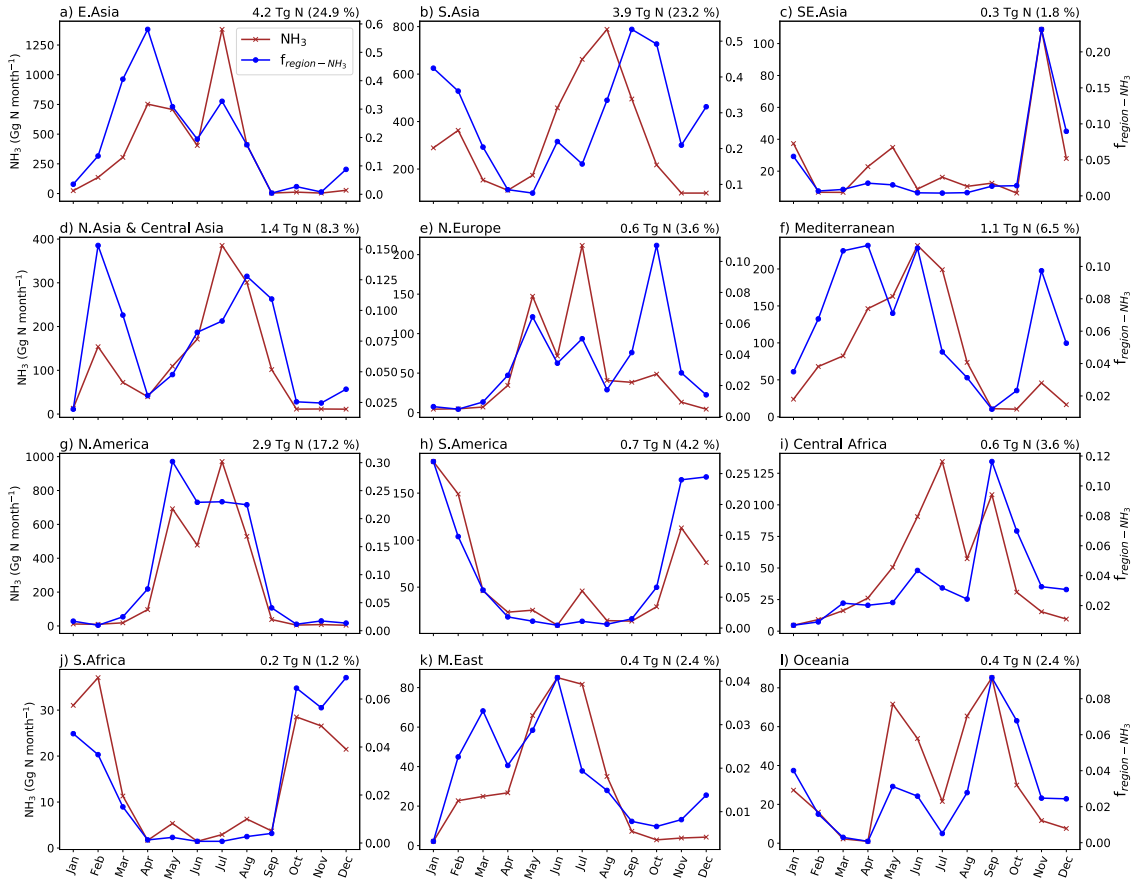

Figure 3.18. Same as Figure 3.17 but for 2018.

Table 3.2 provides a summary of the regional volatilization rates from the use of synthetic fertilizers in both 2010 and 2018. The data show that ammonium application generally results in higher estimated volatilization rates than urea application. Africa and Oceania have the highest volatilization rates for both 2010 and 2018, with over 23 % to 25 % of N in ammonium and urea application volatilized as NH_3, while South America shows the

lowest volatilization rates of less than 13 %. In the listed regions, the volatilization rates of both ammonium and urea application for 2018 are higher than 2010, except for Europe, North America and South Asia.

Table 3.2. Volatilization rates of synthetic fertilizer use in different regions for year 2010 and 2018. Values in the parentheses are volatilization rates when including nitrate application.

Year	Fertilizer	Africa	East Asia	Europe	North America	South Asia	South America	Oceania	Other part of Asia	Global
2010	Ammonium	23.6	17.5	17.6	19.4	25.7	14.2	27.3	19.4	19.3
	Urea	23.6	13.1	14.9	15.3	20.0	11.2	21.1	16.0	16.1
	All	23.6 (19.5)	14.5 (11.7)	16.4 (11.6)	17.9 (15.9)	20.9 (19.9)	12.3 (10.9)	23.7 (22.2)	16.8 (15.1)	17.2 (14.6)
2018	Ammonium	25.8	17.8	15.1	18.0	23.3	13.6	31.1	17.9	18.1
	Urea	24.5	12.7	13.8	14.5	17.4	12.5	26.9	16.6	15.7
	All	25.0 (21.5)	15.0 (11.2)	14.5 (10.6)	16.6 (14.8)	18.3 (17.6)	12.9 (11.7)	28.3 (27.0)	16.9 (15.3)	16.7 (13.9)

3.4 Discussion

3.4.1 Comparisons with other studies

Table 3.3 compares the simulated NH_3 emissions from synthetic fertilizer applications by AMCLIM–Land with those estimated by other studies, including models and inventories, on global, continental and national scales. Table 3.3 also includes volatilization rates, where available. Among all studies for comparisons, DLEM and FAN are both processed-based models (see Table 3.3 for references of all model descriptions/studies), while the other studies are inventories that mainly use EFs methods. DLEM incorporates a bi-directional exchange scheme for NH_3, and FAN is interactively coupled to an Earth System Model.

AMCLIM–Land is more often compared with DLEM and FAN in Table 3.3 due to the availability of results on various spatial scales. Among models, estimated global NH_3 emissions by AMCLIM are the second largest, which are in close agreement with DLEM. For 2010, AMCLIM and DLEM estimate 15.0 Tg N yr^{-1} and 16.7 Tg N yr^{-1} of NH_3 emissions, respectively. By comparison, the FAN model provides lower estimates of 12 Tg N yr^{-1} for 2000 by FANv1 and 11 Tg N yr^{-1} for 2010–2015 by FANv2. The lower NH_3 emissions estimated by FAN is partially due to less total N application in FANv2, which is 79 – 87 Tg N yr^{-1} compared to 102 Tg N yr^{-1} in AMCLIM and DLEM. The volatilization rates estimated by the three models are comparable, ranging between 13 to 16 %. For different types of fertilizers, it is estimated that about 16 % of N in urea fertilizers is lost as NH_3 compared with 19 % by FANv2, and NH_3 emissions from ammonium and nitrate fertilizer application account for 12 to 13 %, which is higher than 7 % estimated by FANv2,

while DLEM does not specifically report NH_3 emissions from urea or ammonium fertilizers. The high volatilization rates of ammonium fertilizers estimated by AMCLIM are possibly due to the following reasons: 1) AMCLIM does not simulate the dissolving process of ammonium fertilizers and instead it assumes that ammonium "pellets" instantly dissolves in soil moisture, which result in large initial emission potential and might cause an overestimation of NH_3 emissions (as shown in Figure 3.3d, the majority of overestimation by AMCLIM occurs in the first day). 2) The drainage and diffusion in AMCLIM might be underestimated so that more N in the ammonium fertilizer is available for volatilization.

Global estimates of emissions from other studies vary significantly, ranging from 5.9 to 28.6 Tg N yr^{-1}. MASSAGE_NH_3 and NH_3_stat both suggest that annual global NH_3 emissions are less than 10 Tg N yr^{-1} for 2008 and 2012. The NH_3_stat model estimates much lower emissions of 5.9 Tg N yr^{-1}, which is only about 35 % of AMCLIM's result. In contrast, estimated emissions by Yang et al. (2023) are the highest (28.6 Tg N yr^{-1}) for the 2010s. The large differences among the studies can be partly explained by the different agriculture activities included and different input data used in each study.

For NH_3 emissions from major continents and emitters (China, India and US), AMCLIM provides consistent estimates as compared with DLEM for regions including Africa, Asia, Europe and China, but higher emissions than FANv2. However, the volatilization rates of AMCLIM and FANv2 agree with each other in Africa, Asia, Oceania, China and India, indicating that the different NH_3 emissions can be partly explained by the different inputs of N fertilizer to the models. As shown in Table 3.3, AMCLIM has similar estimates for NH_3 emissions with other studies for most of regions expect for North America, US and India. For the US, emissions estimated by AMCLIM are higher than EPA by 60 % and

NH_3_stat and MASSAGE_NH_3 by two to four times. The higher estimate for the US by AMCLIM than other studies also caused a higher estimate for North America. Meanwhile, NH_3 emissions from India are also higher in AMCLIM; approximately 10 % to 20 % higher than other models and inventories. Only Yang et al. (2023) suggested even higher NH_3 emissions from India than AMCLIM. However, the volatilization rate for India estimated by AMCLIM is comparable to FANv2. The slightly lower values of AMCLIM than FANv2 indicate that the difference mainly results from different input data used. For example, the total N application in India is 16 Tg N yr^{-1} in AMCLIM compared to 10 Tg N yr^{-1} in FANv2.

Table 3.3. Comparisons of global, continental and national NH_3 emissions from fertilizer (Tg N yr^{-1}) and corresponding volatilization rates (%) between AMCLIM and other inventories, models and studies.

Model/ Study	Year	Global	Africa	Asia	Europe	North America	South America	Oceania	China	India	US
DLEM[a]	2000s, 2010	13.6, 16.7 (16.3%)*	0.5	9.0	1.9	2.0	0.9	0.2			
DLEM[b]	2000-2014								4.1	2.8	
FANv1[c]	2000	12									
FANv2[d]	2010-2015	11 (13%)	0.3 (20%)	5.9 (15.6 %)*	0.7 (6%)	1.3	0.6 (17%)	0.2 (22%)	2.3 (11%)	2.7 (26%)	
Literature[e]	2000	11									
Literature[f]	2010s	28.6			1.4				5.5	6.9	1.3
Literature[g]	2008-2010								2.4-5.2		
Literature[h]	2003-2010									2.2-3.3	
EPA[i]	2011										1.2
MASSAGE_NH_3[j]	2008	9.4							3.0		0.5
NH_3_stat[k]	2012	5.9							0.7	0.6	0.8
AMCLIM (this study)	2010	15.0 (14.6%)	0.6 (19.5%)	9.2 (14.8 %)	1.6 (11.6%)	2.6 (15.9%)	0.6 (10.9%)	0.3 (22.2%)	3.7 (12.0%)	3.4 (21.0%)	1.9 (15. 5%)

[a] Xu et al. (2019) [b] Xu et al. (2018) [c] Riddick et al. (2016) [d] Vira et al. (2020) [e] Beusen et al. (2008) [f] Yang et al. (2023) [g] Kurokawa et al. (2013); Kang et al. (2016); Zhang et al. (2017, 2018) [h] Aneja et al. (2012); Kurokawa et al. (2013) [i] EPA, 2011 [j] Paulot et al. (2014) [k] Aneja et al. (2020) * Values are calculated based on the results in the literature.

Table 3.4 summarizes the crop-specific NH_3 emissions from synthetic fertilizer applications estimated by AMCLIM–Land and other studies. Although there is limited data available for NH_3 emissions from individual crops, the results from each study are generally consistent in magnitude. Zhan et al. (2021) focuses on year 2000, and their values are the smallest. The results from Yang et al. (2023) are average values for the period from 2010 to 2018 and are generally higher. All studies agree that wheat, rice and maize are the top three crops that dominate the NH_3 emissions. AMCLIM has similar estimates for maize but much higher wheat emissions and lower soybean emissions compared to DLEM. The emissions related to rice estimated by AMCLIM are also nearly 50 % lower than estimates by DLEM, which might be partly due to the fact that AMCLIM does not include a flooded paddy scheme for rice simulations. Urea hydrolysis can be faster in flooded rice paddy, which tends to result in higher NH_3 emissions. The differences in crop-specific NH_3 emissions highlight the need for further research to improve the understanding of NH_3 emissions from different crops and fertilizer management practices.

Table 3.4. Crop-specific NH_3 emissions (Tg N yr^{-1}) from synthetic fertilizer use simulated by AMCLIM and comparisons with other studies.

Study	Year	A	B	C	D	E	F	G	H	I	J	K
DLEM[a]	2000s				3.3			3.5		<1.5		3.4
Yang2023[b]	2010s		1.3		3.7			4.9		0.9		6.0
Zhan2021[c]	2000	0.30		0.22	2.2	0.33	0.20	3.0	0.22	0.30	0.38	3.0
AMCLIM	2010	0.58	0.84	0.30	3.0	0.35	0.49	2.4	0.53	0.68	0.41	4.6

[a] Xu et al. (2019) [b] Yang et al. (2023) [c] Zhan et al. (2021)

A – barley; B – cotton; C – groundnuts; D – maize; E – potato; F – rapeseed; G – rice; H – sorghum; I – soybean; J – sugarcane; K – wheat

3.4.2 Spatial and temporal variations in NH_3 emissions

The NH_3 emissions from synthetic fertilizer use are primarily determined by the amount of N applied and are strongly influenced by both environmental conditions and local management practices. High NH_3 emission regions are typically found in countries with intensive agricultural activities such as China, India, Pakistan and US, where large amount of synthetic fertilizer N has been used. The P_V rate is an important indicator that shows the percentage of applied N volatilizes as NH_3, however, the regional pattern of the P_V rate does not always match the distribution of NH_3 emissions due to the combined effect of environmental factors and management practices.

When considering the environmental effects on NH_3 emissions, there are several factors that can cause volatilization rates to vary, including soil pH, soil temperature and moisture and wind speed. Alkaline soils tend to cause higher estimated NH_3 emissions in AMCLIM due to the chemistry involved so that regions with high soil pH, such as western US, Argentina, the Middle East, Namibia, Mongolia and part of northern China show high volatilization rates (Fig.B4). Since the base soil pH distribution is fixed in AMCLIM–Land according to HWSD v1.2 (FAO and IIASA, 2012; Wieder et al., 2014) and does not vary over time, the similar geographical patterns of the volatilization rates in the two simulated years indicates clear climatic dependences (due to temperature, water and wind conditions) featured in NH_3 volatilization.

High temperature leads to faster rates and quicker processes, which can result in larger emissions. Soil moisture influences the concentrations of N species in soils. When the soil is dry, soil TAN concentrations can be high, which may result in a greater emission potential at the soil surface, especially under alkaline soil conditions. This effect could be further amplified for ammonium fertilizer application as AMCLIM does not simulate the initial dissolving of fertilizer pellets. Dry regions, such as Mongolia, Namibia, western US and the Middle East show high volatilization rates. It is worth noting that these regions also have alkaline soils with high pH values, suggesting that the high volatilization may be due to a combined effects of soil dryness and alkalinity. Moreover, when the soil is dry and the subsurface percolation flux is small, there may be a lack of infiltration/drainage, which prevents N from moving from the surface to deeper soil layers. Instead, more N will volatilize as NH_3 from the surface. It is notable that the N fluxes of leaching and diffusion for 2010 are lower but the volatilization rate is higher than 2018. Wind speed is also a critical factor that impacts NH_3 volatilization since it influences the turbulence which affects the atmospheric resistances. Emissions are higher under windy conditions because atmospheric resistances are smaller. Simulations for the GRAMINAE site indicate that the sub-hourly NH_3 emissions vary with temperature and the friction velocity (which is related to wind speed and atmospheric resistances; Fig 3.2) and show strong diurnal cycles. Rainfall can also affect the NH_3 emission, mostly causing a reduction. Nitrogen species are washed off from the land surface during heavy rainfall event, and rain droplets can capture ammonia in the air, limiting the emission through a process known as "scavenging". Although the effects of rainfall are not explicitly included in AMCLIM, they are reflected implicitly by the runoff fluxes, and the magnitude of scavenged NH_3 is small

compared with the emission flux. The above meteorological factors can interactively affect the NH_3 emission.

Management plays another key role in affecting the NH_3 emissions in the agricultural activities, specifically through the timing of fertilizer application during planting seasons, the type of fertilizer used and the application techniques. The temporal variations of NH_3 emissions are largely related to the timing of fertilizer application, since volatilization usually takes place soon after the fertilizers are applied. The regional monthly emissions are closely linked to the planting seasons, with large emissions being found in a few months throughout the year. On the global scale, NH_3 emissions are the highest in MAM and JJA, with the first peak of emissions in May and the largest emissions in July, corresponding to the typical planting seasons for crops in the NH.

The second factor is the type of fertilizer used. According to simulations using AMCLIM–Land, application of ammonium and urea have similar volatilization rates on the global scale. The comparable volatilization rates of the two fertilizer types are possibly because of the following reasons. Ammonium is a direct input to soil TAN pool which is readily to be volatilized as NH_3, while urea must be hydrolysed before it is converted to TAN. The hydrolysis process is limited by water availability. If the soil is very dry, the amount of urea that hydrolyses is reduced (Rodríguez et al., 2005). Furthermore, hydrolysis of urea can cause soil pH to increase, leading to more NH_3 emissions. As a result, NH_3 volatilization from urea application is controlled by two processes with opposite effects. When including both ammonium and nitrate fertilizers (e.g., ammonium nitrate, the N content doubles but volatilization rate of NH_3 halves because the nitrate part does not contribute to NH_3

emissions), urea application is found to result in higher NH_3 emission due to the elevated soil pH by hydrolysis.

The third critical factor is the application techniques. How fertilizers are applied on land can have huge impacts. Broadcasting is the most commonly used method and contributes to the largest fraction of NH_3 emissions, while both immediate incorporation and deep placement of fertilizers are effective methods that can reduce NH_3 emissions to a large extent. Based on current estimates, less than 50 % of applied N is taken up by crops, which may be partly due to the very simple application techniques used. In addition to the three factors discussed above, irrigation can also influence NH_3 emissions as it has been found in literature that less NH_3 emissions occur after irrigation (Dawar et al., 2011; Yang et al., 2022; Zhang et al., 2022), although AMCLIM is not evaluated against observations because of insufficient input data. Irrigation leads to an increase of the soil moisture and reduction of emissions by diluting concentrations of N species and transporting them to deeper soil layers. Proper management practices, such as timely and precise application of fertilizers and adequate application techniques can help reduce NH_3 emissions and improve crop uptake of N.

3.4.3 Uncertainty and limitations

In general, uncertainty in NH_3 emissions arises from two main aspects: input data and model parameters. Input data uncertainty includes the N application rates, the crop calendars that determine the application dates and the soil characteristics. The crop calendars used in AMCLIM are static. Emissions could be influenced if using different crop

calendars as the environmental conditions may also change. AMCLIM assumes that fertilizers are applied twice during the growing season, which is a moderate value used as a representation for fertilization. This value mostly varies between one to three or four times across the globe. For example, there can be two to four times of fertilizer application in North America or zero to three times for South America (Xu et al., 2019a). The heterogeneity of the land during fertilization can also contribute to uncertainty in the overall estimates. In intensive farming countries like China and India, where fertilization can take up to a week or more, the assumption of fertilization being completed within a day in AMCLIM introduces uncertainty. Soil characteristics including soil pH, bulk density, soil constituents and organic matter content, etc., are assumed to remain constant in AMCLIM–Land, which can affect the chemical equilibrium and variables dependent on these data.

Uncertainty is also introduced from various parameters used in the AMCLIM model. First, the representation of soil pH evolution after urea application relies on an empirical relationship due to the complexity in simulating soil pH dynamics. In addition, long term trends of soil pH changes, i.e., soil acidification due to fertilization, are not included in AMCLIM. Instead, simulations for different years used the same base soil pH. Second, AMCLIM assumes the atmospheric concentrations of NH_3 to be zero for convenience, which may cause some overestimation of emissions, although this is expected to be small. Third, the model uses linear relationships to calculate the diffusive and drainage pathways, including irrigation-related drainage, which is difficult to simulate accurately. The overestimation of night-time NH_3 at the GRAMINAE site by approximately a factor of two suggests that the diffusive fluxes were not well represented. Fourth, the relative fraction of techniques used in fertilizer application worldwide are assumed to be dependent on country

income level, which is based on expert judgement due to the lack of statistical data so can introduce uncertainty. There are also sub-national-level variations in techniques used, which can affect the weighted sum and lead to different estimates. Considering all the factors, the estimated uncertainty is 33 % and 20 % for NH_3 emissions from ammonium and urea application, respectively. As a result, the overall expected uncertainty of emissions from synthetic fertilizer use is 3.9 Tg N yr^{-1} in 2010 and 4.3 Tg N yr^{-1} in 2018, which accounts for 26 % of the emission in each year.

The AMCLIM model only simulates NH_3 volatilization and does not include a bi-directional exchange scheme for NH_3, which may overestimate the NH_3 flux when there is enhanced deposition, especially for areas close to agricultural and semi-agricultural land. Another limitation of AMCLIM is the plant N uptake scheme. The current scheme for N uptake by crops has limited interactions with the carbon cycle, and the crop dynamics are represented by fixed empirical parameters that only account for temperature effects. There is also no consideration of water stress constraining the uptake. However, these points are considered beyond the scope of this study due to the complexity involved in simulating the relevant processes.

3.5 Summary and conclusions

This chapter presents the development and operation of AMCLIM–Land, a module in AMCLIM designed to simulate NH_3 emissions from synthetic fertilizer use at both the site scale and global scales. AMCLIM–Land simulates physical, chemical and biological

processes in the soils and at the land surface that control NH_3 volatilization. It incorporates the effects of environmental conditions and important management practices on these processes. AMCLIM–Land employs a four-layer soil structure, allowing for a detailed simulation of the soil processes and evaluation of various application techniques. Besides NH_3 volatilization, AMCLIM–Land also models other important N pathways in the agricultural systems, including surface runoff, nitrification, crop uptake and dissolved N to deep soils via leaching and diffusion.

AMCLIM–Land was tested at the site scale (only one field campaign with detailed measurements) and then applied on the global scale. It demonstrates close agreement with measurements in the GRAMINAE experiment. AMCLIM–Land accurately captures the major features of NH_3 fluxes from a post-cutting grassland after fertilization. On the global scale, using AMCLIM–Land, it is estimated that NH_3 emissions from synthetic fertilizer use are 15.0±3.9 Tg N yr^{-1} in 2010 and 16.8±4.3 Tg N yr^{-1} in 2018, which account for 14.6±3.8 % and 13.9±3.6 % of the total N in synthetic fertilizers in each year. The spatial and temporal variations of NH_3 emissions are significant, with high emissions occurring in regions with intensive agricultural activities, such as China, India and US. Global NH_3 emissions are dominated by East and South Asia, and North America. AMCLIM highlights key factors that tend to cause larger NH_3 emissions, including hot temperatures, low soil moisture, windy conditions and high soil pH. The highest NH_3 emissions occur in July during both simulated years, and the seasonality of emissions was largely driven by planting seasons and temperature. Summer (JJA) contributed to over half of the annual NH_3 emissions.

Based on simulations using AMCLIM–Land, less than 50 % of applied N is absorbed by crops, and NH_3 volatilization to the air is one of the major pathways for N losses. Broadcasting is the most commonly used methods for fertilizer application, but it results in a large fraction of N being lost due to NH_3 emissions. By comparison, incorporation and deep placement are effective methods that can be employed to mitigate NH_3 emissions.

AMCLIM–Land is a valuable tool for exploring the impacts of different agricultural management practices on NH_3 emissions and N pathways, despite the necessary simplifications of complex processes. The main advantages of AMCLIM–Land include: 1) the model is based on understanding at process-level and includes the most important N pathways, 2) responses to environmental variables are included, 3) there are representations of local management, 4) the model performs simulations at high temporal resolution which provides more reliable estimates of NH_3 emissions which are strongly influenced by environmental conditions. Overall, AMCLIM–Land provides insights on how environmental conditions and changes in agricultural management can affect NH_3 emissions and the N pathways.

Future research should focus on improving the soil pH dynamics and a better representative of the diffusion and drainage in the AMCLIM model in order to provide more accurate estimate for NH_3 emissions. Incorporating a bi-directional exchange scheme for NH_3 could be a potential future task so the model can simulate interactions between the soil and the vegetation. More testing and comparisons against site scale measurements will also be helpful to reduce uncertainty and improve the model performance.

Chapter 4
Ammonia emissions from pig and poultry farming

4.1 Introduction

Livestock farming is an important component of agricultural systems. As the global population continues to grow, livestock numbers are also increasing dramatically to fulfil the rising demand for animal products such as meat and eggs. Specifically, pigs and poultry are the sectors which recorded the largest increase in livestock population numbers, with pigs having increased by about 140 % and poultry having increased by nearly five-fold over the past 50 years (FAO, 2018b). This surge in livestock population has also resulted in a substantial increase of nutrient requirements, particularly in N inputs in animal feed. However, N recycling within livestock farming systems is often poor, resulting in a significant amount of N loss instead of being used by the animals. In particular, NH_3 emissions are a major pathway of N loss to the environment and can cause serious environmental problems (Sutton et al., 2011). Therefore, accurate estimation of NH_3 emissions is crucial for assessing the environmental impact of livestock farming systems and optimizing resource utilization.

This chapter presents the development and application of the dynamic process-based model, AMCLIM, to quantify NH_3 emissions from pig and poultry farming. For livestock simulations, the AMCLIM model focuses on three major practices: housing, manure management systems (MMS) and land application of manure. The application of AMCLIM at both the site and global scales and the evaluation against measurements are presented, and the results and implications are discussed.

4.2 Methods and Materials

4.2.1 Overview

Livestock ingest nitrogen from crops or feeds and use the nitrogen for gaining weight, producing meat, milk and eggs. Excess N is excreted (urine and dung) in their manure, which can be a valuable source of fertilizers for land. In general, animal excreta collected from animal houses is stored and then applied to arable land during growing seasons. However, the management of livestock manure can vary greatly across regions, with some farmers spreading manure daily or simply leaving it on pastures without much management rather than storing the manure, while others may use it as fuel. Each of these activities can result in NH_3 emissions.

To simulate the NH_3 emission from pig and poultry farming, all three modules in AMCLIM must be operated. In this section, the Housing (AMCLIM–Housing) and Manure Management (AMCLIM–MMS) Modules in AMCLIM are mainly described, as the Land

Module (AMCLIM–Land) has already been presented in Chapter 3. Different processes of manure application as compared to the synthetic fertilizer application are highlighted in this section. This section also presents the global applications of all three modules for simulating NH_3 emissions from pig and poultry farming.

4.2.2 Simulating pig and poultry housing

4.2.2.1 Processes in animal houses

Animal housing is one of the primary sources of NH_3 emissions in the livestock farming systems as animal houses are often the very first place where emissions take place. Figure 4.1 depicts the processes through which NH_3 emissions originate from excreta in animal houses, ultimately releasing into the exterior atmosphere. In general, there are six processes as follows:

- Livestock excreta contains N in the form of urea in pig (and ruminants') urine and uric acid in poultry excretion, as well as other organic forms of N in pigs' dung and poultry excretion (Process 1).

- Excreted N on the floor surface of the animal house is converted to TAN through hydrolysis of urea or uric acid and decomposition of organic N (Process 2; as expressed by Equation 2.7; details are given in Appendix A1).

- The TAN pool partitions into multiple phases; gaseous NH_3 is in equilibrium with aqueous TAN (Process 3; as expressed by Equations 2.4 and 2.5).

- NH_3 volatilizes to the house atmosphere from the surface (Process 4; as expressed by Equation 2.6).
- Indoor NH_3 level builds up due to NH_3 volatilization (Process 5).
- Indoor NH_3 is continuously removed from the house to the outside atmosphere through ventilation (Process 6).

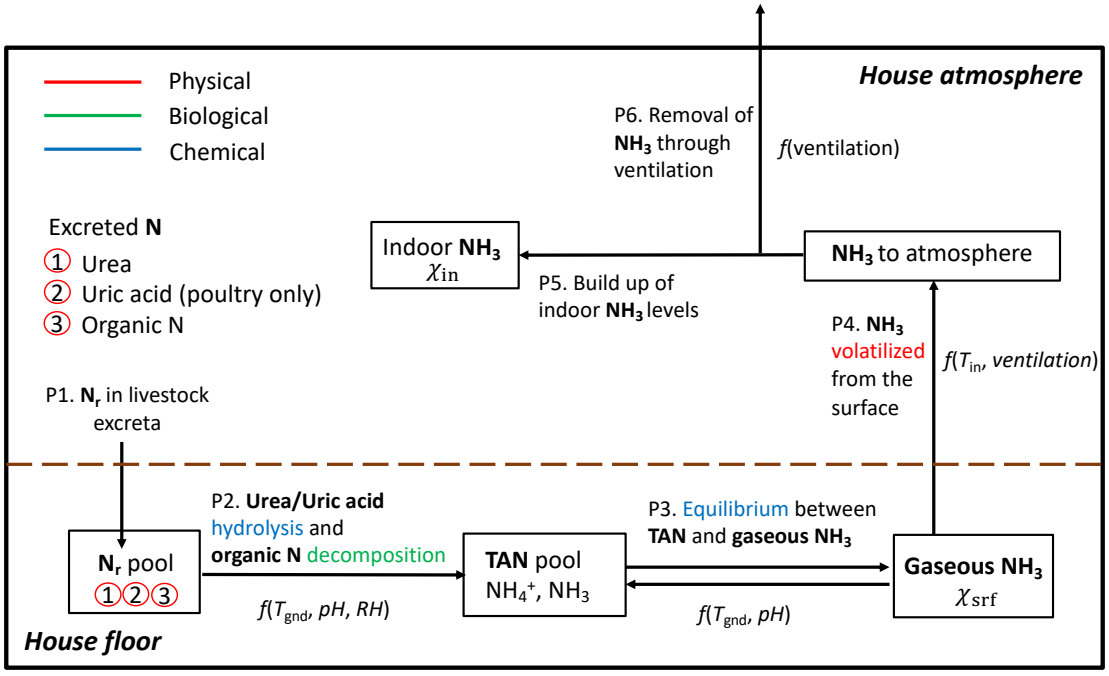

Figure 4.1. Schematic of NH_3 volatilization in animal houses (adapted from Elliott and Collins, 1982 and Jiang et al., 2021). Physical, biological and chemical processes are highlighted in red, green and blue, respectively.

The concentration of NH_3 inside the animal house (χ_{in}, g m^{-3}) is regulated by the balance between NH_3 volatilization from the floor surface ($F_{\mathrm{NH_3\ volatlization}}$) and removal of NH_3 to the outside atmosphere ($F_{\mathrm{NH_3\ removal}}$), which can be expressed by the following equation:

$$\frac{\mathrm{d}\chi_{\mathrm{in}}}{\mathrm{d}t} = F_{\mathrm{NH_3\ volatlization}} - F_{\mathrm{NH_3\ removal}}, \tag{4.1}$$

where the fluxes are expressed as the sum of the flux for the whole animal house (g N s^{-1}), which differs slightly from the standard fluxes given by Equation 2.1. The time-dependent concentration of indoor NH_3 of the animal house can be represented by the following equation:

$$V_{\mathrm{house}}\frac{\mathrm{d}\chi_{\mathrm{in}}}{\mathrm{d}t} = \frac{(\chi_{\mathrm{srf}}-\chi_{\mathrm{in}})}{R_{\mathrm{G,house}}}\cdot S_{\mathrm{house}} - Q_{\mathrm{in}}\,(\chi_{\mathrm{in}} - \chi_{\mathrm{out}}), \tag{4.2}$$

where χ_{in} (g m^{-3}) represents the indoor NH_3 concentration assuming a well-mixed state of air inside the animal house. χ_{srf} (g m^{-3}) is the gaseous NH_3 concentration at the emitting surface, and χ_{out} (g m^{-3}) is the free-atmosphere NH_3 concentration. S_{house} (m^2) and V_{house} (m^3) represent the surface area and the volume of the house, respectively. Q_{in} (m^3 s^{-1}) is the airflow rate of the house with a unit of cubic meter per second. The resistance for NH_3 volatilization in the animal house ($R_{\mathrm{G,house}}$, s m^{-1}) is determined by the inverse of an empirically-derived gaseous transfer coefficient for NH_3 ($k_{\mathrm{G,housing}}$, m s^{-1}), which depends on housing conditions such as temperature and ventilation, as expressed by the following equation:

$$R_{\mathrm{G,house}} = \frac{1}{k_{\mathrm{G,housing}}} \tag{4.3}$$

Animal houses are cleaned after certain amount of time. The frequency of cleaning varies depending on the housing management. The TAN pool (M_{TAN}; given in per unit area; all masses have units of g m^{-2} if not specifically explained) in the animal house can be determined by the following equation:

$$\frac{\mathrm{d}M_{\mathrm{TAN}}}{\mathrm{d}t} = F_{\mathrm{TAN}} - F_{\mathrm{NH_3}} - \psi_{\mathrm{cleaning}}(\mathrm{t}, \mathrm{TAN}), \tag{4.4}$$

where F_{TAN} is the TAN production, i.e., through urea or uric acid hydrolysis and decomposition of organic N for livestock excreta (together with other processes are presented in Appendix A1). $F_{\mathrm{NH_3}}$ is the flux of NH_3 volatilization (all N fluxes/flows have units of g N m^{-2} s^{-1} if not specifically explained). $\psi_{\mathrm{cleaning}}(\mathrm{t})$ represents the cleaning event of the house, as expressed as follows:

$$\psi_{\mathrm{cleaning}}(\mathrm{t}, \mathrm{excreta/N/H_2O}) = \begin{cases} 0, & \text{if "Not a cleaning day",} \\ \frac{M_{\mathrm{excreta/N/H_2O}}}{t_{\mathrm{cleaning}}}, & \text{if "a cleaning day"} \end{cases} \tag{4.5}$$

The cleaning event refers to the removal of livestock excreta (M_{excreta}), all N species (M_{N}) and water ($M_{\mathrm{H_2O}}$) from the animal house within an assumed time scale of 24 h (t_{cleaning}). The removed excreta can either be stored or applied to land as fertilizer, which will be described in the following sections. The pools for other N species, e.g., urea, in the animal houses can be expressed as follow:

$$\frac{\mathrm{d}M_{\mathrm{N}_i}}{\mathrm{d}t} = F_{\mathrm{excretN}} f_{\mathrm{N}_i} - K_{\mathrm{N}_i} M_{\mathrm{N}_i} - \psi_{\mathrm{cleaning}}(\mathrm{t}, \mathrm{N}_i), \tag{4.6}$$

where $F_{excretN}$ is the total N excretion rate from the livestock, and f_N is the fraction of a N form in the excretion. K_N is the conversion rate (s^{-1}) at which a N species decomposes (as Equation 2.7). For pigs, nitrogen is excreted in AMCLIM as urinary N and faecal N in a ratio of 2:1, with 75 % of urinary N being in the form of urea and the rest in organic forms (Vu et al., 2009a, b; Jørgensen et al., 2013). For poultry, AMCLIM assumes 60 % of the excreted N is in the form of uric acid, and the remaining 40 % is in organic forms (Nahm, 2003). The excretion pool is determined using the following equation:

$$\frac{\mathrm{d}M_{\mathrm{excreta}}}{\mathrm{d}t} = F_{\mathrm{excreta}} - \psi_{\mathrm{cleaning}}(\mathrm{t}, \mathrm{excreta}), \tag{4.7}$$

where $F_{excreta}$ is the excretion rate from the livestock, which is derived from the N excretion rates based on the N content in the excreta. The pH of the livestock excretion is used for determining the decomposition rates of N species (see Appendix A1) and chemical equilibria (as described in section 2.3.2) in housing simulations. The pH value is set at 7.7 for pig excreta and 8.5 for poultry (Sommer and Hutchings, 2001).

4.2.2.2 Simulations for pig housing

AMCLIM–Housing includes three types of animal houses, as introduced in Section 2.2.1. The first two housing types are designed for pig housing simulations. The first housing type has slatted floor and pit storage that allows pig excreta to be stored in-situ, keeping the floor area clean. For this housing type, a two-source emission scheme is used to model NH_3 emissions as there are two emitting surfaces: the slats and pit. The two NH_3 emission elements are treated as additive, i.e., the total housing emission is the sum of the emissions from the two housing compartments. To represent the processes on the slats and in the pit,

the pools of N species and other simulated variables are divided into two separate reservoirs. Pig excreta are split proportionally between the two reservoirs depending on the gap space of the slats. For example, if the gap space is 20 %, then 20 % of initial pig excreta will fall into the underneath pit, and the remaining 80 % will stay on the slats. Given the fact that excretions left on the slats will eventually fall to the pit (i.e., through cleaning), but excretions in the pit cannot go back to the slatted floor above, a uni-directional transfer is applied on a daily basis in AMCLIM–Housing. It is assumed that all pools from the slat reservoir go into pit reservoir by the end of each day, and the slat reservoir is reset to zero subsequently. Excreta that go into the pit are stored for longer time, e.g., weeks to months.

The process of NH_3 volatilization differs between the two reservoirs because of the different amount of water held in the two reservoirs. For the slats, excreta are typically a thin wet layer, so the surface concentrations can be expressed by the concentrations of the entire layer. The gaseous NH_3 concentration at the surface is directly derived from the aqueous TAN concentration of this layer. In contrast, the pit reservoir holds more water (and faeces) because urine in the excreta accumulates in the pit. There is an additional aqueous transfer process of TAN from the bulk water to the air-water interface. AMCLIM–Housing incorporates a two-film model that describes the gas exchange across the air-liquid interface (Liss, 1973; Liss and Slater, 1974). Details of the two-film model and the calculation of mass transfer are given in Appendix A10.

The second house type is a normal barn with a solid floor (without pit storage). In AMCLIM–Housing, normal barns are assumed to be cleaned daily so that pig excreta are removed from the house, and all pools are reset to zero every day. Volatilization of NH_3

from the pig excreta on the solid floor is identical to the processes taking place on the slats in the first house type.

For pigs (and ruminants), the water pool simulated in AMCLIM–Housing is determined by sources of water from urination (F_{urine}), water in faecal excreta ($F_{\text{faecal water}}$) and loss by evaporation of water (F_{evap}, mm s^{-1}) A cleaning-day function is included in the equation to account for the effect of cleaning on the water pool as follows:

$$\frac{\mathrm{d}M_{\mathrm{H_2O}}}{\mathrm{d}t} = F_{\text{urine}} + F_{\text{faecal water}} - F_{\text{evap}} - \psi_{\text{cleaning}}(\mathrm{t}, \mathrm{H_2O}) \qquad (4.8)$$

Excess water, such as washing water or drinking water in the houses, is not included since the quantity is unknown. The evaporation rate in the animal houses is approximated by applying an aerodynamic method, which is described in detail in Appendix A11.

4.2.2.3 Simulations for poultry housing

The third type of animal house in AMCLIM–Housing is designed specifically for poultry housing simulations. This accounts for the fact that poultry excreta are in the form of uric acid which hydrolyses to TAN much more slowly than urea (see Appendix A1). Furthermore, poultry excreta are much drier than pig excreta, so the rate of uric acid hydrolysis is also limited by the moisture levels (see Appendix A1). Housing management for poultry can also differ from other livestock. Addition of bedding materials to poultry excreta produces a solid litter. Consequently, poultry litter can be left in houses for a longer period than for other housed livestock, i.e., so called “deep litter” systems.

In AMCLIM–Housing, the water pool in poultry houses is determined by the initial water content in the excreta ($F_{\text{excretion water}}$), evaporation, and the cleaning function, as shown in the following equation:

$$\frac{\mathrm{d}M_{\mathrm{H_2O}}}{\mathrm{d}t} = \max\left(F_{\text{excretion water}} - F_{\text{evap}}, m_{\mathrm{E}} M_{\mathrm{DM}}\right) - \psi_{\text{cleaning}}(\mathrm{t}, \mathrm{H_2O}) \quad (4.9)$$

where m_{E} is the equilibrium moisture content of the excreta as a function of ambient temperature and humidity, which is calculated as described in Appendix A11. M_{DM} is the mass of dry matter (DM) of the excreta, which is used to determine the water at equilibrium moisture.

The high DM content of the poultry litter can result in NH_4^+ adsorption on litter solids, a process similar to NH_4^+ adsorption on soil particles (as described in Section 3.2.1.1; Equation 3.4). Due to the lack of knowledge regarding nitrogen adsorption on livestock manure, AMCLIM–Land uses a constant partitioning coefficient (K_{d}) of 1.0 for all livestock (as introduced in Appendix A3), so the amount of N adsorbed on manure solid is only dependent on the water content of the manure. Moreover, the surface of poultry excreta can dry quickly, forming a natural outer "crust" that prevents further emissions from the old litter below. The quantity of this layer is uncertain, and modelling the drying process is difficult. To simulate the NH_3 volatilization from poultry excreta, AMCLIM–Housing assumes an additional surface resistance of 8640 s m^{-1} (0.1 d m^{-1}) for litter (R_{litter}). This surface resistance is derived using an inversion method as described in the previous version of AMCLIM-Poultry (Jiang et al., 2021). For deep litter system, surface resistance doubles (17280 s m^{-1} or 0.2 d m^{-1}) due to bedding materials added.

4.2.3 Simulations for manure management of pig and poultry

The AMCLIM model simulates manure management for pig and poultry as a subsequent stage after housing, with the exception of in-situ storage of livestock excreta in pits or litter management for broiler poultry, which are counted as housing emissions. In AMCLIM–MMS, there are two types of manure under management: slurry and solid manure, corresponding to liquid and solid phase manure, respectively. As described in Section 2.2.2, four manure management divisions are defined and simulated in AMCLIM–MMS, including three types of storage and one type of land application. This section describes the approach for manure storage, while land application is described in the next section.

Liquid manure or slurry can have a DM content that ranges from 2% to 20%, depending on the amount of water added to the manure. As such, slurry refers to manure with a relatively low DM content, which consists mainly of livestock urine, faeces and added water (Sommer et al., 2006; Vira et al., 2019). In this study, the manure management section uses the term "liquid manure", while the land application section uses "slurry". Note that these two terms are used interchangeably in different modules, and both refer to the same substance. Figure 2.1 illustrates the three types of storage for liquid manure: indoor, outdoor and covered storage.

The indoor storage of liquid manure and pit storage in animal houses are similar, as both reservoirs have high water content (however, as mentioned, it should be noted that NH_3 emissions from pits in animal houses are counted as housing emissions.). The volatilization of NH_3 from indoor storage of liquid manure is calculated using the same two-film mass transfer model as for pit emissions. The TAN pool of the storage unit is determined from

the TAN pool from housing, conversion from other N species, loss through NH_3 volatilization, and removal when manure is used for land application, which can be expressed by the following equation:

$$\frac{\mathrm{d}M_{\mathrm{TAN}}}{\mathrm{d}t} = \psi_{\mathrm{housing}}(\mathrm{t}, \mathrm{TAN}) + F_{\mathrm{TAN}} - F_{\mathrm{NH_3}} - \psi_{\mathrm{to\ land}}(\mathrm{t}, \mathrm{TAN}), \tag{4.10}$$

where $\psi_{\mathrm{housing}}(\mathrm{t})$ is the function that represents the housing excreta that are transferred to the storage unit. The relationship between $\psi_{\mathrm{housing}}(\mathrm{t})$ and the cleaning function $\psi_{\mathrm{cleaning}}(\mathrm{t})$ can be expressed as:

$$\psi_{\mathrm{housing}}(\mathrm{t}) = \frac{\psi_{\mathrm{cleaning}}(\mathrm{t})}{f_{\mathrm{store-housing}}}, \tag{4.11}$$

$f_{\mathrm{store\text{-}housing}}$ is the ratio of storage area to housing area. If the area for manure storage is smaller than the housing area, the pools of manure storage (per unit area) will be larger than housing, as manure concentrates in smaller areas (note that concentrations remain unchanged). The function $\psi_{\mathrm{to\ land}}(\mathrm{t})$ represents stored manure used for land application within 24 h ($t_{\mathrm{to\ land}}$), and is expressed as follows:

$$\psi_{\mathrm{to\ land}}(\mathrm{t}, \mathrm{excreta/N/H_2O}) = \begin{cases} 0, \text{ if "Not an application day",} \\ \frac{MM_{\mathrm{excreta/N/H_2O}}}{t_{\mathrm{to\ land}}}, \text{ if "an application day".} \end{cases} \tag{4.12}$$

Similarly, the other N pools during storage can be expressed as follow:

$$\frac{\mathrm{d}M_{\mathrm{N}_i}}{\mathrm{d}t} = \psi_{\mathrm{housing}}(\mathrm{t}, \mathrm{N}_i) - K_{\mathrm{N}_i} M_{\mathrm{N}_i} - \psi_{\mathrm{to\ land}}(\mathrm{t}, \mathrm{N}_i). \tag{4.13}$$

The water pool of the storage unit is determined by the initial water amount of animal excreta from housing, evaporation, and additional water that may be added ($F_{\text{added water}}$):

$$\frac{\mathrm{d}M_{\mathrm{H_2O}}}{\mathrm{d}t} = \psi_{\text{housing}}(\mathrm{t}, \mathrm{H_2O}) + F_{\text{added water}} - F_{\text{evap}} - \psi_{\text{to land}}(\mathrm{t}, \mathrm{H_2O}). \quad (4.14)$$

By default, the DM content of liquid manure in AMCLIM–MMS is set to 5 %, but it is allowed to vary by a factor of 2, between 2.5 % to 10 %, due to fluctuations in the water pool. Additional water may be added to maintain the DM content within 10 % ($f_{\text{DM.max}}$), as expressed by the following equation:

$$M_{\text{added water}} = \max\left(0, M_{\mathrm{DM}}\left(\frac{1}{f_{\mathrm{DM,max}}} - 1\right) - M_{\mathrm{H_2O}}\right). \quad (4.15)$$

Covered storage of liquid manure is considered a variation of indoor storage in AMCLIM–MMS. A reduction factor of 0.95 is applied to the NH_3 emission from this management system, which represents an effective mitigation by covering the manure with lids or coverings.

Simulations of outdoor storage of liquid manure are similar to those of indoor storage, but the physical and chemical processes are affected by different environmental conditions. The primary difference is the level of turbulence, which is largely related to wind speed and has a significant impact on NH_3 volatilization. While indoor storage provides a less "windy" environment, outdoor storage exposes liquid manure to the outside environment. Temperature differences between indoor and outdoor storage may be less pronounced. In addition, the water pool of outdoor storage is influenced by rainfall (F_{rainfall}, mm s^{-1}), as expressed by the following equation:

$$\frac{\mathrm{d}M_{\mathrm{H_2O}}}{\mathrm{d}t} = \psi_{\mathrm{housing}}(\mathrm{t}, \mathrm{H_2O}) + F_{\mathrm{added\ water}} + F_{\mathrm{rainfall}} - F_{\mathrm{evap}} - \psi_{\mathrm{to\ land}}(\mathrm{t}, \mathrm{H_2O}) \quad . \tag{4.16}$$

A specific management classified as outdoor storage in AMCLIM–MMS is lagoon systems. Lagoon systems are artificial or natural earthen storage structures that usually provide a largely anaerobic environment for liquid manure treatment. In this study, a simplified representation of lagoon systems is used, where a constant TAN concentration of 600 µg mL^{-1} is set for lagoons (Aneja et al., 2001). This simplification is justified reasonable due to the large amount of water present in lagoon systems, resulting in low TAN concentrations. Therefore, the NH_3 emissions are expected to be small, which only disturbs the TAN pool to a limited extent. The process of NH_3 volatilization is simulated by the same two-film model as other liquid storage management systems. Details are presented in Appendix A10.

Compared to liquid manure, solid manure has higher DM contents, typically ranging from 30 to 40 % for pigs and ruminants, and up to 50 to 70 % for poultry manure (Sommer and Hutchings, 2001). With lower water content, solid manure storage can facilitate nitrification, providing an additional chemical pathway that depletes the TAN pool, as expressed by the following equation:

$$\frac{\mathrm{d}M_{\mathrm{TAN}}}{\mathrm{d}t} = \psi_{\mathrm{housing}}(\mathrm{t}, \mathrm{TAN}) + F_{\mathrm{TAN}} - F_{\mathrm{NH_3}} - F_{\mathrm{nitrif}} - \psi_{\mathrm{to\ land}}(\mathrm{t}, \mathrm{TAN}). \tag{4.17}$$

The process of nitrification in solid manure is similar to that in soils, but with some variations in parameters. The details of these calculations can be found in Appendix A4. In solid manure, ammonium can be adsorbed on solid particles, and the manure itself presents

an additional barrier to N transport, as discussed in Section 4.2.2.3. In AMCLIM–MMS, the partition of TAN into different phases in the bulk manure is determined, and the concentrations at the surface are used to calculate NH_3 emission. Further information is provided in Appendix A8.

4.2.4 Simulations for land application of pig and poultry manure

Manure can be used as fertilizer on land either after being stored for a period of time or directly after being removed from animal houses. The land application of pig and poultry manure is simulated by AMCLIM–Land, which employs the four prescribed soil layers (as described in Section 3.2.1). The N processes involved in the simulations for manure application are described in Section 3.2.1 and are the same as those for chemical fertilizer applications. Manure is assumed to be applied only to the soil surface. Modification to allow soil incorporation and deep injection of manure and slurry is possible, but is not included in the current version of AMCLIM applied here. Stored manure is assumed to be spread on croplands, and its application is scheduled according to the local planting seasons. Alternatively, manure can be applied daily if it is spread soon after being removed from animal houses.

Manure application to land provides sources of N to the soil pools. The soil TAN pool in the top layer can be expressed as:

$$\frac{\mathrm{d}M_{\mathrm{TAN}}}{\mathrm{d}t} = \psi_{\mathrm{to\ land}}(\mathrm{t, TAN}) + \psi_{\mathrm{to\ land}}(\mathrm{t, urea/org\ N}) + F_{\mathrm{TAN}} - F_{\mathrm{NH_3}} - F_{\mathrm{TAN\ runoff}} - F_{\mathrm{diffusion}} - F_{\mathrm{leaching}} - F_{\mathrm{nitrif}}, \quad (4.18)$$

where the application rate $\psi_{\text{to land}}(\text{t})$ hase been shown in Equation 4.12. The production of TAN (F_{TAN}) is mainly through the decomposition of organic N. The remaining fluxes are removal processes explained in Section 2.3 and 3.2.1.1 ($F_{\text{TAN runoff}}$ – flux of surface TAN runoff; $F_{\text{diffusion}}$ – diffusive fluxes; F_{leaching} – flux of leaching; F_{nitrif} – nitrification).

Urea in pig manure is assumed to be fully hydrolysed to TAN during storage upon land application as a simplification, which keeps the soil pH constant. This is true for stored manure and is a reasonable assumption for daily spread manure. Uric acid in poultry manure and organic N are assumed to be retained in the top soil layer as these species typically bond with manure and soil particles, and are assumed in AMCLIM not to move to the underlying layers through diffusion or drainage. These N pools in soils are depleted by hydrolysis or decomposition and surface runoff, which can be expressed as:

$$\frac{\mathrm{d}M_{\mathrm{N}_i}}{\mathrm{d}t} = \psi_{\text{to land}}(\mathrm{t}, \mathrm{N}_i) - K_{\mathrm{N}_i} M_{\mathrm{N}_i} - F_{\mathrm{N}_i\,\text{runoff}}. \tag{4.19}$$

The runoff of N species ($F_{\mathrm{N}_i\,\text{runoff}}$) such as uric acid and organic N is determined by the following equation:

$$F_{\mathrm{N}_i\,\text{runoff}} = q_{\mathrm{r}} r_{\mathrm{N}} M_{\mathrm{N}_i}, \tag{4.20}$$

where r_{N} (mm^{-1}) represents the wash-off factor for N species that is set at 1 % per millimetre (Riddick et al., 2017a).

The application of manure, particularly slurry, can significantly affect soil water content. Misselbrook et al. (2006) reported that 6 mm of pig and cattle slurry infiltrate into the soils within an hour after application and cause an increase of the soil moisture content. In

AMCLIM–Land, the immediate change in soil water content after manure application is calculated using Equations 3.11 and 3.12. However, the model does not account for the impact of manure application on soil properties such as porosity or organic matter content. Additionally, AMCLIM–Land allocates N species in solid manure to the top soil layer instead of a separate manure layer above the soils.

4.2.5 Global application

4.2.5.1 Global data for livestock and manure management systems

The Global livestock and MMS data used in the AMCLIM model are obtained from FAO GLEAM2. The global livestock data include information on the geographical distribution of livestock heads, average live bodyweight, and total N excretion rates, which are categorized by production system. The reference year of these data is 2010, and changes in livestock population and N excretion rates over time are based on the variations suggested by Lu and Tian (2017), while the MMS data that determines the fraction of a manure management system are assumed to be constant through the year. Urination and defecation rates of pigs and excretion rates of poultry are derived from the N excretion rates. More information on the properties and characteristics of livestock excreta, including urinary N concentrations, faecal N content, dry matter content and pH, are presented in Appendix B6.

For pig farming, there are three production systems: industrial pigs, intermediate pigs and backyard pigs. It is worth mentioning that only chicken is included in the poultry sector, which accounts for over 95 % of poultry by numbers based on the Food and Agriculture

Organization Corporate Statistical Database (FAOSTAT) data for 2010. Chicken has three production systems: broilers, layers and backyard chicken. The characteristics and housing features of pig and poultry production systems are summarized in Table 4.1, which is adapted from the FAO GLEAM2 model description (FAO, 2018a). The MMS data provide geographical distributions of the fraction that a system is used for manure management, which differs between livestock sectors and production systems for pigs and poultry. As described in previous sections, these MMS are regrouped into the four divisions used in AMCLIM–MMS. More details are available in Appendix B7.

Table 4.1. Characteristics of livestock production systems for pigs and poultry used in GLEAM (information is taken from FAO, 2018).

Production system	Characteristics	Housing
Pigs		
Industrial	Fully market-oriented; high capital input requirements (including infrastructure, buildings, equipment); high level of overall herd performance; purchased non-local feed in diet or on-farm intensively produced feed.	Fully enclosed: slatted concrete floor, steel roof and support, brick, concrete, steel, or wood walls.
Intermediate	Fully market-oriented; medium capital input requirements; reduced level of overall herd performance (compared with industrial); locally sourced feed materials constitute 30 to 50% of the ration.	Partially enclosed: no walls (or made of a local material if present), solid concrete floor, steel roof and support.
Backyard	Mainly subsistence driven or for local markets; level of capital inputs reduced to the minimum; herd performance lower than commercial systems; feed contains maximum 20% of purchased non-local feed; high shares of swill, scavenging and locally sourced feeds.	Partially enclosed: no concrete floor, or if any pavement is present, made with local material. Roof and support made of local materials (e.g., mud bricks, thatch, or timber).
Poultry		
Broilers	Fully market-oriented; high capital input requirements; high level of overall flock productivity; purchased non-local feed or on-farm intensively produced feed.	Broilers assumed to be primarily loosely housed on litter, with automatic feed and water provision.
Layers	Fully market-oriented; high capital input requirements; high level of overall flock productivity; purchased non-local feed or on-farm intensively produced feed.	Layers housed in a variety of cage, barn and free-range systems, with automatic feed and water provision.

Backyard	Animals producing meat and eggs for the owner and local market, living freely. Diet consists of swill and scavenging (20 to 40%) while locally produced feed constitutes the rest.	Simple housing using local wood, bamboo, clay, leaf material and handmade construction resources for supports plus scarp wire netting walls and scrap iron for roof.

4.2.5.2 Housing environments and housing density

There are two housing systems considered in AMCLIM–Housing: fully enclosed houses (with forced heating and ventilation) and partially enclosed houses as described in Section 2.2.1. The inside conditions of animal houses significantly influence the NH_3 emission from livestock housing as they can be very different from the natural environment, with indoor temperature being the most prominent environmental factor. Pigs and poultry have a lower critical temperature (i.e., the minimum managed temperature for optimum chicken performance) of approximately 16–20 ºC (Gyldenkærne, 2005b). Therefore, pigs and poultry from commercial production systems that are intensively managed (e.g., industrial pigs, broilers and layers) are typically kept in insulated buildings equipped with forced heating and ventilation systems. These systems help maintain the ambient temperature within a recommended range throughout the year as far as feasible (Seedorf et al., 1998b). Heating is used on cold days when the temperature is low, while ventilation is used to cool down the house when the temperature is high. Fully enclosed houses require a minimum level of ventilation to remove odours and emissions like NH_3 from the house, which aims to maintain a healthy environment for the animal growth. However, the ventilation should also be below a certain rate to avoid causing an induced draft in the house. For intermediate

and backyard production systems, pigs and poultry are kept in barns that are naturally ventilated. These barns have indoor environments that are closer to the natural environments, with slightly higher temperatures than outdoor temperatures due to the warmth generated by the animals, and local materials are used to block wind and to warm the buildings in cold days.

In AMCLIM–Housing, the indoor temperature and ventilation of animal houses are modelled using a set of empirically derived relationships in relation to the outdoor temperature. These relationships are based on data from the Animal Feeding Operations (AFOs) dataset by the US Environmental Protection Agency (EPA, 2012) and theoretical parameterizations of indoor environments by Gyldenkærne et al. (2005). These relationships can vary between livestock sectors and production systems as each production system of livestock has a corresponding housing system and house type in the global simulations. Table 4.2 lists the housing system and house type of pig and poultry by production systems used in AMCLIM–Housing as described in Section 2.2.1. The parameterizations of housing environments are presented in Appendix A12.

Table 4.2. Housing systems and house types for pig and poultry in AMCLIM–Housing.

Production system	**Housing system**	**House type**
Pigs		
Industrial	Fully enclosed house	Houses with slatted floors and storage pits
Intermediate	Naturally ventilated house	Normal barns
Backyard	Naturally ventilated house	Normal barns

Poultry		
Broiler	Fully enclosed house	Poultry houses
Layer	Fully enclosed house	Poultry houses
Backyard	Naturally ventilated house	Poultry houses

Housing density varies depending on the livestock and production system. Industrial pigs are assumed to be housed at a typical density of 120 kg liveweight per square meter (Lim et al., 2010a). By comparison, intermediate and backyard pigs are housed at lower densities than the industrial production system, with assumed values of 80 and 60 kg liveweight per square meter, respectively. Regarding poultry housing, the assumed density for broilers and layers are 15 and 30 birds per square metre, respectively (Cortus et al., 2010a, b; Wang et al., 2010). Backyard poultry are less densely housed than broilers and layers, with an assumed density of four birds per square meter. The housing area is calculated accordingly by the following equation:

$$S_{\text{house}} = \begin{cases} \dfrac{n_{\text{i}} m_{\text{i}}}{den_{\text{housing}}}, \text{if i is pig} \\ \dfrac{n_{\text{i}}}{den_{\text{housing}}}, \text{if i is poultry} \end{cases}, \tag{4.21}$$

where n_{i} and m_{i} are the number of animals and average body weight (kg head^{-1}), and den_{housing} is the housing density of the livestock (kg animal per m^2 for pigs and number of animal per m^2 for chicken). It is worth noting that pig houses with slatted floor and pit have

two NH_3-emitting surfaces, so the slats areas (S_{slats}, m^2) and pit areas (S_{pit}, m^2) are calculated separately:

$$\begin{cases} S_{\text{slats}} = (1 - f_{\text{gap}}) S_{\text{housing}} \\ S_{\text{pit}} = f_{\text{pit}} S_{\text{housing}} \end{cases}, \tag{4.22}$$

where f_{gap} is the fraction of gap space in the slats (assumed to be 0.2, i.e., 20 % of gap space, for global simulation), and f_{pit} is the relative area of the pit to the housing area (set to be 1.0 in AMCLIM–Housing, meaning that the pit surface has an equivalent size as the area of the house).

To estimate housing NH_3 emissions in global simulations, it is assumed that indoor and atmospheric NH_3 concentrations are negligible, given that animal houses are significant NH_3 sources and their surface concentrations are much higher than indoor and outdoor concentrations. However, as the global volume of animal houses is uncertain (as described in Equation 4.2), the calculation of NH_3 emissions is simplified by using the following equation:

$$F_{\text{NH}_3} = \frac{\chi_{\text{srf}}}{R_{\text{G,house}}}. \tag{4.23}$$

4.2.5.3 Manure storage and manure application

Manure storage, land application of manure, and housing are closely interrelated. In particular, there are several management systems related to housing that should be specifically pointed out. In houses with slatted floor and pits, manure can be stored in the house pit either for long-term or short-term periods. For long-term pit storage, excreta are

assumed in AMCLIM to be stored for two months (60 days) before being applied to the land. For short-term storage, excreta are removed from the pit daily and stored in a separate storage unit (also for the naturally ventilated barns) before ultimately being applied to the land. The specific in-situ storage management systems are determined by the MMS information in the GLEAM database.

For broiler housing with litter management, AMCLIM assumes that excretions remain in the houses for the entire year, being applied to land once being removed. It should be noted that the NH_3 emissions from in-situ storage are counted as part of housing emissions. In contrast, naturally ventilated barns are assumed to be cleaned daily so that excreta are removed from the house and are stored separately.

Livestock excreta removed from the houses are typically stored for a certain period before being applied to the land. However, the area of the storage facilities is uncertain. In the AMCLIM model, it is assumed that the area for manure storage (S_{storage}) is proportional to the housing area, which is expressed as:

$$S_{\text{storage}} = f_{\text{MMS}} f_{\text{store-housing}} S_{\text{housing}}, \tag{4.24}$$

where f_{MMS} is the fraction of manure that is removed for separate storage as part of the MMS. The ratio of storage area to housing area ($f_{\text{store-housing}}$) varies depending on the specific management system. The ratio is set to be 0.5 for liquid manure storage and 0.25 for solid manure storage, and 2.5 for lagoon management, given that liquid manure storage requires a larger area because the volumes are larger than those of solid manure.

In AMCLIM, it is assumed that the stored manure is kept for 180 days and then is applied to the land twice a year during the spring and autumn planting seasons, respectively. The application date is based on the average value of the crop calendars for 18 spring crops and 4 winter crops (see Section 2.4.1, 3.2.3.2 and Appendix B8). For slurry application, the application rate is assumed to be 3 mm of slurry, which is equivalent to a recommended rate of 30 tons per hectare. For solid manure application, a moderate fertilization rate of 10 tons per hectare is used. The N pools and the water pool are calculated accordingly. It should be noted that all stored manure, with the exception of manure in lagoons, is assumed to be applied to agricultural lands. The lagoon system is a small fraction among all management systems, and manure in this system is assumed not to be applied to land but to be kept in the lagoons in AMCLIM.

4.3 Results

4.3.1 Simulations for housing at the site scale

AMCLIM–Housing was applied at site scale and used the AFO monitored data to simulate site-specific NH_3 emissions from pig and chicken houses. The AFO monitored data were gathered by the US EPA as a study of emissions from several types of livestock from 2007 to 2010 (Lim et al., 2010a; Wang et al., 2010). Four houses with slatted floor and pit storage from a pig farm in Indiana (site IN3B) and two layer houses from a chicken farm in North Carolina (site NC2B) were selected for the simulations, as listed in Appendix B9. The AFO

datasets provided animal data and daily mean environmental data for the two sites. Animal data included animal numbers, body weight and biomaterial data. Environmental data included indoor and outdoor temperature and relative humidity and the interior ventilation given as an airflow rate in $m^3\ s^{-1}$. To keep simulations continuous, missing values in the environmental data due to the unavailable measurements were filled by linear interpolation method. AMCLIM–Housing used excreted N that was determined from the livestock excreta data (as shown in Appendix B6) as an input, together with the indoor environmental data. Further information about the pig farm and the chicken farm can be found in USEPA AFOs reports (Lim et al., 2010a; Wang et al., 2010). It is worth noting that the evaluations focused on NH_3 emissions from housing, as the processes involved in manure storage are similar to those in housing, and there were limited available measurements for NH_3 emissions from manure storage. Additionally, the land simulations for synthetic fertilizer application were evaluated against the GRAMINAE experiment discussed in Chapter 3.

4.3.1.1 Pig houses with slat and pit

Figure 4.2 shows the results of simulated NH_3 emissions from a pig house with slatted floor and pit storage, along with comparisons to measurements, stocking data and the indoor environments (other simulations shown in Appendix D1). The simulated period is for two years from 1 July 2007 to 31 July 2009. Gaps shown in the figure represent unavailable measurements, while the model was kept running to produce a continuous output. The indoor temperature of the pig house range between 20 to 30 °C, showing moderate daily and seasonal variations, with higher temperature in summer than winter. There are two obvious temperature drops in March 2008 and March 2009 due to the emptying of pigs from the house as illustrated in Figure 4.2b. This also leads to low values of TAN

concentration on slats for the simulation periods. In contrast, the airflow rate inside the house shows significant seasonal variabilities, with higher ventilation occurring in summer and lower ventilation in winter. The relative humidity exhibits strong daily variations, ranging from 40 % to 80 %.

There were several growth cycles during the simulated period (Fig 4.2b). Over 2000 weaner pigs started in the house, and half of the pigs were moved to other house after three to four weeks once the pigs gained weight (see Appendix D1). As a result, the house had twice as many pigs at the beginning of each growth cycle. Approximately 1000 to 1200 pigs were kept in the house during the subsequent fattening stage.

Daily NH_3 emissions from the pig house generally increase as ventilation increases. High emissions occur mostly in summer, with the highest daily values of over 25 kg d^{-1} in July 2007. AMCLIM–Housing is able to reproduce the overall trend of NH_3 emissions in the first year from July 2007 to July 2008. However, it underestimates the winter emissions (January 2009) by 30 % and overestimates the summer emissions (June 2009 and July 2009) by a factor of two for the second year. The average modelled daily NH_3 emission is 10.4 kg d^{-1} (when measurements available; 9.9 kg d^{-1} for the entire simulation), compared to 8.8 kg d^{-1} recorded by the measurements. According to AMCLIM–Housing, 42 % of total excreted N volatilizes as NH_3. The slats and the pit contribute to 57 % and 43 % of the total emissions, with the average daily emissions being 5.7 kg d^{-1} and 4.2 kg d^{-1}, respectively. As shown in Figure 4.3d, simulated NH_3 emission originating from the slats is typically larger than from the pits, especially in summer when the ventilation is high. Slat NH_3 emissions increase periodically throughout the simulated period, which is closely associated with the animal mass of the house. The pit has been cleaned for a few times as

indicated by the blue dashed lines in Figure 4.2d and 4.2e. Modelled TAN concentrations on the slats are compared with the measurements, as well as the N concentrations in the pit, with reasonably close agreement being found between the modelled and measured values (Fig 4.2e).

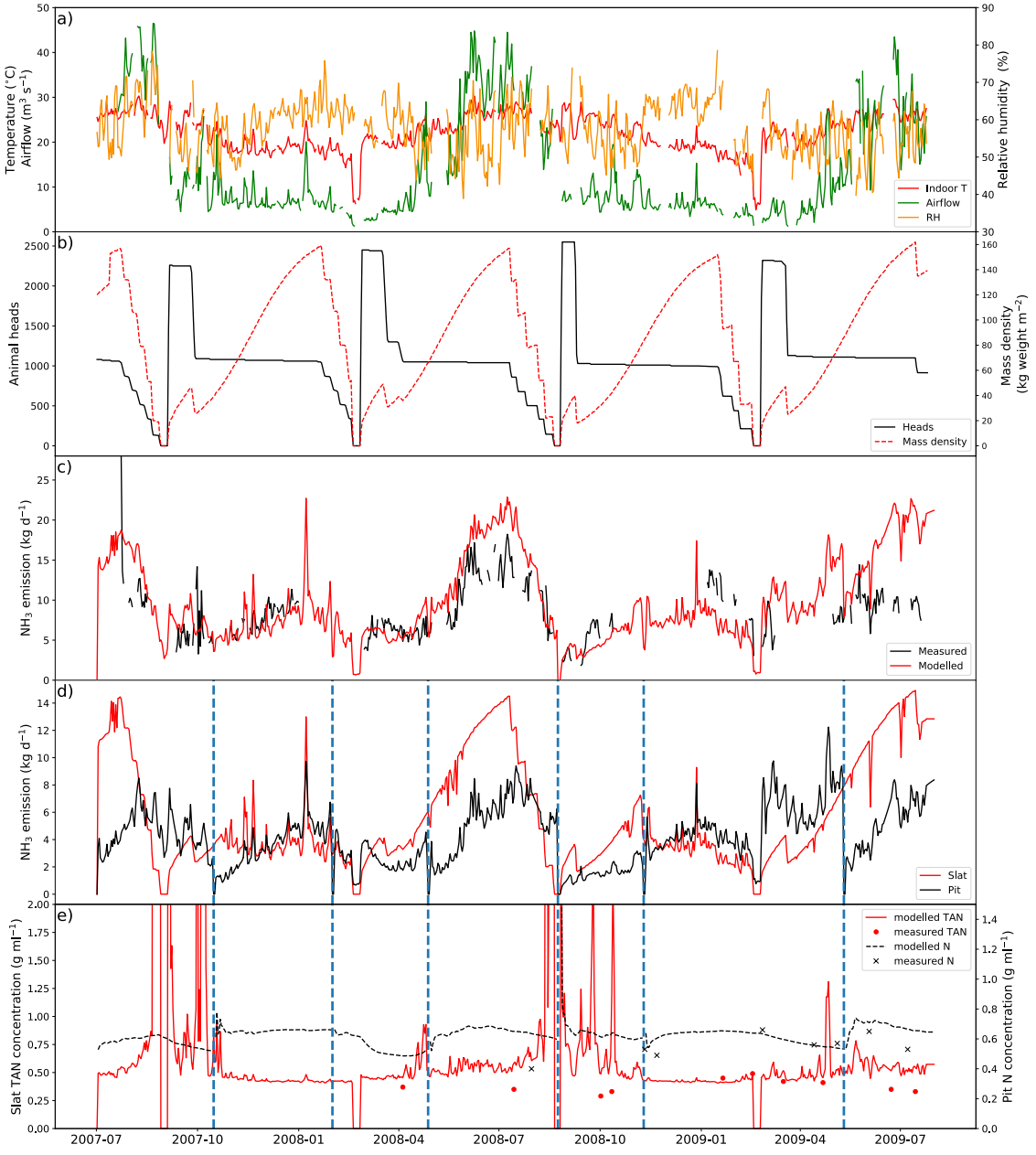
a)
Temperature (°C)
Airflow (m³ s⁻¹)
Relative humidity (%)
Indoor T
Airflow
RH
b)
Animal heads
Mass density (kg weight m⁻²)
Heads
Mass density
c)
NH3 emission (kg d⁻¹)
Measured
Modelled
d)
NH3 emission (kg d⁻¹)
Slat
Pit
e)
Slat TAN concentration (g ml⁻¹)
Pit N concentration (g ml⁻¹)
modelled TAN
measured TAN
modelled N
measured N
2007-07
2007-10
2008-01
2008-04
2008-07
2008-10
2009-01
2009-04
2009-07

Figure 4.2. Site simulations of House 1 in a pig farm at site IN3B, Carroll, Indiana, from 01 July 2007 to 31 July 2009. (a) Measured daily mean indoor temperature, airflow rate, and relative humidity of the house. (b) Animal heads and mass density of the house. (c) Comparison between modelled NH_3 emissions and calculated NH_3 emissions from measured indoor concentrations. (d) Modelled NH_3 emissions from the slats and the pit. (e) Comparisons between measured and modelled TAN concentration of the slats and between measured and modelled N concentration of the pit. Vertical blue dashed lines refer to excreta removal from the pit. See Appendix D1 for results from other pig houses.

4.3.1.2 Layer house

Figures 4.3 shows the simulated NH_3 emissions and indoor concentrations of a layer house compared with the measurements, along with indoor conditions and modelled N species (other simulations shown in Appendix D1). The indoor environments of the layer house are similar to the pig house, with temperature being largely maintained between 20 to 30 °C throughout the year and ventilation working intensively in hot summer. Relative humidity inside the layer house shows strong daily variations, ranging between 40 to 80 %.

The simulated period is from 15 March 2008 to 15 March 2009. The house was fully occupied by more than 90 000 layers for most of the time and was only emptied once (on 04 April 2008) for three weeks. Overall, the model captures the major changes of NH_3 emissions and indoor concentrations well over the simulation period. High emissions occur in summer as the ventilation increases, with the emissions peaking in early June 2008. The maximum daily NH_3 emission is more than 150 kg d^{-1}, and AMCLIM–Housing roughly reproduces this value but with a lag of ~5 days, in the timing of the peak in early June 2008. The average daily emission of NH_3 estimated by the model is 63.6 kg d^{-1} (when measurements available; 62.4 kg d^{-1} for the entire simulation), compared to 54.4 kg d^{-1}

reported by the measurements. Approximately 34 % of total excreted N is lost due to NH_3 emissions according to the simulation.

The indoor NH_3 concentrations show an opposite trend to the emission, which is inversely related to the ventilation. The indoor NH_3 level is typically lower than 10 mg m^{-3} when the airflow rate is high in summer and was much higher in the winter when the ventilation decreases, reaching to around 30 mg m^{-3} from November 2008 to February 2009. AMCLIM–Housing replicates the measured indoor NH_3 concentration well. However, the model largely underestimates both the emissions and concentrations in the first simulated month before the house is emptied. The NH_3 concentration at the surface is much higher than the indoor concentrations, ranging from 0.5 to 4.0 g m^{-3} (500 to 4000 mg m^{-3}), which generates a concentration gradient that drives the emission fluxes.

As shown Figure 4.3c, the uric acid pool in the excreta gradually increases in the first three months of the simulation and then generally stabilizes in the remaining period. There are two decreases in the simulated uric acid pool, with the first drop due to the emptying of the house in early April 2008 and the second due to a sharp increase of indoor temperature that accelerates the hydrolysis process in late May 2008. By comparison, the TAN pool accumulates throughout the year, building up to about 7 g N m^{-2} at the end of the simulation. It is notable that the variations in surface concentration of NH_3 are similar to those in NH_3 emissions. This is because the litter resistance (8640 s m^{-1}) is much larger than the housing resistance that range between 200 to 600 s m^{-1}. As a result, the total resistances show small variability. The NH_3 emissions are mainly constrained by the litter resistance, so the emissions and concentrations broadly display the same feature.

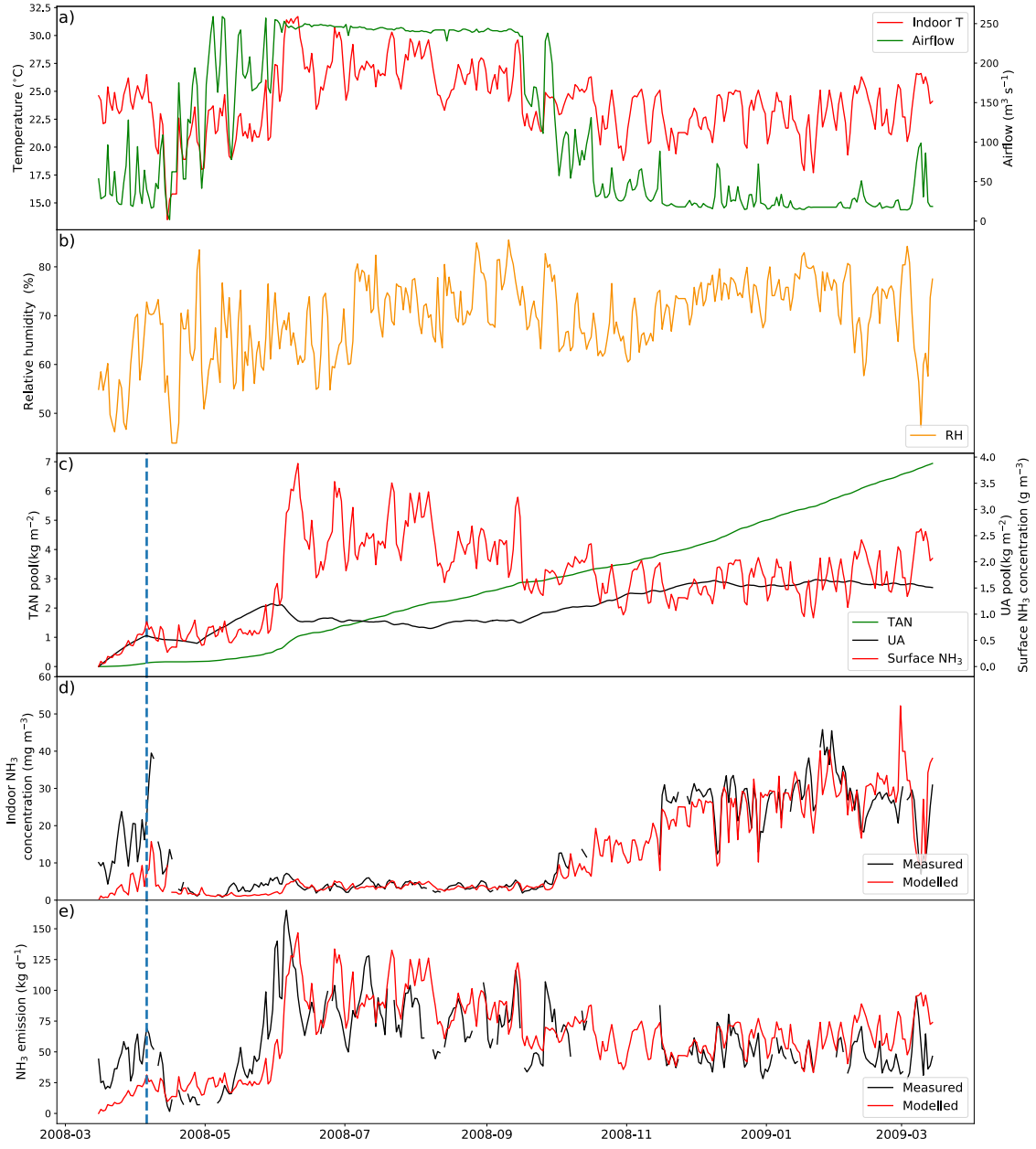
a)
Indoor T
Airflow
Temperature (°C)
Airflow (m³ s⁻¹)
b)
Relative humidity (%)
RH
c)
TAN pool(kg m⁻²)
UA pool(kg m⁻²)
Surface NH₃ concentration (g m⁻³)
TAN
UA
Surface NH₃
d)
Indoor NH₃ concentration (mg m⁻³)
Measured
Modelled
e)
NH₃ emission (kg d⁻¹)
Measured
Modelled
2008-03
2008-05
2008-07
2008-09
2008-11
2009-01
2009-03

Figure 4.3. Site simulations of House A in a layer farm at site NC2B, Nash, North Carolina, from 15 March 2008 to 15 March 2009. (a) Measured daily mean indoor temperature and airflow rate of the house. (b) Measured daily mean relative humidity of the house. (c) Modelled TAN pool and UA pool. (d) Comparison between measured and modelled indoor NH_3 concentrations of the house and surface NH_3 concentrations. (e) Comparison between modelled NH_3 emissions and calculated NH_3 emissions from measured indoor concentrations. Vertical blue dashed lines refer to emptying of the house.

4.3.1.3 Sensitivity tests for model parameters of AMCLIM–Housing

Sensitivity tests were conducted to examine the effects of changes in model parameters on the simulated NH_3 emission from pig and chicken housing. Nine model parameters with varying ranges were selected for the sensitivity analysis, based on expert judgement, and the corresponding percentage changes in the NH_3 emissions are highlighted in Table 3.3. The pH of excreta used in AMCLIM is identified to be the most important parameter which has significant impacts on the NH_3 emissions, especially for layer chicken. Varying the evaporation of water in animal houses (F_{evap}) by a factor of 2 only results in very small changes in emissions compared with other parameters. Moreover, changes in NH_3 emissions from layer chicken housing are almost negligible when varying the indoor NH_3 concentration by a factor of 2 or set to a constant zero, which demonstrates the feasibility of Equation 4.23 that neglects the indoor NH_3 concentration in global simulations for housing.

The NH_3 emissions from pig and layer chicken housing change by the same extent as the changes in N excretion rates ($F_{excretN}$). The impact of the housing resistance ($R_{g,\ house}$) on NH_3 volatilization in the animal house of pigs and layer chicken is different: NH_3 from

layer chicken housing is much less influenced by the housing resistance than pig housing. In contrast, the litter resistance (R_{litter}) plays a more dominant role in affecting the emission than the housing resistance for the layer chicken. The partitioning coefficient for TAN adsorption on excreta solids (K_d) is found to be important for NH_3 emission from layer chicken housing. Excluding the adsorption leads to a 60 % of increase of NH_3 emissions, while doubling the adsorption results in nearly 30 % of less NH_3. Doubling the uric acid hydrolysis rate (K_{UA}) leads NH_3 emissions to increase by 9 %, while the emissions decrease by 15 % if halved the hydrolysis rate.

For pig housing, varying the excreta water (F_{urine} and $F_{fecal\ water}$) by 20 % results in around 5 % changes in NH_3 emissions. Conversely, doubling or halving the urea hydrolysis constant (k_h; details given in Appendix A1) almost has no impacts on the NH_3 emission. Increasing the gap space (f_{gap}) from 0.2 to 0.3 of the house leads NH_3 emissions to decline by 8 %, while the NH_3 emission increases by 9 % when decreasing the gap space to 0.1.

Although the site simulations and the sensitivity tests were only conducted for the housing in this chapter, it still provides valuable insights on how model parameters affect the simulated emissions and how AMCLIM respond to varying processes. AMCLIM was then applied to the global scale to simulate NH_3 emissions from global pig and poultry farming.

Table 4.3. Percentage changes in NH_3 emissions from pig and layer housing in the sensitivity tests for the parameters in AMCLIM.

Model parameters	Value tested	ΔNH_3 emission % (pig)	ΔNH_3 emission % (layer)
$F_{excretN}$	+10 %	+10.0	+10.0
	–10 %	–10.0	–10.0
pH of excreta	+0.5	+22.1	+46.1
	–0.5	–37.4	–50.4
F_{evap}	0.5×	–3.4	–1.3
	2.0×	+2.0	+0.6
$R_{G,\ house}$	0.5×	+15.4	+1.1
	2.0×	–21.1	–2.0
R_{litter}	0.5×	–	+32.3
	2.0×	–	–33.1
K_d	+100 %	–	–27.5
	–100 %	–	+59.7
K_{UA}	0.5×	–	–14.5
	2.0×	–	+9.0
F_{urine} and $F_{fecal\ water}$	+20 %	–5.6	–
	–20 %	+4.1	–
k_h	0.5×	–0.5	–
	2.0×	+0.03	–
f_{gap}	+0.1	–7.9	–
	–0.1	+8.9	–
χ_{in}	0	–	+0.4
	0.5×	–	+0.2
	2.0×	–	–0.4

$F_{excretN}$ – total N excretion rate from the livestock; F_{evap} – evaporation flux of water; $R_{G,\,house}$ – resistance for NH_3 volatilization in the house; R_{litter} – poultry litter resistance; K_d – adsorption coefficient of TAN on excreta solids; K_{UA} – uric acid hydrolysis rate; F_{urine} – water from urination; $F_{fecal\ water}$ – water in feces; k_h – urea hydrolysis constant; f_{gap} – gap space of the slats; χ_{in} – indoor concentration of NH_3

4.3.2 Global simulations for pig farming

4.3.2.1 Annual NH_3 emissions from pig housing

The AMCLIM model was applied at global scale as described in Section 4.2.5. It is estimated that NH_3 emissions from global pig housing are 2.37 Tg N yr^{-1} in 2010 and 2.43 Tg N yr^{-1} in 2018. Total excreted N from pigs is 13.51 Tg N yr^{-1} in 2010 and slightly decreases to 13.43 Tg N yr^{-1} in 2018, with NH_3 emissions accounting for 17.5 % and 18.1 % of the excreted N in the two simulated years, respectively.

Figure 4.4 shows the geographical distributions of NH_3 emissions from pig housing and the volatilization rates for 2010 and 2018. The spatial distributions of both emissions and volatilization rates are similar for both years, with the highest emissions occurring in Brazil, China, northeastern US and Europe. Highest NH_3 volatilization rates of over 35 % are found in Australia, US, Thailand, Malaysia, the northern Africa and the northern South America. European countries and Brazil also show relatively high volatilizations rates of over 20 %, while the rest of the world show low to moderate volatilization, ranging from 5 to 20 %. China, with the highest pig housing emissions, generally have low simulated

volatilization rates of around 10 %. In contrast, Australia shows high volatilization but low emissions.

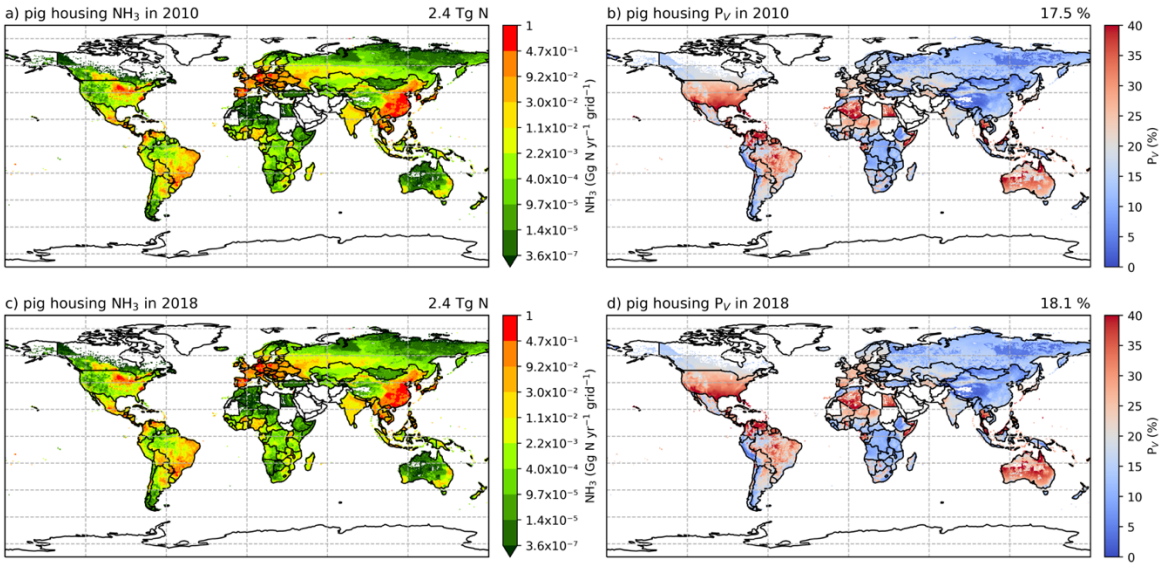

Figure 4.4. Simulated (a) annual global NH_3 emissions (Gg N yr^{-1} $grid^{-1}$) from pig housing in 2010. (b) Percentage of excreted N from pigs that volatilizes (P_V) as NH_3 in 2010. (c) NH_3 emissions (Gg N yr^{-1}) from pig housing in 2018. (d) P_V rates for pig housing in 2018. The resolution is 0.5º × 0.5 º.

Statistical data of estimated NH_3 emissions and volatilization rates for the three pig production systems are presented in Table 4.4. Both industrial and backyard pigs excrete more than 5 Tg N yr^{-1} in 2010 and 2018, while excreted N from intermediate pigs was smaller, which is due to the animal population. Among the three production systems, industrial pigs are the largest emitter group, contributing to over 65 % of estimated housing emissions. Industrial pig housing also shows the highest volatilization rates, with nearly

30 % of excreted N lost due to NH_3 emissions in both simulated years. Backyard pigs are the second largest emitter group, which are responsible for about 25 % of housing emissions, with around 10 % of excreted N volatilized as NH_3. Intermediate pigs have similar volatilization rates of about 10 % as backyard pigs but only contribute less than 10 % of housing emissions.

Table 4.4. Total excreted N (Tg N yr^{-1}), NH_3 emissions (Tg N yr^{-1}), and volatilization rates (%) from housing for three pig production systems.

Production system	Year	Total excreted N (Tg N yr^{-1})	NH_3 from housing (Tg N yr^{-1})	Average P_V (%)
Industrial	2010	5.73	1.55	27.1
	2018	5.68	1.60	28.2
Intermediate	2010	2.18	0.22	10.1
	2018	2.16	0.22	10.2
Backyard	2010	5.60	0.60	10.7
	2018	5.59	0.61	10.9
Total	2010	13.51	2.37	17.5
	2018	13.43	2.43	18.1

4.3.2.2 Annual NH_3 emissions from pig manure management

According to AMCLIM–MMS, NH_3 emissions resulted from pig manure management are 1.0 Tg N yr^{-1} in both 2010 and 2018. As shown in Figure 4.5, high emissions occur regions with high housing emissions, such as China and Europe. High volatilization rates of over 30 % for pig manure management are found in India, northwestern Australia, Southeast Asia, Africa and several countries in South America, while other regions typically have volatilization rates less than 20 %.

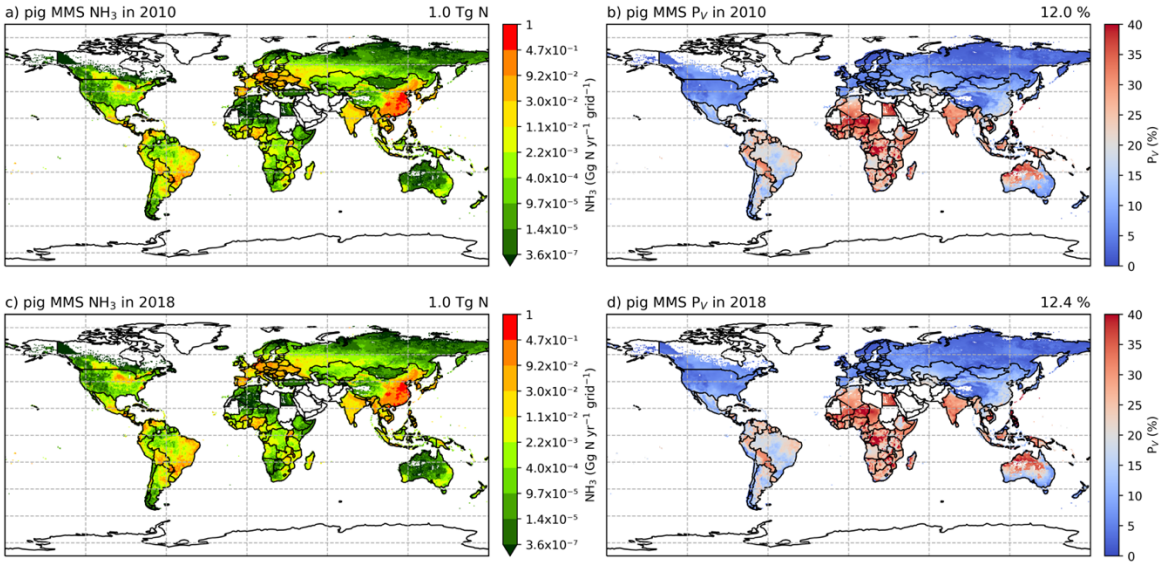

Figure 4.5. Simulated (a) annual global NH_3 emissions (Gg N yr^{-1}) from pig manure management in 2010. (b) Percentage of managed N in pig manure that volatilizes (P_V) as NH_3 in 2010. (c) NH_3 emissions (Gg N yr^{-1}) from pig manure management in 2018. (d) P_V rates for pig manure management in 2018.

Based on the MMS data from GLEAM2 and simulations using AMCLIM–MMS, more than 2.7 Tg N yr^{-1} excreted by pigs are either burned as fuel or lost to the environment through practices like dumping and sewage (together termed as "unmanaged" in Table 4.5) for both simulated years, accounting for approximately 20 % of total excreted N from pigs. For manure that are stored or left on lands, about 12 % of N volatilizes as NH_3 from a total managed 8.3 Tg N yr^{-1}. Manure N under management for backyard pig manure is 3.6 Tg N yr^{-1} and leads to 0.6 Tg N yr^{-1} of NH_3 emissions, accounting for 60 % of total estimated manure management emissions. Managed manure N for industrial pigs is comparable to that for backyard pigs, but the volatilization rates are about 7 % compared to 17 % for backyard pigs. The higher volatilization rates of manure management for backyard pigs are due to more manure that is left on land instead of being stored. The intermediate production system results in less than 0.2 Tg N yr^{-1} of NH_3 emissions in both 2010 and 2018, with volatilization rates of 12 %.

Table 4.5. Total managed N (Tg N yr^{-1}), NH_3 emissions (Tg N yr^{-1}), and volatilization rates (%) from manure management for three pig production systems. * Total unmanaged N (Tg N yr^{-1}) includes manure N that is dumped to rivers and fishponds and enters public sewage. Manure used as fuel are also included in unmanaged N (although this is technically managed but is not simulated in AMCLIM).

Production system	Year	Total managed N (Tg N yr^{-1})	NH_3 from MMS (Tg N yr^{-1})	Average P_V (%)	*Total unmanaged N (Tg N yr^{-1})
Industrial	2010	3.55	0.24	6.8	0.63
	2018	3.47	0.24	6.9	0.61
Intermediate	2010	1.23	0.15	12.2	0.73
	2018	1.22	0.15	12.3	0.72
Backyard	2010	3.58	0.62	17.3	1.42
	2018	3.57	0.63	17.6	1.41
Total	2010	8.36	1.01	12.0	2.78
	2018	8.26	1.02	12.4	2.74

4.3.2.3 Annual NH_3 emissions from pig manure application to land

In 2010, estimated NH_3 emissions from pig manure application to land are 1.9 Tg N yr^{-1}, indicating that 33.9 % of applied manure N is lost due to NH_3 emissions. As shown in Figure 4.6, high emissions mostly occur in China and Europe, and most of the regions show high volatilization. Highest volatilization rates that exceeded 50 % are found in northern

and southern Africa, India and western Australia. China, Southeast Asia, Europe, US and South America showed slightly lower volatilization rates but also higher than 30 % (Fig 4.6). Only certain countries in Africa, Canada, Scandinavia and northern and eastern Russia exhibit lower volatilization rates less than 30 %.

By comparison, land application of pig manure results in 1.7 Tg N yr^{-1} of NH_3 emissions for the year 2018, with high emissions found in the same regions as in 2010, such as China and Europe. Globally, 34 % of applied N volatilizes as NH_3. The regional pattern of P_V for the year 2018 is similar compared to 2010 but shows stronger spatial variation.

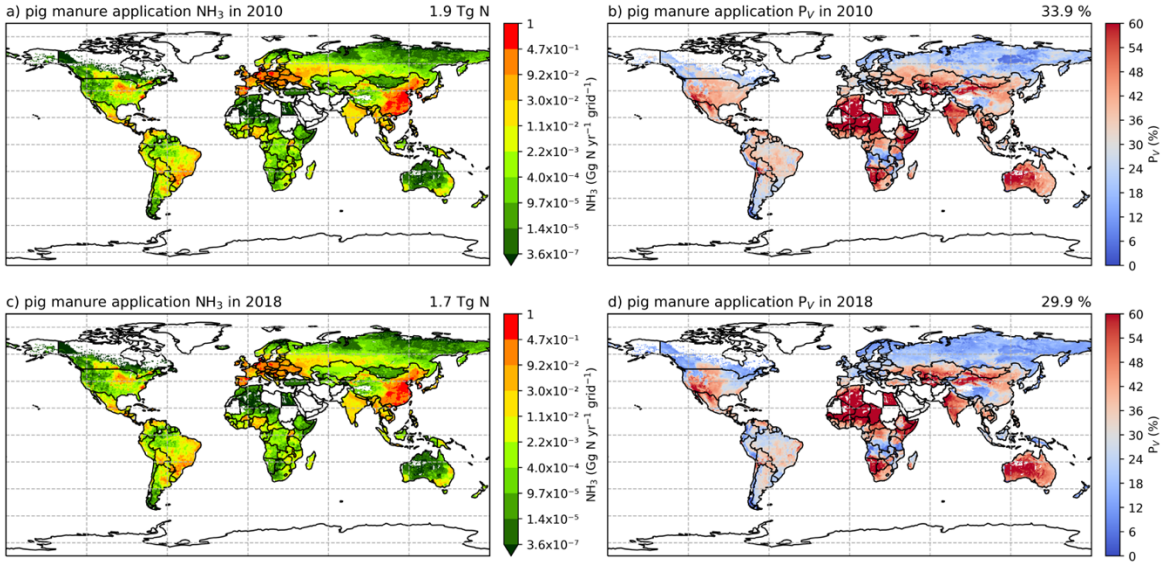

Figure 4.6. Simulated (a) annual global NH_3 emissions (Gg N yr^{-1}) from pig manure application in 2010. (b) Percentage of applied N in pig manure that volatilizes (P_V) as NH_3 in 2010. (c) NH_3 emissions (Gg N yr^{-1}) from pig manure application in 2018. (d) P_V rates for pig manure application in 2018.

As presented in Table 4.6, all three production systems show relatively high volatilization rates of manure application to land, particularly in 2010. Overall, volatilization rates of 2018 are lower than those of 2010 for all production systems. The backyard production system is responsible for the largest emissions (over 40 %). Industrial pigs contribute comparable emissions to backyard pigs, while the around 20 % of emissions are from the land application of intermediate pig manure.

Table 4.6. Total applied N (Tg N yr^{-1}), NH_3 emissions (Tg N yr^{-1}), and volatilization rates (%) from manure application to land for three pig production systems.

Production system	Year	Total applied N (Tg N yr^{-1})	NH_3 from application (Tg N yr^{-1})	Average P_V (%)
Industrial	2010	2.45	0.72	29.4
	2018	2.38	0.59	24.6
Intermediate	2010	1.00	0.37	37.0
	2018	0.98	0.32	32.7
Backyard	2010	2.26	0.85	37.6
	2018	2.25	0.77	34.2
Total	2010	5.71	1.94	33.9
	2018	5.61	1.68	29.9

4.3.2.4 Nitrogen flows and NH_3 emissions of global pig farming

Figure 4.7 illustrates the N flows of global pig farming for the reference year 2010, which are allocated to housing, manure management and application to land, with a focus on NH_3 emissions. Global total excreted N from pigs is 13.51 Tg N yr^{-1} in 2010. All excreted N is allocated to housing, which resulted in NH_3 emissions of 2.37 Tg N yr^{-1}. A further 2.78 Tg N yr^{-1} is lost because of manure burning (0.50 Tg N yr^{-1}) and unmanaged manure (2.27 Tg N yr^{-1}). The remaining 8.36 Tg N yr^{-1} undergoes management and leads to 1.01 Tg N yr^{-1} of NH_3 emission. A small part (0.33 Tg N yr^{-1}) is either washed off, nitrified or left in lagoon systems, while 1.32 Tg N yr^{-1} are left on land without being stored. Subsequently, 5.71 Tg N yr^{-1} from storage are applied to land, which results in 1.94 Tg N yr^{-1} of NH_3 emission, 2.87 Tg N yr^{-1} entering soils and plants and 0.90 Tg N yr^{-1} being depleted by other processes (e.g., runoff, nitrification, leaching and diffusion to deep soils). Manure left on land was assumed to be completely incorporated into soils or used by plants and was not simulated anymore by AMCLIM. Nitrified N was also not further simulated in the model.

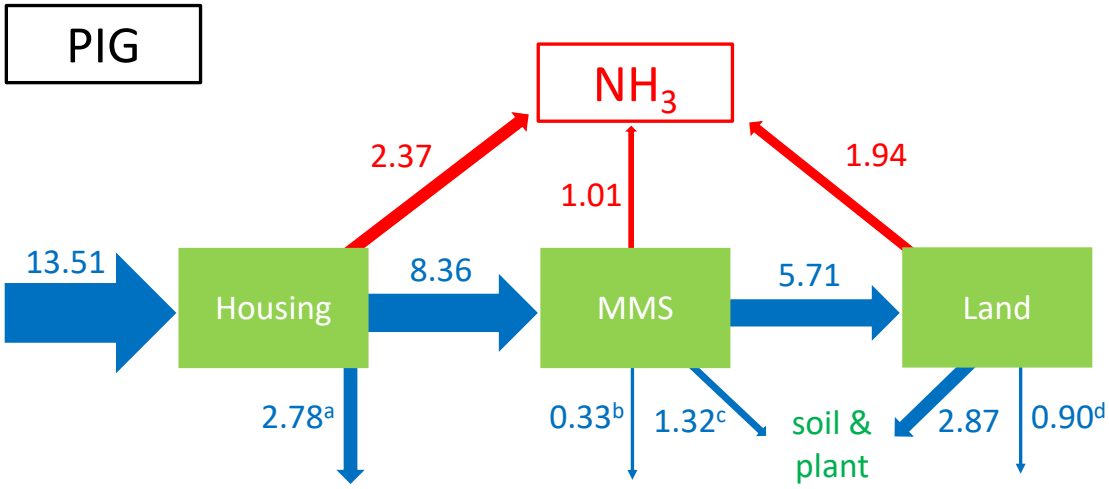

[a]manure used as fuel (0.50) unmanaged manure (2.27)
[b]runoff (0.02) nitrification (0.27) lagoon (0.04)
[c]this 1.32 represents the amount of manure N left on land (not stored) and is not further simulated; NH_3 emission counted as MMS emissions
[d]runoff (0.19) nitrification (0.48) leaching & diffusion to deep soil (0.23)

Figure 4.7. Nitrogen budget of global pig farming including housing, manure management and application to land estimated by AMCLIM for the year 2010. Dark blue arrows are N flows. Red arrows represent NH_3 emissions. All numbers have the unit of Tg N yr^{-1}. Size of the arrows is proportional to the flux.

Global total NH_3 emissions from pig farming (in housing, manure management and land application) estimated by the AMCLIM model are 5.3 Tg N yr^{-1} in 2010 and 5.1 Tg N yr^{-1} in 2018, with 39.3 % and 38.2 % of excreted N lost due to NH_3 emissions in each year. Around 40 to 50 % of the emissions are from housing, while manure management and manure application result in 20 % and 30 to 40 % of emissions, respectively. As shown in Figure 4.8, high emissions are found across Brazil, China, India, Nigeria, northeastern US and Europe, as well as several countries in Southeast Asia. High volatilization rates can be

seen in India, Australia, southern US, northern and southern Africa and South America. Regions with high emissions are not always consistent with high volatilization. For example, the overall percentage volatilization in China is smaller than India, Australia and Africa. It is found that N lost through NH_3 volatilization can reach up to 70 % of total excreted N in some places, such as countries in northern Africa.

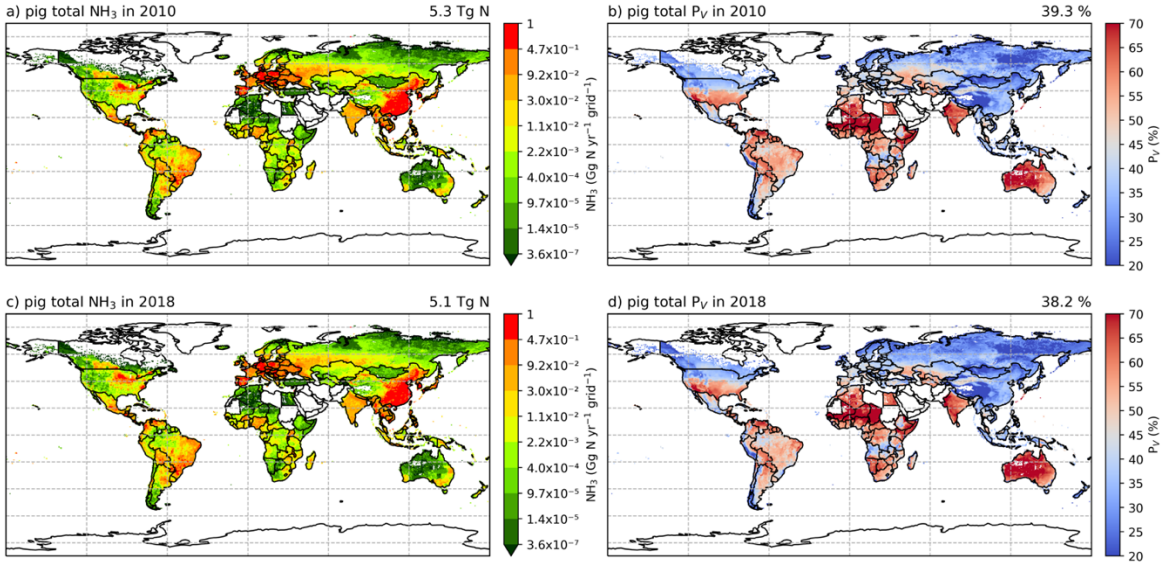

Figure 4.8. Simulated (a) annual global NH_3 emissions (Gg N yr^{-1}) from pig farming (including housing, manure management and manure application) in 2010. (b) Percentage of excreted N from pigs that volatilizes (P_V) as NH_3 in 2010. (c) NH_3 emissions (Gg N yr^{-1}) from pig farming in 2018. (d) P_V rates for pig farming in 2018.

As summarized in Table 4.7, industrial pigs contribute nearly 50 % of the total estimated emissions from pig farming, whereas intermediate and backyard pigs are responsible for 37 % and 13 %, respectively. Industrial pigs are not only the largest emitter group but also

have the highest volatilization rates of more than 40 %. For the two simulated years, estimated emissions and the overall volatilization rates are higher for 2010 than 2018 for all production systems.

Table 4.7. Total excreted N (Tg N yr^{-1}), total NH_3 emissions (Tg N yr^{-1}, including housing, manure management and application) and volatilization rates (%) from pig farming categorized between three pig production systems.

Production system	Year	Total excreted N (Tg N yr^{-1})	Total NH_3 emission (Tg N yr^{-1})	Average P_V (%)
Industrial	2010	5.73	2.50	43.6
	2018	5.68	2.43	42.7
Intermediate	2010	2.18	0.73	33.5
	2018	2.16	0.70	32.4
Backyard	2010	5.60	2.07	37.0
	2018	5.59	2.01	36.0
Total	2010	13.51	5.30	39.3
	2018	13.43	5.14	38.2

Estimated global monthly emissions of NH_3 from pig farming in 2010 and 2018 are shown in Figure 4.9. The seasonality of both years is very similar, with the highest emission occurring in April and a second emission peak in September. Emissions in JJA are less

varied compared to MAM and SON as shown in Figure 4.9. It is evident that the monthly variations are largely due to the emissions resulting from manure application, and emissions from housing and manure management are less varied throughout the year.

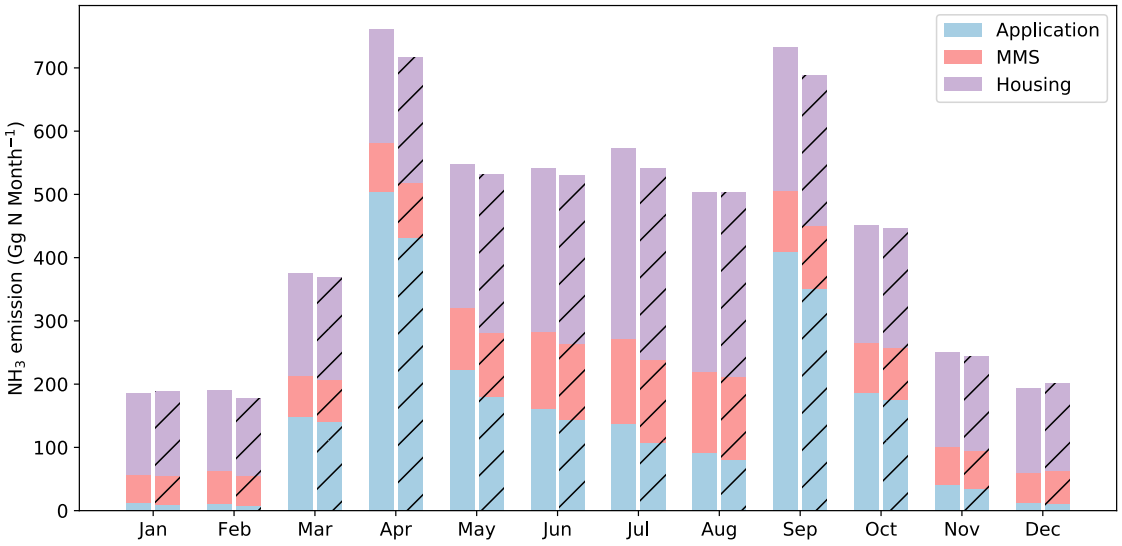

Figure 4.9. Global monthly NH_3 emissions (Gg N month^{-1}) from pig housing, manure management and manure application to land in 2010 and 2018 (hatched), simulated by AMCLIM.

4.3.3 Global simulations for poultry farming

4.3.3.1 Annual NH_3 emissions from chicken housing

According to simulations using AMCLIM–Housing, estimated NH_3 emissions from global chicken housing are 3.1 Tg N yr^{-1} and 3.2 Tg N yr^{-1} in 2010 and 2018, accounting for 27.8 %

and 28.2 % volatilization of total chicken excretal N, respectively. As shown in Figure 4.10, in both 2010 and 2018, highest emissions occur in China, India, Pakistan, the Middle East, Southeast Asia and Western Africa, with emission hot spots in southeast US and south Brazil. Highest NH_3 volatilization rates of around 40 % are found in tropical regions along the equator, such as northern South America, central Africa and Southeast Asia. Meanwhile, India and southeast China also show high volatilization rates of over 30 %. Northern Africa, the Middle East and western Russia have moderate volatilization, ranging between 20 to 30 %, while the other parts of the world have volatilization rates of less than 20 %.

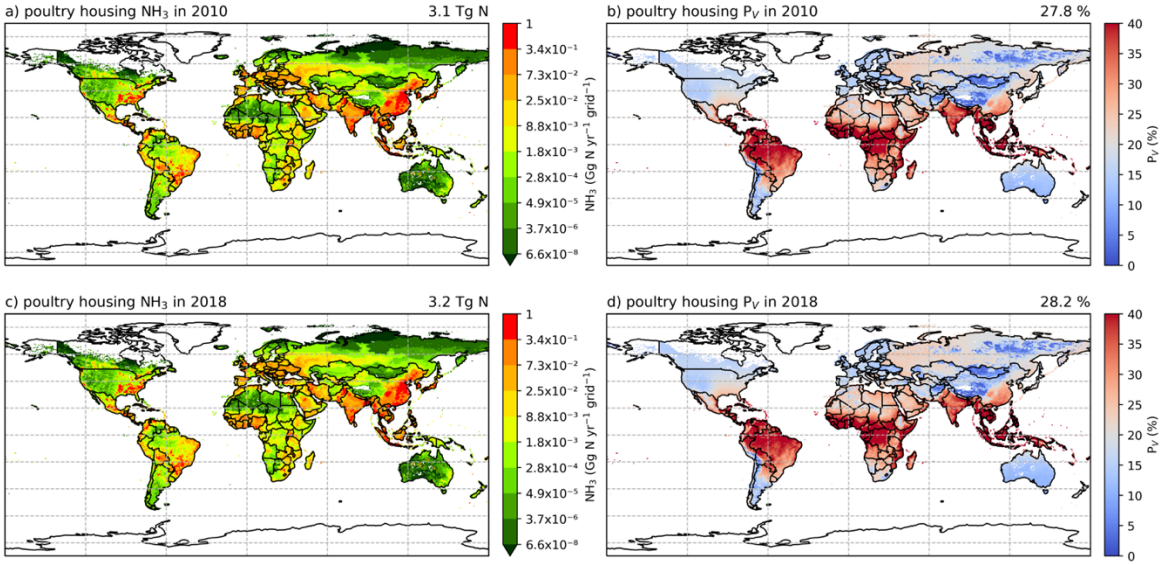

Figure 4.10. Same as Figure 4.4 but for chicken housing.

Estimated excreted N from chicken is 11.2 Tg N yr^{-1} in 2010 and 11.5 Tg N yr^{-1} in 2018. In both years, broiler chicken contribute over 1.3 Tg N yr^{-1} of estimated housing NH_3

emissions, which accounts for over 40 % of total housing emissions from chicken and is the largest among all three production systems (Table 4.8). More than 35 % and 20 % of housing emissions are from layer chicken housing and backyard chicken housing, respectively. Regarding the volatilization rates, over 30 % of excreted N volatilizes as NH_3 during housing for both layer chicken and backyard chicken, while broiler chicken housing has slightly lower volatilization rates of around 25 %.

Table 4.8. Total excreted N (Tg N yr^{-1}), NH_3 emissions (Tg N yr^{-1}) and volatilization rates (%) from housing for three chicken production systems.

Production system	Year	Total excreted N (Tg N yr^{-1})	NH_3 from housing (Tg N yr^{-1})	Average P_V (%)
Broiler	2010	5.37	1.32	24.7
	2018	5.47	1.37	25.1
Layer	2010	3.67	1.11	30.4
	2018	3.70	1.14	30.8
Backyard	2010	2.18	0.67	30.7
	2018	2.29	0.71	31.0
Total	2010	11.22	3.10	27.8
	2018	11.46	3.22	28.2

4.3.3.2 Annual NH_3 emissions from chicken manure management

Managing chicken manure results in 0.8 Tg N yr^{-1} of NH_3 emissions in 2010 and 2018 based on simulations using AMCLIM–MMS. As shown in Figure 4.11, the highest emissions occur in China, and high emissions are also found in India, Southeast Asia, with hot spots occurring in southeast US. Overall, less than 10 % of managed manure N is lost through NH_3 emissions in both simulated years. Volatilization rates are generally lower than 20 % across the globe, with larger values occasionally occurring in southeast Asia, Africa and the Middle East.

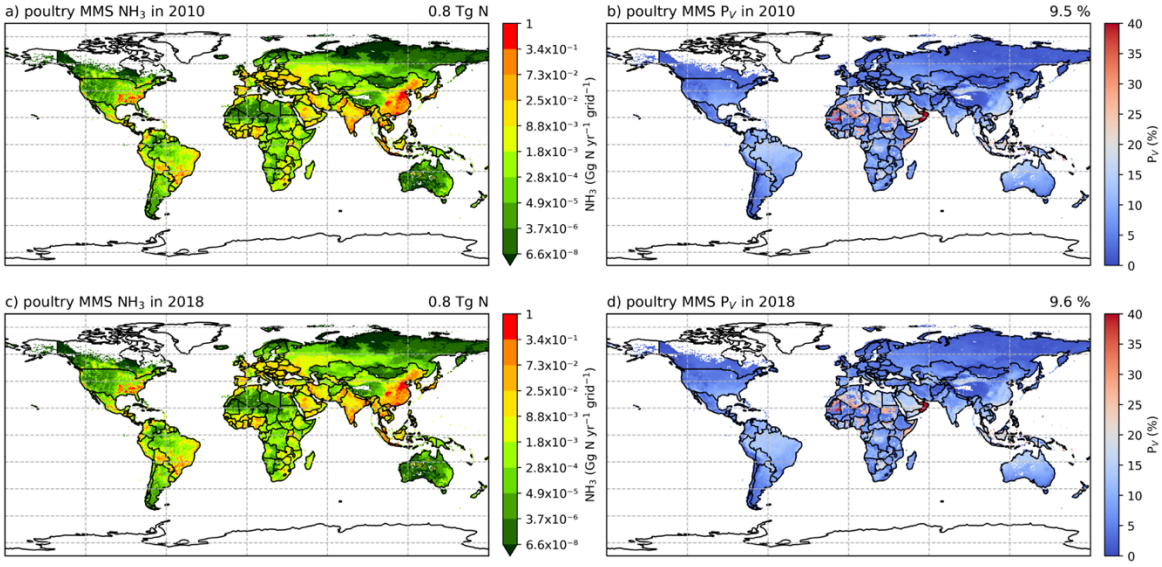

Figure 4.11. Same as Figure 4.5 but for chicken manure management.

According to the MMS data from GLEAM2 and simulations using AMCLIM–MMS, most of the chicken manure is under management compared to pigs. Layer chicken result in 0.5

Tg N yr^{-1} of NH_3 emissions, accounting for 60 % of total NH_3 emissions from manure management and have the highest volatilization rates of 18 % (Table 4.9). By comparison, broiler and backyard chicken have much lower volatilization rates of around 6 % and contribute less to NH_3 emissions than layer chicken, which together result in the remaining 40 % of NH_3 emissions (0.3 Tg N yr^{-1}).

Table 4.9. Total managed N (Tg N yr^{-1}), NH_3 emissions (Tg N yr^{-1}) and volatilization rates (%) from housing for three chicken production systems.

Production system	Year	Total managed N (Tg N yr^{-1})	NH_3 from MMS (Tg N yr^{-1})	Average P_V (%)
Broiler	2010	4.02	0.22	5.5
	2018	4.07	0.22	5.5
Layer	2010	2.55	0.46	18.2
	2018	2.55	0.47	18.5
Backyard	2010	1.50	0.09	6.0
	2018	1.58	0.09	5.7
Total	2010	8.07	0.77	9.5
	2018	8.20	0.78	9.6

4.3.3.3 Annual NH_3 emissions from chicken manure application to land

Annual NH_3 emissions from chicken manure application to land estimated by AMCLIM–Land are 0.9 Tg N yr^{-1} in 2010 and 0.8 Tg N yr^{-1} in 2018, accounting for 40.5 % and 37.6 % of applied manure N, respectively. As shown Figure 4.12, high emissions mainly occur in China, India, Iran, southeastern US and Europe. Highest volatilization rates that exceeded 50 % of total applied N can be seen in India, Australia, Mexico, part of US, northern and southern Africa and the Middle East in both 2010 and 2018. China, Europe and South America also show high volatilization rates of over 30 %. Volatilization rates are generally lower for the year 2018 than 2010, with obvious difference found in Southeast Asia.

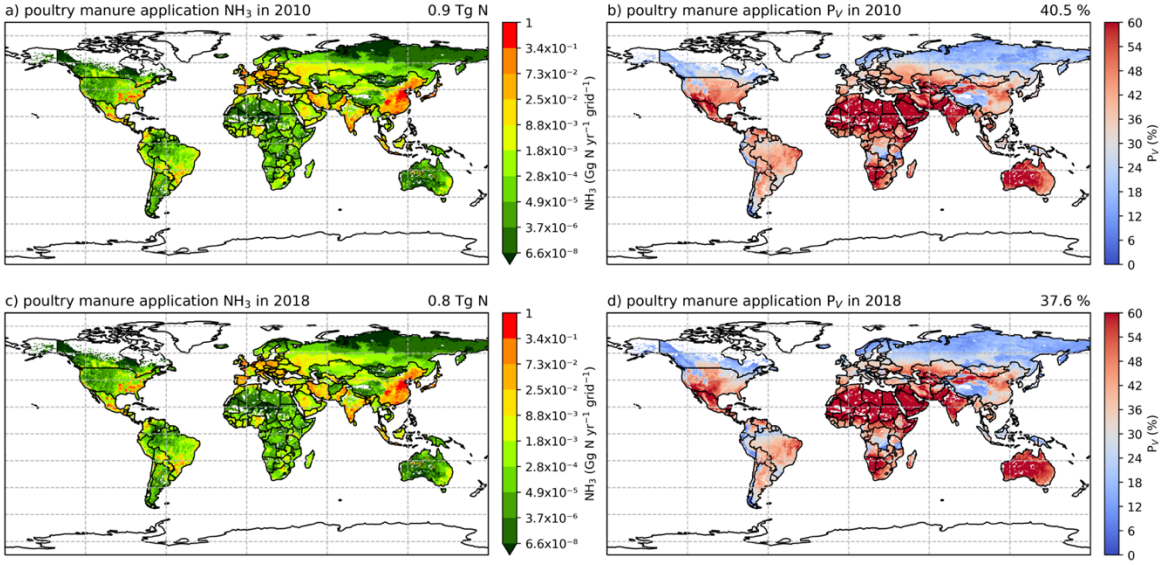

Figure 4.12. Same as Figure 4.6 but for chicken manure application to land.

Layer chicken dominate the N application to land and the associated NH_3 emissions, while broiler chicken only result in less than 10 % of total emissions (Table 4.10). The two production systems show similar volatilization rates in both years, with layer chicken having slightly higher values. As there is no manure from backyard chicken being stored according to the GLEAM MMS data, the applied manure N for this production system was zero in AMCLIM.

Table 4.10. Total applied N (Tg N yr^{-1}), NH_3 emissions (Tg N yr^{-1}) and volatilization rates (%) from manure application to land for three chicken production systems.

Production system	Year	Total applied N (Tg N yr^{-1})	NH_3 from application (Tg N yr^{-1})	Average P_V (%)
Broiler	2010	0.24	0.08	33.3
	2018	0.23	0.07	31.2
Layer	2010	1.92	0.79	41.1
	2018	1.91	0.73	38.4
Backyard	2010	--	--	--
	2018	--	--	--
Total	2010	2.15	0.87	40.5
	2018	2.14	0.80	37.6

4.3.3.4 Nitrogen flows and NH_3 emissions of global chicken farming

Nitrogen flows of global chicken farming for 2010 are shown in Figure 4.13. Global total excreted N from chicken is 11.22 Tg N yr^{-1} in 2010, which results in NH_3 emissions of 3.10, 0.77 and 0.87 Tg N yr^{-1} from housing, manure management and application to land, respectively. Only 0.04 Tg N yr^{-1} is burned as fuel and the majority of manure N (8.07 Tg N yr^{-1}) is managed. Nitrification and N loss associated with runoff are tiny (0.11 Tg N yr^{-1}) during chicken manure management. By comparison, a large fraction of manure N (5.04 Tg N yr^{-1}) is left on land rather than being stored, which is mostly from the deeplitter system of broiler chicken. Afterwards, 2.15 Tg N yr^{-1} of manure N from storage that is mainly from layer chicken is applied to land. In addition to NH_3 emission, 0.99 Tg N yr^{-1} entering soils and plants, and the remaining 0.29 Tg N yr^{-1} is nitrified or lost via runoff, leaching and diffusion to deep soils.

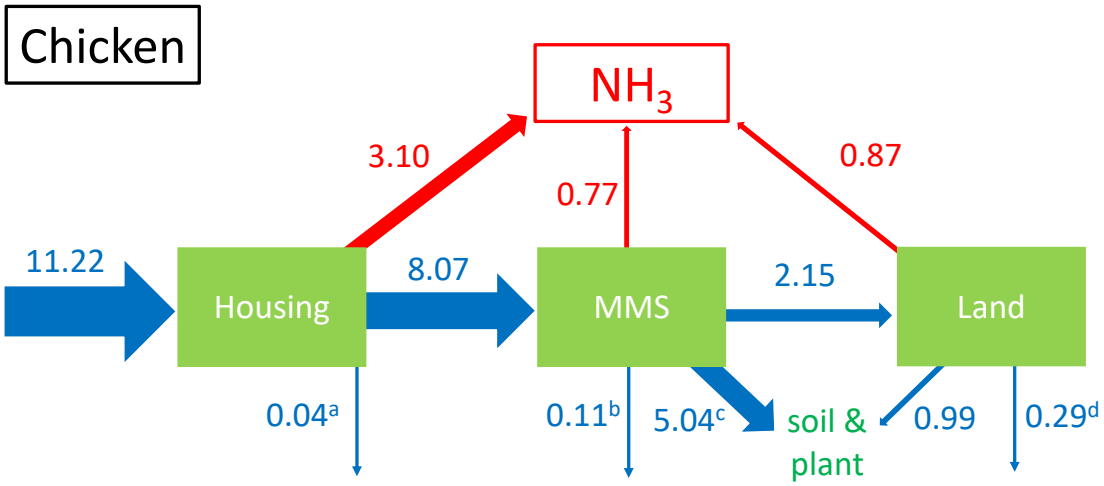

[a]manure used as fuel (0.04)
[b]runoff (0.01) nitrification (0.10)
[c]this 5.04 represents the amount of manure N left on land (not stored) and is not further simulated; NH_3 emission counted as MMS emissions
[d]runoff (0.08) nitrification (0.13) leaching & diffusion to deep soil (0.08)

Figure 4.13. The same as Figure 4.7 but for global chicken farming.

Using AMCLIM, it is estimated that the global NH_3 emissions from chicken farming are 4.8 Tg N yr^{-1} in 2010 and 2018, accounting for about 42 % of the total excreted N (Table 4.11). No clear differences are found between the two simulated years. Housing contributed to over two-thirds of total emissions, and both manure management and application are responsible for 15 to 20 % of emissions. As shown in Figure 4.14, high emissions occur in China, India, the Middle East, Europe, Southeast Asia and Western Africa, and high volatilization rates are mostly found in tropical regions along the equator, with up to 60 % of excreted N lost due to NH_3 emissions.

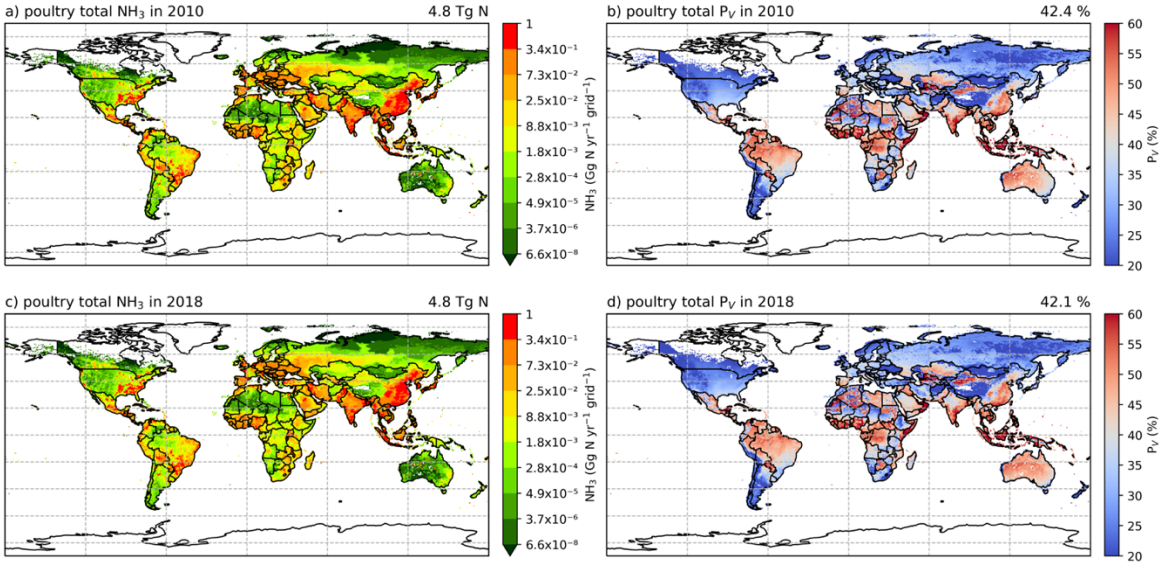

Figure 4.14. Same as Figure 4.7 but for chicken farming.

Among the three production systems, layer chicken are the largest emitter, which contributed approximately 50 % of total NH_3 emissions, followed by broiler chicken that are responsible for over 30 % of emissions (Table 4.11). Backyard chicken result in the lowest emissions of 0.8 Tg N yr^{-1}. Broiler chicken and backyard chicken have similar volatilization rates of over 30 %, while layer chicken show much higher volatilization rates, exceeding 60 %.

Table 4.11. Total excreted N (Tg N yr^{-1}), NH_3 emissions (Tg N yr^{-1}) and volatilization rates (%) from chicken farming (in housing, manure management and application to land) categorized between three chicken production systems.

Production system	Year	Total excreted N (Tg N yr^{-1})	Total NH_3 emission (Tg N yr^{-1})	Average P_V (%)
Broiler	2010	5.37	1.63	30.4
	2018	5.47	1.67	30.6
Layer	2010	3.67	2.37	64.6
	2018	3.70	2.35	63.4
Backyard	2010	2.18	0.76	34.9
	2018	2.29	0.80	34.9
Total	2010	11.22	4.76	42.4
	2018	11.46	4.82	42.1

Figure 4.15 shows the global monthly emissions of NH_3 from chicken farming in 2010 and 2018, with both years exhibiting generally the same seasonal variations. The highest emissions can be seen in July and the second highest emissions are in April, exceeding 0.5 Tg N $month^{-1}$. Emissions in MAM and JJA are generally larger than SON and DJF. Both manure application and manure management show more significant seasonal variability compared to housing, with MAM and JJA emissions being larger than other seasons.

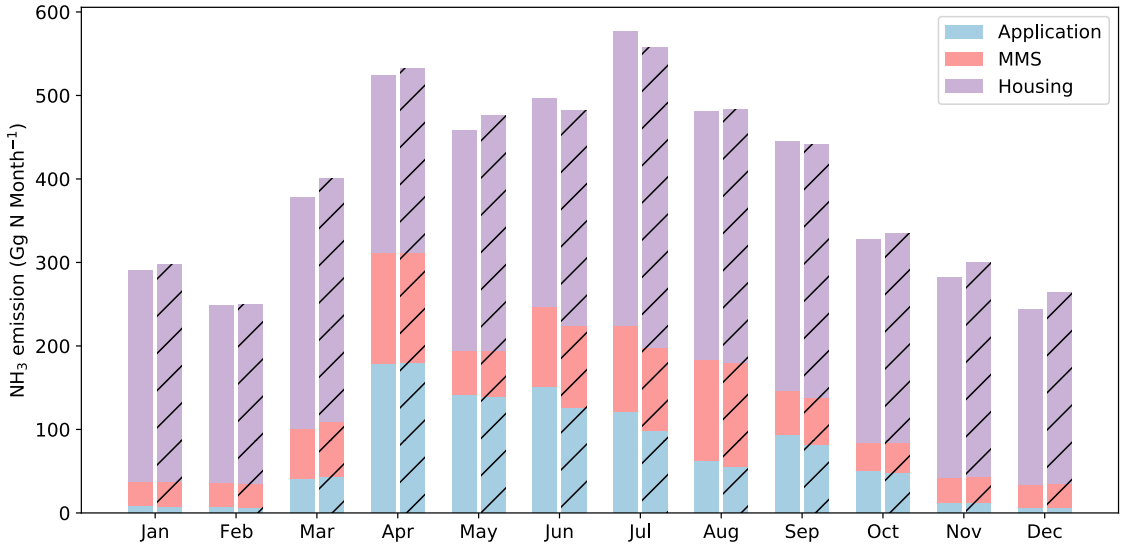

Figure 4.15. Same as Figure 4.8 but for chicken farming.

4.4 Discussion

4.4.1 General discussion

Ammonia emissions can occur from a variety of stages in livestock agricultural systems, from housing to subsequent manure storage and the ultimate spreading of manure. All three modules in the AMCLIM model are involved in simulating NH_3 emissions from pig and poultry farming.

AMCLIM–Housing was applied at the site scale to simulate pig and chicken housing emissions and provided reasonable estimates that had close agreement with the measurements. The NH_3 emissions are found to be strongly related to environmental conditions of the animal house, where emissions increase as inside temperature and ventilation increase. Meanwhile, management practices also play an important role in affecting the emission. Emissions of NH_3 vary with the growing cycles in the pig farm at site IN3B, and the removal of the excreta causes a short "stoppage" of emissions.

Although AMCLIM is a dynamical process-based model, results of its simulations can be converted into emissions factors. On the global scale, the estimated average NH_3 EF using AMCLIM is 5.5 kg N yr^{-1} $head^{-1}$ (2.8 to 9.4 kg N yr^{-1} $head^{-1}$ between the 10^{th} and 90^{th} percentile of global data) for pigs and 0.24 kg N yr^{-1} $head^{-1}$ (0.11 to 0.29 kg N yr^{-1} $head^{-1}$ between the 10^{th} and 90^{th} percentile of global data) for chicken. The EFs derived from AMCLIM are generally comparable to values from literature, with EFs ranging from 1.2 to 7.2 kg N yr^{-1} $head^{-1}$for pigs and 0.08 to 0.37 kg N yr^{-1} $head^{-1}$ for chicken (Yang et al., 2023). For housing-specific emissions, pigs have an average EF of 2.4 kg N yr^{-1} $head^{-1}$ (0.8 to 4.4 kg N yr^{-1} $head^{-1}$ between the 10^{th} and 90^{th} percentile), while the average EF for chicken is 0.15 kg N yr^{-1} $head^{-1}$ (0.08 to 0.21 kg N yr^{-1} $head^{-1}$ between the 10^{th} and 90^{th} percentile).

The spatial distributions of both emissions and the percentage volatilization rates show significant variations. High emissions coincide with high animal populations in countries and regions with intensive livestock farming, such as China, India, US and Europe. The volatilization rates differ across the globe due to a combined effect of environmental conditions and management practices. For example, high volatilization rates of chicken housing are found in the tropical regions along the equator, showing how hot and humid

conditions tend to cause larger emissions. Housing of industrial pigs show higher volatilization compared to intermediate and backyard pigs because the industrial pigs are kept in buildings with heating systems and excreta are kept longer in the houses as in-situ storage is available. Moreover, the pits for manure storage provides an additional emitting surface of NH_3.

Various manure management practices can lead to very different volatilization rates. For pig manure management, as shown in Appendix D3, manure that is left on land without much management results in much higher NH_3 emissions than manure that is stored either as liquid or solid manure. Regions including Africa, Southeast Asia and India clearly exhibit much higher total volatilization rates than other places because of warmer climate and because manure is less often stored for further use but is simple left on land without much further management. Conversely, manure storage with covering only leads to small NH_3 emissions.

As presented in the result section, the estimated volatilization rates of both pig and poultry farming for the year 2010 are very similar to the value for the year 2018. Specifically, NH_3 emissions from housing and manure management of both pigs and poultry show small differences between 2010 and 2018, with slightly higher P_V occurring in 2018 compared to 2010, indicating that 2018 is generally hotter than 2010. Such "stable" housing and manure management emissions are possibly due to largely controlled indoor environments of animal houses and storage barns compared with natural conditions. Enclosed animal houses have their own regulated temperature inside, and naturally ventilated barns are not as windy as outside and the floor temperature of these barns are less varied than air temperature. In contrast, emissions from land application of manure vary between the two years. There are

relatively large differences between the two years, with 2010 showing both higher emissions and volatilization rates than 2018. This annual trend of manure application to land is found to be consistent with synthetic fertilizer application, as discussed in Chapter 3. The relevant processes that govern the NH_3 emissions from land application are dependent on natural environmental conditions, and there are more N pathways, such as runoff, drainage and diffusion. As more processes are involved under natural conditions, NH_3 emissions may show larger variations. Simulations for synthetic fertilizer application indicates that the lower volatilization rates in 2018 than 2010 can be attributed to larger leaching and diffusive fluxes in 2018 that depletes the soil N and results in less significant NH_3 emissions. The different P_V of manure application to land between the two years can result from the same reason. Detailed analysis and further explanations are given in Chapter 6 (see Section 6.3.1).

4.4.2 Global chicken farming: comparison with the previous version of AMCLIM

In Jiang et al. (2021), the development of the AMCLIM-Poultry model ("Poultry Model" for short in the following text) is described, which is a starting point and a pilot study that uses a process-based model to simulate NH_3 emissions from global chicken farming. The Poultry Model has been incorporated in the full AMCLIM model as a component unit, and several processes have been improved. Major advances in the current AMCLIM model (for simulating poultry farming) compared with the Poultry Model include the following:

- The adsorption of TAN on manure particles is included in the current AMCLIM by using a linear equation that describes the equilibrium between aqueous TAN and solid exchangeable TAN (see Section 4.2.2.3 and Appendix A3).

- Initial water content of the excreta is taken into account rather than assuming an immediate equilibrium moisture content of the excreta.

- Organic forms of N in the excreta are included in addition to uric acid.

- A separate manure management stage is included by operating the AMCLIM–MMS. Litter management is distinguished from other management.

- Housing of backyard chicken and subsequent manure management replace the original "manure left on land" scenario, according to the characteristics of the production system and the corresponding MMS information (Table 4.1).

- The simulations for housing were operated in the updated model at an hourly time-step instead of daily time-step.

- Land application of manure is simulated by the Land Module of AMCLIM, which includes more soil processes and N pathways and employs a four-layer soil profile compared to the simpler land application scheme in the Poultry Model.

- Nitrogen application rates are derived from recommended or reference manure application rates.

Other changes in the AMCLIM model include:

- The new resistance scheme in the poultry houses consists of a resistance for gas transfer and a litter resistance rather than using a single constant housing resistance in the Poultry Model. The former resistance is dependent on temperature and ventilation inside the house, while the latter one is a constant value used the same inversion method as in the previous Poultry Model (see Section 4.2.2.1 and 4.2.2.3).

- Manure is no longer only applied to the six prescribed crops based on expert judgement. Instead, manure is assumed to be applied to land depending on a generalised crop calendar which is derived from 16 major crops.

With the improvements and modifications, the current AMCLIM model provides very similar estimates of the housing simulations at the site scale, which is due to the updated processes that have opposite effects. The inclusion of organic forms of N gradually expands the TAN pool, which leads to more N that is available for NH_3 emissions. Conversely, the adsorption of TAN on manure solids and more moisture in the excreta decrease the aqueous TAN concentration so compensating this effect.

For the global simulations, NH_3 emissions from chicken farming are 4.8 Tg N yr^{-1} in 2010 estimated by current AMCLIM, which is about 13 % less than those from the Poultry Model's estimation of 5.5 Tg N yr^{-1}. The relative contribution to the total emissions shifts from the land application of manure to the housing, which is largely due to the fact that emissions from backyard chicken were counted as housing emissions in current AMCLIM rather than land application emissions as in the Poultry Model. Housing emissions from broilers are comparable between AMCLIM and the Poultry Model, while AMCLIM suggests higher housing emissions from layers compared to the earlier model. Lower land

application emissions were estimated by the current AMCLIM model, which is possibly because 1) less N is applied to land, 2) more N pathways that are included act as competing fluxes to volatilization could decrease the emission, 3) the adsorption of TAN on soil solids leads to lower emission potential.

4.4.3 Uncertainty and limitations

Uncertainty in NH_3 emissions from pig and poultry farming simulations arises from multiple sources of which stated by the sensitivity analysis (Table 4.3). For the housing simulations, the relationships used to parameterize the indoor conditions may not be representative, especially the ventilation in the naturally ventilated barns can be uncertain, which can influence the rates of the simulated processes. In addition, the gap area and the solid floor area of animal houses with slatted floor are uncertain, whilst AMCLIM used a fixed value assuming a 20 % of gap space. Meanwhile, the surface area of the pit for manure storage may not be the same as the floor area above but was assumed to be equivalent to the floor area in AMCLIM.

For manure management simulations, the largest uncertainty comes from the source area. In AMCLIM, the area for NH_3 emissions in this stage was assumed to be proportional to the housing area based on the logic that more area might be required for manure storage for more animals, which is a reasonable assumption, but the ratio is unclear. The determination of the emitting surface of NH_3 emission during manure storage is a major limitation of AMCLIM.

For land spreading of manure, only broadcasting was simulated, which may not reflect the reality in countries with policies that require manure to be incorporated in soils, such as Netherlands and Demark. Emissions from manure application are probably overestimated in these places. Other uncertainty in the land application has been discussed in the previous chapter in Section 3.4.3.

According to the sensitivity tests (Table 4.3), the pH of excreta can greatly influence the NH_3 emissions, which can result in uncertainty in the estimated emissions. The adsorption of TAN on manure particles is represented by a linear relationship with a constant coefficient that describes the equilibrium, which may influence the calculation for TAN concentrations. Uncertainty associated with the adsorption scheme mainly exists in solid manure simulations such as poultry simulations and solid manure storage.

As a result, these factors are likely to introduce 18 % uncertainty to pig housing emissions and 37 % to chicken housing emissions based on the sensitivity tests. The uncertainty in emissions from manure management and application is estimated to be 20 % and 26 % (the same as synthetic fertilizer application in Chapter 3), respectively. However, it should be noted that the NH_3 emissions at different stage are dependent on each other. There is a "compensating" effect on emissions from livestock farming, i.e., emissions tend to be higher in subsequent manure storage and application when housing emissions decrease. By assuming a negative correlation between emissions from different activities, the combined uncertainty in pig farming NH_3 is 0.4 and 0.3 Tg N yr^{-1} for 2010 and 2018, while chicken farming NH_3 has uncertainty of 1.3 Tg N yr^{-1} for both years.

4.5 Summary and conclusions

This chapter presents the development and application of all three modules in AMCLIM to simulate NH_3 emissions from pig and poultry farming. AMCLIM follows the N flow from animal housing, manure management to ultimate the land application of manure, with impacts of environmental factors being included in the model. AMCLIM–Housing includes two housing systems and three housing types, and AMCLIM–MMS includes four major manure management divisions, which allows the impacts of management practices to be reflected, i.e., simulations for livestock sectors and production systems can be differentiated. AMCLIM also has substantial updates for simulating poultry farming emissions, with more processes being included compared with the previous version (Section 4.4.2).

In this chapter, major effort has been given to the evaluation of AMCLIM–Housing against measurements by USEPA AFO. The simulated NH_3 emissions from pig and chicken housing showed close agreement with measurements. AMCLIM–Housing was able to broadly reproduce the NH_3 emissions from two types of animal houses with different processes and settings, and roughly replicate the daily variations in NH_3 emissions. The other two modules were not specifically tested against measurements because of the similarities in the processes for housing and manure management and lack of available datasets (AMCLIM–Land has been tested and details are given in Chapter 3).

Based on simulations using AMCLIM, pig farming is estimated to result in NH_3 emissions of 5.3±0.4 Tg N yr^{-1} in 2010 and 5.1±0.3 Tg N yr^{-1} in 2018, while chicken farming results in 4.8±1.3 Tg N yr^{-1} NH_3 emissions in both 2010 and 2018. This indicates that overall, around 40 % of total excreted N is lost due to NH_3 emissions. Specifically, NH_3 emissions

from housing and manure management account for 60 to 70 % of total emissions from pig farming, which is equivalent to 24 % of total excreted N from pigs. The remaining 30 to 40 % of NH_3 emission is from land application of pig manure. For poultry, over 80 % of NH_3 emissions are from housing and manure management, and manure application only contributes to less than 20 % of total emissions. It is evident that the manure application shows lower volatilization rates in 2018 than 2010 (relative 7 to 12 % decrease in P_V), which exhibits the same trend as the results of synthetic fertilizers (see Section 3.3.2). By comparison, housing and manure management show less interannual variability in volatilization rates than manure application.

High emissions from pig farming are found in Brazil, China, India, US and Europe, and high emissions from chicken farming occur in China, India, Europe, Southeast Asia and Western Africa, which is consistent with regions that have high livestock population numbers. The volatilization rates show strong spatial variations across the globe, with the highest volatilization rates being up to 60 % or 70 % of excreted N. This demonstrate that simple EFs are not sufficient enough to reflect real world conditions, and the need to refine current EFs to incorporate climate dependence of NH_3 emissions.

Chapter 5
Ammonia emissions from cattle, sheep and goat farming

5.1 Introduction

Ruminant farming is a crucial source of agricultural NH_3 emissions. In particular, cattle is the sector that contributes to the largest NH_3 emissions among livestock. Existing studies have reported that over 50 to 60 % of animal–related NH_3 originates from cattle agriculture (including buffaloes), while sheep and goat farming together resulted in around 10 % of livestock NH_3 emissions (Dentener and Crutzen, 1994; Bouwman et al., 1997b; Behera et al., 2013). According to FAO statistical data, stocks of ruminants have increased by 60 % over the past 50 years (FAO, 2018b). Compared with pigs and poultry, excreted nitrogen deposited on pastures during grazing is an additional source of NH_3 emissions, which needs to be investigated.

This chapter focuses on presenting the development of the Grazing Submodule of AMCLIM–Land, and the application of the model to quantify NH_3 emissions from ruminant farming. The AMCLIM model simulates ruminants including cattle, sheep and goat, and focuses on four agricultural activities: housing, manure management, manure

application and grazing. The application of AMCLIM at both the site and global scales and the evaluation against measurements are presented. The results and implications are discussed.

5.2 Methods and Materials

As described in Chapter 4, modelling NH_3 emissions from livestock farming requires utilizing all three modules of the AMCLIM model. Ruminant and pig farming share several common features, such as housing and manure management. Ruminants can be kept in animal houses, and the excreta are stored and are eventually used as fertilizers. However, ruminants can graze outside year-round, which is an additional source of NH_3 that must be counted. In-depth descriptions of the processes involved in the simulations for livestock housing, manure management and manure application have been covered in previous Chapters. This section aims to expand upon and differentiate the processes specific to grazing livestock.

5.2.1 Simulations for ruminant housing, manure management and land application of manure

Ruminants including cattle, sheep and goats, are typically kept in naturally ventilated animal houses as these animals have higher tolerances to cold temperatures than pigs and poultry. In AMCLIM, it is assumed that the excreta from these animals are removed from

the houses on a daily basis. Meanwhile, ruminants also graze outside, which leads to the deposition of excreta on pastures. Two grazing systems are considered: year-round grazing and seasonal grazing. In the case of year-round grazing, all ruminant excreta are assumed to be deposited on pastures. For seasonal grazing, the excreta are split into two parts, with a fraction of excreta remaining in the animal houses, while the rest is left outside while grazing. The time evolution of N pools (M_{N}; given in per unit area; all masses have units of g m^{-2} if not specifically explained) in the animal houses can be modified from Equation 4.6 as follows:

$$\frac{\mathrm{d}M_{\mathrm{N}_i}}{\mathrm{d}t} = (1 - f_{\mathrm{grazing}})F_{\mathrm{excretN}}f_{\mathrm{N}_i} - K_{\mathrm{N}_i}M_{\mathrm{N}_i} - \psi_{\mathrm{cleaning}}(\mathrm{t}, \mathrm{N}_i), \qquad (5.1)$$

where f_{grazing} is the fraction of ruminant excreta that is deposited on pastures and is dependent on the grazing time. As described in Section 4.2, F_{excretN} is the total N excretion rate from the livestock, and f_{N} is the fraction of a N form in the excretion. K_{N} is the conversion rate (s^{-1}) at which a N species decomposes. $\psi_{\mathrm{cleaning}}(\mathrm{t})$ represents the cleaning event of the house (see Equation 4.5).

The characteristics of ruminant excreta are similar to pigs, as they contain both urine and dung, with excreted N mainly existing as urea in urine and organic N in faeces. The differences between ruminant and pig excreta stem from the biological and behavioural features that are varied between livestock, such as urinary N concentration, faecal N content, urination and defecation volume/mass and frequency etc. Further information is given in Appendix B6. The TAN pool can be calculated by Equation 4.4. Similarly, the water pool is calculated from urination (F_{urine}), water in faecal excreta ($F_{\mathrm{faecal\ water}}$), loss by evaporation of water (F_{evap}, mm s^{-1}), and the cleaning event by the following equation:

$$\frac{\mathrm{d}M_{\mathrm{H_2O}}}{\mathrm{d}t} = (1 - f_{\mathrm{grazing}})(F_{\mathrm{urine}} + F_{\mathrm{faecal\ water}}) - F_{\mathrm{evap}} - \psi_{\mathrm{cleaning}}(\mathrm{t}, \mathrm{H_2O}). \quad (5.2)$$

Ruminant excreta in houses are collected and stored (or managed in other ways, e.g., used as fuel but not used as fertilizers to fields), and will eventually be mainly used as fertilizers on land. Conversely, excreta deposited on pastures while grazing are assumed not to be collected for storage or to be used as added fertilizers in the AMCLIM model. Emissions of NH_3 from grazing are simulated by the Grazing submodule of AMCLIM–Land. Manure management and land application of manure for ruminants are simulated by AMCLIM–MMS and AMCLIM–Land respectively, as described in Sections 4.2.3 and 4.2.4. In addition to the four MMS divisions, information on manure management for ruminants includes a system in which manure deposited on pastures is simulated by the Grazing submodule (discussed in the next section).

5.2.2 Simulations for ruminants grazing

Grazing practice is an important component of ruminant farming systems. Animals can spend the whole year or part of the year outside (i.e., on pastures), corresponding to the year-round and seasonal grazing, respectively. Based on the GLEAM2 livestock data, ruminants are categorised into grassland and mixed production systems. In AMCLIM, ruminants in the grassland production system are assumed to graze year-round, whereas those in the mixed production system graze seasonally (Vira et al., 2020a). The NH_3 emissions during seasonal grazing are considered as a counterpart to the housing emissions. The N pools for seasonal grazing can be expressed as follows:

$$\frac{\mathrm{d}M_{\mathrm{N}_i}}{\mathrm{d}t} = f_{\mathrm{grazing}} F_{\mathrm{excretN}} f_{\mathrm{N}_i} - K_{\mathrm{N}_i} M_{\mathrm{N}_i}. \quad (5.3)$$

The amount of ruminant excreta deposited on pastures depends on grazing time, and is determined from the MMS information provided by the GLEAM2 model and a temperature condition. Specifically, the fraction of excreta deposited on pastures f_{grazing}, is calculated as follows:

$$f_{\mathrm{grazing}} = \begin{cases} \begin{cases} \frac{f_{\mathrm{MMS(pasture)}}}{N_{\mathrm{T}_{10}^{\mathrm{min}}>10°\mathrm{C}}/365}, if\ T_{10}^{\mathrm{min}} \geq 10°\mathrm{C} \\ 0, if\ T_{10}^{\mathrm{min}} < 10°\mathrm{C} \end{cases}, & \text{if } f_{\mathrm{MMS(pasture)}} \leq \frac{N_{\mathrm{T}_{10}^{\mathrm{min}}>10°\mathrm{C}}}{365} \\ f_{\mathrm{MMS(pasture)}}, & \text{if } f_{\mathrm{MMS(pasture)}} > \frac{N_{\mathrm{T}_{10}^{\mathrm{min}}>10°\mathrm{C}}}{365} \end{cases}, \quad (5.4)$$

where $f_{\mathrm{MMS(pasture)}}$ is the fraction of annual total manure deposited on pastures. T_{10}^{min} (ºC) is the 10-day running average of daily minimum temperature (calculated for each day of the year), and $N_{\mathrm{T}_{10}^{\mathrm{min}}>10°\mathrm{C}}$ is the number of days with T_{10}^{min} higher than 10 ºC in a year (Pinder et al., 2004). The temperature condition justifies the number of days suitable for grazing in a year, while the MMS statistical data constrains the annual total value of excreted N that is deposited on pastures.

If the values of MMS data ($f_{\mathrm{MMS(pasture)}}$) are smaller than the fraction of suitable days ($N_{\mathrm{T}_{10}^{\mathrm{min}}>10°\mathrm{C}}$) in the year, ruminants only graze on suitable days (i.e., when T_{10}^{min} is higher than 10 ºC). If the MMS value is larger, the AMCLIM model assumes that animals graze throughout the year, but spend only a fraction of time outside on pastures every day. This situation counts as seasonal grazing in AMCLIM, even though animals are grazing year-round, as the grazing system is determined by the production system. Emissions

during seasonal grazing can be crucial, particularly if animals are kept outside for a considerable amount of time.

As previously mentioned, grazing practices can result in NH_3 emissions. The AMCLIM model includes two schemes for simulating these emissions: the urine patch scheme and the dung pat scheme, as shown in Figure 5.1. The urine patch scheme is focused on NH_3 emission from urine deposition, while the dung pat scheme considers NH_3 from both dung-only and dung/urine mixtures situations. These two schemes are analogous to land application of slurry and solid manure, respectively, with the same simulated processes as for the manure application to land (as described in Section 4.2.4).

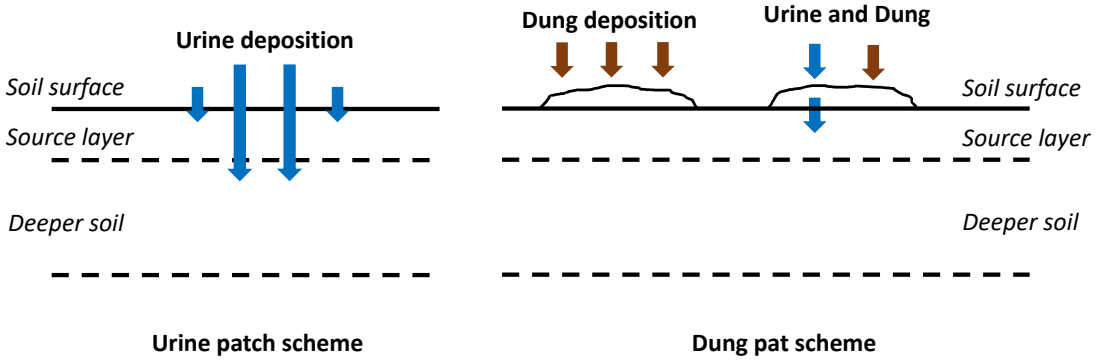

Figure 5.1. Sketch of the urine patch scheme and the dung pat scheme used in the AMCLIM model for grazing simulations.

Urine can infiltrate into soils relatively quickly and change the water content of the soil surface. Meanwhile, urinary N mainly exists as urea. Hydrolysis of urea in fresh urine results in soil pH change (as introduced in Section 3.2.1.4), which is different from slurry

application where urea is assumed to be completely converted to TAN and not to affect soil pH. Another difference is the vertical soil layering. In the urine patch scheme, only the surface soil layer is modelled, rather than all four soil layers as in simulations for fertilizer applications. Also, considering the smaller water volume of ruminant urine compared with slurry application or irrigation, AMCLIM defines a 4 mm source layer in which all simulated processes take place. The thickness of this source layer is based on Móring et al. (2016).

In the dung pat scheme, NH_3 is mainly emitted from the excreta rather than the underlying soils, as the excreta act as a substrate to hold the excreted N. Therefore, an excreta layer is set up above the soil surface in the dung pat scheme, and the underlying soils are not further simulated. All simulated processes in both schemes are the same as those for the top soil layer of manure applications, and the transport distances for diffusive transport are modified accordingly.

Simulating NH_3 emissions from grazing is challenging due to the heterogeneity of grazing fields. It is crucial to determine the area of emitting surfaces with the matched N pools. Since animals roam freely and do not urinate and defecate in the same area during every excretion event, fresh excreta do not accumulate on old excreta. In AMCLIM, excreta and excreted N from each day are simulated independently, and not accumulated into the common pools. This means that each day's excreta go into new pools instead of being added to the previous day's pools. The total NH_3 emission from a grazing field can be calculated by the following equation:

$$F_{\mathrm{NH_3}} = \sum_{\mathrm{n=1}}^{\mathrm{n}} F_{\mathrm{NH_3(n)}}, \tag{5.5}$$

where $F_{NH_3(n)}$ represents the NH_3 emission from the area where excreta are deposited on day n. Pools from each day are simulated for 60 days, after which, all N pools are assumed to be naturally incorporated into soils and are not simulated further. During the simulation period, input is only from the first day of this 60-day window, and the source area for emissions of each day is a constant value under the assumption that daily excretion rates (urine and dung) remain the same.

5.2.3 Global application

Global application of the AMCLIM model for simulating NH_3 emissions from ruminant farming requires input of livestock and MMS data. The model is driven by reanalysis meteorology, which has been introduced in previous chapters. Information about ruminant excreta is provided in Appendix B6, along with data for pigs and poultry. Livestock and MMS data are available for cattle, sheep and goats. GLEAM2 provides five types of cattle: beef, dairy, other dairy, feedlot cattle and buffaloes. Ruminants typically have two production systems: grassland and mixed production systems, except for feedlot cattle, which is treated as a specialized production system: feedlot. In feedlots, cattle are fed with a specialized diet to stimulate weight gain and are normally kept in concentrated areas to facilitate the fattening processes with high stocking densities according to FAO (FAO, 2018a).

An important parameter for the global simulations is stocking density, which determines the source area for emissions. For cattle, the housing density of 100 kg liveweight per square meter is assumed for beef, 80 kg liveweight per square meter for all dairy, and 150

kg liveweight per square meter for feedlot cattle. The grazing density for all cattle is set at 2500 square meter per head (equivalent to four animals per hectare; Saarijärvi et al., 2006; Saarijärvi and Virkajärvi, 2009). For sheep and goats, a housing density of 50 kg liveweight per square meter is assumed and a grazing density of 400 square meter per head (equivalent to 25 animals per hectare). The housing areas are calculated by Equation 4.21 as for pigs. For grazing, the area (S_{grazing}, m^2) can be calculated by the following equation:

$$S_{\text{grazing}} = n_{\text{i}} den_{\text{grazing}}, \tag{5.6}$$

note that grazing "density" (den_{grazing}, m^2 $head^{-1}$) has a different unit from housing density (den_{housing}, kg animal weight m^{-2}) as mentioned. It is important to clarify that the source areas of NH_3 emissions from grazing are not equivalent to the grazing area. Saarijärvi et al. (2006) have shown that the annual average surface coverage of urine and dung on a grazing field is 17 % and 4 %, respectively. In AMCLIM, the source areas of NH_3 emissions from urine patch ($S_{\text{urine patch}}$) and dung pat ($S_{\text{dung pat}}$) can be expressed as follows:

$$S_{\text{urine patch}} = f_{\text{urine}} S_{\text{grazing}}, \tag{5.7}$$

$$S_{\text{dung}} = f_{\text{dung}} S_{\text{grazing}}, \tag{5.8}$$

where f_{urine} is 0.17 and f_{dung} is 0.04. The areas for dung-only and dung mixtures in the dung pat scheme are the same, which accounts for 2 % of the total grazing area.

The housing environments are close to the natural environments as ruminants are kept in naturally ventilated barns. The generalised relationships used for parameterizing the

temperature and ventilation rates of animal houses are presented in Appendix A12. The simulations for manure storage and land application have been described in Chapter 4.

5.3 Results

5.3.1 Simulations for dairy housing at the site scale

AMCLIM–Housing simulated NH_3 emissions from dairy barns and were compared with USEPA AFO measurements. Two free stall barns in a dairy farm in Indiana were monitored for two years (as presented in Appendix B8), with around 1600 Holstein cows being housed in each barn. The barns have exhaust fans to facilitate ventilation, and scrapers were used to clean the barns and to remove manure. More information about the dairy farm can be found in Lim et al. (2010).

The simulated period is from 01 July 2007 to 31 July 2009, as shown in Figure 5.2. Daily average temperature inside the barn is very close to the outdoor temperature, ranging from -10 to 25 °C (Fig 5.2 and Fig E1). Strong seasonal variations are found in ventilation, with higher ventilation in summer and lower ventilation in winter, while inside temperature exhibits the same trend. The relative humidity also shows strong daily variations, with the highest RH being over 85 % and lowest values being below 55 %.

Overall, AMCLIM–Housing well reproduces the NH_3 emissions and captures the daily variations of the emissions (Fig 5.2). The average modelled NH_3 emission from the dairy

barn is 32.4 kg d^{-1} (when measurements available; 35.2 kg d^{-1} for the entire simulation), compared with 32.5 kg d^{-1} reported by the measurements. As shown in Figure 5.2, high NH_3 emissions occur not only in summer but also in spring, especially in 2009, resulting from high temperature and high ventilation. Meanwhile, emissions decrease in winter when both temperature and ventilation are low. The highest emission is over 100 kg d^{-1} in April 2009, while the lowest emission is less than 10 kg d^{-1} in winter days. According to the model, 15 % of excreted N from dairy is lost due to NH_3 emissions.

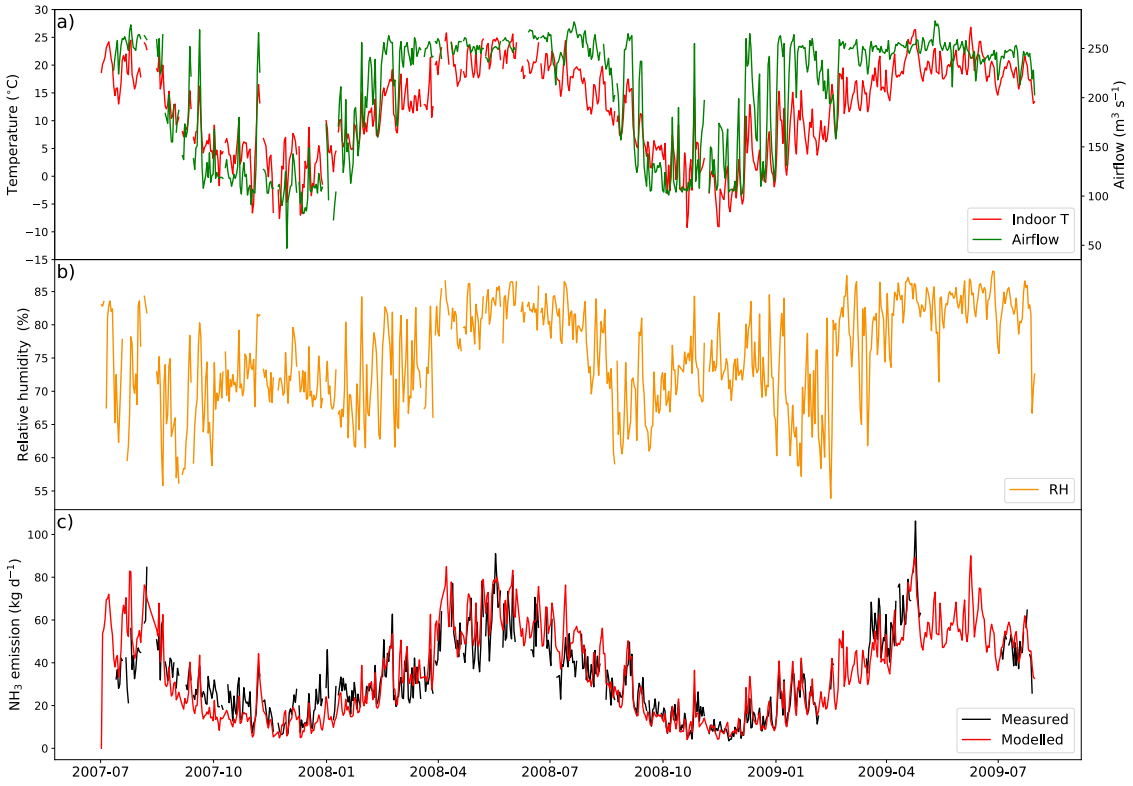

Figure 5.2. Site simulations of Barn 1 in a dairy farm at site IN5B, Jasper, Indiana, from 01 July 2007 to 31 July 2009. (a) Measured daily mean indoor temperature and airflow rate of the barn. (b) Measured daily mean relative humidity of the barn. (c) Comparison between modelled NH_3 emissions and calculated NH_3 emissions from measured indoor concentrations.

5.3.2 Global simulations for ruminants housing, manure management and land application of manure

5.3.2.1 Cattle NH_3 emissions

Global cattle housing results in 3.49 Tg N yr^{-1} of NH_3 emissions in both 2010 and 2018, according to simulations by AMCLIM–Housing, accounting for about 12 % of total excreted N from cattle. The geographical distributions of the housing NH_3 emission and the volatilization rates are shown in Figure 5.3ab and 5.4ab, with no significant difference between the two years. India has the highest emissions, and high emissions also occur in the southern Brazil, North China Plain (NCP), France, Pakistan and middle US. Countries in South America such as Bolivia, Brazil, Paraguay and Venezuela show the highest volatilization rates of over 25 %, as well as New Zealand. Part of India and several Sahel countries show moderate volatilization rates of 15 to 20 %, while the other regions in the world generally have volatilization rates of less than 10 %.

Emissions of NH_3 from cattle manure management estimated by AMCLIM–MMS are 3.59 Tg N yr^{-1} in 2010 and 3.65 Tg N yr^{-1} in 2018, respectively. In both years, approximately 17 % of managed N is lost due to NH_3 emissions. The spatial distributions of the manure management emissions (Fig 5.3c and 5.3d) are similar to the housing emission (Fig 5.3a and 5.3b). Highest emissions occur in India and Pakistan, with hot spots being found in NCP, southern Brazil and part of US. For the volatilization rates (Fig 5.3d and 5.4d), highest rates of more than 35 % are found in countries in northern South America (Bolivia, Brazil, Paraguay and Venezuela), the Sahel and Southeast Asia. India, Pakistan, central and southern Africa also show high volatilization rates of over 20 %. China, US and Europe

have lower volatilization than the regions mentioned above, with typically less than 10 % of N lost through NH_3 emissions.

Using AMCLIM–Land, it is estimated that NH_3 emissions from cattle manure application are 3.1 Tg N yr^{-1} in 2010, accounting for 36 % of applied N in cattle manure. High emissions can be seen across India, NCP, mid US and Europe (Fig 5.3e and Fig 5.4e). The volatilization rates are high across most of the regions on the globe (>36 %), with India having particular high rates of nearly 60 % (Fig 5.3f and Fig 5.4f). Only Brazil, northern Europe and Southeast Asia show lower rates of less than 30 %.

In 2018, cattle manure application results in 2.7 Tg N yr^{-1} of NH_3 emissions. Globally, about 32 % of applied N is estimated to be volatilized as NH_3. Compared with 2010, Russia, eastern US and Europe show lower volatilization rates, while volatilization rates remain high in Australia, India, NCP and western US.

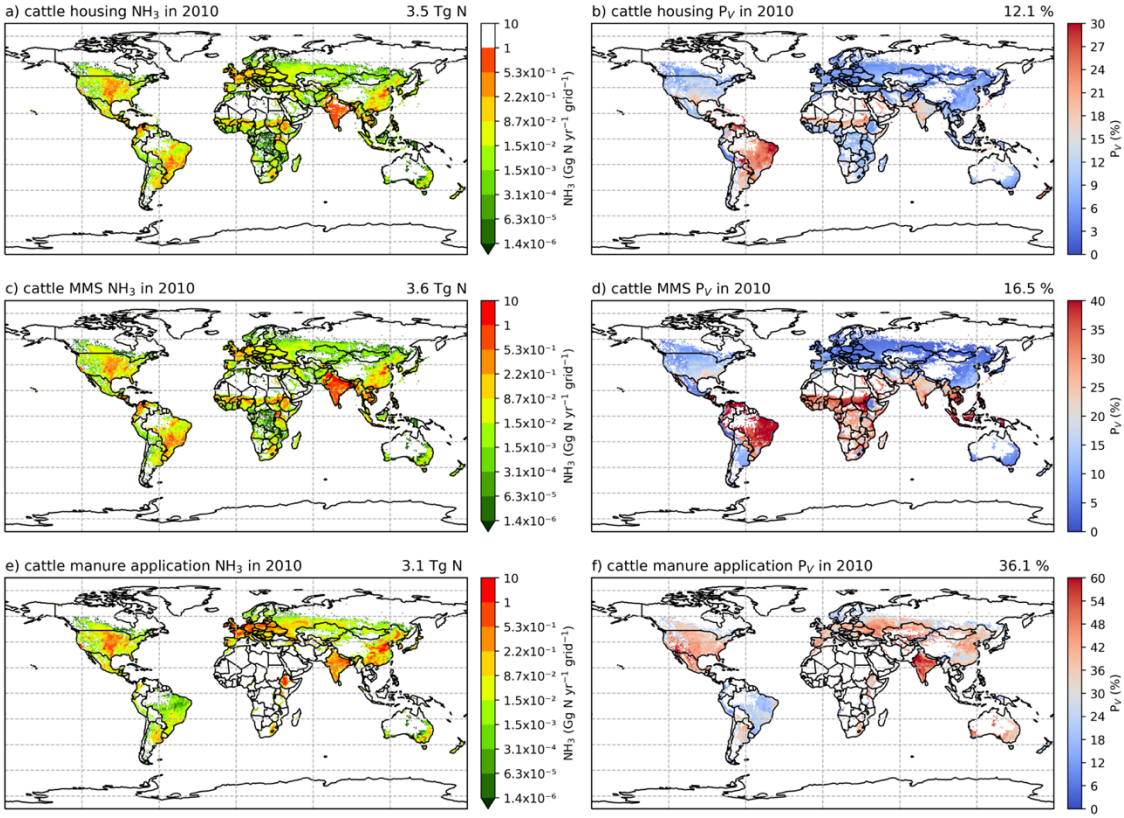

Figure 5.3. AMCLIM cattle simulations for the year 2010: NH_3 emissions (a, c, e) and percentage volatilization rates (P_V) (b, d, f), for housing, MMS and manure application, respectively. The resolution is 0.5º × 0.5 º.

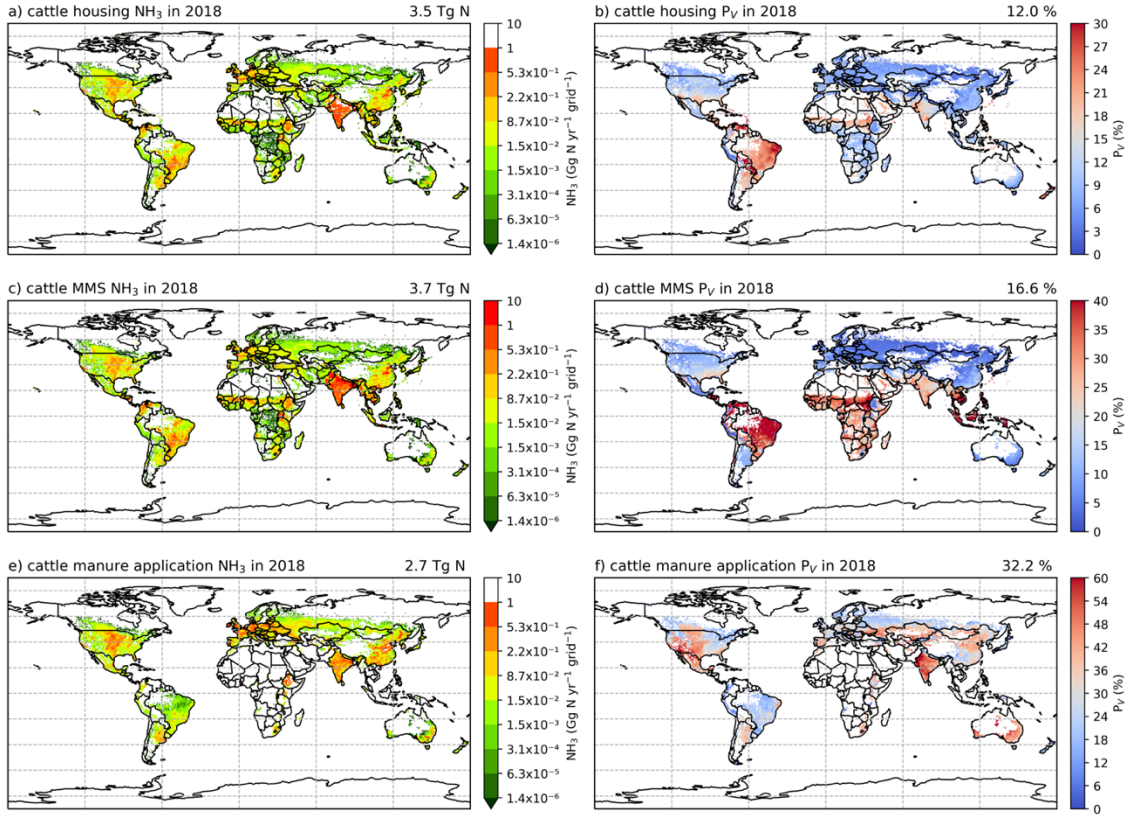

Figure 5.4. Same as Figure 5.3 but for the year 2018.

Simulated NH_3 emissions from cattle housing and volatilization rates for each cattle type are presented in Table 5.1. Dairy (including other dairy) and beef cattle are the largest emitters, which contribute to 1.6 Tg N yr^{-1} and 1.1 Tg N yr^{-1}, respectively, accounting for around 12 to 13 % of excreted N in houses. Among all types, buffalo (including buffalo beef and dairy) housing has the highest volatilization rates of more than 15 %, while the volatilization rates are less than 10 % for feedlot cattle.

Similar to housing, dairy (including other dairy) and beef cattle are responsible for the largest NH_3 emissions from manure management. Buffalo (including buffalo beef and buffalo dairy) show substantially higher volatilization rates compared with other types of cattle, exceeding 25 %, while the volatilization rates for the remaining cattle species typically range between 13 to 17 %.

Application of dairy (including other dairy) and beef manure to land contribute over 90 % of total manure application NH_3 emissions in both simulated years (Table 5.3). Volatilization rates in 2010 are typically higher than those in 2018 for all types of cattle. Emissions from buffaloes are almost negligible compared with other types of cattle due to buffaloes contributing much less manure N application.

Table 5.1. Total excreted N (Tg N yr^{-1}), NH_3 emissions (Tg N yr^{-1}) and volatilization rates (%) from housing for major types of cattle.

Ruminants	Year	Total excreted N in houses (Tg N yr^{-1})	NH_3 from housing (Tg N yr^{-1})	Average P_V (%)
Beef cattle	2010	8.78	1.08	12.3
	2018	8.76	1.07	12.2
Dairy cattle	2010	7.19	0.93	12.9
	2018	7.31	0.93	12.7
Other dairy	2010	7.02	0.65	9.3
	2018	7.24	0.65	9.0
Feedlot cattle	2010	1.60	0.15	9.4
	2018	1.51	0.14	9.3
Buffalo beef	2010	1.22	0.19	15.6
	2018	1.21	0.19	15.7
Buffalo dairy	2010	2.95	0.49	16.6
	2018	3.09	0.51	16.5
Total	2010	28.76	3.49	12.1
	2018	29.12	3.49	12.0

Table 5.2. Total managed N (Tg N yr^{-1}), NH_3 emissions (Tg N yr^{-1}) and volatilization rates (%) from manure management for major types of cattle.

Ruminants	Year	Total managed N (Tg N yr^{-1})	NH_3 from MMS (Tg N yr^{-1})	Average P_V (%)
Beef cattle	2010	6.91	1.13	16.4
	2018	6.89	1.15	16.7
Dairy cattle	2010	5.40	0.75	13.9
	2018	5.49	0.75	13.7
Other dairy	2010	5.43	0.80	14.7
	2018	5.61	0.81	14.4
Feedlot cattle	2010	1.45	0.23	15.9
	2018	1.36	0.22	16.2
Buffalo beef	2010	0.80	0.22	27.5
	2018	0.79	0.22	27.8
Buffalo dairy	2010	1.78	0.46	25.8
	2018	1.87	0.50	26.7
Total	2010	21.77	3.59	16.5
	2018	22.01	3.65	16.6

Table 5.3. Total applied N (Tg N yr^{-1}), NH_3 emissions (Tg N yr^{-1}) and volatilization rates (%) from manure application to land for major types of cattle.

Ruminants	Year	Total applied N (Tg N yr^{-1})	NH_3 from application (Tg N yr^{-1})	Average P_V (%)
Beef cattle	2010	2.84	1.00	35.2
	2018	2.77	0.90	32.5
Dairy cattle	2010	2.79	1.01	36.2
	2018	2.77	0.88	31.8
Other dairy	2010	2.37	0.87	36.7
	2018	2.41	0.77	32.0
Feedlot cattle	2010	0.43	0.17	39.5
	2018	0.39	0.14	35.9
Buffalo beef	2010	0.03	0.01	33.3
	2018	0.03	0.01	33.3
Buffalo dairy	2010	0.05	0.02	40.0
	2018	0.05	0.01	20.0
Total	2010	8.51	3.08	36.1
	2018	8.42	2.71	32.2

5.3.2.2 Sheep and goat NH_3 emissions

Emissions of NH_3 from sheep and goat housing are estimated to be 0.27 Tg N yr^{-1} in 2010 and 2018, accounting for 20.5 % and 19.7 % of excreted N in housing each year, respectively. As shown in Figure 5.5a, India, NCP and Europe typically show higher emissions than other regions in the world. However, regions with high emissions are not consistent with regions with high volatilization rates. Highest volatilization rates are found in Africa, South Africa and southern North America, while Asia and Europe generally have lower volatilization rates of less than 20 % (Fig 5.5b).

Management of sheep and goat manure are estimated to result in 0.27 Tg N yr^{-1} NH_3 emissions in 2010 and 0.28 Tg N yr^{-1} NH_3 emissions in 2018. For each simulated year, 26.6 % and 26.1 % of managed N is lost through volatilization, respectively. Emissions from manure management are the same as the housing emissions for sheep and goat, and the geographical distributions are also very similar (Fig 5.5a and 5.5c; Fig 5.6a and 5.6c). Overall, the volatilization rates for manure management are higher than housing. High volatilization rates are found in Africa, Central and South Asia, Europe, South America and Southeast Asia (Fig 5.7b and 5.7d).

Estimated NH_3 emissions from sheep and goat manure application are 0.18 Tg N yr^{-1} in 2010 and 0.17 Tg N yr^{-1} in 2018. The emissions from manure application are lower than emissions from housing and manure management, but the volatilization rates are higher. Figure 5.5ef and 5.6ef show the geographical distributions of emissions and the corresponding volatilization rates. High emissions mostly can be seen in India, NCP, Pakistan and Europe. In 2010, high volatilization rates are found across all the regions with

emissions, while high volatilization rates occurr only in NCP, Spain, western US and South Asia.

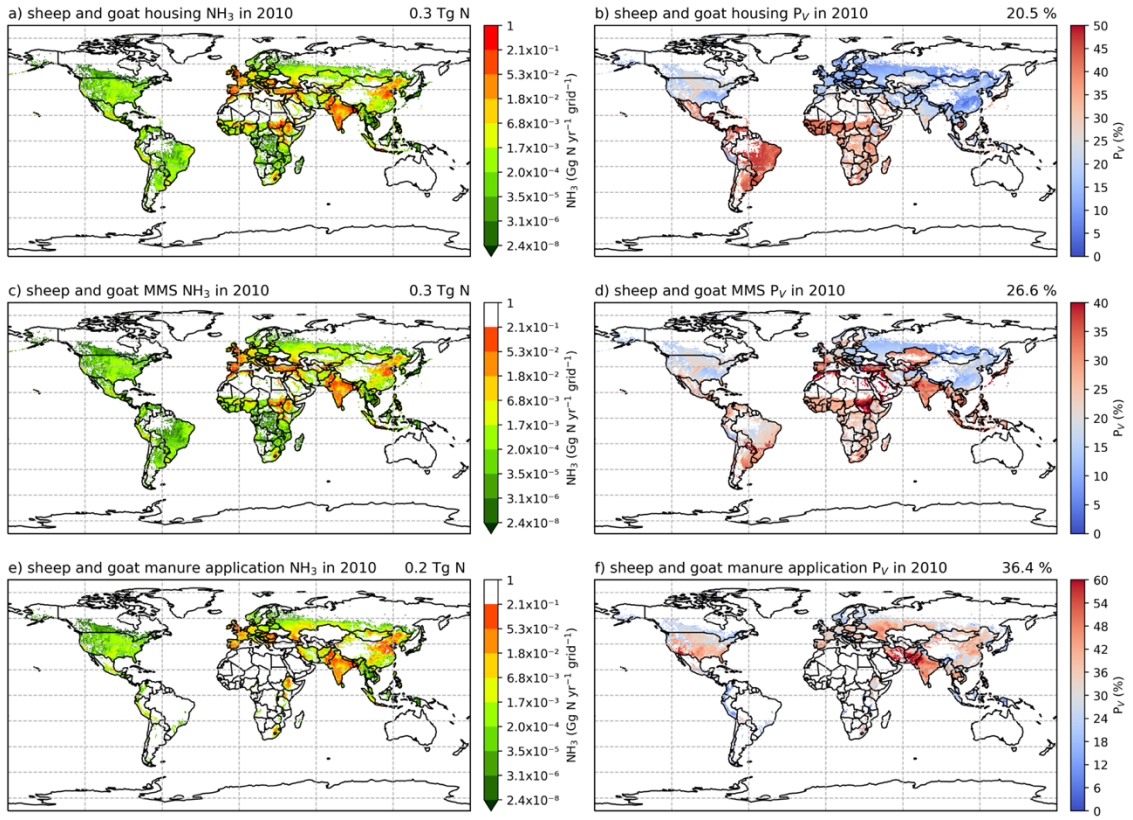

Figure 5.5. Same as Figure 5.3 but for sheep and goat in year 2010.

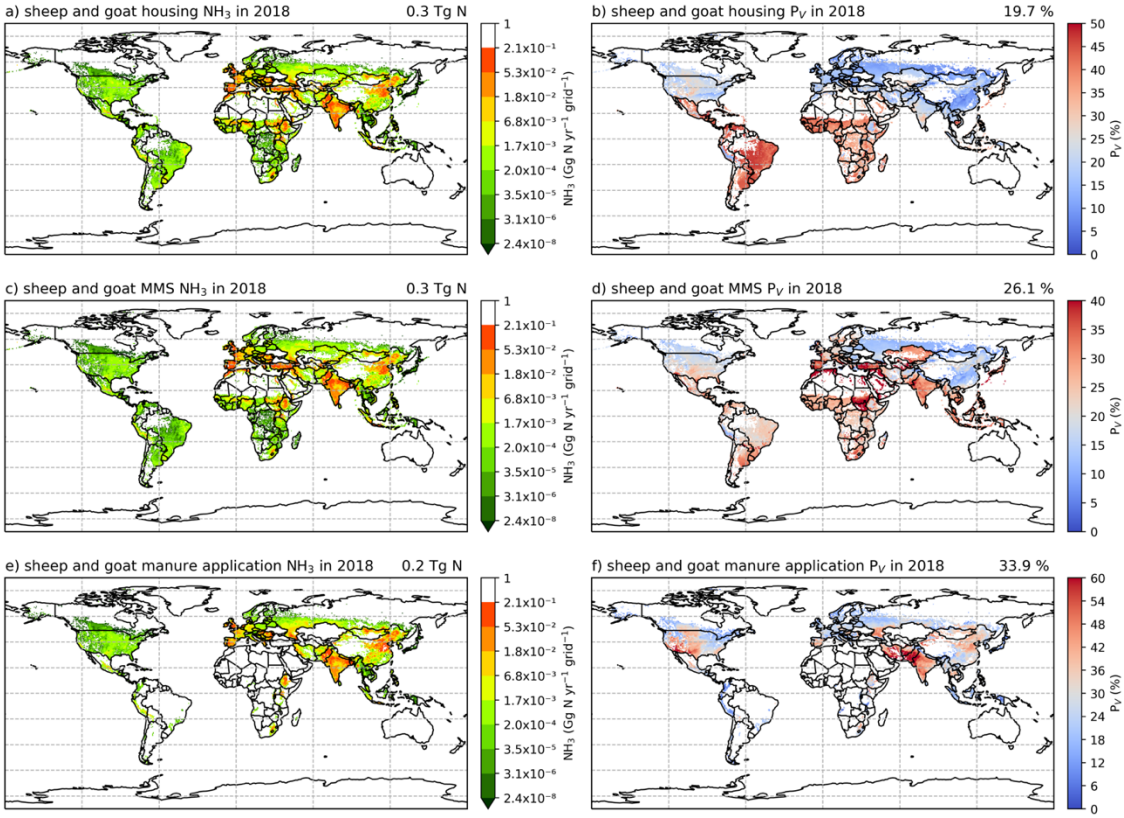

Figure 5.6. Same as Figure 5.5 but for the year 2018.

Estimated NH_3 emissions from both sheep and goat housing are comparable, with sheep contributing to about 60 % of the total emission (Table 5.4). Sheep housing shows higher volatilization rates than goat housing. Both the emissions and the volatilization rates from two simulated years are very similar, with 2018 having slightly lower volatilization rates.

On average, over 25 % of managed sheep and goat manure N is lost due to NH_3 emissions (Table 5.5). Both years have very similar volatilization rates, and sheep result in slightly higher emissions and show higher volatilization rates than goat.

Unlike housing and manure management, application of goat manure is responsible for higher NH_3 emissions than sheep, and the volatilization rates for goat manure application are also higher than sheep (Table 5.6). In 2018, the overall volatilization rates are lower than in 2010, which is consistent with other land simulations (synthetic fertilizer application in Chapter 3; pig and chicken manure application in Chapter 4).

Table 5.4. Total excreted N (Tg N yr^{-1}), NH_3 emissions (Tg N yr^{-1}) and volatilization rates (%) from housing for sheep and goat.

Ruminants	Year	Total excreted N in houses (Tg N yr^{-1})	NH_3 from housing (Tg N yr^{-1})	Average P_V (%)
Sheep	2010	0.71	0.16	22.5
	2018	0.74	0.16	21.6
Goat	2010	0.59	0.11	18.6
	2018	0.60	0.11	18.3
Total	2010	1.30	0.27	20.5
	2018	1.34	0.27	19.7

Table 5.5. Total managed N (Tg N yr^{-1}), NH_3 emissions (Tg N yr^{-1}) and volatilization rates (%) from manure management for sheep and goat.

Ruminants	Year	Total managed N (Tg N yr^{-1})	NH_3 from MMS (Tg N yr^{-1})	Average P_V (%)
Sheep	2010	0.55	0.15	27.3
	2018	0.57	0.16	28.1
Goat	2010	0.48	0.12	25.0
	2018	0.49	0.12	24.5
Total	2010	1.03	0.27	26.6
	2018	1.06	0.28	26.1

Table 5.6. Total applied N (Tg N yr^{-1}), NH_3 emissions (Tg N yr^{-1}) and volatilization rates (%) from manure application to land for sheep and goat.

Ruminants	Year	Total applied N (Tg N yr^{-1})	NH_3 from application (Tg N yr^{-1})	Average P_V (%)
Sheep	2010	0.23	0.08	34.8
	2018	0.24	0.07	29.2
Goat	2010	0.26	0.10	38.5
	2018	0.28	0.10	35.7
Total	2010	0.49	0.18	36.4
	2018	0.52	0.17	33.9

5.3.3 Global simulations for ruminants grazing

Ammonia emissions from ruminants grazing consist of two parts: emissions from seasonal grazing and emissions from year-round grazing. For the mixed production system, N excreted in houses and on pastures both results in NH_3 emission. Such ruminants graze seasonally, so the emission is counted as seasonal grazing emission. For the grassland production system, as ruminants stay outside throughout the entire year, the emission is counted as year-round grazing emission.

5.3.2.1 Cattle NH_3 emissions

According to simulations using AMCLIM–Land, NH_3 emissions from cattle grazing are 7.5 Tg N yr^{-1} in 2010, with 3.3 Tg N yr^{-1} of emissions from the mixed production system ("seasonal grazing") and 4.2 Tg N yr^{-1} of emissions from the grassland production system ("year-round grazing"). By comparison, total grazing emissions are about 10 % lower (6.7 Tg N yr^{-1}) in 2018. The mixed production system contribute to 3.0 Tg N yr^{-1}, while the grassland production system contribute to 3.7 Tg N yr^{-1}.

For the seasonal grazing, N excreted by the mixed production system cattle is 15.3 Tg N yr^{-1} in 2010 and 15.8 Tg N yr^{-1} in 2018, respectively, accounting for around 35 % of total excreted N, with the remaining 65 % of N being excreted in animal houses (Table 5.7 and 5.1). Overall, 21 % and 19 % of the N volatilized as NH_3 in 2010 and 2018, respectively. High emissions are found in India, Pakistan and South America (Fig 5.7a and 5.7c), and

high volatilization rates are found in France, Mexico, Spain, southern US, Africa, South Asia and the Middle East (Fig 5.7b and 5.7d).

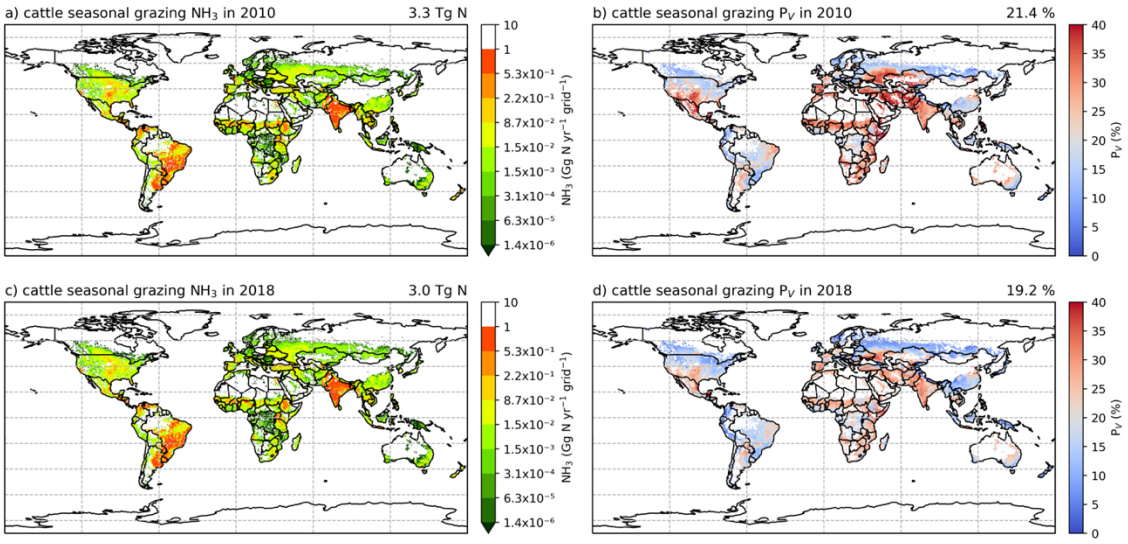

Figure 5.7. Simulated (a) annual global NH_3 emissions (Gg N yr^{-1}) from cattle seasonal grazing in 2010. (b) Percentage of excreted N from cattle while grazing seasonally that volatilizes (P_V) as NH_3 in 2010. (c) NH_3 emissions (Gg N yr^{-1}) from cattle seasonal grazing in 2018. (d) P_V rates for cattle seasonal grazing in 2018.

Beef is the largest emitter that contributes to over 50 % of emissions, whereas dairy and buffalo are responsible for 30 % and 20 % of emissions, respectively (Table 5.7). Buffaloes have the highest volatilization rates of more than 25 %, while beef and dairy generally have lower volatilization rates of less than 20 %.

Table 5.7. Total excreted N (Tg N yr^{-1}), NH_3 emissions (Tg N yr^{-1}) and volatilization rates (%) from seasonal grazing for major types of cattle.

Ruminants	Year	Total excreted N while grazing (Tg N yr^{-1})	NH_3 from grazing (Tg N yr^{-1})	Average P_V (%)
Beef cattle	2010	8.67	1.67	19.3
	2018	8.98	1.58	17.6
Dairy cattle	2010	2.09	0.45	21.5
	2018	2.16	0.40	18.5
Other dairy	2010	2.25	0.52	23.1
	2018	2.33	0.46	19.7
Buffalo beef	2010	0.67	0.18	26.9
	2018	0.66	0.16	24.2
Buffalo dairy	2010	1.59	0.46	28.9
	2018	1.63	0.42	25.8
Total	2010	15.27	3.28	21.4
	2018	15.76	3.02	19.2

For the year-round grazing, total excreted N from the grassland production system cattle is 23.8 Tg N yr^{-1} in 2010 and 24.4 Tg N yr^{-1} in 2018, with 18 % and 15 % of excreted N being lost through NH_3 emissions in each simulated year, respectively. The overall estimated volatilization rate for year-round grazing of cattle is lower than that for seasonal grazing. Countries and regions with high seasonal grazing emissions also have high emissions from year-round grazing (e.g., Argentina, Brazil, India and Pakistan). Moreover, high emissions also occur in Mexico and US. Compared to seasonal grazing, the volatilization rates of year-round grazing are generally smaller. High volatilization rates are found across the Africa, South Asia, the Middle East and part of Australia (Fig 5.8b and 5.8d).

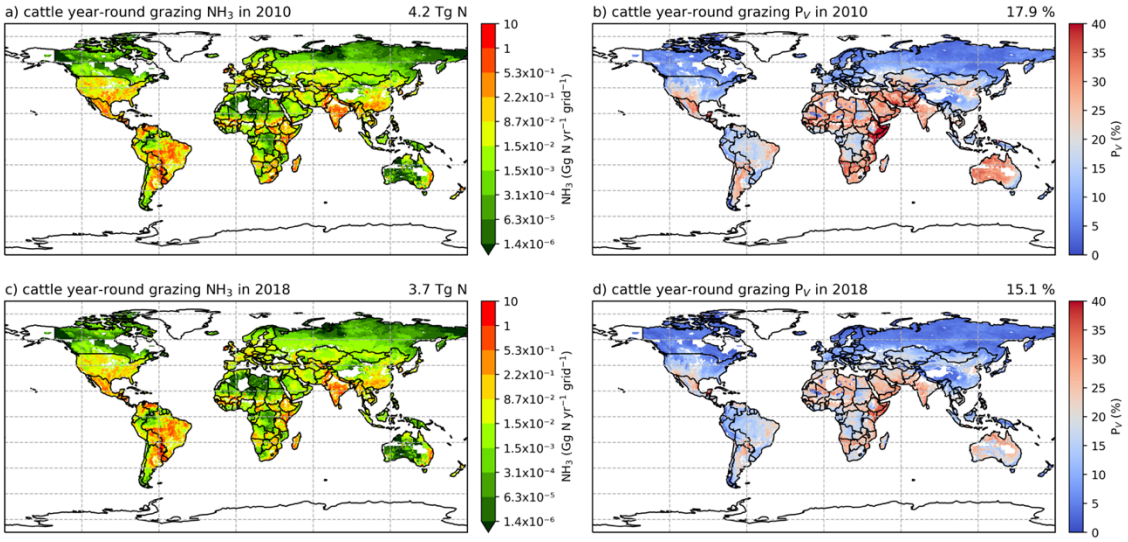

Figure 5.8. Simulated (a) annual global NH_3 emissions (Gg N yr^{-1}) from cattle year-round grazing in 2010. (b) Percentage of excreted N from cattle while grazing year-round that volatilizes (P_V) as NH_3 in 2010. (c) NH_3 emissions (Gg N yr^{-1}) from cattle year-round grazing in 2018. (d) P_V rates for cattle year-round grazing in 2018.

As summarised in Table 5.8, beef contributes over 50 % of total year-round grazing emissions, which is the largest emitter. Dairy contributes 40 % of emissions, while buffaloes result in less than 10 %. All types of cattle exhibit similar volatilization rates, with rates in 2018 being lower than 2010.

Table 5.8. Total excreted N (Tg N yr^{-1}), NH_3 emissions (Tg N yr^{-1}) and volatilization rates (%) from year-round grazing for major types of cattle.

Ruminants	Year	Total excreted N while grazing (Tg N yr^{-1})	NH_3 from grazing (Tg N yr^{-1})	Average P_V (%)
Beef cattle	2010	12.01	2.18	18.2
	2018	12.47	1.99	16.0
Dairy cattle	2010	5.48	0.86	15.7
	2018	5.54	0.71	12.8
Other dairy	2010	4.88	0.91	18.6
	2018	4.88	0.72	14.8
Buffalo beef	2010	0.54	0.10	18.5
	2018	0.56	0.08	14.3
Buffalo dairy	2010	0.87	0.19	21.8
	2018	0.92	0.17	18.5
Total	2010	23.78	4.24	17.9
	2018	24.37	3.67	15.1

5.3.3.2 Sheep and goat NH_3 emissions

Sheep and goat grazing results in 1.4 Tg N yr^{-1} of NH_3 emissions in 2010 and 2018 according to simulations using AMCLIM. The mixed production systems contribute 0.6 Tg N yr^{-1} of emissions, while the grassland production systems contribute 0.8 Tg N yr^{-1}.

Contrary to cattle, around 65 % of N in excreta from mixed production system sheep and goat is deposited on pastures rather than in houses, with 25 % and 20 % of excreted N being lost through NH_3 volatilization in 2010 and 2018, respectively. High emissions occur in India, Iran, NCP, Pakistan, Spain, Turkey and several Sahel countries (Fig 5.9a and 5.9c). The highest volatilization rates are found in southwestern Russia. India, Africa and Europe also have high rates (Fig 5.9b and 5.9d). Sheep contribute to over 60 % of total emissions, while goats contribute to the remaining 40 % (Table 5.9). The volatilization rates for both livestock were comparable.

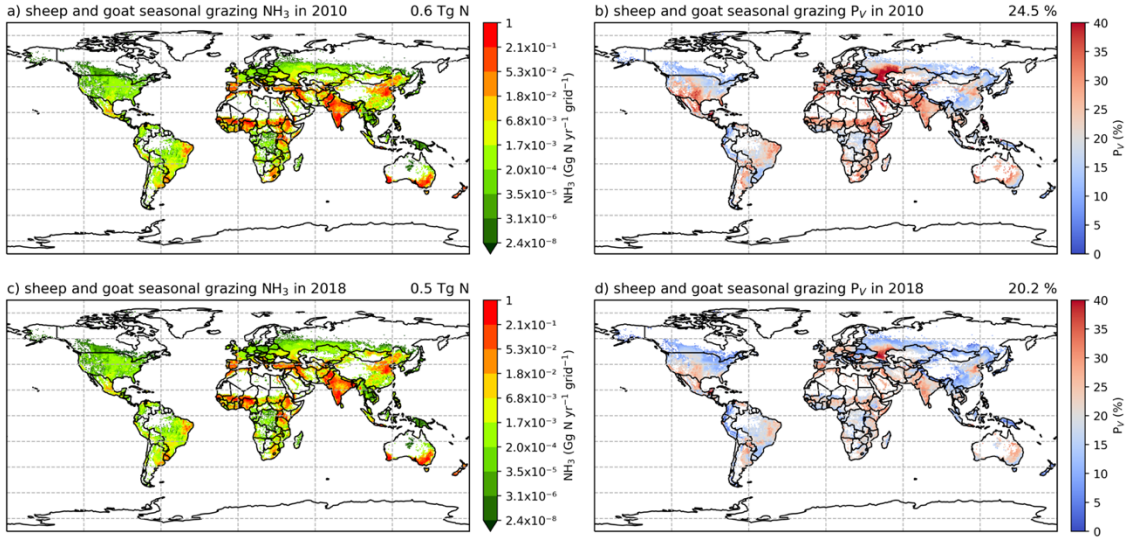

Figure 5.9. Same as Figure 5.7 but for sheep and goat.

Table 5.9. Total excreted N (Tg N yr^{-1}), NH_3 emissions (Tg N yr^{-1}) and volatilization rates (%) from seasonal grazing for sheep and goat.

Ruminants	Year	Total excreted N while grazing (Tg N yr^{-1})	NH_3 from grazing (Tg N yr^{-1})	Average P_V (%)
Sheep	2010	1.51	0.37	24.5
	2018	1.59	0.32	20.1
Goat	2010	0.89	0.22	24.7
	2018	0.96	0.19	19.8
Total	2010	2.40	0.59	24.5
	2018	2.55	0.51	20.2

For the grassland production system of sheep and goat, it is estimated that around 25 % and 20 % of excreted N volatilizes as NH_3 during the year-round grazing in 2010 and 2018, respectively. As shown in Figure 5.10, high emissions are found in southeaster Australia, northern China, eastern Africa, the Middle East and South Asia. High volatilization rates occur in Australia, Mexico, part of US, Africa, the Middle East, South Asia and South America (Fig 5.10b and 5.10d). Sheep are responsible for two-thirds of the emissions, and the volatilization rates for sheep and goat are around 20 % (Table 5.10). It is notable that

year-round grazing of sheep and goat generally result in similar volatilization rates to seasonal grazing, which is different from cattle grazing.

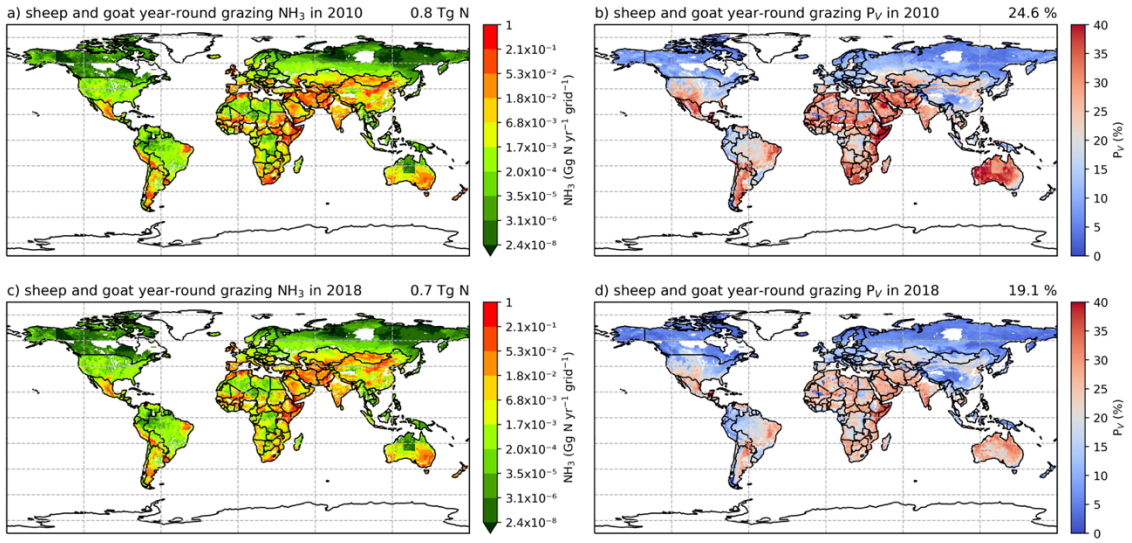

Figure 5.10. Same as Figure 5.8 but for sheep and goat.

Table 5.10. Total excreted N (Tg N yr^{-1}), NH_3 emissions (Tg N yr^{-1}) and volatilization rates (%) from year-round grazing for sheep and goat.

Ruminants	Year	Total excreted N while grazing (Tg N yr^{-1})	NH_3 from grazing (Tg N yr^{-1})	Average P_V (%)
Sheep	2010	2.23	0.55	24.6
	2018	2.32	0.43	18.5
Goat	2010	1.09	0.27	24.8
	2018	1.09	0.23	21.1
Total	2010	3.32	0.82	24.6
	2018	3.41	0.66	19.1

5.3.3.3 Emissions from urine patches and dung pats

Emissions of NH_3 from the different grazing schemes estimated by AMCLIM–Land are summarised in Table 5.11. In both years, urine patches contribute the highest estimated NH_3 emissions, along with the highest volatilization rates. About 70 to 75 % of NH_3 emissions from grazing result from urine patches according to AMCLIM, while the remaining 25 to 30 % is from dung pat (dung only and mixed dung and urine). Within the dung pat scheme, around 3 % of excreted N volatilizes as NH_3 from dung itself. By comparison, about 17 % N is lost as NH_3 from the mixture of dung and urine.

Table 5.11. Total excreted N (Tg N yr^{-1}), NH_3 emissions (Tg N yr^{-1}) and volatilization rates (%) from each grazing scheme for ruminants.

Year	Scheme	Total excreted N while grazing (Tg N yr^{-1})	NH_3 from grazing (Tg N yr^{-1})	Average P_V (%)
2010	urine patch	24.66	6.78	27.5
	dung pat (dung only)	8.61	0.25	2.9
	dung pat (mixed)	11.51	1.92	16.7
	Total	44.78	8.95	19.9
2018	urine patch	25.42	5.64	22.2
	dung pat (dung only)	8.87	0.29	3.3
	dung pat (mixed)	11.88	1.96	16.5
	Total	46.17	7.89	17.1

5.3.3.4 Comparison of AMCLIM grazing with measurements

The simulated NH_3 volatilization from grazing by AMCLIM were compared with measurements, which mainly focuses on evaluating against experimental studies that measured NH_3 emissions from urine deposition, as NH_3 emissions are mainly resulted from urine patches during grazing. Two types of observations were selected for the comparisons: real livestock grazing or urine application. Since there are insufficient input data in the reported measurements to operate AMCLIM, simulated volatilization rates were extracted

from the global results and compared with the measured volatilization rates from these experimental studies, depending on geographical locations and time of the year.

Figure 5.11a shows the comparisons between modelled and measured P_V for real livestock grazing. Simulated P_V of the urine patch for cattle grazing is comparable to the measurements at sites in the UK (Ryden et al., 1987; Jarvis et al., 1989a), Switzerland (Voglmeier et al., 2018), France (Bell et al., 2017) and New Zealand (Laubach et al., 2013). The annual mean volatilization rate (% NH_3/total excreted N) of grazing in the northern Europe estimated by AMCLIM (9.5 %) also agrees with Hutchings et al. (1996) (<10 %). However, large differences exist in between the modelled and measured P_V (% NH_3/urinary N) for cattle and sheep grazing in the UK (Jarvis et al., 1989b, 1991), as well as the volatilization rate (% NH_3/total excreted N) of cattle grazing in the Netherlands (Bussink, 1992), where AMCLIM largely overestimates the volatilization rates. These overestimations might be due to local management practices. Bussink (1992) and Jarvis et al. (1989; 1991) measured NH_3 loss from grazed land with different levels of synthetic fertilizer inputs that varied between 210 kg N ha^{-1} to 550 kg N ha^{-1}. The observed volatilization rates are normally very low (< 5%), while simulated volatilization rates are much higher (8 to 22 %). It remains unclear how additional fertilizer affects the NH_3 volatilization from livestock excreta on grasslands.

By comparison, there is closer agreement between the volatilization rates estimated by AMCLIM and those measured for urine application than for real animal grazing (Fig 5.11a vs. Fig 5.11b). Figure 5.11b shows that the majority of the modelled P_V is within a factor of 2 relative to the measured P_V (FAC2 = 0.86), and the correlation between the model and measurements was 0.47 (r=0.47). Specifically, P_V estimated by AMCLIM is generally

consistent with real livestock urine application experiments conducted at sites in Australia (Vallis et al., 1982, 1985), Ireland (Fischer et al., 2016) and New Zealand (Ball et al., 1979; Sherlock and Goh, 1984; Laubach et al., 2012), as well as two studies using artificial urine in Finland (Saarijärvi et al., 2006) and US (Frank and Zhang, 1997). In particular, AMCLIM captures a very high P_V measured for cattle urine application in a tropical place in Australia (symbol "A" in Fig 5.11b). However, only very limited measurements have been taken under tropical climates, indicating a need for more experiments in hot regions. It is worth mentioning when comparing with experiments carried out under dry soil conditions, the volatilization rates of urine application estimated by AMCLIM are either overestimated for three experiments in UK summer by Lockyer and Whitehead (1990), or underestimated for one experiment in New Zealand summer by Carran et al. (1982). Low P_V measured by Lockyer and Whitehead (1990) in June and July at a UK site shows clear differences compared to other measurements of the same study (symbol "D"s in Fig 5.11b), which remained unclear to the original authors, and no explanations were provided (Lockyer and Whitehead, 1990). However, since AMCLIM was not applied at each site and was not driven by the same environmental and meteorological variables, the modelled P_V is not distinguished between dry or wet soil conditions. Higher P_V in dry soils (soil moisture close to wilting point) than wet soils (soil moisture close to field capacity) reported by Carran et al. (1982) might be related to the retention of urine in soils and slower drainage.

There is less literature on investigating NH_3 volatilization from dung compared to urine. In general, the P_V of dung was found to vary between 1 to 5 % in Europe (Whitehead, 1990; Fischer et al., 2016), while Laubach et al. (2013) reported that 11 % of N in dung was lost

through NH_3 emissions in an experiment in New Zealand. Meanwhile, it is broadly agreed that NH_3 emissions from grazing mainly comes from urine deposition, which ranges from 87 to 96 % based on existing studies (Saarijärvi et al., 2006; Laubach et al., 2013). Simulations using AMCLIM suggest a lower contribution from the urine patch because the mixture of urine and dung in the dung pat scheme were also included in the model. So the results from AMCLIM can be considered as broadly consistent with experimental studies.

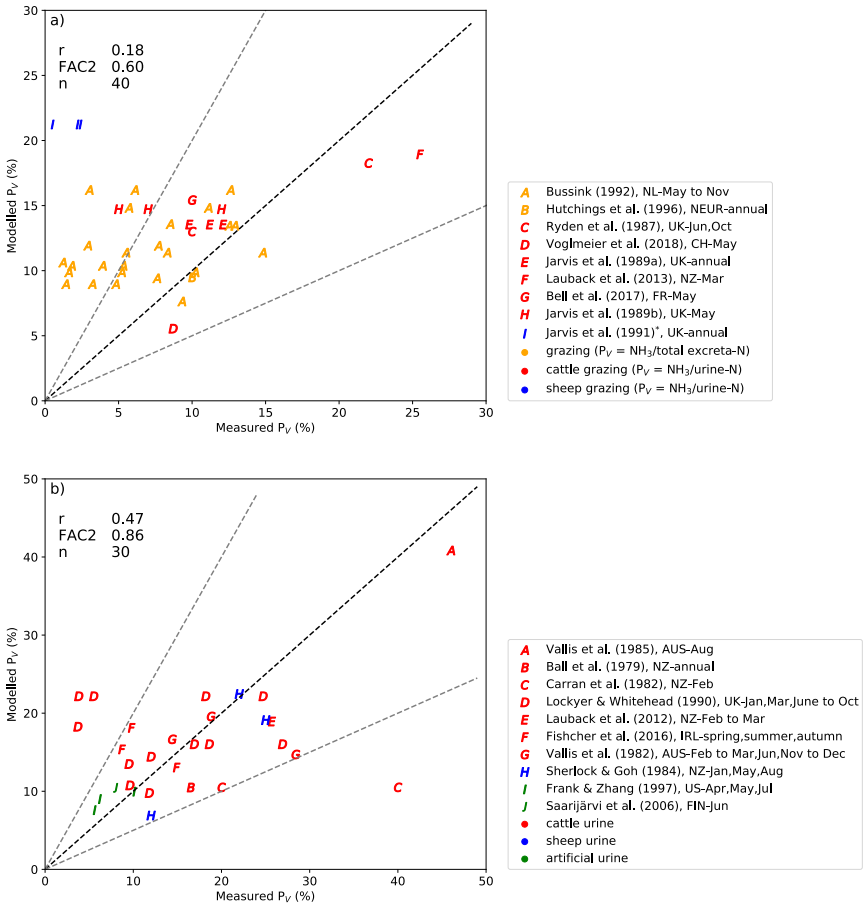

Figure 5.11. Modelled percentage volatilization rates (P_V, %) compared with field measurements. Measurement data were from literature that studied real ruminant grazing (a) and ruminant urine application (b). Pearson's correlation coefficient (r), fraction of values within a factor of 2 (FAC2) and number of measurements (n) are presented at the top left corner. *In Jarvis et al. (1991), P_V of the grazed land with 0 and 420 kg N ha^{-1} fertilizer input and mixed grass/clover were 0.5 %, 2.2 % and 2.4 %, respectively.

5.3.4 Nitrogen flows and NH_3 emissions of global ruminant farming

5.3.4.1 Nitrogen flows of ruminant farming

Figure 5.12 shows the N flows of global ruminant farming for the reference year 2010. Global total excreted N from ruminants including cattle, sheep and goats is 74.84 Tg N yr^{-1}. About 40 % of excreted N (30.06 Tg N yr^{-1}) is allocated to housing, and 60 % (44.78 Tg N yr^{-1}) is from grazing. Ruminant housing results in 3.75 Tg N yr^{-1} of NH_3 emission, while 3.53 Tg N yr^{-1} of manure N is used as fuel. Manure management results in 3.89 Tg N yr^{-1} of NH_3 emission, accounting for 17 % of total managed manure N (22.79 Tg N yr^{-1}). During manure management, nitrogen that is left on land without being stored was 8.28 Tg N yr^{-1}, while runoff and nitrification together account for 1.62 Tg N yr^{-1}. Nitrogen that is introduced to land consisted of two parts: 9.01 Tg N yr^{-1} from manure storage and 44.78 from grazing, which together result in 12.20 Tg N yr^{-1} of NH_3 emission. Meanwhile, 26.07 Tg N yr^{-1} enters soils and is used by plants, and 15.55 Tg N yr^{-1} of N undergoes other processes (e.g., runoff, nitrification, leaching and diffusion to deep soils).

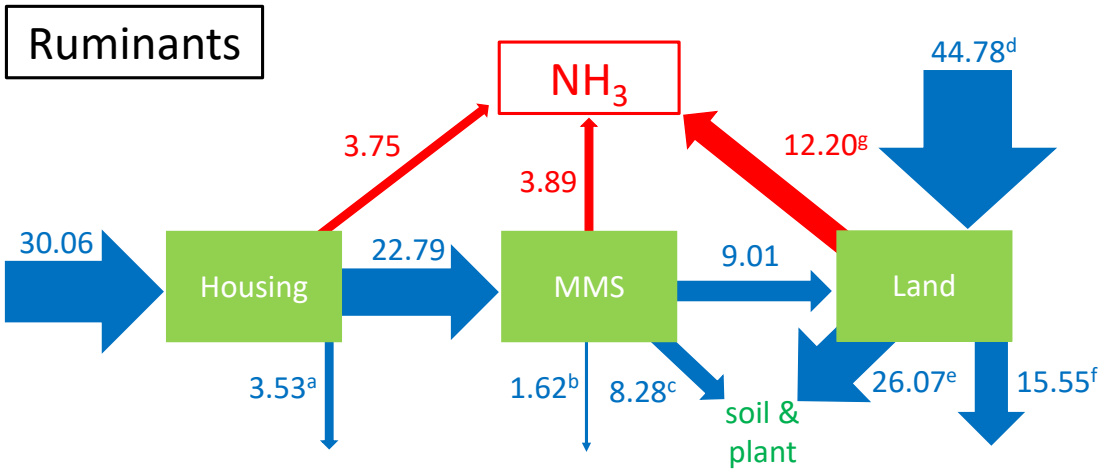

[a]manure used as fuel (3.53)
[b]runoff (0.22) nitrification (1.44) lagoon (<0.01)
[c]this 8.28 represents the amount of manure N left on land (not stored) and is not further simulated; NH_3 emission counted as MMS emissions
[d]excreted N deposited on pastures while grazing
[e]manure application (4.43) grazing (21.64)
[f]runoff (1.13) nitrification (1.47) leaching & diffusion to deep soil (12.95)
[g]manure application (3.25) grazing (8.95)

Figure 5.12. Nitrogen budget of global ruminant farming including housing, manure management, manure application to land and grazing estimated by AMCLIM for year 2010. Dark blue arrows are N flows. Red arrows represent NH_3 emissions. All numbers have the unit of Tg N yr^{-1}. Size of the arrows is proportional to the flux.

5.3.4.2 Cattle NH_3 emissions

According to simulations using AMCLIM, the estimated global NH_3 emissions from cattle farming are 17.7 Tg N yr^{-1} in 2010 and 16.6 Tg N yr^{-1} in 2018, indicating 26 % and 24 % of excreted N lost through NH_3 volatilization in each year, respectively. Housing, manure management and manure application each contribute to around 20 % of total NH_3, and

grazing resulted in the remaining 40 % of emissions. As shown in Figure 5.13, high emissions occur in Brazil, China, India, eastern US, Caribbean and Europe, as well as several African countries. High volatilization rates are found across India, NCP, part of Russia, Ukraine, eastern US, Africa, Europe and Southeast Africa. Regions with high emissions are broadly consistent with high volatilization.

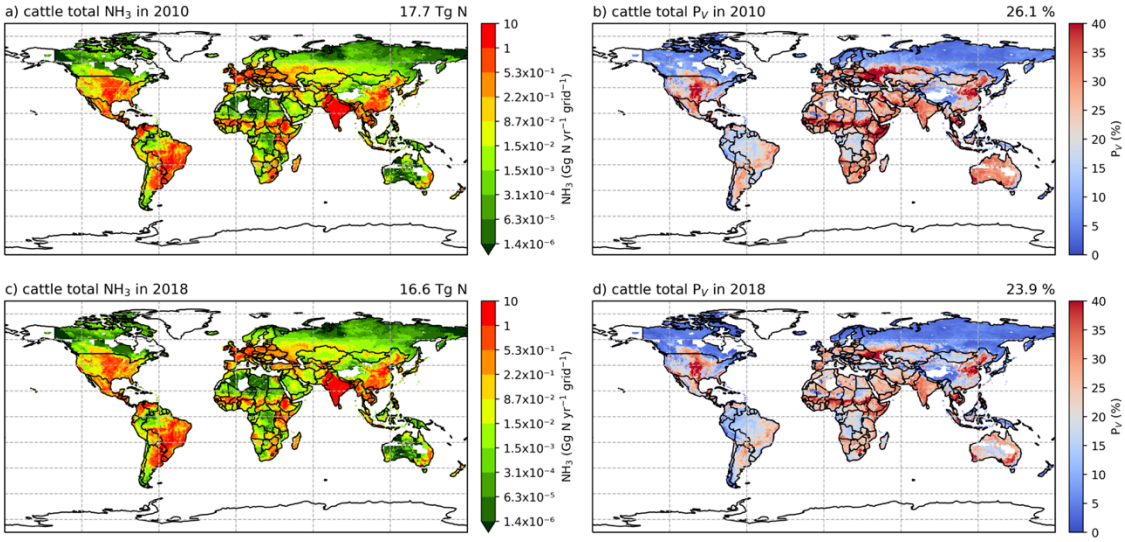

Figure 5.13. Simulated (a) annual global NH_3 emissions (Gg N yr^{-1}) from cattle farming (including housing, manure management, manure application and grazing) in 2010. (b) Percentage of excreted N from cattle that volatilizes (P_V) as NH_3 in 2010. (c) NH_3 emissions (Gg N yr^{-1}) from cattle farming in 2018. (d) P_V rates for cattle farming in 2018.

Figure 5.14 shows the global monthly emissions of NH_3 from cattle farming in 2010 and 2018, with emissions from each stage. The two simulated years show similar seasonal variability, with the year 2010 exhibiting more significant seasonality. In 2010, the largest

monthly emission exceeds 2.0 Tg N $month^{-1}$ in April, and a second emission peak occurs in September. Monthly emissions in 2018 are generally lower than the year 2010.

Housing and manure management have very similar monthly emissions, and both show much higher emissions in MAM and JJA than other seasons. Meanwhile, NH_3 emissions from grazing are also high in MAM and JJA, with seasonal grazing exhibiting more varied monthly emissions compared to year-round grazing. By comparison, NH_3 emissions resulting from manure application showed seasonality that is different from other activities but similar to the total emissions, indicating that the seasonal variations in cattle farming emissions are largely driven by the manure application.

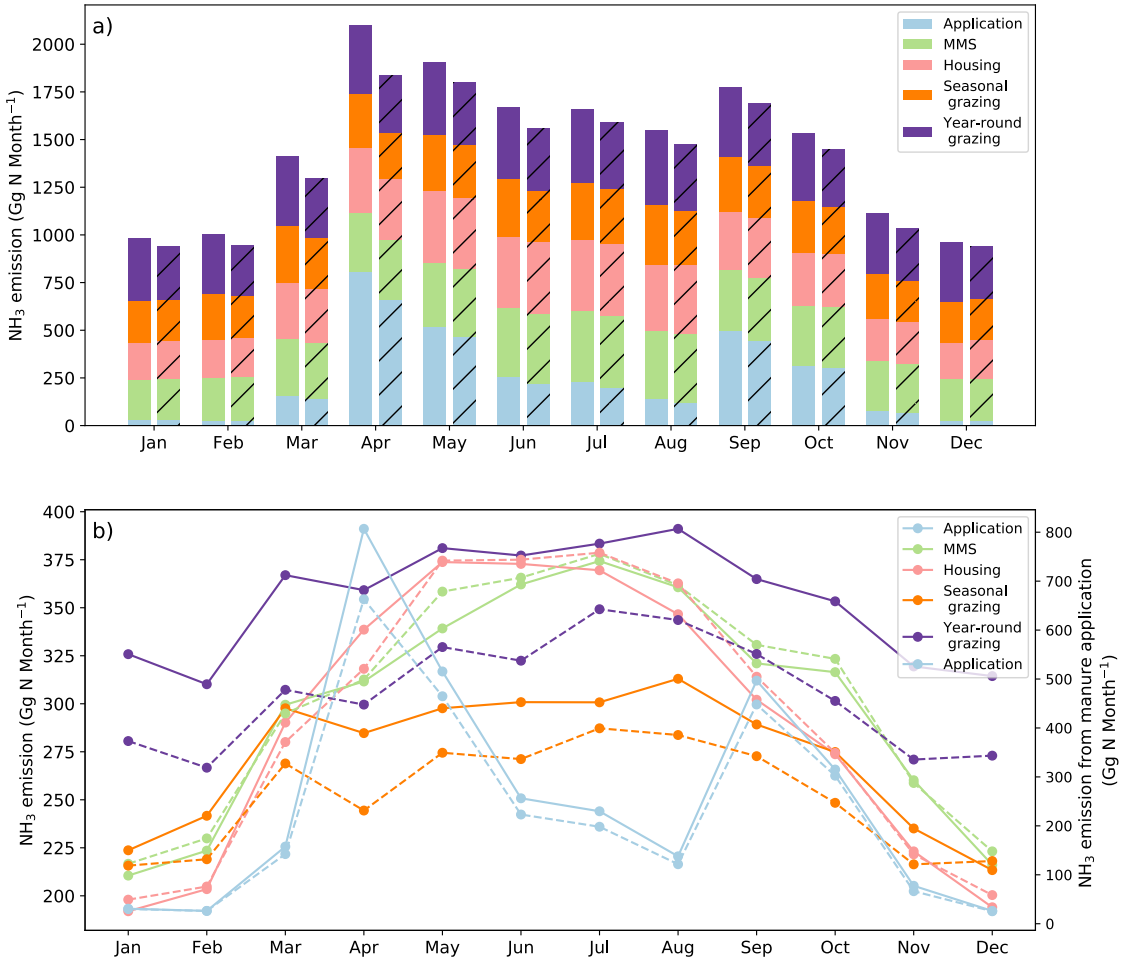

Figure 5.14. Global monthly NH_3 emissions (Gg N month^{-1}) from cattle housing, manure management, manure application, seasonal grazing and year-round grazing in 2010 (a–bars on the left; b–solid lines) and 2018 (a–bars on the right with hatch; b–dashed lines) simulated by AMCLIM.

5.3.4.3 Sheep and goat NH_3 emissions

The global NH_3 emissions from sheep and goat farming estimated by AMCLIM are 2.1 Tg N yr^{-1} and 1.9 Tg N yr^{-1} in 2010 and 2018, accounting for 30 % and 26 % of excreted N in each year, respectively. Grazing results in around 60 % of the total emissions, while housing, manure management and application are each responsible for about 10 to 15 % of emissions. As shown in Figure 5.15, high emissions are found in southeastern Australia, India, NCP, western and eastern Africa, Europe and the Middle East, and high volatilization rates generally occurred in these regions with high emissions, as well as the US.

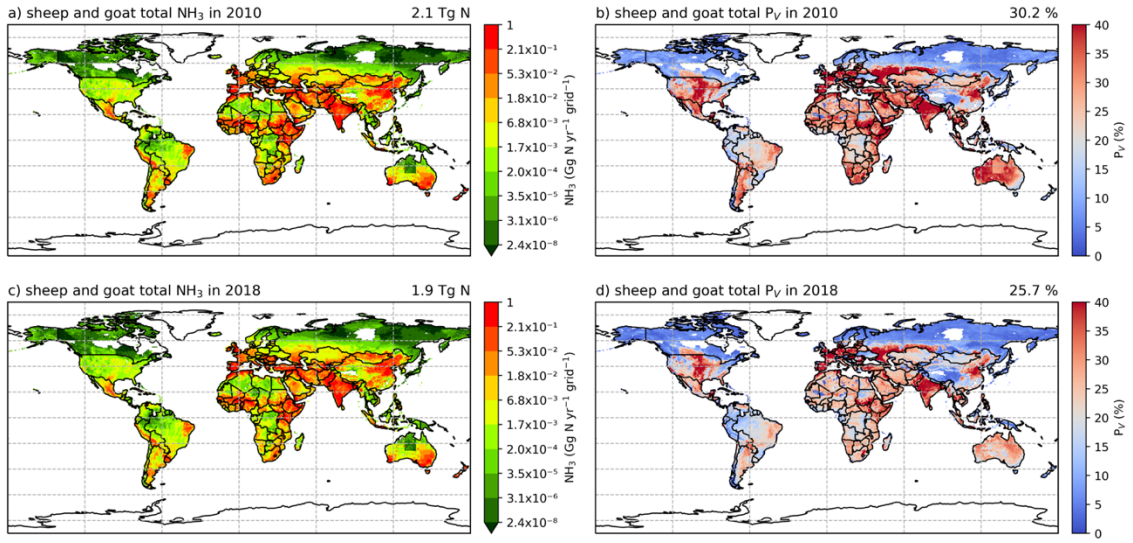

Figure 5.15. Same as Figure 5.11 but for sheep and goat farming.

As shown in Figure 5.16, the highest monthly emissions from sheep and goat farming are in April in both simulated years, with high emissions from May to October. Compared with

cattle farming, seasonal variations in NH_3 emissions from sheep and goat housing and manure management are less pronounced, and grazing generally shows slightly higher emissions in JJA than other seasons. The most predominant seasonal variations are found in emissions from manure application, with the highest emissions occurring in April, which is largely related to the simulated planting seasons.

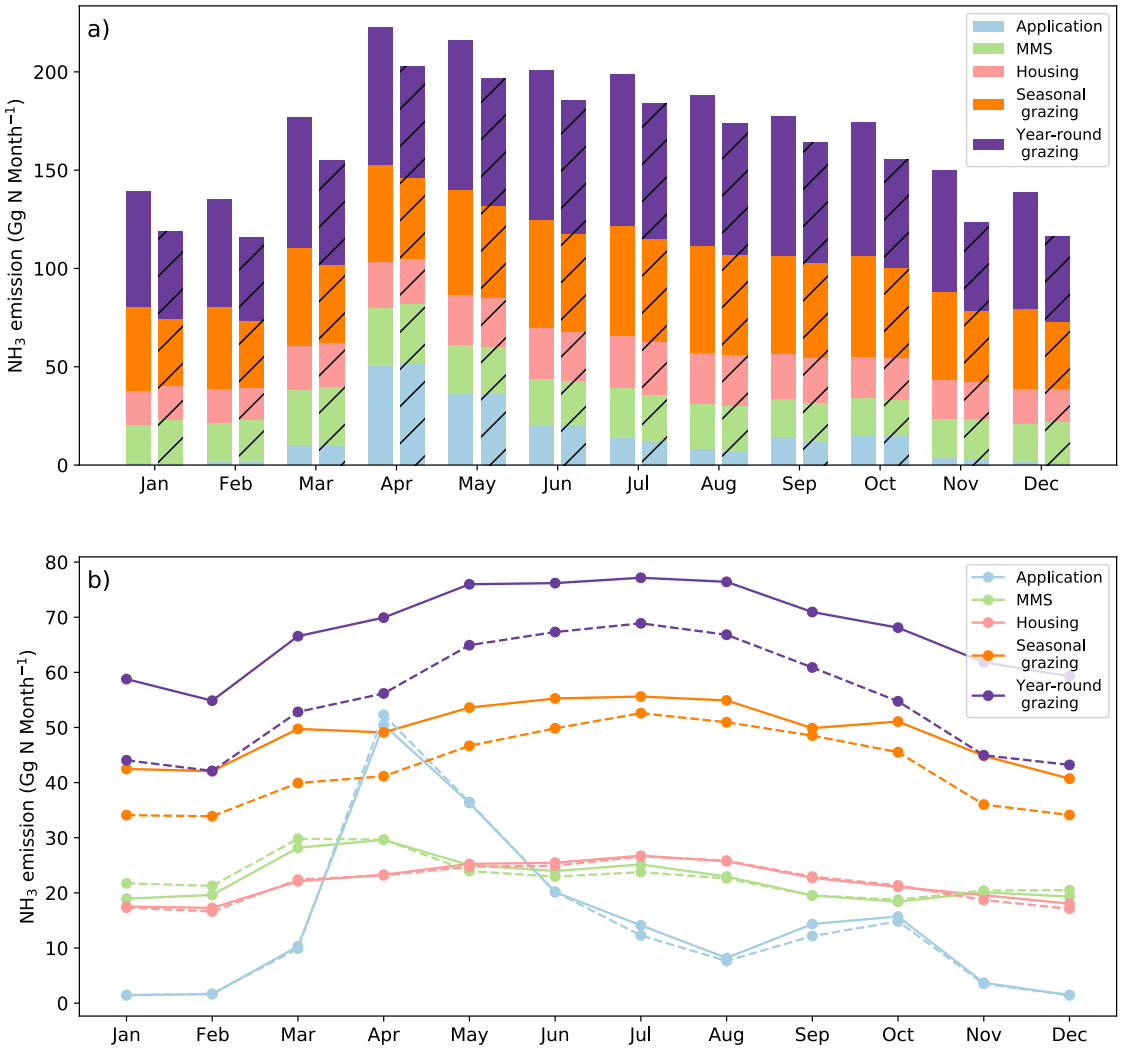

Figure 5.16. Same as Figure 5.14 but for sheep and goat farming.

5.4 Discussion

AMCLIM–Housing applied at the site scale was capable of reproducing the NH_3 emissions from a dairy barn, with close agreement between the modelling results and measurements. Both simulated and measured emissions show a positive relationship with indoor temperature and ventilation. Distinct from the site simulation of pig and layer chicken housing presented in Chapter 4, the indoor conditions of the dairy barn are closer to the natural environment than the pig and layer houses. The simulated processes are similar to those in the simulations for the "slatted floor" in the pig house. With less processes involved (only one emitting surface in the dairy houses for simulations), the model performance is actually better.

The global application of AMCLIM focused on cattle, sheep and goat. The cattle sector includes six types of cattle, and this is the largest NH_3 emission sector in livestock farming. Estimated NH_3 emissions resulted from cattle farm are nearly nine times the emissions from sheep and goat farming. Large emissions related to cattle farming occur in regions with high animal populations, such as India, NCP, US, Caribbean, Europe, South America and several Sahel countries. These regions generally show high volatilization rates, and high volatilization rates are also found in Australia and southeast Asia. The geographical distribution of high emissions from sheep and goat farming are also consistent with high animal populations.

The impacts of environmental conditions and management practices on NH_3 volatilization can be reflected on multiple aspects from the simulations for ruminant farming. First, it is notable that the simulated volatilization rates of housing, manure management and grazing

for buffaloes are higher than other types of cattle. This is because buffaloes are predominantly reared in hot regions such as southern China, South Asia and southeast Asia compared to cattle that are widely distributed across the globe, resulting in higher P_V due to generally hotter conditions. Second, the estimated P_V rates of ruminant housing are slightly higher for the year 2010 than 2018, which is different compared with pig and poultry housing. This can be partly attributed to the management for ruminants, which are often not confined to housing throughout the year but can let the animal spend considerable time outdoors on pastures, particularly in warmer weather. Therefore, the lower P_V in 2018 might result from a warmer condition that influences the allocation of excreta, leading to different distributions between houses and pastures. Meanwhile, land application of manure and grazing show relatively higher volatilization rates in 2010 than 2018. The same feature has also been found for land applications of synthetic fertilizer (see Chapter 3), pig and poultry manure (see Chapter 4). The lower P_V of these outdoor activities in 2018 than 2010 might be due to larger leaching and diffusive fluxes that transport N to the deeper soils and result in less NH_3 released to the atmosphere, which has been discussed in Chapter 3 and 4.

Ruminant-specific NH_3 emission factors (EFs) derived from ACMLIM simulations and comparisons with EFs from literature are summarised in Table 5.12. Global average EFs for beef, sheep and goat estimated by AMCLIM are generally within the range reported by literature (Yang et al., 2023). AMCLIM predicted higher EFs for buffaloes and lower EFs for dairy cattle than literature.

Table 5.12. Simulated animal NH_3 emission factors (EFs) (kg N $head^{-1}$ yr^{-1}) for ruminants based on simulations of AMCLIM compared with Yang et al. (2023) which summarizes the range of EFs from literature. The AMCLIM values in the first row are the global mean EF, and values in the brackets represent the 10th and 90th percentile, respectively.

Study	Ruminants EFs (kg N $head^{-1}$ yr^{-1})				
	Beef	Buffaloes	Dairy	Goat	Sheep
AMCLIM	9.7 (2.5 – 15.9)	11.8 (3.7 – 15.5)	11.6 (2.1 – 19.1)	0.8 (0.2 – 1.7)	1.2 (0.2 – 2.0)
Yang2023[a]	3.0 – 14.3	2.8 – 8.7	14.5 – 21.8	0.6 – 5.0	0.6 – 2.5

[a] Yang et al., 2023

Globally, the estimated volatilization rates for sheep and goat farming are higher than those of cattle farming (see Fig 5.13 and 5.15), which is partly due to the higher N concentration in sheep and goat's urine compared to cattle. Another reason is that sheep and goat are more "concentrated" in the Middle East and South Asia where they tend to have higher volatilization rates due to warmer climates. For housing, the housing density used in AMCLIM also affect the volatilization rates. It is worth noting that the volatilization rates of feedlot cattle housing are the second lowest among ruminants, partly because the feedlot cattle had the highest stocking density in the model. Increasing the stocking density results in smaller source area for NH_3 emission, which leads to lower emissions. Application of ruminant manure showed the highest volatilization rates among all activities, with the volatilization rates being lower in 2018 than 2010, which is also found for pig and poultry

manure. By comparison, housing and manure management showed less variations in volatilization rates between years.

Grazing is an additional component of simulations for ruminant farming compared to pigs and poultry. Overall, the estimated NH_3 emissions from grazing are 7.9 to 9.0 Tg N yr^{-1}, accounting for around 16 to 19 % of excreted N from ruminants while grazing. Emissions related to grazing exhibit the largest annual difference between the two simulated years compared with other activities. The grazing emissions estimated by AMCLIM are lower than the 12 Tg N yr^{-1} suggested by FANv2, but the volatilization rates are comparable to the 18 % by FANv2 (Vira et al., 2020a). The differences in emissions between AMCLIM and FANv2 are partly due to the different estimates of excreted N on pastures. In general, excreted N on pastures during grazing results in lower simulated volatilization loss of NH_3 compared with manure application.

For the "mixed" production system, about 65 % of N in cattle excreta is excreted in animal houses, compared with less than 40 % for sheep and goat, based on the GLEAM2 MMS data. The volatilization loss of excreted N during seasonal grazing of cattle is around 20 %, which is similar to the value for sheep and goats. It should be noted that the regional variations in the volatilization rates of year-round sheep and goat grazing are more significant than the seasonal grazing (Fig 5.9 b, d and Fig 5.10 b, d). By comparison, the regional variations in year-round grazing of cattle are similar to the seasonal grazing (Fig 5.7 b, d and Fig 5.8 b, d). As a result, with the "grassland" production system (year-round grazing) being more spread across the globe especially in temperate and cold regions than the "mixed" production system, year-round grazing of cattle shows lower volatilization

rates compared with seasonal grazing, while there is not much difference between year-round and seasonal grazing for sheep and goat.

It is evident that the urine patch scheme in the grazing simulations results in much higher NH_3 emission and higher volatilization rate compared with the dung pat scheme. Urea in urine deposited on pastures is readily to hydrolyse to TAN, which can lead to higher emission than dung itself due to the slower decomposition of organic forms of N in dung. As presented in Section 5.3.3.3, existing experimental studies have reported that NH_3 loss accounts for 0.5 % to up to 46 % of urinary N, while AMCLIM predicted 5.5 to 41 %. The differences can be caused by different environmental and meteorological conditions such as temperature, soil moisture, precipitation and soil texture, between the year when experiments were conducted and the modelled year 2010. It also remains unclear why several experiments showed very small volatilization rates, which were not clearly provided by experimentalists, and needs further investigations. Overall, estimated volatilization rates by AMCLIM are broadly consistent with measurements, especially in warm regions such as Australia and New Zealand. The differences indicate that the infiltration and drainage (also diffusion) in AMCLIM might not be representative enough and need improvement. By comparison, dung contributes less NH_3 emissions than urine resulting from the lower volatilization rates. However, from the mixture of dung and urine scheme, it implies that urine deposited on dung can also result in considerable NH_3 emissions, which is due to the slow infiltration of urine to the soil underneath as dung holds the liquid. A similar example is farmyard manure which can cause large NH_3 emissions.

Uncertainty in NH_3 emissions from livestock housing, manure management and application has been discussed in Chapter 4. For ruminants, uncertainty related to these activities is

assumed to be the same as that of pigs, with additional uncertainty also existing in emissions from grazing. Uncertainty of grazing emissions is considered the same as urea application, which is 20 % (as discussed in Chapter 3). The overall estimated uncertainty of NH_3 from ruminants farming is 8 to 10 % for cattle and 11 to 14 % for sheep and goat.

5.5 Summary and conclusions

This chapter presents the quantification of NH_3 emissions from ruminants farming, including cattle, sheep and goat. In addition to housing, manure management and land application of manure (where the modelling is similar to pigs and poultry, as described in Chapter 4), the AMCLIM Grazing Submodule has been developed for ruminants compared to pigs and poultry. The AMCLIM model simulates both seasonal and year-round grazing of ruminants and implements two grazing schemes (seasonal and year-round) that consider emissions from urine and dung. Ruminant housing and seasonal grazing are closely associated with each other, in which AMCLIM incorporates the meteorological condition, production system information and MMS information to determine the quantity of N excreted in animal houses and on pastures.

In this chapter, AMCLIM was applied at the site scale to simulate the NH_3 emission from dairy houses. The simulated NH_3 emissions from dairy housing agree well with measurements. For global simulations, it is estimated that NH_3 emissions from ruminants farming are 19.8±1.5 Tg N yr^{-1} in 2010 and 18.5±1.3 Tg N yr^{-1} in 2018, with cattle contributing to 17.7±1.5 and 16.6±1.3 Tg N yr^{-1} and sheep and goat contributing to 2.1±0.3

and 1.9±0.2 Tg N yr^{-1} emission in each simulated year. This indicates that over a quarter of excreted N from ruminants volatilizes as NH_3. For cattle, about 40 % of emissions result from housing and manure management, while over 17 % of emissions come from manure application. The remaining 42 % of emissions are from the two types of grazing. For sheep and goat, grazing is the most important source, which results in over 60 % of total emissions because of shorter housing periods. Emissions from other activities are comparable to each other (ca. 10 to 14 %). Emissions from the land simulations (manure application and grazing) for ruminants also exhibited the same trend as application of synthetic fertilizers, pig and poultry farming, of which higher volatilization rates occurred in 2010 than 2018.

High emissions from cattle farming are found in Brazil, China, India, US, Europe and several African countries, while high emissions resulting from sheep and goat farming are found in Australia, China, Europe, the Middle East and South Asia. These regions are largely consistent with places with high livestock population numbers.

Chapter 6
Outlook: present and future agricultural ammonia emissions

6.1 Introduction

Global agricultural NH_3 emissions are estimated to have more than doubled over the past 50 years, from about 20 Tg N yr^{-1} in the 1970s to over 45 Tg N yr^{-1} in the 2010s (EDGAR, 2022), mainly as a result of large increases in livestock farming and fertilizer use. As an unintentional nitrogen loss from agricultural systems, NH_3 emission not only compromises the resource use efficiency (i.e., increase the fraction of nitrogen that is not used by plants or livestock), but also adversely affect the environment (i.e., reducing air, water and soil quality and damaging vegetation). Agricultural NH_3 emissions have been found to be strongly dependent on environmental conditions such as temperature, wind speed, water availability and many other meteorological factors (Gyldenkærne, 2005b; Misselbrook et al., 2005; Sommer et al., 2006; Sutton et al., 2013; Bittman et al., 2014). Global NH_3 emissions have been projected to treble the present value by the end of the century when considering climate warming and increasing agricultural activities (Sutton et al., 2013). Meanwhile, local management practice is a crucial factor that determines the NH_3

emissions. Better management practices can effectively reduce NH_3 emissions, which is beneficial for the environment, while wasting less nitrogen as a valuable resource.

In this chapter, estimated NH_3 emissions from the whole agricultural sector by AMCLIM are presented that synthesize the results from previous chapters (Chapter 3 – synthetic fertilizer; Chapter 4 – pigs and chicken; Chapter 5 – ruminants). Analysis, sensitivity tests and experimental tests are reported that investigate the impacts of environmental variables and local management practices on NH_3 emissions, with explorations of potential measures and techniques for NH_3 abatement. This chapter also presents past NH_3 emissions for the last two decades and projects the future NH_3 emissions to the end of the 21st century.

6.2 Ammonia emissions from the agricultural system

6.2.1 Annual global agricultural NH_3 emission and nitrogen flows in the agricultural sector

Using AMCLIM, it is estimated that NH_3 emissions from global agriculture are 44.9±4.4 Tg N yr^{-1} in 2010, indicating that approximately 22±2 % of a total 201.8 Tg N yr^{-1} from synthetic fertilizer and livestock excreta is lost due to NH_3 volatilization. As shown in Figure 6.1, high NH_3 emissions (per grid) occur in Brazil, China, eastern US, Europe, South Asia, and several African and South American countries, which largely corresponds to the regions with intensive agricultural activities. Specifically, China, India, US, Brazil and

Pakistan are estimated to be the top five countries that have the largest emissions as 8.8, 7.4, 4.5, 3.0 and 2.0 Tg N yr^{-1}, respectively, accounting for nearly 60 % of the global total NH_3 emissions.

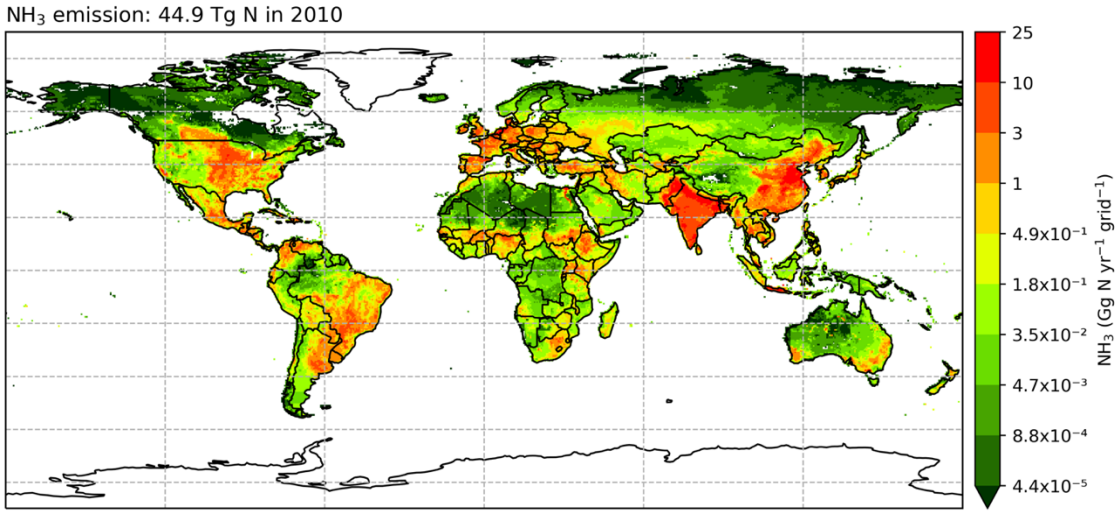

Figure 6.1. Geographical distribution of global agricultural NH_3 emissions (Gg N yr^{-1} $grid^{-1}$) in 2010 estimated by AMCLIM. The resolution is 0.5º × 0.5 º.

About 1/3 of NH_3 emissions result from the use of synthetic fertilizer (as presented in Chapter 3), with 2/3 of emissions from livestock farming (as presented in Chapter 4 and 5; including housing, manure management, land application of manure and grazing). Cattle (including buffaloes) is the largest emitter group among livestock, contributing nearly 40 % of total emissions and over 60 % of livestock emissions (Fig 6.2b). Both pigs and poultry result in more than 10 % of total NH_3 emissions, while sheep and goats are responsible for the remaining 5 %.

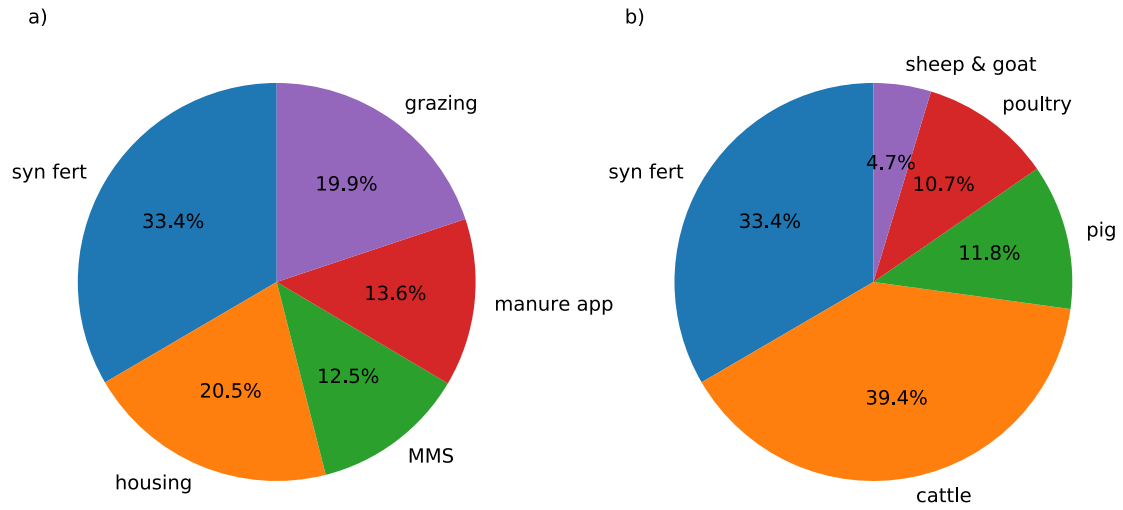

Figure 6.2. Global agricultural NH_3 emissions from different (a) agricultural activities and (b) sectors for 2010 as estimated by AMCLIM. The cattle sector includes beef cattle, dairy cattle, other dairy, feed cattle and buffaloes. The poultry sector only includes chicken that accounts for over 95 % of poultry numbers globally (FAOSTAT). Other minor livestock such as non-chicken poultry (e.g., duck and turkey), horse and camel, which only account for a small fraction are not simulated in AMCLIM.

AMCLIM was also used to assess the nitrogen budget for the whole agricultural sector, with a focus on NH_3 emissions and processes associated with anthropogenic activities as in previous chapters. Global total nitrogen intake by livestock is estimated at 122.2 Tg N yr^{-1} in 2010, with 99.6 Tg N yr^{-1} excreted, according to GLEAM2 that provides input data of livestock to AMCLIM (FAO, 2018a; Uwizeye et al., 2020). As illustrated in Figure 6.3, it is estimated that 14.8 Tg N yr^{-1} is lost as NH_3 emissions from livestock housing and manure management, with further 6.4 Tg N yr^{-1} being used as fuel/biogas or lost to other

environmental compartments due to lack of proper management (e.g., excreta dumped into fishpond). During manure management, a small fraction of nitrogen is estimated to be washed away (0.2 Tg N yr^{-1}) by surface runoff and converted into nitrate (and nitrite) through nitrification (1.8 Tg N yr^{-1}). Meanwhile, 14.6 Tg N yr^{-1} is either left on land without further attention (without being stored) or applied to field directly (without being stored), which is assumed to be added to the soil nitrogen pool or uptake by plants. The remaining 61.7 Tg yr^{-1} of livestock excreted nitrogen is introduced to land through two pathways: 16.9 Tg N yr^{-1} is applied as manure fertilizer after storage, and 44.8 Tg N yr^{-1} is directly deposited on pastures through grazing.

Land receives nitrogen input from both livestock manure and synthetic fertilizer. An additional 102.3 Tg N yr^{-1} is added to land as synthetic fertilizer, and the majority of which is in the form of urea and ammonium (85.1 Tg N yr^{-1}), with 15.2 Tg N yr^{-1} added as nitrate. A total 30.0 Tg N yr^{-1} of NH_3 emissions are estimated by AMCLIM to result from these activities, with both manure and synthetic fertilizer contribute half of these emissions. Around 53 % (86.9 Tg N yr^{-1}) of nitrogen input to land is either used by crops or stored in soils, 10 % (16.7 Tg N yr^{-1}) is nitrified, and about 20 % (30.4 Tg N yr^{-1}) was lost due to runoff, leaching and diffusion.

Overall, around 50 % (101.5 Tg N yr^{-1}) of the total nitrogen input from anthropogenic sources (201.8 Tg N yr^{-1}) enters the soil including plant uptake, and over 40 % (81.9 Tg N yr^{-1}) of nitrogen is estimated to be lost through different processes. The remaining 10 % of N that undergoes nitrification is not simulated further, which potentially ends up being converted to N_2O and N_2 through denitrification and leaching.

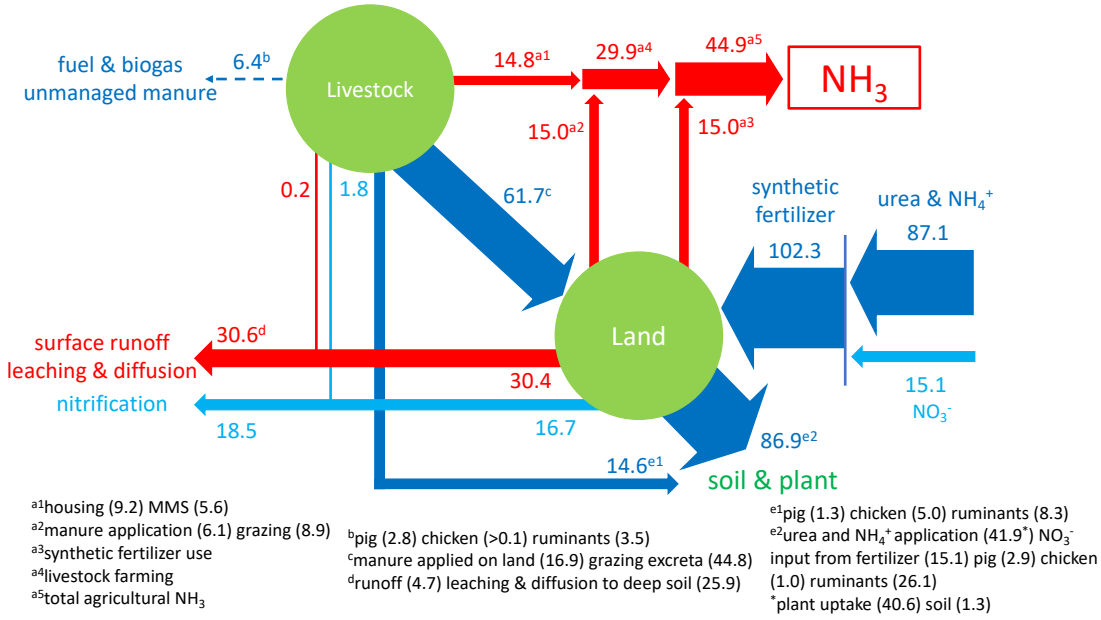

Figure 6.3. Global nitrogen budget of the agricultural sector by AMCLIM. Natural nitrogen input or sources are not included. Dark blue arrows are nitrogen flows. Red arrows represent physical processes including emissions, runoff, leaching and diffusion. Light blue arrows represent nitrification or nitrate inputs. All numbers have the unit of Tg N yr^{-1}. Size of the arrows is proportional to the flux. The fluxes of NH_3 are labelled by a1 – a5, and N flows enter the soil including plant uptake are labelled by e1 – e2, detailing the individual sources or pathways.

6.2.2 Ammonia emissions from agricultural activities

Annual NH_3 emissions from each agricultural activity as estimated by AMCLIM are summarised in Table 6.1, along with the corresponding percentage volatilization rates. In 2010, both livestock housing and grazing result in an estimated 9 Tg N yr^{-1} NH_3, together accounting for approximately 40 % of total emissions. Manure management and

application to land each contribute around 6 Tg N yr^{-1} NH_3, respectively (Fig 6.2a and Table 6.1). The highest percentage volatilization rate is from manure application, with 36 % of applied manure nitrogen estimated to be lost through NH_3 emissions. Grazing has the second highest estimated volatilization rates of nearly 20 %. Use of synthetic fertilizer, livestock housing and manure management show similar volatilization rates, ranging from 14 to 17 %.

Table 6.1. Annual global NH_3 emissions (Tg N yr^{-1}) and corresponding volatilization rate P_V (%) for agricultural activities in 2010.

Agricultural activities	NH_3 emission (Tg N yr^{-1})	N available for Emissions (Tg N yr^{-1})	Average P_V (%)
Synthetic fertilizer	15.0	102.3	14.7
Livestock housing	9.2	54.8	16.8
Manure management	5.6	39.2	14.4
Manure application	6.1	16.9	35.9
Grazing	8.9	44.8	19.9
Whole agricultural sector	44.9	201.9	22.2

Table 6.2 compares the NH_3 emissions simulated by AMCLIM with estimates from other studies, including models and inventories. The comparisons are against research conducted later than 2000 with volatilization rates if available. DLEM, FAN (both introduced in Chapter 3; see section 3.4.1) and CAMEO (Beaudor et al., 2023) are processed-based

models, while the other studies or inventories mainly use EFs methods (see Table 6.2 for references of all model descriptions/studies). For global agricultural emissions, AMCLIM produces similar results to other process-based models, i.e., CAMEO (44 Tg N yr^{-1}) and FANv2 (48 Tg N yr^{-1}). Emissions estimated by AMCLIM are also similar to the EDGAR emission inventory (44.2 Tg N yr^{-1}), with slightly higher emissions estimated by AMCLIM than EDGAR. By comparison, NH_3 emissions reported by EFs-based studies vary between 32 to 54 Tg N yr^{-1}. Paulot et al. (2016) estimates global agricultural NH_3 emissions at 34 Tg N yr^{-1} for 2008, which is more than 20 % lower than the process-based models (in year 2010 or averaged over the 2010s) and is close to the results for year 2000 suggested by Beusen et al. (2008; 32 Tg N yr^{-1}) and FANv1 (33 Tg N yr^{-1}; Riddick et al., 2016), while emissions by Yang et al. (2023; 54.4 Tg N yr^{-1}) are 23 % higher compared with models and the EDGAR inventory.

Each of these studies used a different methodology and estimated emissions based on different sectors or activities. For example, CAMEO and the EDGAR inventory reported NH_3 from two major sources: agricultural soils and manure management (EDGAR) or indoor emissions (CAMEO; including housing, animal yards and manure storage), and the estimated emissions from these two sources were in close agreement between CAMEO and EDGAR. By comparison, AMCLIM and FANv2 have more detailed component emissions that are related to agricultural activities. Emissions from synthetic fertilizer use estimated by AMCLIM (as discussed in Section 3.4.1) are higher but emissions from livestock farming are lower than the estimates from FANv2. This is partly due to the different inputs used by the two models as discussed in Chapter 3. The overall volatilization rates for emissions from the whole agricultural sector, synthetic fertilizer use and livestock farming

are comparable between AMCLIM and FANv2. The largest difference between the two models exists in the volatilization rates of manure application, where AMCLIM suggests a volatilization rate that is nearly double that of FANv2. Compared with FANv2, DLEM is closer to AMCLIM for the NH_3 emissions from synthetic fertilizer use (16.7 Tg N yr^{-1} vs. 15.0 Tg N yr^{-1}), as well as the estimated volatilization rates (16.3 % vs. 14.7 %).

There are also variations in the simulated processes among the process-based models. AMCLIM is the only model that has a detailed simulation for processes involved in all agricultural activities, including use of synthetic fertilizers (as discussed in Chapter 3), livestock housing, manure management, land application of manure and grazing (as discussed in Chapter 4 and 5), which accounts for climatic effects on NH_3 volatilization. Other models are considered as semi-empirical process-based models that also use EFs for several agricultural components. For example, CAMEO and FANv2 applied EFs for livestock housing and manure management, with corrections for environmental conditions. Meanwhile, AMCLIM also considers the impacts of local management practices on NH_3 emissions by including several housing systems and housing types, as well as the manure management systems that vary across the globe.

Table 6.2. Comparison of NH_3 emissions (Tg N yr^{-1}) from global agriculture and agricultural activities, and corresponding volatilization rates of total N inputs (%) between AMCLIM and other inventories, models and studies.

Model/ Study	Year	Global total	Synthetic fertilizer	Manure application to land	Grazing	Housing and manure management	Livestock total
CAMEO[a]	2005-2015	44	34* (fertilizer and manure application)		10** (livestock housing, yarding and storage)		
DLEM[b]	2000s,		13.6				
DLEM[c]	2010		16.7 (16.3%)				
FANv1[d]	2000	33	12				
FANv2[e]	2010-2015	48 (23.6%)	11 (13%)	6.5 (19%)	12 (18%)	18	37 (31%)
Beusen2008[f]	2000	32	11				21
Yang2023[g]	2010s	54.4	28.6				25.8
EDGAR v6.1[h]	2011	44.2	31.8* (agricultural soils)			11.1** 1.3 (manure burning)	
MASSAGE_NH_3[i]	2008	34	9.4				24.6
NH_3_stat[j]	2012		5.9				
AMCLIM (this study)	2010	44.9 (22.3%)	15.0 (14.7%)	6.1 (35.9%)	8.9 (19.9%)	14.8 (15.8%)	29.9 (30.1%)

[a] Beaudor et al. (2023) [b] Xu et al. (2019) [c] Xu et al. (2018) [d] Riddick et al. (2016) [e] Vira et al. (2020) [f] Beusen et al. (2008) [g] Yang et al. (2023) [h] EDGAR (2023) [i] Paulot et al. (2014)

[j] Aneja et al. (2020) * NH_3 emissions from agricultural soils ** NH_3 emissions from livestock manure management.

The geographical distributions of NH_3 emissions from each activity are shown in Figure 6.4, and the corresponding percentage volatilization rates are shown in Figure 6.5. Results and discussion for synthetic fertilizer and grazing have been given in Chapter 3 and Chapter 5, respectively. For livestock housing and manure management of all livestock sectors, the spatial distributions of NH_3 emission are similar, with high emissions occurring from China, India and Pakistan and hot spots in Brazil, US and Europe. The dominant source of NH_3 emissions differs across the globe (Fig 6.4; also as shown in Fig F1 in Appendix F1). For example, the Northern China Plain (NCP) has high NH_3 emissions from the use of synthetic fertilizer but rather low grazing emissions, while Brazil shows the opposite, with low emissions related to synthetic fertilizer use and high emissions from grazing. Grazing is identified to be the most frequent dominant source for NH_3 emissions (Fig F1a), which is largely due to its wide spatial coverage while other activities concentrate in particular regions. Further discussion is presented in Section 6.2.4.

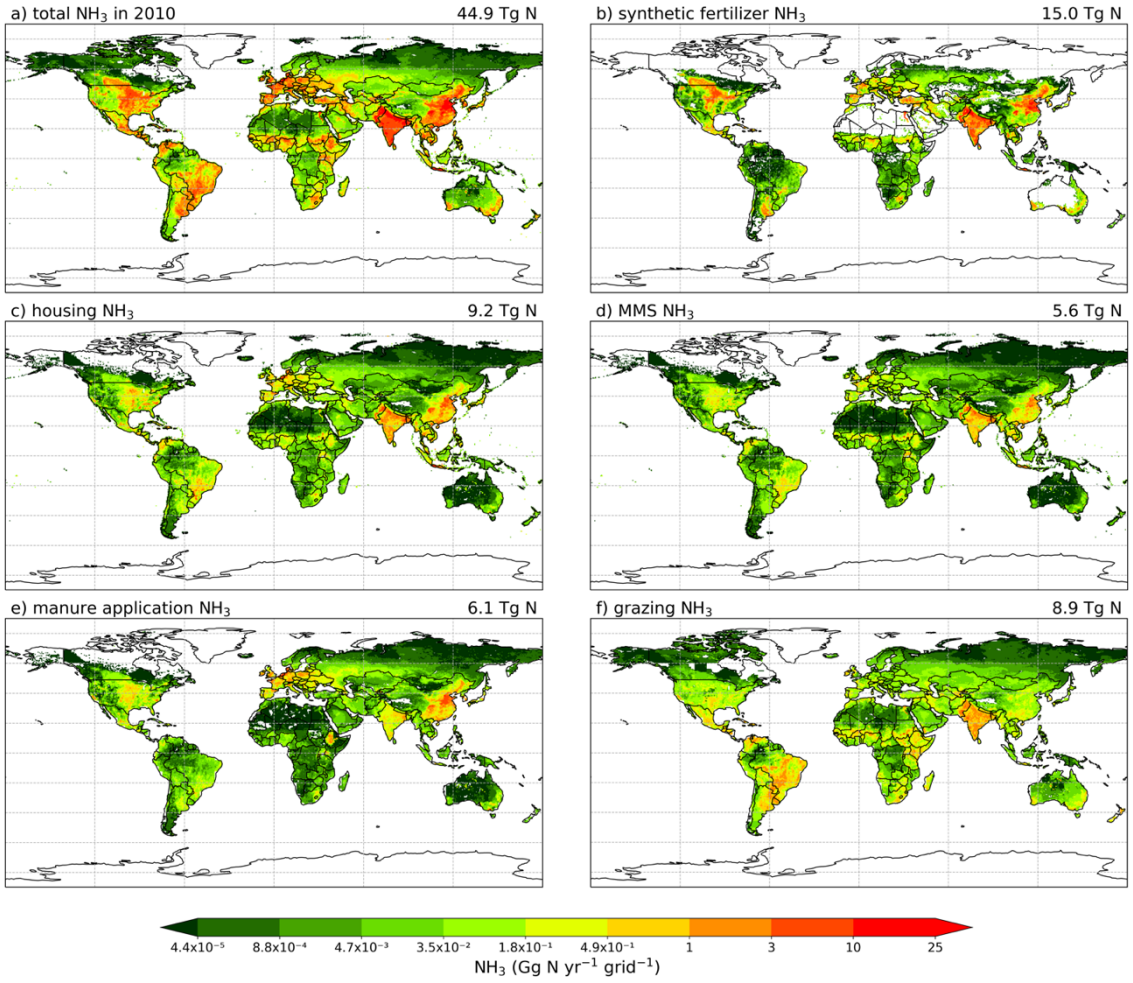

Figure 6.4. Simulated annual global NH_3 emissions (Gg N yr^{-1} $grid^{-1}$) from (a) the whole agricultural sector, (b) synthetic fertilizer use, (c) livestock housing, (d) manure management, (e) manure application to land and (f) grazing in 2010. The resolution is 0.5º × 0.5 º.

As shown in Figure 6.5a, estimated NH_3 volatilization rates differ across the globe. For 2010, up to 40 % of nitrogen are estimated to be lost due to NH_3 volatilization in regions such as Australia, Pakistan, the Middle East and several countries in eastern Africa and the Sahel region. High P_V is not necessarily consistent with high emission regions (Fig 6.5a and Fig 6.4a), but often occurs in hot regions. Manure application showed very high P_V values across the globe. This is partly because the pH of manure can be higher than soil pH in regions with acidic soils, which facilitates NH_3 volatilization. Meanwhile, nitrogen in applied manure has decomposed to TAN after being stored for weeks to months and is readily volatilized. In addition, manure is assumed in AMCLIM to be applied only at the surface. Therefore, the volatilization of manure application is generally higher than that of synthetic fertilizer application (some of which is incorporated or placed below the soil surface). Particularly high volatilization rates for manure application can be found in dry regions, e.g., the Middle East and Sahel region, which is consistent with that of synthetic fertilizer. Grazing P_V displays similar geographical distributions to that of manure application, but with lower volatilization rates (Fig 6.5f). Compared with manure application and grazing, livestock housing and manure management exhibited lower volatilization rates. High volatilization rates of housing and manure management mostly occurred in tropical regions (Fig 6.5c and 6.5d). The spatial variation in the simulated P_V is driven by the combined effects of both the environmental conditions and local management practices. For example, land application in hot and dry regions tends to have higher P_V than cold and wet places. High volatilization rates of indoor practices (e.g., housing or manure storage) are frequently found in hot tropical regions, which reflects the environmental dependences inherent in AMCLIM. Moreover, the volatilization rates for

fully enclosed animal houses with heating and ventilation are normally higher than naturally ventilated barns.

It is worth emphasizing that N species decompose to TAN at different rates, i.e., the hydrolysis of urea to TAN is much faster than the decomposition of organic N. Therefore, the majority of NH_3 emissions related to livestock farming have been found to be originated from urine, of which urea is the major composition (Sommer and Hutchings, 2001). By comparison, NH_3 emissions due to organic N break down can be lower as a result of slower mineralization rates on a longer time scale. Figure F2 (see Appendix F2) shows a variation of the volatilization rates ($P_{V(TAN)}$) that is expresses as percentage of TAN (approximated by urea or urinary N) that volatilizes as NH_3. The regional patterns of $P_{V(TAN)}$ are generally the same as P_V, while the values of $P_{V\ (TAN)}$ are higher than those of P_V.

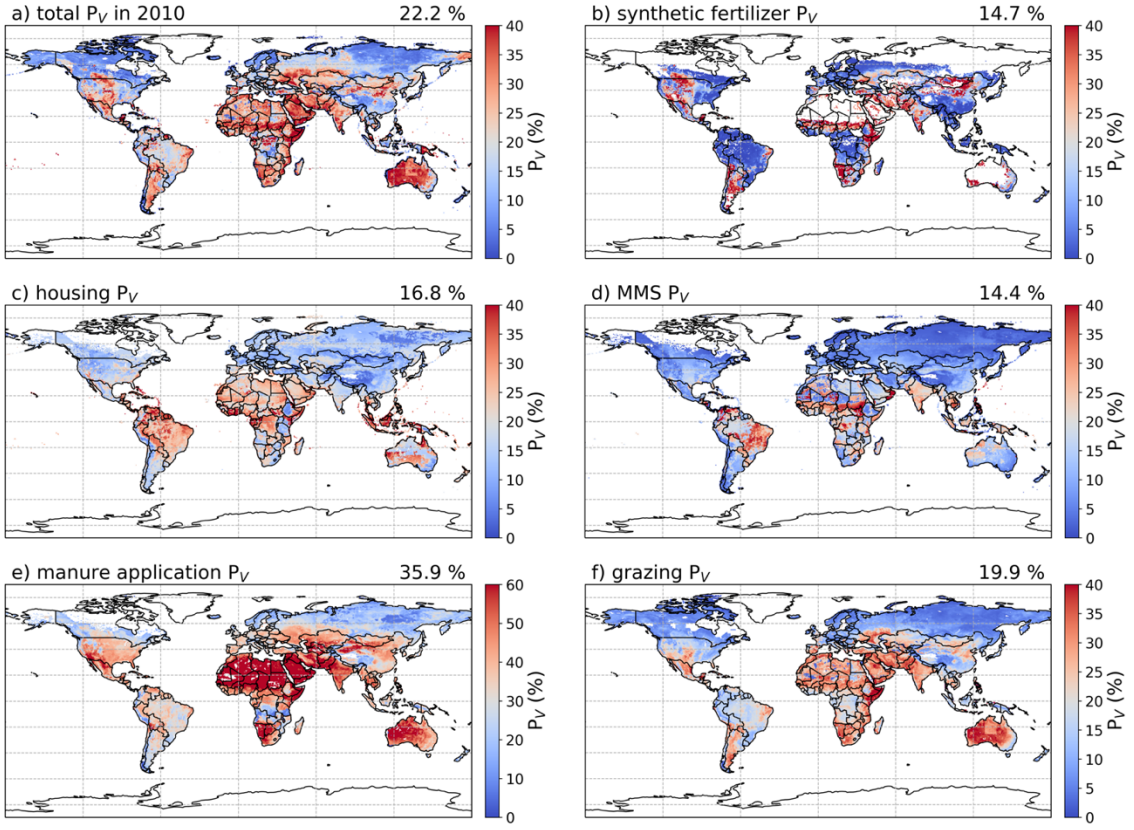

Figure 6.5. Percentage of nitrogen that volatilizes (P_V) as NH_3 in 2010 as estimated by AMCLIM for (a) whole agricultural sector, (b) synthetic fertilizer use, (c) livestock housing, (d) manure management, (e) manure application to land (note the different scale) and (f) grazing.

6.2.3 Ammonia emission factors for livestock farming as estimated using AMCLIM

As a process-based model, AMCLIM does not depend on fixed EFs, i.e., NH_3 emission per animal or per unit fertilizer input. This is one of the key advantages of AMCLIM compared with many other inventory approaches (e.g., Yang et al., 2023). Nevertheless, for comparison with other inventories, it is of interest to derive EFs, and show how these vary spatially.

Livestock-specific EFs were derived from the normalised NH_3 emissions simulated by AMCLIM as shown in Figure 6.6. Ruminants EFs exhibit similar features in spatial distributions, with regions such as Australia, US and Europe having high EFs, which is mainly due to animals in these regions excrete more nitrogen (see Fig F3 in Appendix F3). The regional patterns of EFs for pigs and chicken are different from ruminants. High EFs for pigs are mostly found in India, southwestern Russia and Ukraine, while EFs for chicken are high in Australia, Brazil, India and Southeast Asia. High EFs for pig and chicken not only result from high nitrogen excretion rate, but also are affected by the environmental conditions and management practices (Fig F3 in Appendix F3; Fig 4.4 – 4.6 and Fig 4.10 – 4.12).

The global average EFs for major livestock estimated by AMCLIM have been compared with values reported from literature, which has been presented in Chapter 4 and Chapter 5. Estimated EFs derived from AMCLIM's simulations are generally comparable to livestock in Europe, but different values in China, India, US and other countries or regions (cf. Yang et al., 2023). Moreover, it should be noted that livestock EFs can also vary across

sub-national scale according to AMCLIM, which is not normally reflected from existing EF studies. For example, cattle and chicken EFs differ across China, with high cattle EFs in the NCP and high chicken EFs in the south and east regions in China reflecting climatic and soil differences. Such sub-national variations in EFs can also be found in countries that have different climates and soil types such as Argentina (Fig 6.6a, b, c, f), Australia (Fig 6.6e), Brazil (Fig 6.6a), Canada (Fig 6.6a, b, c, d), Russia (Fig 6.6 a, c, d, e) and US (Fig 6.6e, f). These indicate that current EFs might not be representative enough depending on the purpose or interests. Using a single EF for a country may satisfy the requirement of reporting national emissions, but EFs need further refinement and improvement for investigating other scientific questions such as providing input to atmospheric chemistry and air quality modelling, assessing the environmental impacts of NH_3 emission and proposing mitigating measures.

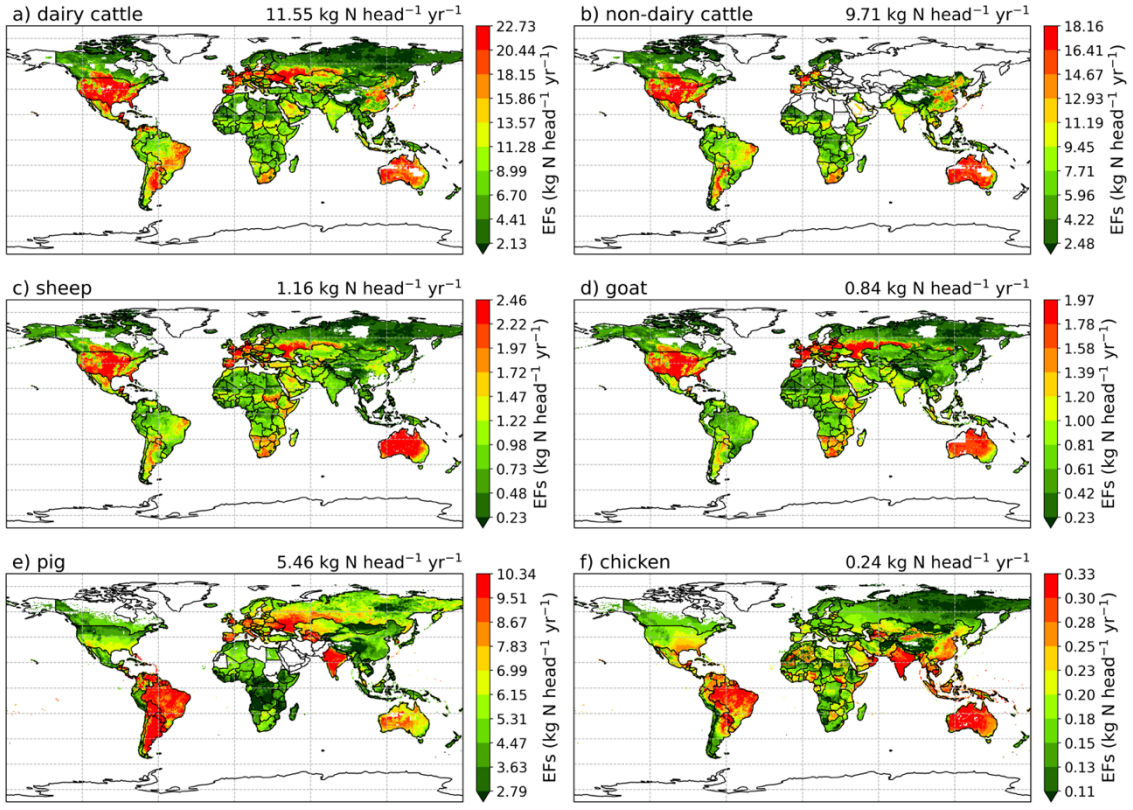

Figure 6.6. Estimated EFs (kg N head^{-1} yr^{-1}) of (a) dairy cattle, (b) non-dairy cattle, (c) sheep, (d) goat, (e) pigs and (f) chicken based on simulations for year 2010 using AMCLIM.

6.2.4 Spatial distribution and temporal profile of NH_3 emissions

As shown in Figure 6.7, over 80 % of global NH_3 emissions in 2010 come from the northern hemisphere (NH), with extremely high emissions occurring between 20 ~ 40 °N, where several large emitter countries are located, such as China, India, Pakistan and US. In

contrast, NH_3 emissions are negligible beyond 40 °S or 60 °N (Fig 6.7). Emissions related to synthetic fertilizer use are mainly from the NH compared with other agricultural activities (Fig 6.7a). By comparison, NH_3 emissions from grazing are found to be more evenly distributed across each latitudinal band. For sectoral emissions, emissions from pig and chicken farming are concentrated between 20 ~ 60 °N (Fig 6.7b), while the SH NH_3 emissions are dominated by emissions resulted from cattle farming.

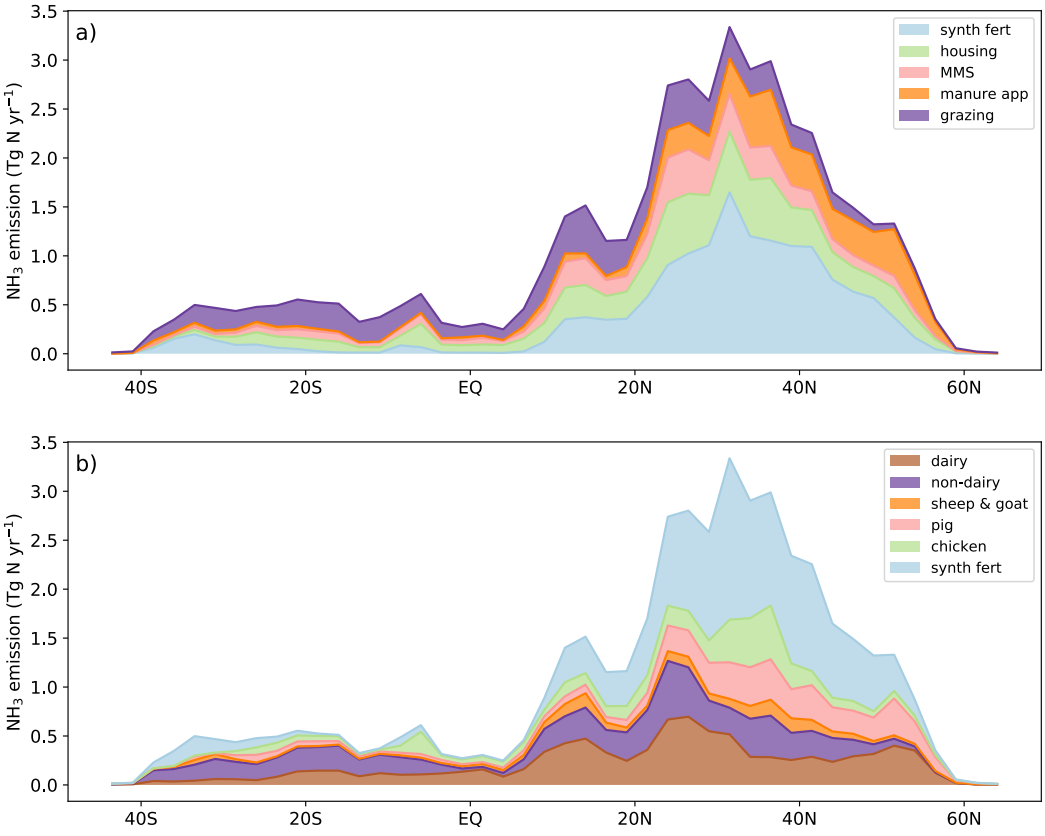

Figure 6.7. Simulated latitudinal NH_3 emissions (Tg N yr^{-1}) from (a) agricultural activities and (b) sectors in 2010 by AMCLIM. Emissions are aggregated every 2.5 °.

Agricultural NH_3 emissions exhibit important seasonal variation as shown in Figure 6.8. In the NH, emissions in JJA are higher than other seasons, and the highest monthly emissions from the NH are in July, exceeding 6 Tg N $month^{-1}$. By comparison, emissions are generally smaller in the SH. Highest emissions from the SH are from November to January, with the highest emission of 0.7 Tg N $month^{-1}$ occurring in January, mainly from grazing, synthetic fertilizer application and livestock housing. The seasonal variations in NH_3 from both hemispheres are largely due to the monthly variability in synthetic fertilizer use, which is linked especially to the estimated timing of planting seasons, i.e., high emissions associated with synthetic fertilizer use occurred from May to August in the NH and occurred from November to February in the SH. It is also found that manure application resulted in higher emissions in May to August in SH than other months, which can be explained by the planting seasons used in AMCLIM (as shown in Fig B5 in Appendix B8), i.e., the planting season mostly begin in May to July in SH. The planting season suggests that most of the manure was applied to land in SH autumn/winter, which might be an overestimation, indicating the application date derived from the average crop calendar needs further improvement. However, it is worth noting that the NH_3 emissions from manure application to land in the SH are relatively small compared to other sources in the SH, so this problem only influences the temporal profile of the SH NH_3 emissions and have very limited impacts on the global emissions. For other activities such as livestock housing, manure management and grazing, the seasonal variation is less significant, especially in the SH. On the global scale, emissions resulting from manure application to land show large monthly variation but differ from the synthetic fertilizer emissions, with the highest emission occurring in April and a second peak occurring in September (Fig 6.8b). Meanwhile, the NH_3 emissions from housing, manure management and grazing in JJA are generally higher than other

months, which indicates that higher temperature in the NH results in more NH_3 emissions from these practices.

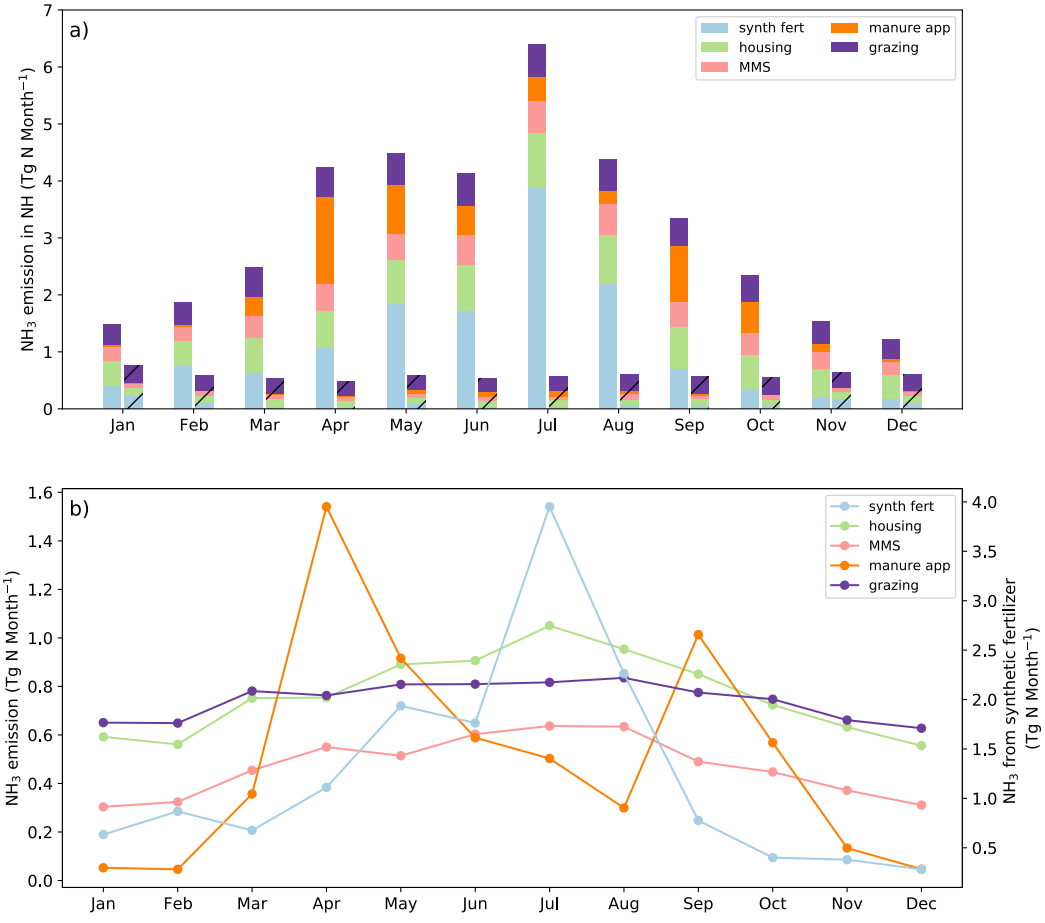

Figure 6.8. (a) Monthly NH_3 emissions from the northern hemisphere (NH) and the southern hemisphere (SH). Columns with hatch represent emissions from SH. (b) Global monthly NH_3 emissions (Gg N month^{-1}) from synthetic fertilizer use, livestock housing, manure management, manure application and grazing in 2010, as simulated by AMCLIM.

6.3 Effects of environmental conditions on ammonia emissions

6.3.1 Investigation of influences of environmental factors on NH_3 volatilization rates

Ammonia emissions are primarily associated with N source activities (i.e., more fertilizer application and more intensive livestock farming tend to result in higher NH_3 emissions), while the volatilization rates are more often influenced by environmental conditions than the amount of nitrogen input. Temperature, wind speed and water availability have been found to have the most prominent impacts on the NH_3 volatilization (Gyldenkærne, 2005b; Misselbrook et al., 2005; Sommer et al., 2006; Sutton et al., 2013; Bittman et al., 2014).

Figure 6.9 shows the latitudinal mean of annual air temperature and wind speed for where NH_3 emission occurs, along with the percentage volatilization rates. The highest volatilization rates occur between 10 ~ 15 °N, corresponding to the latitudinal zone with the highest temperature of around 25 °C and moderate wind speed of 2.5 to 3 m s^{-1}. The P_V in most of latitudinal zones is between 15 to 25 %, while zones with high NH_3 emissions (20 ~ 40 °N; as shown in Fig 6.7) show less variation in P_V, ranging between 20 to 25 %. The P_V values are generally lower in the subpolar regions in the NH than the tropical and temperate regions, and there is a sharp decline in the P_V beyond 55 °N, which can be explained by the low temperature. The zonal mean P_V is occasionally lower than its 25th percentile value (solid black line vs. low end of shaded grey area in Fig 6.9b) because regions with particularly large emissions have lower volatilization rates than most other grids in the same latitudinal band, indicating that high volatilization rates frequently occur

in places with low emissions in these latitudinal bands. This can also partly explain the spikes in P_V between 45 ~ 50 °S and 60 ~ 65 °N (Fig 6.9b), i.e., regions with large emissions and high volatilization rates.

The zonal mean volatilization rates increase towards higher temperature (Fig 6.9c). It is evident that the volatilization rates increase as a function of temperature in the low temperature regime of which annual mean temperature was less than 0 °C (T-r1). In the high temperature regime (T-r3), higher P_V broadly corresponds to higher temperature, but it can vary from 18 % to over 25 % under similar temperature condition, e.g., around 25 °C. By comparison, the relationship between temperature and P_V is much less obvious in the intermediate temperature regime (T-r2). The volatilization rates are found to vary by up to five times different under similar temperature conditions, e.g., around 10 °C.

The volatilization rates are found to be lower in high wind speed zones than low wind speed zones as shown in Figure 6.9d. However, it does not necessarily mean higher wind speeds result in low P_V values. In the low wind regime (u-r1), the volatilization rates exhibit an increasing trend as wind speed increases. In contrast, in other two regimes (u-r2 and u-r3), P_V is scattered instead of showing either positive or negative correlation with wind speed (Fig 6.9d). The lower P_V values for u-r3 may simply reflect high wind speeds in cold locations (T-r3).

The T-r1 regime indicates that temperature is often the limiting factor that affects the volatilization rates under cold conditions, and a small increase in temperature potentially leads to a relatively large increase in NH_3 emissions in these regions (Fig 6.9c). Figure 6.9a shows that the zonal mean wind speeds increase northward beyond 60 °N, while the

temperature decreases to negative values. The corresponding P_V drops, which is positively correlated to the temperature, demonstrating that temperature plays a more important role in influencing NH_3 volatilization than wind speed. Meanwhile, as temperature has a dominant impact in cold environments where wind speeds are usually high (i.e., zonal mean wind speeds are larger than 3.5 m s^{-1} when zonal mean temperature is lower than 0 °C), this partly explains the scattered P_V in the high wind regime u-r3. In hot regions represented by T-r3, since temperature still positively affect the volatilization but is no longer a limiting factor, the variability in wind speeds results in the varying volatilization rates. In regions with zonal mean temperature higher than 15 °C, the zonal mean wind speed ranges from less than 2 m s^{-1} to around 3 m s^{-1} (Fig 6.9a), which illustrates that T-r3 corresponds to u-r1. Therefore, higher P_V under similar temperature conditions in T-r3 might be the result of higher wind speeds. For T-r2 and u-r2, the large variations in the volatilization rates are partly due to an integrated effect of both temperature and wind speed. It is worth noting that regimes T-r2 and u-r2 align with regions where large NH_3 emissions occur and intensive agricultural activities take place (Fig 6.7 and 6.9a), so local management practices can also lead to very different P_V. The impacts of management practices are discussed in later sections.

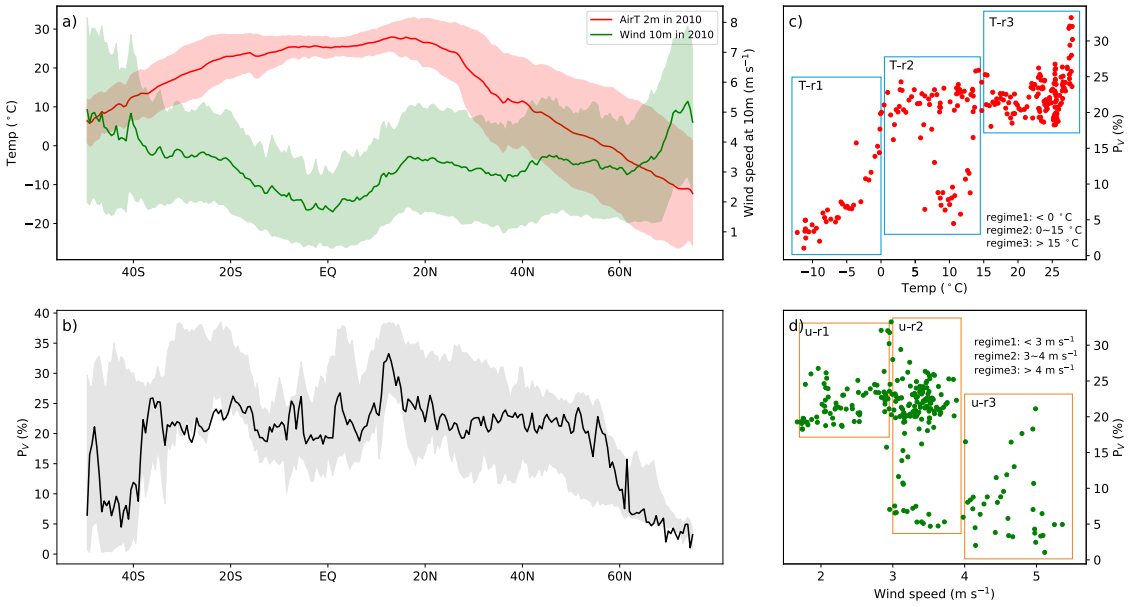

Figure 6.9. Annual mean meteorological variables and NH_3 volatilization rates. (a) Zonal mean air temperature at 2 m and wind speed at 10 m at locations where NH_3 emissions occurred in year 2010. Shaded areas represent the standard deviation. (b) Zonal mean P_V (%) simulated by AMCLIM. Shaded areas represent the 25th to 75th percentile values (25th and 75th percentile of grids with valid values). The simulated zonal mean P_V plotted against zonal mean air temperature at 2 m (c) and wind speed at 10 m (d). There are three temperature regimes: T-r1 (< 0 °C), T-r2 (0~15 °C) and T-r3 (> 15 °C), and three wind speed regimes: u-r1 (< 3 m s^{-1}), u-r2 (3 ~ 4 m s^{-1}) and u-r3 (> 4 m s^{-1}).

The latitudinal mean volatilization rates of individual agricultural activities are shown in Figure 6.10, and volatilization rates are plotted against zonal mean temperature. Manure application generally show the highest P_V (over 30 %) across the world, which is consistent with the geographical distributions shown in Figure 6.5. Applications of synthetic fertilizer show relatively high P_V of up to 30 % in 10 ~ 20 °N and 30 ~ 40 °S and very low P_V near

the equator and subpolar zones. Manure management and grazing exhibit similar features, with P_V peaking in 10 ~ 20 °N and decreasing towards polar regions. A notable spike in P_V for grazing in the SH polar region, i.e., ca. 50 °S can be seen (Fig 6.10a). Grazing is the dominant source of NH_3 emissions for this latitudinal bands (see Fig F1 in Appendix F1), and the high P_V is also displayed in the whole agricultural sector, as shown in Figure 6.9b. This is probably due to the high soil pH in Argentina (see Fig B4 in Appendix B5) The P_V of livestock housing ranges from 10 to 25 % in most regions, with the highest values reaching 35 % in southern hemispheric tropics between 5 ~ 10 °S.

The volatilization rates increase as temperature increases for all agricultural activities (Fig 6.10b-d). Specifically, a strong temperature effect on NH_3 volatilization is found in manure management and grazing, especially in cold environments (Fig 6.10b and 6.10d). For housing, the overall volatilization rates are not as sensitive as those for manure management and grazing, but higher temperature generally results in higher P_V (Fig 6.10b). This is largely because the P_V varies between different livestock sector and the overall P_V of housing is an averaged-out value of all livestock. Compared with other activities, the temperature effect in land application is much less obvious, especially in intermediate and high temperature regimes, which is due to the complicated interactions between more processes and factors involved, such as soil moisture, substrate pH (i.e., manure or soil pH) and fertilizer types.

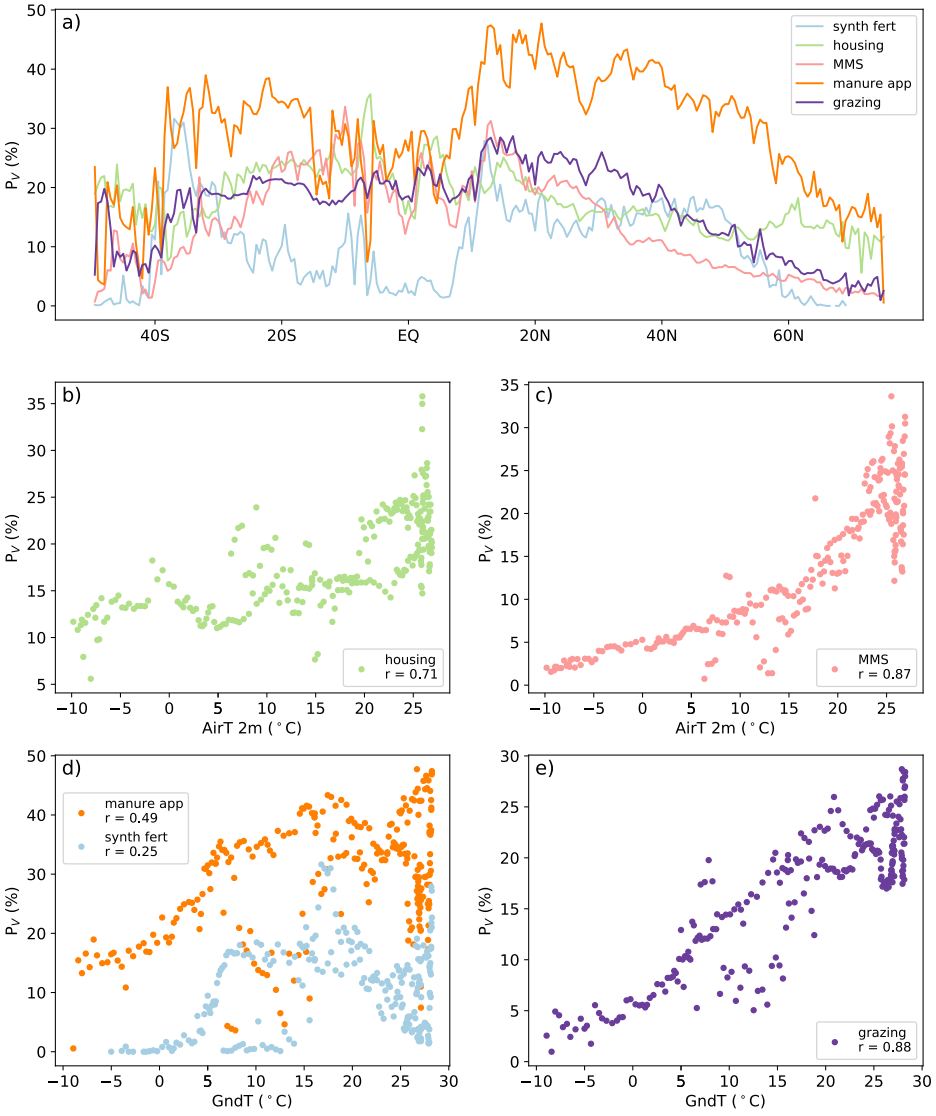

Figure 6.10. Zonal mean P_V (%) of five agricultural activities in 2010 simulated by AMCLIM (a). Simulated P_V of housing (b) and manure management (c) plotted against air temperature at 2 m, and simulated P_V of manure and synthetic fertilizer application (d) and grazing (e) plotted against ground temperature.

In addition to temperature and wind speed, water availability can also greatly impact NH_3 volatilization. The effect of water availability is more important for land emissions such as NH_3 from fertilizer and manure application. Figure 6.11 shows the latitudinal mean of volumetric soil water content and subsurface percolation flux (where NH_3 emissions occur), along with the NH_3 volatilization rates of synthetic fertilizer and manure application to land. Low P_V related to synthetic fertilizer use in the equatorial regions (5 °S ~ 5 °N) might be explained by wet soils and large drainage and leaching. Between 5 ~ 10 °N, both the soil moisture and the percolation flux drop dramatically, corresponding to the sharp increase in P_V of these two activities, which is difficult to explain by the changes in temperature or wind speed.

From Figure 6.11 c-f, volatilization rates generally display a reverse correlation with soil moisture, as well as the subsurface percolation flux, suggesting P_V decreases as soil moisture and percolation flux increases. As discussed in previous chapters, in principle, NH_3 emissions tend to be larger in dry soils than wet soils because of higher TAN concentrations. Meanwhile, drainage/leaching is closely associated with the soil water conditions, which can also influence the emission by transporting nitrogen to deeper soils instead of being volatilized. However, the gaseous and aqueous diffusion that move TAN in soils are influenced by soil moisture (and other variables and parameters such as soil pH and adsorption), which result in a non-linear response of NH_3 emissions to the soil moisture. The emission does not always increase towards higher soil moisture but is also dependent on soil pH (Vira et al., 2020, Fig 2; also see Fig F4 – F5 in Appendix F4). This suggests that low soil moisture alone may not always result in high emissions. Therefore, lowering the soil moisture affects the NH_3 emissions in three possible aspects: 1) it increases aqueous

TAN concentrations, which has a positive impact (+), i.e., emission increases; 2) it either accelerates or slows down diffusion depending on soil pH and temperature, which can be a positive (+) or a negative impact (–); and 3) it potentially decreases the subsurface percolation fluxes so drainage and leaching becomes less significant, which results in higher volatilization rates and has a positive impact (+).

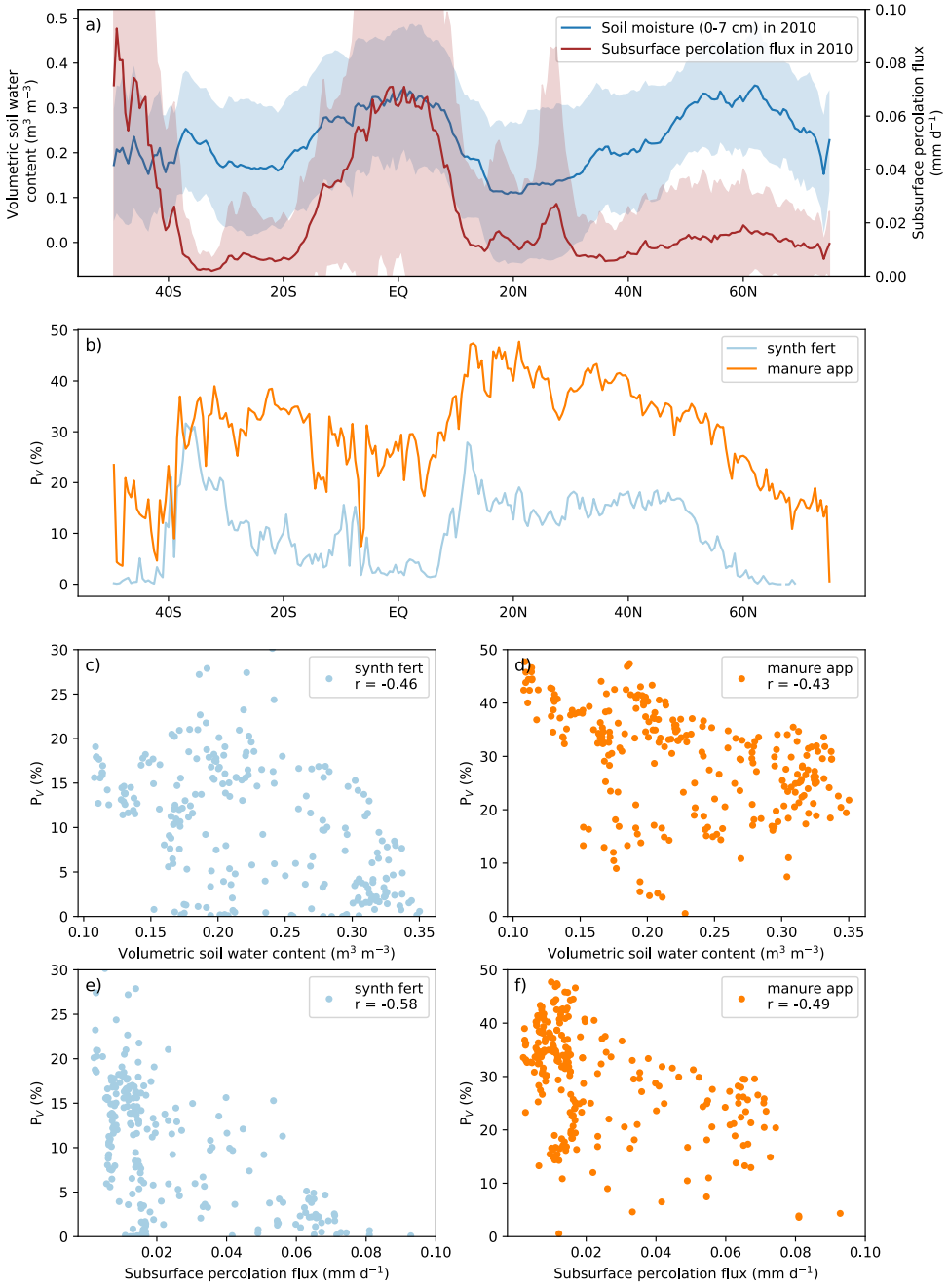
a)
Soil moisture (0-7 cm) in 2010
Subsurface percolation flux in 2010
Volumetric soil water content (m³ m⁻³)
Subsurface percolation flux (mm d⁻¹)
40S
20S
EQ
20N
40N
60N
b)
synth fert
manure app
P_V (%)
c)
synth fert
r = -0.46
d)
manure app
r = -0.43
Volumetric soil water content (m³ m⁻³)
e)
synth fert
r = -0.58
f)
manure app
r = -0.49
Subsurface percolation flux (mm d⁻¹)

Figure 6.11. Annual mean environmental variables and NH3 volatilization rates. (a) Zonal mean soil moisture (0-7 cm) and subsurface percolation flux where NH3 emissions occurred in year 2010. Shaded areas represent the standard deviation. (b) Zonal mean PV (%) of land application of synthetic fertilizer and manure in 2010 simulated by AMCLIM. Simulated PV of synthetic fertilizer (c) and manure application (d) plotted against soil moisture, and PV of synthetic fertilizer (e) and manure application (f) plotted against subsurface percolation flux.

The water availability effect is also reflected by the interannual variability in the NH_3 volatilization of three outdoor activities. As presented in previous chapters and summarised in Table 6.3, the P_V of synthetic fertilizer use, manure application and grazing are lower in 2018 than year 2010, but temperatures in 2018 were generally 0.1 to 0.2 °C higher than 2010, indicating that there are other processes affecting the volatilization. The soil water contents were slightly higher in 2018 than that in 2010, while the subsurface percolation fluxes were much larger in 2018 than 2010 by 40 to 50 % (Table 6.3). It is notable that there are more estimated N leaching and diffusion to deep soils in 2018 compared to 2010 (see Section 3.3.2, Figure 3.12). Overall, year 2018 was a "hotter" but "wetter" year compared to 2010, and the effect of water availability outweighed the temperature effect in 2018, which resulted in larger leaching and diffusive fluxes but smaller NH_3 volatilization fluxes from outdoor activities.

It is worth mentioning that precipitation is also an important indicator for the water availability, which influences runoff and soil water, but is not investigated in the analysis. This is because AMCLIM does not explicitly take precipitation into account for determining water availability when simulating emissions from synthetic fertilizer and manure application to land. Instead, reanalysis data of soil moisture and runoff are used as

input variables which implicitly included the impacts of precipitation (as described in Section 3.2.1.3).

Table 6.3. Annual mean volatilization rates of land application of synthetic fertilizer and manure and grazing in years 2010 and 2018. Annual mean temperature, soil water content and subsurface percolation flux for locations where NH_3 emissions occur and where these three activities took place in 2010 and 2018.

	Activity	Year	
		2010	2018
P_V (%)	Synthetic fertilizer	14.6	13.9
	Manure app	35.9	32.2
	Grazing	19.9	17.0
Meteorological and environmental variable			
T (°C)	Synthetic fertilizer	15.8	15.9
	Manure app	12.2	12.4
	Grazing	10.9	11.0
Soil water (m^3 m^{-3})	Synthetic fertilizer	0.26	0.28
	Manure app	0.25	0.26
	Grazing	0.23	0.26
Subsurface percolation flux ($\times 10^{-2}$ mm d^{-1})	Synthetic fertilizer	2.3	3.3
	Manure app	2.0	2.8
	Grazing	1.8	2.7

Further investigations for influences of environmental factors on NH_3 volatilization rates were carried out for livestock housing, manure management and land application of synthetic fertilizer and manure. For livestock housing, industrial pig, backyard chicken and beef cattle that are kept in different types of houses and different housing systems were selected for analysis. For land application, analysis for synthetic fertilizer use mainly focused on maize and wheat, which are the major crops that have the largest coverage across the globe, while both manure management and manure application to land were investigated as whole sectors.

Each panel of Figure 6.12 shows heat maps (number density of grid points) of annual mean P_V against annual mean air temperature, wind speed and RH, using values from each model grid point for a different agricultural system. Among the three investigated factors, temperature has the most profound impacts on the volatilization rates, with a strong impact on the industrial pig housing (Fig 6.12a). The volatilization rates of backyard chicken housing and manure management also show positive correlation with temperature (i.e., the volatilization rates with high number density increase as a function of temperature), while exhibiting some variation as shown in Figure 6.12b and 6.12d. By comparison, the P_V of beef cattle housing shows large variations and is less well correlated with temperature, reflecting a role of other factors. It is obvious that there are two "hot zones" with high number density of P_V points for beef cattle housing when temperature is over 20 °C (Fig 6.12c), indicating that temperature is not the sole limiting factor that influences the NH_3 volatilization.

The features in the temperature-P_V plots may be explained as follows. Houses for industrial pigs are typically fully enclosed with self-regulating heating and ventilation systems, which

why the P_V is between 10 to 20 % even when temperature is below 0 °C. The indoor conditions such as temperature and ventilation rates are dependent on the outdoor temperature, so temperature becomes the most important factor impacting the volatilization. Backyard chicken and beef cattle are kept in partially enclosed, naturally ventilated houses, so the P_V can be affected by wind speeds. The P_V of backyard chicken and beef cattle housing is between 0 to 10 % under negative temperature conditions, which is lower than that of industrial pig housing. Meanwhile, grazing may result in different volatilization from housing as some beef cattle are allowed to graze on pastures rather than staying in houses if weather conditions are ideal, which partly explains the two "high density zones" in Figure 6.12c. For manure management, the storage condition is closer to the ambient environment than housing, and P_V generally increases as temperature goes up. However, there is also management other than storage, such as lagoon or manure that is simply left on land without further treatment. As a result, the P_V of manure management has a scattered relationship with temperature (e.g., compared with industrial pigs housing).

Compared with temperature, wind speed and RH have less consistent impacts on the volatilization rates of housing and manure management. This is largely due to the fact that industrial pig houses have their own ventilation that is independent from the outdoor wind speed. Other types of animal houses can also have facilities that mechanically block strong wind. The RH effect is also not obvious, suggesting it plays a less important role than temperature in affecting the volatilization. RH is expected to have a critical impact on chicken housing, but little evidence was found from this analysis in Figure 6.12. Further investigation is presented in Section 6.3.2.

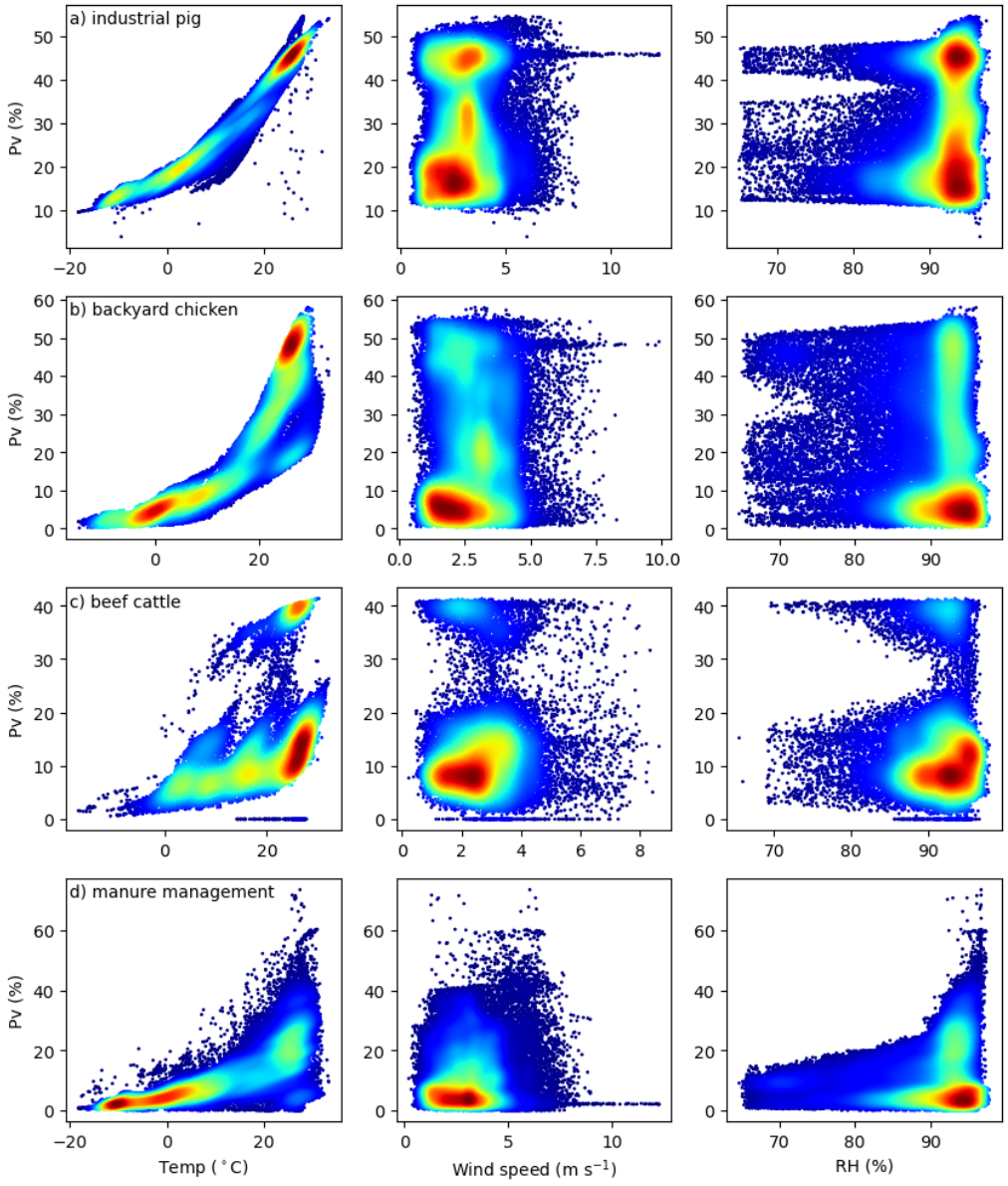

Figure 6.12. Simulated P_V plotted against annual mean air temperature at 2 m, wind speed at 10 m and RH for (a) industrial pig housing, (b) backyard chicken housing,

(c) beef cattle housing and (d) manure management in 2010. Each point is the result of a grid taken from the global simulations. Contour colours represent the number density of points.

Compared with NH_3 emissions from housing, NH_3 related to synthetic fertilizer use and manure application can be influenced by more environmental variables, such as soil moisture and soil pH. Consequently, the volatilization rates are less clearly related to a single factor. For instance, P_V of land applications is less as temperature-dependent than livestock housing and manure management (cf. Fig 6.13 vs. Fig 6.12). Moreover, as more processes were included in the land simulations, increasing temperature also accelerates the rates of other processes, e.g., nitrification and downward diffusion, which are competing pathways that act to reduce NH_3 volatilization. Figure 6.13 shows that P_V does not correlate well with the investigated variables, and the negative correlation between soil moisture and P_V found in the previous analysis (Fig 6.10) does not explicitly show here. Maize and wheat show consistent features, while manure application exhibits a different pattern due to its characteristics (e.g., moisture and substrate pH). Slurry application to land is common in many places, so the impact of soil moisture might not be critical when investigating at smaller scales, e.g., each grid point (Fig 6.13c), because there is lots of water from slurry. In addition, manure pH is often higher than soil pH so that the volatilization rates are less influenced by soil pH. The complex interactions between processes make it difficult to isolate a specific variable that affects the NH_3 volatilization from land applications.

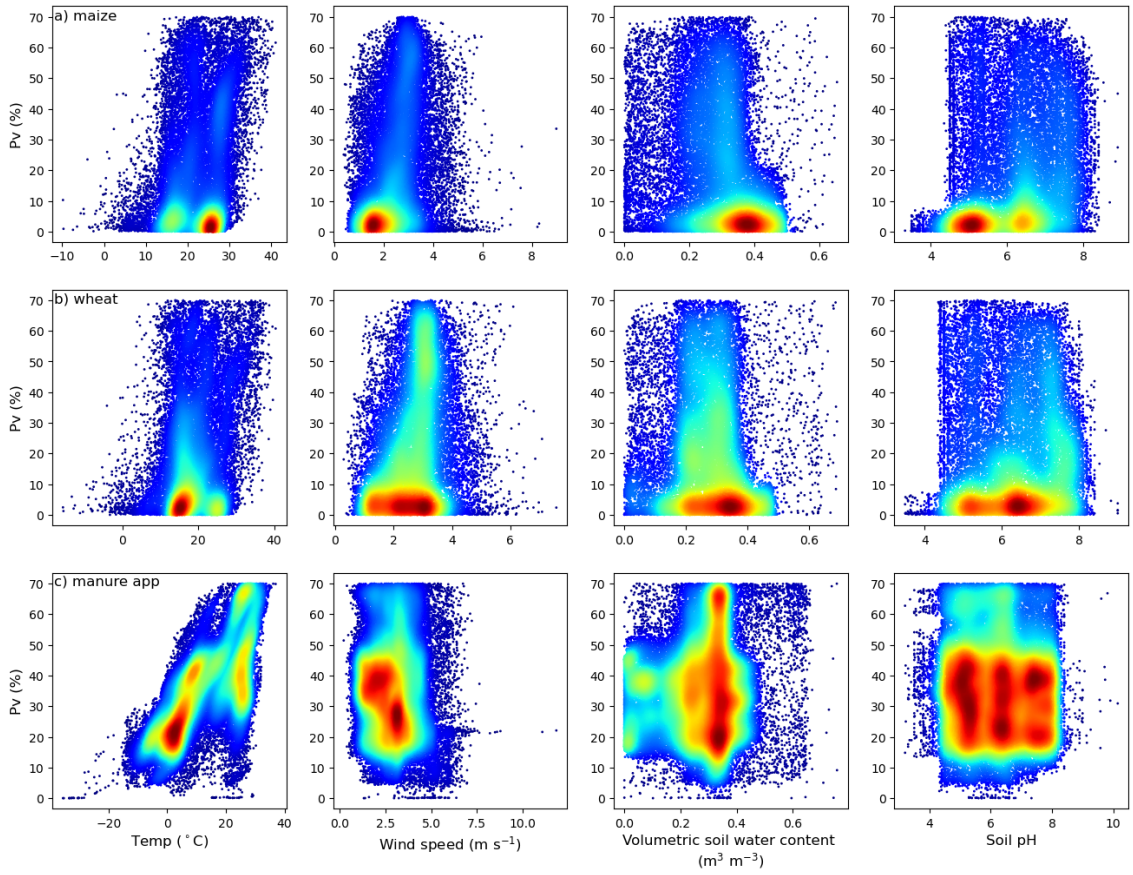

Figure 6.13. Simulated P_V plotted against ground temperature, wind speed at 10m, volumetric soil water content and soil pH for (a) application of ammonium fertilizer for maize, (b) application of ammonium fertilizer for wheat and (c) manure application in 2010.

6.3.2 Sensitivity analysis to environmental factors

Sensitivity tests were conducted using AMCLIM to further investigate the impacts of environmental factors on NH_3 volatilization at both site scale and global scale.

6.3.2.1 Housing emissions

For three animal housing sites (as introduced in Section 4.3.1 for pigs and layer chicken, and Section 5.3.1 for dairy cattle), AMCLIM-Housing simulated NH_3 emissions by varying a single variable with two sets of values: 10 % of the difference between the maximum and the minimum and 1× standard deviation (standard deviation of all values across the simulated period) of the tested variable, while keeping other variables unchanged over the simulation period. Table 6.4 presents the percentage changes in NH_3 emission from the sensitivity tests compared with the results from the base run. Emissions are found to be the most sensitive to the changes in indoor temperature and less sensitive to ventilation, while varying RH only has very small effects on the emission.

In addition to the sensitivity tests, AMCLIM-Housing was used to conduct two sets of experimental tests to simulate NH_3 emissions using constant temperature or constant RH for the three sites. The differences in NH_3 emissions between the experiments and the base run are shown as percentage change in Figure 6.14. When simulating with the mean temperature, the emissions from IN3B and NC2B are almost the same as the base run, while emission from IN5B decreased by 18 % (Fig 6.14a). Houses of pigs and layer chicken have heating systems, and the temperature inside is generally higher than the dairy house, especially during winter. The indoor temperature of the dairy house has larger variability as shown in Table 6.4. Therefore, when using the mean temperature that is lower than that of hot days for simulations, less NH_3 is resulted from a more moderate conditions (i.e., no significant NH_3 volatilization occurs under hot conditions), so the overall emissions are lower from the dairy house than the base run. It is also found that perturbing temperature conditions has greater impacts on dairy (and layer chicken housing) than pig housing,

which is due to the same reason. Meanwhile, the rate of urea hydrolysis is typically faster than uric acid hydrolysis, which can explain the more significant impacts of temperature on layer chicken housing than pig housing.

Contrary to the consistent effects of perturbing temperature conditions on the emissions (i.e., higher temperature resulted in more emissions for all livestock), the RH effects differ across the three sites. For pig and dairy cattle, higher emissions result from lower RH, because the TAN concentration increases when the water pool is depleted due to higher water evaporation. However, the RH effect is much less prominent for pig housing as the water pool of the pit is rather stable compared with dairy housing, which does not have the pit. By comparison, decreasing RH of the layer housing led to lower emissions (Fig 6.14b). This is because the hydrolysis of uric acid is also RH dependent, and hydrolysis rate can be very slow under a relatively low RH condition.

Table 6.4. Results of sensitivity tests to perturbed indoor environmental variables for livestock housing of three sites, including IN3B for pigs, IN5B for dairy cattle and NC2B for layer chicken. Indoor temperature (T_{in}), airflow rate (Q_{in}) and relative humidity (RH_{in}) were changed by ±1×diff (i.e., (max-min)/10) and ±1×SD (standard deviation). The changes in NH_3 emissions due to perturbed variables are presented as percentage change compared with the base run.

		Value tested		ΔNH_3 emission (%)			
Site	Variable	1× diff	1×SD	+diff	–diff	+SD	–SD
IN3B (pigs)							
	T_{in} (°C)	2.50	4.20	+10.85	–11.70	+17.99	–20.47
	Q_{in} (m^3 s^{-1})	4.50	11.50	+2.57	–3.76	+5.70	–8.99
	RH_{in} (%)	4.00	6.90	–0.31	+0.24	–0.67	+0.40
IN5B (dairy)							
	T_{in} (°C)	3.60	8.30	+31.67	–24.47	+81.84	–47.91
	Q_{in} (m^3 s^{-1})	21.80	55.30	+2.85	–2.84	+7.24	–7.19
	RH_{in} (%)	3.60	7.30	–0.85	+0.87	–1.70	+1.77
NC2B (layer)							
	T_{in} (°C)	1.80	3.00	+15.72	–16.14	+25.27	–26.28
	Q_{in} (m^3 s^{-1})	25.70	97.80	+1.25	–3.46	+2.46	–6.67
	RH_{in} (%)	4.20	8.10	–0.48	+0.19	–1.31	+0.13

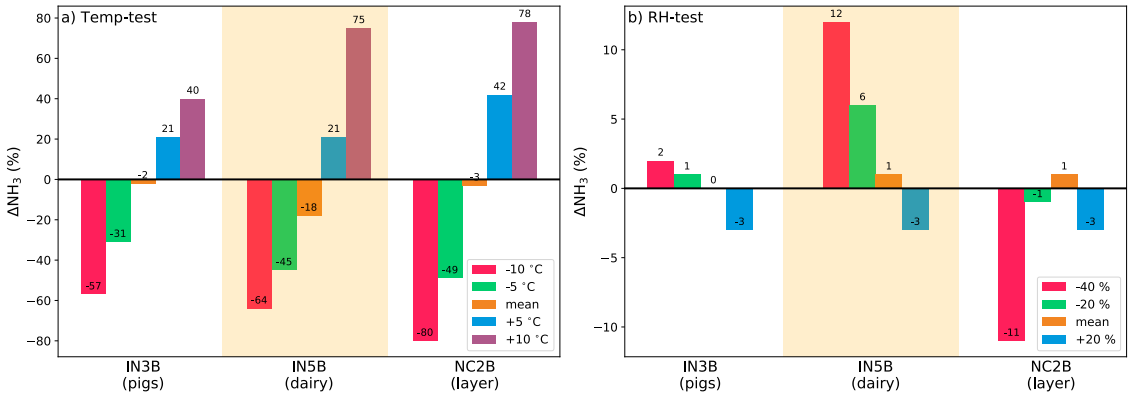

Figure 6.14. Summary of changes in NH_3 emissions based on experiments that use constant (a) temperature and (b) RH for livestock housing simulations for three sites. Five rounds of experiments using fixed indoor temperature throughout the simulations include: 10 °C lower or higher than mean temperature, 5 °C lower or higher than mean temperature, and mean temperature. Four rounds of experiments using fixed RH throughout the simulations include: 40 % (absolute value) lower than mean RH, 20 % (absolute value) lower or higher than mean RH, and mean RH.

6.3.2.2 Fertilizer emissions

The sensitivity of NH_3 emissions to environmental variables for fertilizer was tested using the GRAMINAE site conditions. Here, simulated NH_3 emissions are found to be the most sensitive to soil pH and temperature (Table 6.5). Emissions change by around 40 % and 80 to 90 % when soil pH varies by 0.5 unit and 1.0 unit, respectively, which is the largest change. A 2.8 °C and 5.5 °C increase in ground temperature result in 15 % and 31 % of higher simulated emissions, while decreasing the ground temperature by the same degrees causes emissions to decrease by 15 % and 28 %. Changes in simulated NH_3 emissions are

found to be positively correlated with wind speed, which is the same as soil pH and ground temperature, but the effects are smaller. The sensitivity of temperature and soil pH is broadly linear, while the wind sensitivity exhibits non-linearity.

Increasing soil moisture alone results in higher simulated emissions at the GRAMINAE site, according to the sensitivity test. This does not necessarily contradict the results from large scale analysis, because the impact of soil moisture on drainage was ignored, i.e., subsurface percolation fluxes were kept unchanged. A similar phenomenon is reported by Vira et al. (2020) at a soil pH of 7. When the soil pH is modified to 8.5, an opposite trend is found as emissions decrease at higher soil moistures (Table 6.5). The results of tests with a broader range of perturbed soil pH and moisture are presented in Figure F5 in Appendix F4, illustrating the complex interaction between these two variables. By comparison, it is evident that emissions are lower due to larger subsurface percolation fluxes. The relatively small change in emissions is mainly due to a small perturbation (2 % and 7 %) of the fluxes. Precipitation has the same effect on the NH_3 emissions as the percolation flux. Emissions are not very sensitive to the increasing rainfall, but reduction in rainfall tends to have bigger impacts on the emissions.

Table 6.5. Results of sensitivity tests to perturbed environmental variables for GRAMINAE site simulation. Ground temperature, wind speed, soil water content and precipitation were changed by ±1× diff (i.e., (max-min)/10) and ±1× SD (standard deviation). Soil pH were changed by ±0.5 and ±1 unit. The changes in NH_3 emissions due to perturbed variables are presented as percentage change compared with the base run. Note that the wind speed, soil moisture and precipitation cannot be negative in tests of –diff and –SD. Changes in precipitation only occur when there was precipitation originally. [a]Excluding changes in subsurface percolation flux, soil pH is 6.3, the same as the base run. [b]Excluding changes in subsurface percolation flux, but soil pH was modified to 8.5.

	Value tested		% ΔNH_3 emission			
Variable	1× diff	1×SD	+diff	–diff	+SD	–SD
T_{gnd} (°C)	2.8	5.5	+15.01	–14.51	+30.53	–28.30
u (m s^{-1})	0.56	1.36	+4.20	–8.66	+5.15	–27.94
θ (m^3 m^{-3})[a]	3.1×10^{-3}	8.2×10^{-3}	+4.27	–4.37	+11.09	–11.68
θ (m^3 m^{-3})[b]	3.1×10^{-3}	8.2×10^{-3}	–0.97	+0.99	–2.36	+2.61
q_p (mm d^{-1})	1.5×10^{-2}	4.9×10^{-2}	–1.79	+1.83	–5.68	+6.14
F_{rain} (mm hr^{-1})	1.1	1.9	–1.56	+5.51	–1.58	+6.31
Variable	Value tested		+ 0.5	– 0.5	+ 1.0	– 1.0
soil pH			+38.27	–41.96	+87.28	–81.31

6.3.2.3 Global sensitivity tests

Two global sensitivity tests were carried out using AMCLIM. Temperatures were increased/decreased everywhere by 2 °C, while other conditions were kept the same as the base simulation. As presented in Table 6.6, a 2 °C rise in temperature results in global agricultural NH_3 increasing by 6.9 %, while emissions decline by 6.7 % when temperature decreases 2 °C. The largest percentage change in emissions is from livestock housing (+10.3 % and –9.4 %). Global NH_3 emissions from each activity increase in the +2 °C test and decrease in the –2 °C test. The relative P_V changes are the same as the changes in emissions for synthetic fertilizer application, livestock housing and grazing because these are independent activities, compared with manure management and application of which available nitrogen is dependent on the loss from previous stages. As higher NH_3 emissions are originated from housing and manure management, less nitrogen in livestock excreta is available for NH_3 volatilization for the subsequent application stage. As result, NH_3 emissions from manure application only increase by 1.6 %, when temperature increases by 2 °C.

Table 6.6. Results of sensitivity tests of perturbed temperature for global simulations. Percentage changes in global NH_3 emissions and P_V due to perturbed variables are presented by agricultural activities. Note that the unit of P_V is also in percentage, while the reported values are relative changes expressed in percentage.

	ΔNH_3 emission (%)		ΔP_V (%)	
Activity	+2 °C	–2 °C	+2 °C	–2 °C
Synthetic fertilizer	+7.4	–6.4	+7.4	–6.4
Livestock housing	+10.3	–9.4	+10.3	–9.4
Manure management	+8.5	–8.3	+10.4	–10.3
Manure application	+1.6	–3.0	+6.1	–5.8
Grazing	+5.3	–5.4	+5.3	–5.4
Total	+6.9	–6.7	+6.3	–7.1

The temperature sensitivity of volatilization, $k_{Pv(T)}$ (% K^{-1}), was derived from a linear approximation based on the global sensitivity tests. The overall temperature sensitivity of P_V for the whole agricultural sector is 3.4 % K^{-1}, indicating a 3.4 % relative increase in NH_3 volatilization for each 1 K increase in mean temperature (equivalent to 3.4 % of increase in NH_3 emissions for each 1 °C increase in mean temperature; a direct comparison between NH_3 emissions under 2 °C warming and the base NH_3 emissions expressed as a ratio is shown in Figure F6 and F7 in Appendix F5), compared to the base simulations for the year 2010. As shown in Figure 6.15a, high $k_{Pv(T)}$ is found not only in cold temperate regions in

the NH such as Canada, Russia and northern Europe, but also in hot and humid regions like southern China, central Africa, northern South America and Southeast Asia. The grazing $k_{Pv(T)}$ shows a spatial distribution similar to that of the whole agricultural sector (Fig 6.15f), as well as manure application (Fig 6.15e). The temperature sensitivities for synthetic fertilizer application (Fig 6.15b) and manure management (Fig 6.13d) show large but different regional patterns. High values of $k_{Pv(T)}$ for synthetic fertilizer are generally consistent with the agricultural sector, with much higher values being over 10 %. For manure management which has the highest overall temperature sensitivity (5.2 % K^{-1}) among all activities, high $k_{Pv(T)}$ mainly occurs in cold places, but Iran, Mexico and Oceania also have high values. By comparison, the temperature sensitivities for livestock housing show smaller spatial variations, with higher $k_{Pv(T)}$ in tropical and temperate regions than in cold regions (Fig 6.15c). The effect of warming is estimated to be less significant compared to Sutton et al. (2013). Specifically, the temperature sensitivity is found to be extremely low for manure application to land and grazing in Australia, the Middle East and Sahel regions, which is largely because a big fraction of N (see Fig 6.5ef) and particularly TAN (see Fig F2 cd) has already lost as NH_3. Hence it is difficult for regions with high P_V (and $P_{V(TAN)}$) to further increase the volatilization rates due to hotter temperature. Similarly, high temperature sensitivities for synthetic fertilizer use occur in places that show low P_V values (see Fig 6.5b and Fig 6.15a).

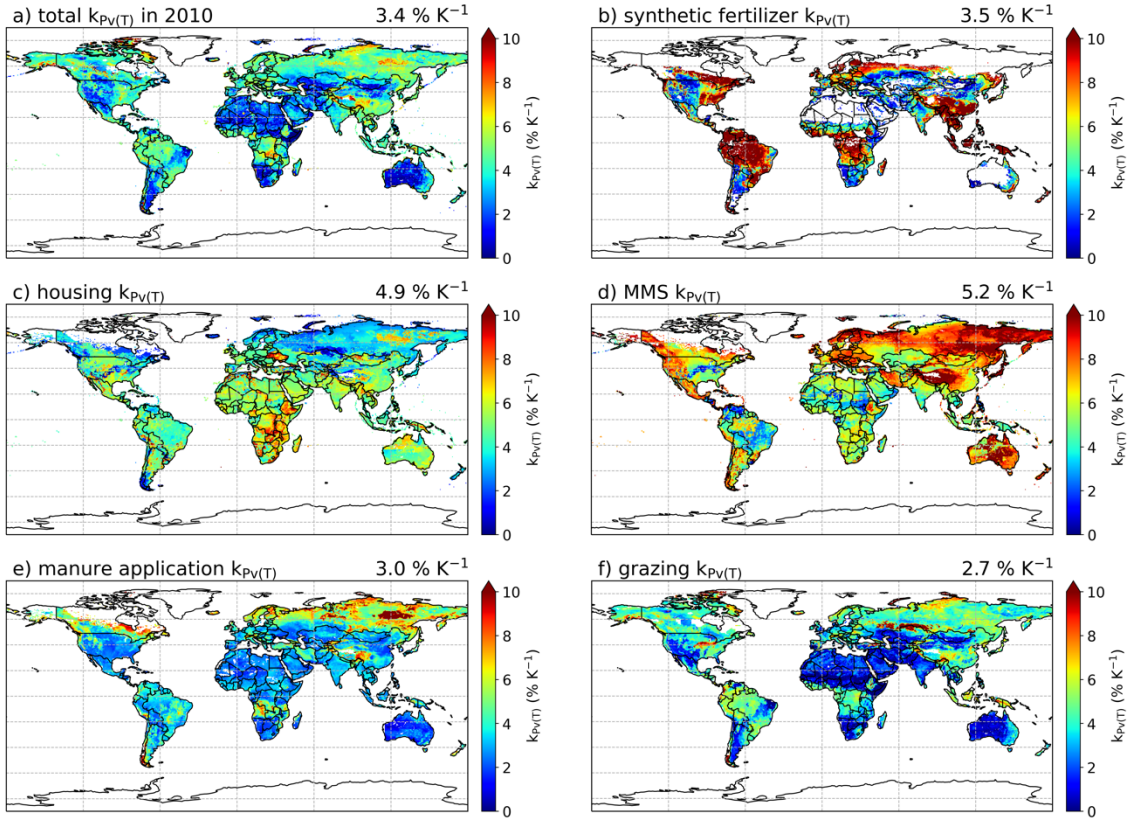

Figure 6.15. Simulated temperature sensitivity of the NH_3 volatilization rates ($k_{Pv(T)}$, % K^{-1}) for (a) whole agricultural sector, (b) synthetic fertilizer use, (c) livestock housing, (d) manure management, (e) manure application and (f) grazing derived from the global sensitivity tests in 2010.

The AMCLIM simulations estimate that the largest absolute increases in agricultural NH_3 emissions due to 2 °C warming occur between 20 N ~ 40 °N, with the majority of increased emissions in the NH, as shown in Figure 6.16a. The highest relative increase in NH_3 (and

also the P_V) is found in polar regions beyond 60 °N where very little emissions occurred, while the changes for other regions range between 5 to 9 %.

The zonal mean temperature sensitivities for individual activities are shown in Figure 6.16b. The $k_{Pv(T)}$ of manure management, manure application and grazing showed higher temperature sensitivities in the polar regions than the temperate and tropical regions. It indicates that the temperature sensitivities of these activities tend to be higher in colder areas, which is also demonstrated by Figure F8 (see Appendix F6). By comparison, the latitudinal $k_{Pv(T)}$ of synthetic fertilizer application is higher, not only in polar regions, but also in equatorial regions than regions between 20 ~ 40 °S and 20 ~ 60 °N, with a remarkable peak between 5 ~ 10 °N. These zones with high temperature sensitivity generally have low P_V in the base simulation. The $k_{Pv(T)}$ of synthetic fertilizer use shows a reverse correlation with the base P_V (Fig F8 in Appendix F6), indicating that substantial increase in NH_3 volatilization due to temperature increase might occur in places with low original volatilization rates. The housing $k_{Pv(T)}$ typically ranges between 4 to 6 % K^{-1} in most latitudinal bands, but is lower (2 to 4 % K^{-1}) in polar regions, which is also reflected in Figure 6.15c. This is largely because the indoor temperature of animal houses for livestock like pigs and poultry are regulated especially in cold regions (e.g., western Russia), so the changes in ambient temperature in cold places do not lead to a change in indoor temperature so do not have significant impacts on the NH_3 volatilization from housing.

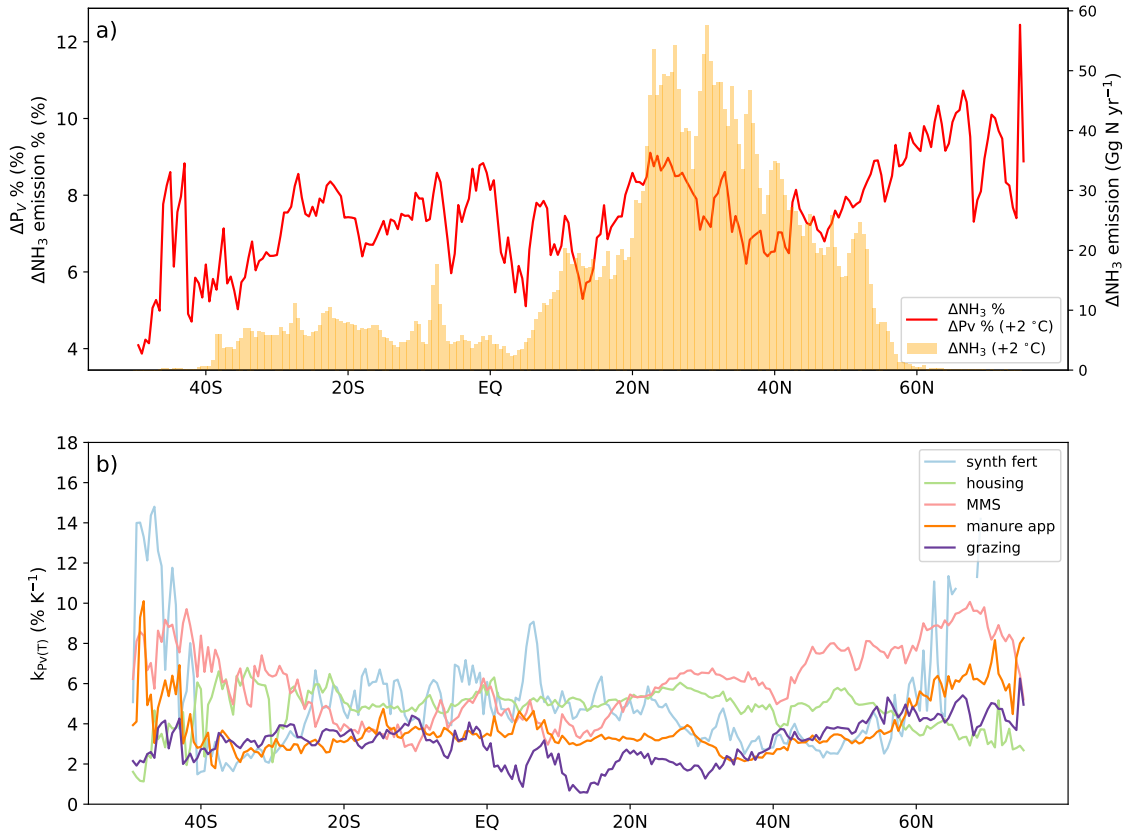

Figure 6.16. Zonal percentage change in P_V (%) and agricultural NH_3 emissions when temperature increases by 2 °C based on global sensitivity tests for 2010 using AMCLIM (a). Zonal mean $k_{Pv(T)}$ for the agricultural activities (b).

6.4 Impacts of management practices on ammonia emissions and potential mitigation measures

6.4.1 Investigation of influences of management practices on NH_3 volatilization rates

Agricultural NH_3 emissions are determined by agricultural activities and influenced by environmental conditions (Gyldenkærne, 2005b; Sommer et al., 2006; Vira et al., 2020a). The impacts of environmental factors on NH_3 volatilization have been discussed in the previous section. This section mainly investigates how local management practices affect NH_3.

AMCLIM was used to perform two sets of model experiments for both indoor simulations and land simulations with modified management practice. In each set of experiments, a single model parameter that represents a management practice was selected and perturbed in a certain range. In experiments for livestock housing, a 10 % change in nitrogen excretion rate (under the assumption that reducing nitrogen excretion does not change the behaviour, e.g., urination and defecation, and biomaterial characteristics of livestock) resulted in the same change of 10 % in NH_3 emissions for all livestock (Fig 6.17a). Varying the indoor temperature by 2 °C results in large change in emissions especially for dairy cattle and layer chicken, which has also been tested in the previous section. For pigs and dairy cattle, decreasing emitting surface area of the excreta by 20 % leads to around 20 % of reduction in emissions, and an expansion in the emitting surface results in the NH_3 increasing linearly. While layer housing is slightly less responsive to the 20 % varying emitting surface, with

emissions changing by –14 % and 13 %, respectively (Fig 6.17a). The differences are mostly due to the different characteristics of chicken as chicken excreta is much drier than other livestock, which poses additional surface resistance for NH_3 volatilization.

From the experiments for land application of fertilizer (the GRAMINAE site), the changes of NH_3 emissions resulting from different nitrogen application rates and application techniques were estimated. Modifying the nitrogen application rate by 10 % and 20 % causes NH_3 emissions to vary by 12 % and 25 % accordingly. Unlike livestock housing, decreasing the nitrogen source (i.e., nitrogen fertilizer) does not result in the same amount of reduction in emission for land application for a relatively short time period of 11 days. Meanwhile, incorporation and deep placement of fertilizer resulted in massive NH_3 emissions reduction by 85 % and 100 %, respectively.

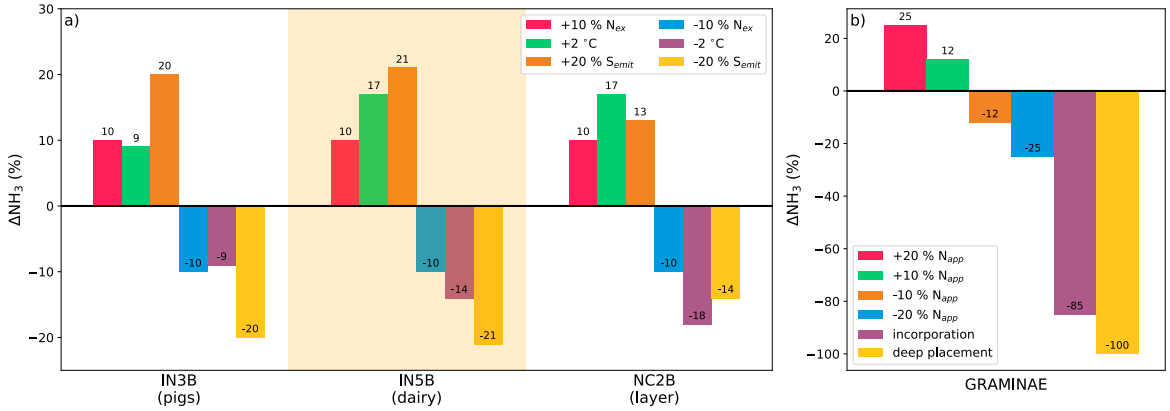

Figure 6.17. Changes in NH_3 emissions based on experiments with varying management practices for (a) livestock housing and (b) fertilizer application (GRAMINAE). For livestock housing (a), livestock nitrogen excretion rate (N_{ex}) was varied by 10 %. Indoor temperature was varied by 2 °C, and the area of emitting surface (excreta surface) were varied by 20 %. For experiments of fertilizer application (b), nitrogen application rates (N_{app}) were varied by 10 % and 20 %. Application techniques including incorporation and deep placement were simulated.

6.4.2 Measures for mitigating NH_3 emissions

Since NH_3 emission is a major unintentional loss of nitrogen input from various agricultural practices, which impacts the environment, reducing NH_3 emissions not only can improve the nitrogen cycling efficiency within the agricultural system but also have great environmental benefits. As discussed, management is a critical factor that determines the agricultural NH_3, which implies that improvement in local management practices can be helpful for NH_3 emission abatement. This section focuses on presenting and discussing the effects of mitigation measures.

Based on the simulations using AMCLIM, a primary reduction of NH_3 emissions is found to be related to lower amount of nitrogen in sources as shown in Table 6.7. Decreasing the N application rate by 20 % (measure A1) leads to 20 % less NH_3 emissions from synthetic fertilizer use. Note this impact is slightly different from the site analysis for GRAMINAE (Fig 6.17) because global simulations had longer period (i.e., whole planting seasons) than site simulations (11 days for GRAMINAE). Similarly, emissions from livestock housing and grazing also decrease by 10 % if nitrogen excretion rates of livestock were 10 % lower (measure B1), which can be achieved by improving the diets and feeds of the livestock. Another effective measure is improving the application techniques. If the fraction of using incorporation techniques rise 0.2 in each country (measure A2; compared to the base scenario used in AMCLIM, see Appendix B3), it is estimated that NH_3 emissions resulting from application of synthetic and manure fertilizers decline by 24 %, while NH_3 emissions decline by 34 % if the fraction of using deep placement techniques rise 0.1 globally. More specifically, incorporation of fertilizers can reduce more than 50 % emissions, and fertilizer deep placement may potentially cut down all the NH_3 volatilized to the atmosphere (over 97 %). Meanwhile, AMCLIM also suggests that roughly 20 to 30 % of less nitrogen fertilizer is required globally to achieve the equivalent nitrogen uptake by crops if incorporation and deep placement are used.

For livestock housing, decreasing the surface area fouled by manure is helpful for emissions reduction (measure B2), which is also proved from the site analysis (Fig 6.17). Improvements in manure management, including covering the stored manure (measure C1) and storing manure rather than leaving it uncovered on land (measure C2) are very effective measures that can reduce about 30 to 40 % of NH_3 emissions. Meanwhile, if ruminant

manure (mainly dung) can be collected timely from the pasture (measure D1), there will be roughly a quarter less NH_3 resulting from grazing.

AMCLIM estimates that 16.6 Tg N yr^{-1} or 37 % of current total agricultural NH_3 emissions (for the reference year 2010) can be avoided globally by applying all mitigation measures A1–D1 as listed in Table 6.7. About 1/3 of the NH_3 reduction is due to improvements in synthetic fertilizer use, which is equivalent to 40 % of less emissions from this single activity. For livestock farming, grazing emissions decreased by about 40 %. Emissions from manure management and application are dependent on previous stages, i.e., housing and storage, and 35 % of emissions from these three activities can be mitigated when applying measures A2 and B1 – C2. Manure management has the largest mitigation potential. A substantial decline of nearly 70 % in manure management NH_3 emissions can be achieved if manure can be stored in a better way, e.g., apply coverings. Details of the calculations and methods are presented in Appendix F7. A critical point is that sometimes it is necessary for mitigation measures to target on multiple activities at the same time, otherwise the effectiveness may be compromised. For example, higher NH_3 emissions can be resulted from the manure management and land application when only focusing on the reduction of housing emissions.

Table 6.7. Reductions (R_{A1} to R_{D1}) in global NH_3 emissions as a result of each mitigation measure (A1 – D1) for agricultural activities. Changes are expressed as percentage difference compared with the original base simulations of the corresponding activities (not the total emission). [a] Overall changes in NH_3 by assuming the fraction of using incorporation and deep placement techniques in each country increased 20 % and 10 % compared to the original value, respectively. [b] Changes in NH_3 when all synthetic fertilizer is applied by incorporation or deep placement. [c] Changes in NH_3 relative to total NH_3 emissions from the whole manure management systems. [d] Changes in NH_3 relative to component NH_3 emissions from a specific manure management system. * Faeces/manure collected within a day after being excreted on pastures.

Activity	Measure	ΔNH_3 emission %
Synthetic fertilizer use	A1: –20 % N application rate	R_{A1}: –20 %
	A2: incorporation, deep placement	$R_{A2\ (syn\ fert)}$: –24 %[a] (–50 %, –97 %)[b]
Livestock housing	B1: –10 % N excretion rate	R_{B1}: –10 %
	B2: –20 % manure surface area	R_{B2}: –16 %
Manure management	C1: covering manure	R_{C1}: –29 %[c] (–95 %)[d]
	C2: storing manure left on land	R_{C2}: –41 %[c] (–60 %)[d]
Manure application	A2: incorporation, injection	$R_{A2\ (manure)}$: –34 %[a] (–57 %, –98 %)[b]
Grazing	B1: –10 % N excretion rate	R_{B1}: –10 %
	D1: collecting faeces/manure*	R_{D1}: –24 %

In addition to the above measures, there are several other effective techniques for NH_3 mitigation that are reported by literature and recommended by the *UNECE* Ammonia Guidance Document (Bittman et al., 2014). For example, adding bedding, separating urine and faeces, cleaning the floor more frequently, acidifying manure and drying manure can reduce housing NH_3 emissions (Misselbrook and Powell, 2005; Bittman et al., 2014). Decreasing the velocity and temperature of the air is also reported as a potential mitigation method, which is also demonstrated by the sensitivity tests by AMCLIM. However, it remains uncertain how livestock performance is influenced, and also it is not easy to adjust the temperature for naturally ventilated barns. For land application, lowering the DM content of slurry is found to result in less NH_3 due to faster infiltration (Misselbrook et al., 2005; Bittman et al., 2014), and proper irrigation (with at least 5 mm of water) is also beneficial. Using urease inhibitors and polymer coated urea granules are good options for reducing NH_3 from urea application because the hydrolysis process is slowed down (Bittman et al., 2014).

6.5 Global agricultural ammonia emissions in the 21st century

6.5.1 Ammonia emissions from 2000 to 2018

Global agricultural NH_3 emissions in the reference year 2010 estimated by AMCLIM have been discussed in detail in Section 6.2, along with emissions from a more recent year in 2018 having been presented in Chapters 3 to 5. In addition, three full AMCLIM simulations

for the years 2000, 2005 and 2015 were made, as shown in Figure 6.18a. This shows that estimated global NH_3 emissions have increased from 39.8 Tg N yr^{-1} to 47.8 Tg N yr^{-1} over the period 2000 to 2015 and decreased to 45.2 Tg N yr^{-1} in 2018. From 2000 to 2015, China and India have experienced a substantial increase in NH_3 emissions with annual increase rates of 0.11 Tg N yr^{-1} and 0.09 Tg N yr^{-1}, respectively, due to more synthetic fertilizer use and the larger scale of livestock agriculture (Fig 6.18a). By comparison, NH_3 from Brazil, US and Africa have a lower rate of increase, varying between 0.02 to 0.07 Tg N yr^{-1}. Estimated emissions from Europe have declined from 5.7 Tg N yr^{-1} in 2000 to 2010 by about 4 % and then increased to 6.0 Tg N yr^{-1} in 2015.

In 2018, global NH_3 emissions, as well as emissions from the major regions mentioned above were lower than 2015, but larger than 2010 (Fig 6.18a). However, the NH_3 volatilization rates in 2018 expressed as P_V are lower than previous years as shown in Figure 6.18b. In particular, P_V of manure application and grazing in 2018 drop by 10 % relative to 2010 and 2015, which results in an overall lower volatilization rate. For other years, the P_V of the whole agriculture sector is around 22 %, with relatively small inter-annual variability. As P_V of housing and manure management exhibits a slightly increasing trend from 2010 to 2018, the lower P_V in 2018 than other years is largely due to less intensive volatilization of outdoor simulations including synthetic fertilizer use, manure application to land and grazing. The lower P_V of these outdoor activities are largely associated with wetter soil conditions and larger drainage/leaching as discussed previously (see Section 6.3.1), resulting in more nitrogen being transported to deeper soils instead of volatilizing from the surface. Moreover, the simulated atmospheric resistances in 2018 are found to be generally larger than earlier years, which can be due to lower wind speeds or

different atmospheric conditions, e.g., stability etc. Nonetheless, it should be noted that the overall yearly variability is driven by complex integrated effects from multiple factors, and it is difficult to isolate completely the impact from a single variable or process.

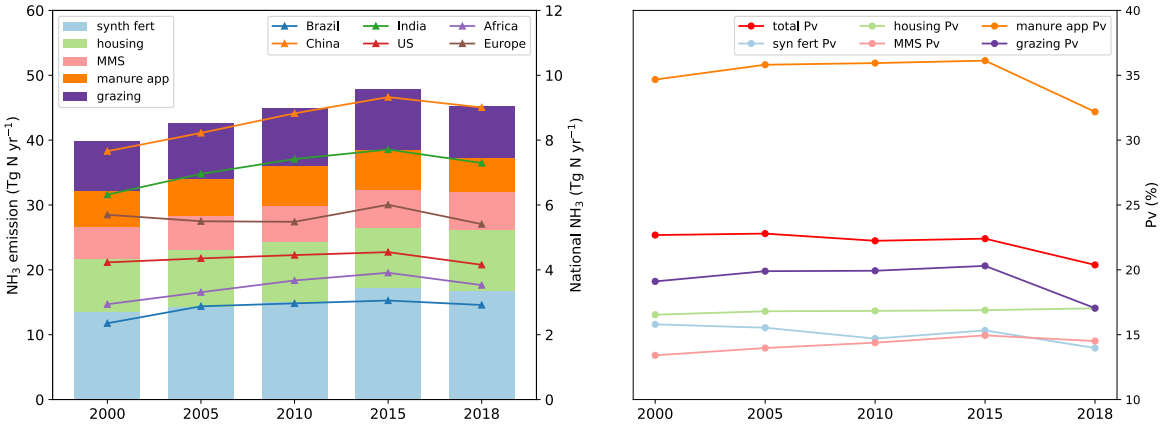

Figure 6.18. Global agricultural NH_3 emissions and volatilization rates of year 2000 to 2018. (a) Global NH_3 from agricultural activities and regional NH_3 emissions from major countries and regions with high emissions. (b) Volatilization rates of agricultural activities.

6.5.2 Projections of future NH_3 emissions to the end of 21st century

Future NH_3 emissions are expected to keep increasing due to more intensive agricultural activities and the changing climate. With more livestock and synthetic fertilizer use, the amount of N introduced to the Earth System goes up. More nitrogen inputs to the environment in a warming planet tend to result in higher NH_3 emissions in the future.

AMCLIM was used to simulate future agricultural NH_3 emissions to the end of 21st century (including 2100) based on N scenarios developed from expert judgement under three Shared Socioeconomic Pathways (SSPs) (Van Vuuren et al., 2017). These three simple N scenarios are summarised in Table 6.8. As discussed, NH_3 originates from two types of nitrogen in the agricultural systems: nitrogen from synthetic fertilizer and nitrogen from livestock excreta. AMCLIM assumed that synthetic fertilizer is likely to increase by 0.5 %, 1.0 % and 2.0 % per year under SSP126, SSP245 and SSP370, respectively. These values are derived from ×0.25, ×0.5 and ×1 of the mean annual increase rate for the period from 2005 to 2015 relative to the value in the reference year 2010. Similarly, livestock numbers increase by 1.4 %, 2.8 % and 5.6 % per 10 years under the three SSPs, respectively, based on the same assumptions. As presented in Table 6.8, projected nitrogen varies enormously between different SSPs. For example, synthetic fertilizer nitrogen under SSP370 in 2100 (286.4 Tg N yr^{-1}) is almost double the value from SSP126 (148.3 Tg N yr^{-1}), and the nitrogen from livestock excreta in 2100 is over 30 % higher under SSP370 compared to SSP126. For the intermediate SSP245, annual total nitrogen reaches to 254 Tg N yr^{-1} in 2050 and 319 Tg N yr^{-1} in 2100, which is higher than the 2010 value by 26 % and 59 %, respectively.

Table 6.8. Nitrogen scenarios based on three Shared Socioeconomic Pathways (SSPs) in AMCLIM. *Changes in "Livestock N" are due to changes in livestock number while the nitrogen excretion rates are assumed to be constant values.

	SSP126	SSP245	SSP370
N scenarios	×0.25 mean annual increasing rate of year 2005 to 2015	×0.5 mean annual increasing rate of year 2005 to 2015	×1 mean annual increasing rate of year 2005 to 2015
Syn fert N	+0.5 % per year	+1.0 % per year	+2.0 % per year
Projected (Tg N yr^{-1})			
2050	122.8	143.2	184.1
2100	148.3	194.4	286.4
Livestock N*	+1.4 % per 10 years	+2.8 % per 10 years	+5.6 % per 10 years
Projected (Tg N yr^{-1})			
2050	105.2	110.8	121.9
2100	112.1	124.6	149.8

In addition to the changes in nitrogen inputs and excreta, the changing climatic conditions are also critical factors influencing future NH_3. As full simulations for future predictions are not achievable due to insufficient environmental and meteorological inputs such as soil

moisture and runoff fluxes, AMCLIM focused on addressing the temperature effect and used air temperature projections by UKESM1-0-LL under three SSPs from the Coupled Model Intercomparison Project Phase 6 (CMIP6) (Senior et al., 2020). The original temperature projections were monthly average and were converted to annual means. Combining the projected annual mean temperature and the temperature sensitivity derived from the global sensitivity tests (as shown in Figure 6.13), the projected annual mean volatilization rates were calculated from the following equation:

$$P_{\mathrm{V,future}}(T_{\mathrm{future}}) = k_{P_{\mathrm{V}}(T)}(T_{\mathrm{mean}} - T_{2010}) + C_{P_{\mathrm{V}}(T)}, \quad (6.1)$$

where T_{future} and T_{2010} are annual mean temperature of a future year and year 2010, and $C_{P_{\mathrm{V}}(T)}$ is solved from the global sensitivity tests for year 2010. Subsequently, the NH_3 emissions were calculated from the following equations:

$$F_{\mathrm{NH_3}} = \sum P_{\mathrm{V,activity}} F_{\mathrm{N,activity}}, \quad (6.2)$$

where $F_{\mathrm{N,activity}}$ is the annual total nitrogen from an agricultural activity such as synthetic fertilizer application, housing and grazing etc. Since it is difficult to determine the amount of nitrogen from manure management and application as it is related to previous stages, an aggregated temperature sensitivity is determined to calculate the overall volatilization from housing, manure management and application together. Equations 6.1 and 6.2 include the spatial variability of the temperature sensitivity, and the global total projected emissions are the sum of emissions from each grid box.

Figure 6.19 shows the estimated NH_3 emissions from 2000 to 2100 using the temperature sensitivity method, along with NH_3 emissions from the AMCLIM full simulations. For the

period from 2000 to 2018, NH_3 estimated by the simplified $k_{Pv(T)}$ method agrees well with the AMCLIM full simulations, indicating that this method is reasonably robust and generally are able to predict comparable global totals. The temperature sensitivity method provides higher estimations for year 2018 than the full simulations, which is largely due to the effects of variables other than temperature such as soil moisture and subsurface drainage as discussed previously.

There are two sets of projections as shown in Figure 6.19: future NH_3 due to temperature effect alone and with N scenarios. It is evident that with increased nitrogen use and inputs, there will be higher NH_3 emissions (dashed coloured lines vs. solid coloured lines). In each set of projections, NH_3 emissions vary due to different temperature conditions under SSPs. Simply speaking, the extent of global mean temperature rise is the smallest under SSP126 and the highest under SSP370 (see Figure F9 in Appendix F8). By the end of the century, NH_3 emissions increase to 51 to 55 Tg N yr^{-1} when soley considering the temperature effect and can reach 59 to 102 Tg N yr^{-1} when also combining with the growing livestock numbers and synthetic fertilizer usage.

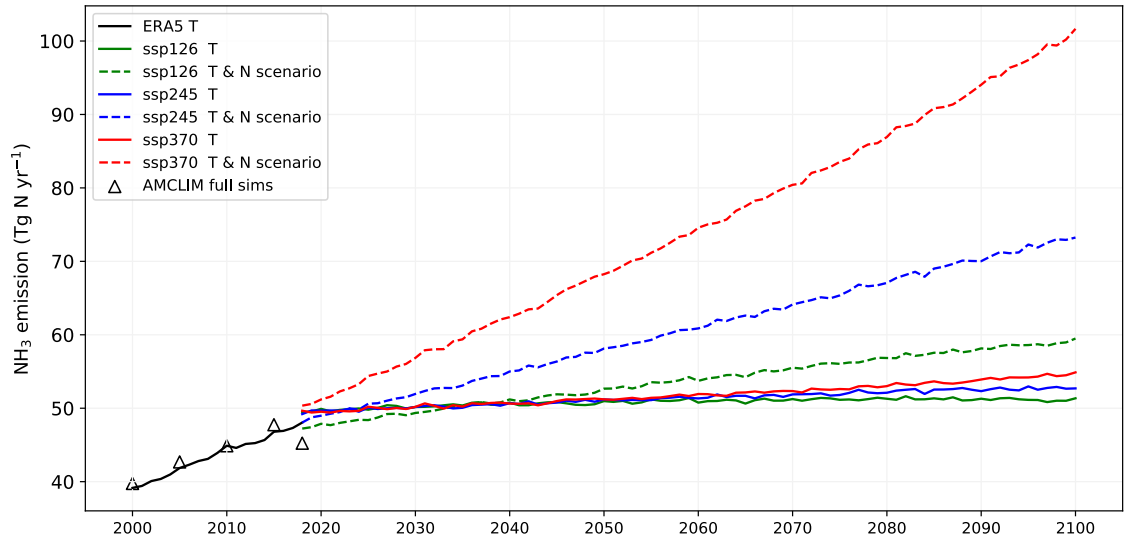

Figure 6.19. Global annual agricultural NH_3 emissions from 2000 to 2100. The triangles represent results from AMCLIM full simulations for year 2000, 2005, 2010, 2015 and 2018. The black solid line is the estimated annual NH_3 using the temperature sensitivity method with ERA5 reanalysis temperature as inputs. The solid lines in green, blue and red are projections for NH_3 emissions only due to temperature change (nitrogen inputs are the same as year 2018) under three SSPs, while dashed lines are projections that also consider the different N scenarios.

Unlike Sutton et al. (2013), that estimated future NH_3 emissions can increase from 45 to 85 Tg N yr^{-1} in 2008 to 64 to 125 Tg N yr^{-1} due to warming alone (under a 5 °C warming scenario) and 89 to 179 Tg N yr^{-1} with increased livestock and fertilizer, AMCLIM's projections are more conservative, especially for the global total emissions. Based on simulations using AMCLIM, regions that contribute to large NH_3 emissions already have high volatilization rates, such as India and Pakistan, then the future warming effect might be little on these places, hence the increase of global total agricultural NH_3 due to

temperature increase is moderate. However, the temperature effect plays a more crucial role on the regional scale (see Fig F10 in Appendix F8). Areas with relatively low emissions and low volatilization rates can experience dramatic increase under a warming climate, which subsequently harm the air quality and reduce nutrient use efficiency. These locations generally have temperate or relatively cold climates, such as Canada, Russia, Tibet, northeastern US and northern Europe (see Fig F10). Also, when considering the potential activity change, i.e., more synthetic fertilizer use and livestock, the situation can be even worse, not only for these areas with low P_V, but also for the globe. As shown in Figure 6.19, global total NH_3 emissions can more than double 2010s' value by the end of 21st century under SSP370, indicating that food production is still likely to be the primary driver resulting in NH_3 emissions increases in most regions.

These projections suggest that climate change will pose a threat on regional and local scales, while food demand can lead to global challenges. The results further imply that it is of great importance to follow an ideal pathway that is sustainable, e.g., SSP126, to limit nitrogen losses through the NH_3 emission and its adverse effects. If mitigation measures can be applied effectively (as discussed in Section 6.4.2), it is possible to control the future NH_3 emissions to a level that benefits both the environment and the human society.

It is worth acknowledging the limitations of these projections. The N scenarios are quite simple and do not explicitly consider potential future policies and regulations, and the projections only take into account of the temperature effect. Changes in future wind conditions, soil conditions as well as land use change can also significantly influence the NH_3 emissions that are originated from the agricultural activities. Although it remains extremely difficult and complicated to carry out more comprehensive future projections,

AMCLIM currently still provides very insightful and useful implications on how NH_3 will vary in the future.

6.6 Summary and conclusions

This chapter synthesizes the global agricultural NH_3 emissions from individual sectors (Chapter 3 – synthetic fertilizer; Chapter 4 – pigs and chicken; Chapter 5 – ruminants). In 2010, global NH_3 emissions from agriculture are estimated at 44.9±4.4 Tg N yr^{-1} based on simulations by AMCLIM, equivalent to 22±2 % of anthropogenic nitrogen input being lost due to NH_3 volatilization.

The results by AMCLIM are comparable to process-based models and EDGAR emission inventory. Around 1/3 of the emissions result from synthetic fertilizer use, with 2/3 associated with livestock farming (including housing, manure management, land application of manure and grazing). Cattle is the largest emitter group among livestock, following by pigs, chicken, and sheep and goats.

AMCLIM also focuses on simulating the NH_3 emission from five major agricultural activities: synthetic fertilizer use, livestock housing, manure management, manure application to land and grazing. Both livestock housing and grazing contribute approximately 20 % of total emissions, and manure management and application to land contribute around 13 %, respectively. The highest percentage volatilization rate is from

manure application, reaching 36 %. Other activities show volatilization rates that are generally lower than 20 %.

Agricultural NH_3 emissions show large spatial variations. High emissions are found in regions with intensive agricultural activities. In particular, China, India, US, Brazil and Pakistan result in the largest emissions, together accounting for nearly 60 % of the global NH_3 emissions. Meanwhile, over 80 % of global NH_3 emissions are found to be resulted from the NH, with extremely high emissions occurring between 20 ~ 40 °N. Temporal variation in NH_3 emissions is also large. Highest emissions occur from June to August in the NH and from November to February in the SH, which is largely driven by the seasonality in NH_3 emissions related to synthetic fertilizer use, depending on the planting seasons.

As NH_3 emissions are greatly influenced by environmental conditions, three major factors were mainly analysed to investigate the impacts on NH_3 volatilization, including temperature, wind speed and water availability. Overall, high volatilization rates are found in hot and dry places. Temperature is the most critical factor affecting NH_3 volatilization under cold environment, and increasing in temperature facilitates volatilization to cause more NH_3 emissions. Wind speed also positively affects NH_3 volatilization, but its impact is less significant compared to temperature especially when temperature is the limiting factor.

Contrary to temperature and wind speed, water availability plays a more complicated role on NH_3 volatilization. In general, NH_3 emissions tend to be larger under dry conditions due to a higher concentration, which generates higher emission potential. Soil moisture and

subsurface percolation flux are two indicators for water availability, and volatilization rates are found to be reversely correlated to these two variables. However, wetter soils can either result in higher or lower emissions, depending on interactions with other variables. For global simulations of year 2018, the estimated volatilization rates of outdoor emissions (land application of synthetic fertilizer and manure and grazing) are lower than 2010. This is mainly due to larger subsurface percolation fluxes that caused larger drainage and leaching, which depletes soil nitrogen and results in less NH_3 emission.

Mitigation measures were simulated and were found to be effective in reducing NH_3 emissions, including decreasing nitrogen application rates and improving livestock feeding materials, covering stored manure and better land application techniques (e.g., incorporation and deep placement) etc. It is estimated that a potential 40 % abatement of global NH_3 emissions can be achieved when applying a suite of the tested measures.

Based on simulations using AMCLIM, NH_3 emissions have increased from 39.8 Tg N yr^{-1} in 2000 to 45.2 Tg N yr^{-1} in 2018. Temperature sensitivity was derived from global sensitivity tests, indicating that global total NH_3 emissions can increase by 3.4 % each 1 K warming relative to year 2010. For each agricultural activity, temperature sensitivity varies across the globe, with the highest temperature sensitivity being over 12 % K^{-1} in cold regions for land application of fertilizer and manure. Future NH_3 emissions are projected to go up to 51 to 55 Tg N yr^{-1} due to warming alone (with 2018 activity) and can reach 59 to 102 Tg N yr^{-1} when also combining with the growing livestock number and synthetic fertilizer usage. It is suggested that climate change and food production pose risks for future agricultural NH_3 emissions at different spatial scales. Regional and local environment and

agricultural systems may suffer the consequences of the warming effect, while the globe may face challenges due to increased food production.

Chapter 7
Conclusions

7.1 Thesis overview

Ammonia emissions mainly originate from agricultural activities, as a result of NH_3 volatilization from synthetic fertilizer and livestock excreta. As a major unintended N loss, NH_3 emissions not only compromise the nutrient recycling within the agricultural systems but also have adverse impacts on the environment (Galloway et al., 2003a; Sutton et al., 2011b). Previous studies have found that NH_3 emissions are strongly dependent on the environmental conditions, such as temperature, water availability and many other factors (Gyldenkærne, 2005b; Misselbrook et al., 2005; Sommer et al., 2006; Sutton et al., 2013; Bittman et al., 2014). However, existing emission inventories that use emission factors (EFs) to estimate NH_3 emissions usually lack consideration of the impacts of these factors, which may introduce uncertainty and bias in estimations of the NH_3 emission. In addition to the environmental factors, management practices also influence NH_3 emissions. To address the deficiencies in current EFs-based approaches, process-based models have been developed and used, which simulate the processes that determine NH_3 emissions (Riddick et al., 2017b; Móring et al., 2016; Pinder et al., 2004; Beaudor et al., 2023; Vira et al., 2020a).

In this thesis, the development of a dynamic emission model AMmonia–CLIMate (AMCLIM) for simulating climate-dependent NH_3 emissions has been described. AMCLIM has high spatial and temporal resolution, with high level of detail. The AMCLIM model focuses on modelling NH_3 emissions from the use of synthetic fertilizer and major livestock farming that includes cattle (including buffaloes), pigs, poultry (chicken), sheep and goats. AMCLIM simulates climate-sensitive physicochemical and biological processes involved in the agricultural activities that determine the NH_3 emissions, including livestock housing, manure management, land application of both synthetic fertilizer and manure, as well as ruminant grazing. There are three main modules in AMCLIM: the Housing Module (AMCLIM–Housing), the Manure Management Module (AMCLIM–MMS) and the Land Module (AMCLIM–Land). Site scale simulations were carried out using AMCLIM for livestock housing and synthetic fertilizer applications, and the modelled results have been evaluated by comparison with measurement data from the USEPA AFO and the GRAMINAE projects, respectively, and a wide range of grazing studies. When AMCLIM was applied on the global scale, it was driven by the ERA5 reanalysis meteorology and used a variety of input data, such as livestock and manure management information from the GLEAM2 model (FAO, 2018), nitrogen application rates and crop calendar from GGCMI 3 (Mueller et al., 2012; Hurtt et al., 2020; Jägermeyr et al., 2021) and soil data from multiple databases.

Global simulations were performed using AMCLIM for the period from 2000 to 2018, with full model runs for the years 2000, 2005, 2010, 2015 and 2018. The results of estimated NH_3 emissions produced by AMCLIM are thoroughly explained and discussed, with a focus on the reference year 2010 and a comparative analysis for the year 2018. Budgets

detailing the N flows within individual livestock sectors and the entire agricultural sector have been generated based on the AMCLIM simulations, which emphasizes the NH_3 volatilization process. The thesis contains a range of analyse aimed at investigating the impacts of environmental factors and management practices, as well as identifying effective measures for reducing NH_3 emissions. Sensitivity tests were conducted at both site-specific and global scales, with a particular emphasis on how temperature affects the volatilization and other processes. Furthermore, projections for future NH_3 emissions by the end of the 21st century have been developed by combining temperature sensitivity with various N scenarios under different Shared Socioeconomic Pathways (SSPs) (Van Vuuren et al., 2017).

7.2 Summary of key results

The key results of this thesis are summarised below, which addresses the objectives and research questions as presented in Chapter 1 (Section 1.1).

1. **Presenting the development and evaluation of a dynamic, process-based NH_3 emission model.**

    a) **How can a model be developed for quantifying climate-dependent NH_3 emissions based on knowledge at the process-based level?** In general, the development of AMCLIM focused on three core aspects: 1) representation of the volatilization process of NH_3 from the emitting surface to the atmosphere;

2) determination of masses and concentration of TAN (and other N species); and 3) simulations for processes/pathways that deplete the TAN pool. First, the volatilization of NH_3 is calculated by assuming a resistance model that uses the gas concentration gradient of NH_3 between the surface and a reference height, which is constrained by a set of resistances that are dependent on atmospheric conditions. Gas phase NH_3 concentrations at the surface are determined from both a temperature response of combined Henry's constant and dissociation equilibria and the emission potential ($[NH_4^+]/[H^+]$). Second, the mass of the TAN pool is solved by estimating the sources and losses. The sources include direct input of ammonium fertilizers, hydrolysis of urea and uric acid and decomposition of organic forms of nitrogen that can be temperature-dependent. The concentration of TAN depends on the water pool of the system (e.g., water and urine in livestock houses or manure stores, and soil moisture on croplands and grazed pastures) and is also related to substrate (e.g., manure or soil) characteristics as adsorption processes are important. Third, the depletion of the TAN pool (or the loss pathways of the TAN) includes multiple processes. For indoor simulations such as livestock housing and manure storage, the TAN pool is mainly depleted by NH_3 volatilization. For outdoor simulations such as land application of synthetic fertilizer and manure and grazing, AMCLIM also simulates surface runoff, nitrification, plant uptake of N, leaching and diffusion to deep soils. These physical, chemical and biological processes are influenced by environmental conditions.

b) **How well does the model agree with the measurements for NH_3 emissions from different agricultural activities?** AMCLIM was applied at site scale, and the simulated results were evaluated against measurement data for NH_3 emissions from livestock housing and fertilizer application to land. By comparing with measurements of eight livestock houses by USEPA AFO (Cortus et al., 2010a, b; Lim et al., 2010a, b; Wang et al., 2010), the simulated NH_3 emissions from dairy cattle, pig and chicken housing showed close agreement with measurements. AMCLIM was able to reproduce the NH_3 emissions from three different types of animal houses with different processes and settings, and generally replicate the daily variations in NH_3 emissions. For the simulation of a fertilized grassland at the GRAMINAE site (Sutton et al., 2009b), AMCLIM model captured the main features (long-term decay following application and diurnal variation) of the measured NH_3 emissions throughout the simulated period and produced estimates for daily NH_3 emissions and sub-hourly variations comparable to the measurements. AMCLIM broadly reproduced the measured NH_3 emissions, with overestimation on the first day and during night time.

2. **Applying the model at the global scale to estimate agricultural NH_3 emissions.**

a) **What is the magnitude of global agricultural NH_3 emission?** For the reference year 2010, global agricultural NH_3 emissions estimated by AMCLIM are 44.9±4.4 Tg N yr^{-1}, equivalent to globally 22±2 % of anthropogenic nitrogen input from synthetic fertilizer and livestock excreta being lost through NH_3 emissions. China, India, US, Brazil and Pakistan are the top five countries that

resulted in the largest emissions, together accounting for nearly 60 % of the global NH_3 emissions. The global estimates of AMCLIM are consistent with other models, e.g., CAMEO, 44 Tg N yr^{-1} for 2005 to 2015 (Beaudor et al., 2023) and FANv2, 48 Tg N yr^{-1} for 2010s (Vira et al., 2020a) and the EDGAR emission inventory, 44.2 Tg N yr^{-1} for the year 2010 (EDGAR, 2023). However, the climate-dependent estimates of AMCLIM generate a different spatial pattern of emissions (see details in Section 6.2.2). and also allow year-to-year fluctuations from meteorological variability and longer-term influences from climate change to be simulated (see Section 6.5)

b) **What are the sectoral NH_3 emissions (e.g., from synthetic fertilizer use and different livestock types) and what is the contribution of each major agricultural activity?** Around 1/3 of the emissions result from synthetic fertilizer use (15.0 Tg N yr^{-1}), with 2/3 associated with livestock farming (29.9 Tg N yr^{-1}; including housing, manure management, land application of manure and grazing). Cattle (17.7 Tg N yr^{-1}) are the largest estimated emitter group among livestock, contributing about 40 % of total NH_3 emissions. Both pigs (5.3 Tg N yr^{-1}) and poultry (4.8 Tg N yr^{-1}) contribute more than 10 % of total emissions, with sheep and goats (2.1 Tg N yr^{-1}) together responsible for about 5 %. Regarding the agricultural activities, the NH_3 emissions from both livestock housing (9.2 Tg N yr^{-1}) and grazing (8.9 Tg N yr^{-1}) each represent about 20 % of the total emission. Manure management (5.6 Tg N yr^{-1}) and manure application to land (6.1 Tg N yr^{-1}) contribute 13 and 14 % of the total emission, respectively.

c) **What is the spatial distribution of agricultural NH_3 emissions and the corresponding volatilization rates (i.e., the percentage of agricultural N that is volatilized as NH_3)?** According to simulations by AMCLIM, in general, high NH_3 emissions are found to have occurred in regions with intensive agricultural activities (i.e., countries with the largest emissions as mentioned above). Over 80 % of NH_3 emissions are from the NH, and the largest NH_3 emissions are found between 20 ~ 40 °N (i.e., where large parts of China, India, US and Pakistan are located), where also the highest emissions related to synthetic fertilizer use are found. Emissions from grazing are more evenly distributed across latitudinal bands compared to other activities. Compared with studies that do not take account of climatic impacts or only to a limited extent, AMCLIM estimates more NH_3 emissions from in warm and dry locations and less NH_3 emissions in cold and wet places. An exception is emission for poultry, where a certain amount of water is necessary to stimulate hydrolysis of uric acid (UA). This tends not be a barrier for other livestock as urine typically provides sufficient water to allow hydrolysis of urea.

The spatial distribution of volatilization rates is not always necessarily consistent with the spatial distributions of emissions. The regional patterns of the volatilization rates of individual practices are different. A common feature is that high volatilization rates are frequently found in hot and dry places, while cold regions typically show lower volatilization rates. Specifically, the volatilization rates of manure application to land are generally higher than other activities across the globe.

d) **What are the daily/seasonal temporal profiles of agricultural NH_3 emissions?** Meanwhile, NH_3 emissions also show strong temporal variations. At a daily scale, the highest NH_3 emissions typically occur in the hottest period of the day, i.e., early afternoon. Over the year, the NH_3 emissions are the highest in summer, with the seasonality being largely determined by the temporal variations in the emissions resulted from synthetic fertilizer use, which is associated with the planting season. Different agricultural activities show different seasonality, i.e., manure application emissions peak in April and September, while emissions related to other activities including housing, manure management and grazing are generally higher in the NH summer than other seasons.

e) **What are the major N flows and pathways in the agricultural systems?** The amount of N in livestock excreta and synthetic fertilizer input in 2010 is estimated to be 99.6 Tg N yr^{-1} and 102.3 Tg N yr^{-1}, respectively. Based on simulations using AMCLIM, around 22 % of this nitrogen is estimated to be lost through NH_3 volatilization (44.9 Tg N yr^{-1}), and approximately 50 % of nitrogen enters the soil pool and is used by plants (101.5 Tg N yr^{-1}). About 3 % of nitrogen is lost due to burning or lack of proper management (6.4 Tg N). Less than 10 % of nitrogen undergoes nitrification (18.5 Tg N yr^{-1}), and the remaining 15 % is lost through runoff (4.7 Tg N yr^{-1}), leaching and diffusion in soils (25.9 Tg N yr^{-1}).

3. **Enhancing understanding of the impacts of environmental factors and management practices on NH_3 emissions.**

a) **How do environmental conditions/factors affect NH_3 emissions from agriculture?** The impacts of temperature, wind speed and water availability on NH_3 volatilization have been mainly investigated. Increasing temperature and wind speed facilitates volatilization, thus producing higher NH_3 emissions. Temperature is found to be the most critical factor especially under cold conditions. Ammonia emissions tend to be larger under dry conditions, but wetter soils can result in emissions either increasing or decreasing, depending on interactions with other variables such as soil pH. Wetter conditions can generate larger subsurface percolation fluxes, which lead to lower NH_3 emissions by depleting soil nitrogen through larger drainage and leaching. Sometimes the water availability effects outweighed the temperature effects. As 2018 was a generally hotter and wetter year compared to 2010, the estimated volatilization rates of grazing and land application of fertilizer and manure in 2018 were lower than 2010, which was largely the result of larger drainage in 2018 compared with 2010. Moreover, soil pH is also a critical factor that determines the NH_3 emissions from land applications, with simulated emissions increasing at higher pH conditions.

b) **How to improve agricultural practices to reduce NH_3 emissions?** Improved management practices are found to have positive effects on NH_3 mitigation. For land application of synthetic fertilizer and manure, AMCLIM estimated that using better application techniques such as incorporation and deep placement/injection can reduce NH_3 emissions by a large degree, i.e., emissions might decrease by over 50 % and 95 % when applying the techniques

themselves. Using AMCLIM, it is estimated that by combining sophisticated application techniques with lower N application rates, NH_3 emissions can be reduced whilst saving fertilizer and achieving comparable crop yields. For livestock farming, more scientific feeding strategies can possibly decrease N surplus and there will be less N excreted from the livestock. Meanwhile, reducing the manure surface area, covering stored manure, and not leaving excreta on land without attention will all also benefit NH_3 abatement. By incorporating a suite of mitigation measures mentioned above in AMCLIM, it is estimated that global agricultural NH_3 emissions could be reduced by up to 40 %.

4. **Estimating present and future NH_3 emissions.**

   a) **How have NH_3 emissions changed over the past two decades in this century?** Using AMCLIM, it is estimated that global NH_3 emissions have increased from 39.8 Tg N yr^{-1} in 2000 to 45.2 Tg N yr^{-1} in 2018, mainly as a result of agriculture intensification (i.e., more N from synthetic fertilizer use and increasing livestock numbers). The small inter-annual variability of the volatilization rates indicates that environmental change (i.e., temperature, wind and water availability) has not been the main drive of increasing in NH_3 emissions over the past two decades.

   b) What could future NH_3 emissions from agriculture look like (emission totals and spatial patterns)? A global sensitivity test to temperature indicates that annual NH_3 emissions may increase by around 7 % due to a (uniform) 2 °C

warming, compared to the base value of year 2010. The temperature responses vary between individual activities and regions. The largest absolute increase in emissions occurs between 20 ~ 40 °N, while the most significant relative increases tend to take place in cold regions. By applying a simplified temperature sensitivity method, AMCLIM estimated that future NH_3 emissions by the end of the 21st century are projected to rise to 51 to 55 Tg N yr^{-1} due to the temperature effect alone (with 2018 activity). When combining with the N scenarios developed under different SSPs in which livestock number and synthetic fertilizer usage keep increasing, NH_3 emissions can go up to 59 to 102 Tg N yr^{-1}. Climate change and food production are found to have significant impacts on future agricultural NH_3 emissions but on different spatial scales. Locations with low volatilization rates (usually in cold and temperate regions, such as Canada, Russia, Tibet, northeastern US and northern Europe) tend to be most influenced by the effects of warming, in these regions the local air quality and nutrient use efficiency may be adversely affected. On the global scale, food production is growth likely to be the primary factor that generates increasing of NH_3 emissions. In summary, these projections suggest that climate change poses a threat on regional and local scales, while food production pressures will lead to global scale challenges.

7.3 Significance and implications

This thesis presents the quantification of climate-dependent NH_3 emissions from global agriculture. The development, evaluation and application of a dynamic process-based emission model, AMCLIM, have been elaborated and explained, with detailed parameterization given. Simulations have been performed for estimating historical NH_3 emissions over the past two decades, and future NH_3 emissions have been projected based on a simplified temperature sensitivity method derived from the model sensitivity analysis.

The AMCLIM model itself is considered to be a valuable asset. AMCLIM has been specifically designed and built from scratch to simulate the NH_3 volatilization by modelling the N flows within global agricultural systems. AMCLIM is thought to be the first dynamical emission model that simulates NH_3 emission from all individual sectors by a consistent process-based modelling approach, with high levels of detail. AMCLIM not only includes important N processes that are sensitive to environmental factors, but also takes into account the impacts of management practices. AMCLIM can be applied at multiple scales depending on the objectives. Global application of AMCLIM is operated at a relatively high temporal and spatial resolution, i.e., hourly time-step and 0.5° latitude × 0.5° longitude (equivalent to 39 km × 55 km at 45° latitude), which can more accurately capture the temporal and spatial features of NH_3 emissions compared with previous studies.

AMCLIM results were used to calculate EFs for livestock NH_3 emissions on the model's native grid (Figure 6.6). Comparing these EFs with existing national values in the literature (Yang et al., 2023), it is clear that there are important sub-national variations due to local variations of environmental and management factors that are typically overlooked in these

national values. It is emphasized that conducting more experimental studies on measuring NH_3 fluxes is necessary, especially in hot tropical regions where there very few published studies. Such studies need to report sufficient environmental and soil data to make them most useful for comparison with model simulations. AMCLIM is suitable for further development or augmented to investigate other N_r fluxes and provides a starting point for modelling the wider nitrogen cycle. Code of the currently version of the AMCLIM model is written in Python and is managed on github (https://github.com/jjzwilliam/AMCLIM) with version control and can be run on a local PC or on a High Performance Computing (HPCs), depending on the workload and purposes. The full application of the AMCLIM model has been ported on the UK National HPC ARCHER2.

The major output of the AMCLIM model is a dataset that documents daily agricultural NH_3 emissions with a global coverage for several years, with meteorological inputs from ERA5. This emission dataset may serve as a reference for national and regional monitoring needs and can be used as input for atmospheric chemistry/transport modelling, with implications for air quality evaluation. The volatilization rate (P_V) is a useful indicator to identify where and which activity results in a large fraction of N loss due to NH_3 volatilization and needs particular attention when seeking to avoid significant nutrient losses. From a broader perspective, the N budgets derived from the AMCLIM simulations are helpful for developing a comprehensive assessment of N_r recycling within the agricultural system and the environmental impact of N_r from anthropogenic sources. By carrying out analysis, sensitivity and experimental tests, this thesis provides insights on how environmental factors and management practices influence NH_3 volatilization. The future projections of NH_3 emissions highlight the critical impacts of global warming and increasing

anthropogenic N due to activity change. Potential measures for mitigating NH_3 emissions have been examined, with effectiveness quantified at the global scale. Consequently, this thesis can provide a basis for guiding policy development and regulations, which has real-world impacts.

7.4 Limitations and future work

Major limitations of this study exist in two aspects: limited measurement data for model evaluation and uncertain model parameters or parameterizations of simulated processes. First, AMCLIM has been intensively evaluated against measurement of livestock housing and synthetic fertilizer application, which represents two major categories of NH_3 emissions that are from indoor facilities and from land application, respectively. However, simulations for manure management, manure application to land and grazing are not explicitly evaluated in detail with any measurements at site scale. This is partly due to the difficulties in measuring NH_3 fluxes and also because of insufficient input data from experimental studies to drive the AMCLIM model. Since the simulations for manure management and application to land are at least similar to what has been evaluated against site scale measurements, this leaves NH_3 emissions from grazing estimated by AMCLIM, which is considered to be the most uncertain model subcomponents. To address this limitation, simulated grazing volatilization rates were compared with reported values from literature, as a broader method of evaluation.

Second, several modelled processes in AMCLIM are uncertain and need further investigation, which is either due to very complicated processes that are challenging to simulate or due to lack of knowledge and measurement data, including soil pH dynamics after urea application, the drainage and diffusion processes in soils, the adsorption of TAN on manure solids and the land-air exchange process of NH_3 when considering vegetation effects. In AMCLIM, these processes are generally simplified under various assumptions. Therefore, it is important to note that all the results must be interpreted carefully within the context of a modelling approach with uncertainty and limitations. Another limitation that is worth mentioning is from the computational perspective. AMCLIM requires large number of inputs (as presented in Chapter 2), while the computational requirements for running the specific Grazing Submodule can be high.

This research can be further expanded in a variety of directions. In principle, future work could be carried out to address the limitations summarised above. Conducting more experimental studies that take NH_3 emission measurements in regions from a wide spectrum of climatic conditions, e.g., measurements in tropical regions where NH_3 volatilization can be intense, is very likely to benefit model development. This includes the benefit of sufficient observations for evaluation, which can also advance a better understanding of the critical processes involved in the NH_3 emission modelling.

Additional possible future work includes, but is not limited to:

1) **Developing a bi-directional exchange scheme for NH_3.**

Current evidence indicates that the air-surface flux of NH_3 can be either uni-directional or bi-directional, influenced by ambient NH_3 concentrations. This dynamic behaviour is

particularly relevant for semi-natural vegetation in agricultural regions, especially in wet and cold areas. To capture this complexity, it is worth developing a sophisticated exchange scheme for NH_3. Conventional deposition velocity methods in atmospheric models can be enhanced by accounting for the multi-dimensional surface interactions, including leaf surfaces, stomatal exchange, and interactions with the underlying soil. Sutton et al. (2013) proposed a resistance-based approach for NH_3 exchange including cuticular, stomatal and ground pathways, and several studies have demonstrated the feasibility of implementation of the bi-directional exchange into large scale atmospheric modelling (Bash et al., 2013; Fu et al., 2015; Chen et al., 2021). Though it is a great challenge to develop models at the process level because of the relatively complicated dynamics exchange, the integration of such processes into AMCLIM could provide better insights into quantifying net NH_3 fluxes.

2) **Running atmospheric chemistry/transport models with the high resolution NH_3 emissions estimated by AMCLIM or incorporating the AMCLIM model into a sophisticated Earth System Model (ESM).**

Precise NH_3 emissions are crucial for accurate atmospheric modelling, particularly on a global scale. Existing atmospheric chemistry/transport models often rely on prescribed NH_3 emissions or emission inventories with limited consideration for climatic influences. These emissions typically have low temporal resolution, reflecting only monthly averages based on simplified activity profiles. This can introduce uncertainty in simulating NH_3 concentrations, deposition, and aerosol formations. By substituting the prescribed NH_3 emission inputs with estimates from AMCLIM, atmospheric models could potentially generate more accurate simulations, benefiting air quality assessments (Ge et al., 2023). Running atmospheric models with AMCLIM-derived NH_3 emissions can be a useful way

to further evaluate emission quality. Additionally, integrating AMCLIM into an Earth System Model (ESM) is promising as it can allow for comprehensive coupling of nitrogen and carbon cycles and more consistent meteorological and environmental drivers, i.e., making the AMCLIM model online rather than offline, expanding the scope of research.

3) **Evaluating economic damage cost linked to NH_3 emissions and cost-benefit measures for NH_3 emission abatement.**

Future research could explore different N scenarios and assess the economic damage costs associated with NH_3 emissions, and conduct cost-benefit analysis to identify the cheapest measures for reducing net NH_3 emissions. The increasing challenges posed by N_r emissions could have substantial environmental and societal impacts. Evaluating these costs from an economic perspective can provide insights into potential policy development. A climate-dependent modelling approach (such as AMCLIM) is helpful for providing more reliable estimates.

Model Symbols

a_{plant}	dimensionless parameter for plant activity	
a_{Σ}	empirical factor for nitrification process	2.4 (manure) or 1.8 (synthetic fertilizer)
A_h	temperature correction dependence for urea hydrolysis	
A_m	temperature correction dependence for organic N decomposition	
B	boundary layer Stanton number	5
B_a	mineralization constants for available organic N	8.94×10^{-7} s^{-1}
B_r	mineralization constants for resistant organic N	6.38×10^{-8} s^{-1}
B_{vap}	vapor transfer coefficient	m Pa^{-1} s^{-1}
BD_{manure}	bulk density of manure	g cm^{-3}
BD_{soil}	bulk density of soil	g cm^{-3}
c_p	specific heat capacity of dry air	1005 J kg^{-1} K^{-1}
C	substrate concentration of carbon	g C m^{-2}
$C_{Pv(T)}$	constant of temperature sensitivity	% K^{-1}
$den_{grazing}$	grazing density	m^2 $head^{-1}$
$den_{housing}$	housing density of livestock	kg animal per m^2 (pigs and ruminants)

		or number of animal per m^2 (chicken)
$D_{NH_4/NH_3}^{aq/gas}$	molecular diffusivity	$m^2\ s^{-1}$
D_{pot}	water drainage potential	$m\ s^{-1}$
D_{temp}	temperature difference between indoor and outdoor temperature due to the warmth generated by animals	3 ºC
e_a	actual vapor pressure at present state	Pa
e_s	saturation vapor pressure	Pa
$f_{blocking}$	blocking factor of animal house	
f_{clay}	fractional soil clay content	
$f_{DM.max}$	maximum DM content of slurry	
f_{dung}	fraction of dung pat of pastures	
f_{fert}	fraction of fertilizer type used	
f_{gap}	fraction of gap space in the slats	0.2
$f_{grazing}$	fraction of ruminant excreta deposited on pastures	
f_{MMS}	fraction of a manure removed for separate storage as part of the MMS	
$f_{MMS(pasture)}$	fraction of annual total manure deposited on pastures	
f_N	fraction of N form in excretion	
f_{pit}	relative area of pit to area of animal house	1.0

f_{silt}	fractional silt content of soil	
f_{som}	fractional soil organic matter content	
$f_{store\text{-}housing}$	ratio of manure storage area to housing area	
f_{tech}	fraction of application technique used	
f_{T}	temperature dependence of root activity	
f_{urine}	fraction of urine patch of pastures	
$F_{added\ water}$	flux of additional water added to slurry	g m^{-2} s^{-1}
$F_{diffusion\ to\ surface}$	upward diffusive fluxes to surface	g N m^{-2} s^{-1}
$F_{diffusion(aq/gas)}$	diffusive fluxes	g N m^{-2} s^{-1}
$F_{drainge}$	flux of N drainage	g N m^{-2} s^{-1}
F_{evap}	evaporation of water	g m^{-2} s^{-1}
$F_{excreta}$	excretion rate from livestock	g m^{-2} s^{-1}
$F_{excretion\ water}$	initial water content in poultry excreta	g m^{-2} s^{-1}
$F_{excretN}$	total N excretion rate from livestock	g N m^{-2} s^{-1}
$F_{faecal\ water}$	flux of water from faeces	g m^{-2} s^{-1}
$F_{leaching}$	flux of leaching	g N m^{-2} s^{-1}
F_{L_N}	sum of losses of N compound	g N m^{-2} s^{-1}
F_{NH_3}	flux of NH_3	g N m^{-2} s^{-1}
$F_{NH_3\ removal}$	flux of NH_3 from house atmosphere to outside	g N s^{-1}
$F_{NH_3\ volatlization}$	flux of NH_3 from floor surface to house atmosphere	g N s^{-1}

$F_{\text{N runoff}}$	flux of surface N runoff	g N m^{-2} s^{-1}
$F_{\text{N,activity}}$	annual total nitrogen from agricultural activity	g N m^{-2} yr^{-1}
$F_{\text{nitrate runoff}}$	flux of surface nitrate runoff	g N m^{-2} s^{-1}
F_{nitrif}	flux of nitrification	g N m^{-2} s^{-1}
F_{P_N}	sum of production (including inputs) of N compound	g N m^{-2} s^{-1}
F_{rainfall}	rainfall	mm s^{-1}
F_{TAN}	production of TAN	g N m^{-2} s^{-1}
$F_{\text{TAN runoff}}$	flux of surface TAN runoff	g N m^{-2} s^{-1}
F_{uptake}	flux of N uptake by plants/crops	g N m^{-2} s^{-1}
$F_{\text{urea runoff}}$	flux of surface urea runoff	g N m^{-2} s^{-1}
F_{urine}	flux of water from livestock urination	g m^{-2} s^{-1}
g	acceleration of gravity	9.81 m s^{-2}
H	sensible heat flux	J m^{-2} s^{-1}
I_{TAN}	direct input of TAN species	g N m^{-2} s^{-1}
$J_{\text{C,N}}$	combined response factor for substrate C and N level	
k	von Karman constant	0.41
k_{G}	gaseous transfer coefficient for NH_3	m s^{-1}
$k_{\text{G,housing}}$	gaseous transfer coefficient for NH_3 in animal house	m s^{-1}
k_{h}	urea hydrolysis constant	s^{-1}

k_{L}	aqueous transfer coefficient for TAN	m s^{-1}
$k_{nitrif,pH}$	pH dependence of nitrification rate	
$k_{nitrif,T}$	temperature dependence of nitrification rate	
$k_{nitrif,WFPS}$	water-filled pore space dependence of nitrification rate	
k_{pH}	pH dependence of uric acid hydrolysis rate	
$k_{Pv(T)}$	temperature sensitivity	% K^{-1}
k_{RH}	humidity dependence of uric acid hydrolysis rate	
k_{T}	temperature dependence of uric acid hydrolysis rate	
K_{d}	partition coefficient of soil adsorbed of TAN	m^3 m^{-3}
K_{N}	conversion rate at which a N compound decomposes to form TAN	s^{-1}
K_{Neff}	correction constant for root activity	g N m^{-2}
K_{NH_3}	combined coefficient of Henry and dissociation equilibria	
K_{nitrif}	rate of nitrification	s^{-1}
$K_{nitrif,opt}$	optimum nitrification rate	0.1 d^{-1}
K_{OrgN}	rate of organic N decomposition	s^{-1}
K_{s}	soil hydraulic conductivity	m s^{-1}
K_{sat}	soil hydraulic conductivity at saturation	m s^{-1}
K_{UA}	rate of uric acid hydrolysis	s^{-1}

K_{uptake}	plant water uptake coefficient	0.096 d^{-1}
K_{Urea}	rate of urea hydrolysis	s^{-1}
L	Monin-Obukhov length	m
m	average body weight of animal	kg $head^{-1}$
m_{air}	molecular weight of air	29 g mol^{-1}
m_{E}	equilibrium moisture content of excreta	
m_{NH_3}	molecular weight of NH_3	17 g mol^{-1}
$M_{\text{added water}}$	mass of additional water added to slurry	g m^{-2}
M_{DM}	mass of DM of excreta	g m^{-2}
M_{excreta}	mass of livestock excreta	g m^{-2}
M_{faeces}	mass of faeces	g m^{-2}
$M_{\text{H}_2\text{O}}$	mass of water	g m^{-2}
M_{N}	mass of N species	g N m^{-2}
M_{Neff}	mass of effective available N for the plant	g N m^{-2}
M_{nitrat}	mass of nitrate	g N m^{-2}
$M_{\text{NH}_3,\text{g}}$	mass of gas NH_3	g N m^{-2}
$M_{\text{NH}_4^+}$	mass of NH_4^+	g N m^{-2}
M_{OrgN}	mass of organic N	g N m^{-2}
M_{TAN}	mass of TAN in all phases	g N m^{-2}
$M_{\text{TAN,aq}}$	mass of aqueous TAN	g N m^{-2}

$M_{TAN,s}$	mass of exchangeable solid TAN (adsorbed NH_4^+)	g N m^{-2}
M_{UA}	mass of uric acid	g N m^{-2}
M_{Urea}	mass of urea	g N m^{-2}
n	number of animals	
N	substrate concentration of nitrogen	g N m^{-2}
$N_{T_{10}^{min}>10°C}$	number of days with T_{10}^{min} higher than 10 ºC in a year	
p	atmospheric pressure	Pa
P_V	percentage of N volatilizes as NH_3	%
$P_{V,activity}$	annual mean percentage volatilization rate for agricultural activity	%
$P_{V(TAN)}$	percentage of TAN volatilizes as NH_3	%
q_p	subsurface percolation flux of water	m s^{-1}
q_r	surface runoff flux of water	m s^{-1}
Q_{in}	airflow rate of animal house	m^3 s^{-1}
r_N	wash-off factor for N species	% mm^{-1}
R	resistance constraining fluxes	s m^{-1}
R_a	aerodynamic resistance	s m^{-1}
$R_{aq/gas}$	resistance that constrains the aqueous or gaseous diffusion processes	s m^{-1}
R_{atm}	atmospheric resistances	s m^{-1}

R_b	boundary layer resistance	s m^{-1}
$R_{G,house}$	resistance for NH_3 volatilization in animal house	s m^{-1}
R_{GL}	combined resistance for transfer of NH_3 across the gas-liquid interface	s m^{-1}
R_{litter}	surface resistance of poultry litter	8460 s m^{-1}
$R_{manure,aq/gas}$	manure resistances	s m^{-1}
RH	relative humidity	%
$S_{dung\ pat}$	area of dung pat of pastures	m^2
$S_{grazing}$	area of grazing pastures	m^2
S_{house}	surface are of animal house	m^2
S_{pit}	area of pit in animal house	m^2
S_{slats}	area of slats in animal house	m^2
$S_{storage}$	area of manure storage unit	m^2
$S_{urine\ patch}$	area of urine patch of pastures	m^2
Sc	Schmidt number	
$t_{cleaning}$	cleaning time	24 h
t_{fc}	reference time for soil water content reaching field capacity	24 h
t_{max}	maximum temperature for microbial activity for nitrification	313 K
t_{opt}	optimum temperature for microbial activity for nitrification	301 K

t_{r1}	temperature correction constant for organic N decomposition	0.0106 K^{-1}
t_{r2}	temperature correction constant for organic N decomposition	0.12979 K^{-1}
T	temperature	K or °C
T_{2010}	annual mean temperature of year 2010	K or °C
T_{floor}	floor temperature of animal house	°C
T_{future}	annual mean temperature of future year	°C
T_{gnd}	ground temperature	°C
T_{in}	indoor temperature of animal house	°C
T_{max}	indoor temperature when ventilation reaches maximum in animal houses with forced ventilation	12.5 ºC
T_{min}	indoor temperature when heating is installed in animal houses with forced ventilation	0 ºC
T_{10}^{min}	10-day running average of daily minimum temperature	°C
T_{out}	outdoor temperature	°C
T_{ref}	recommended temperature for livestock	20 ºC
u	wind speed at reference height z	m s^{-1}
u_*	friction velocity	m s^{-1}
v	kinematic viscosity	m^2 s^{-1}
v_i	root activity weighting parameter	

V_{house}	volume of animal house	m s^{-1}
V_{H_2O}	volume of water	mL m^{-2}
V_{in}	ventilation of animal house	m s^{-1}
V_{max}	maximum ventilation of animal house	0.38 m s^{-1} (pigs) or 0.4 m s^{-1} (poultry)
V_{min}	minimum ventilation of animal house	0.2 m s^{-1}
$WFPS$	water-filled pore space	
w_{irr}	irrigation	m
$W_{r,i}$	root structural dry matter components	g m^{-2}
W_{uptake}	water uptake by crops	m s^{-1}
z_0	roughness length	m
z_i	thickness of soil layer i	m
α_{root}	integrated root activity parameter for N uptake	g N m^{-2} s^{-1}
Γ	emission potential ($[NH_4^+]/[H^+]$)	
σ_{20}	reference root activity parameter at 20 °C	0.05 (20 °C)
σ_N	temperature-dependent root activity parameter	g N g^{-1} d^{-1}
ε	porosity of soil	m^3 m^{-3} or m m^{-1}
ε_{manure}	porosity of manure	m^3 m^{-3} or m m^{-1}
θ	soil volumetric water content	m^3 m^{-3} or m m^{-1}
θ_{fc}	field capacity	m^3 m^{-3} or m m^{-1}

θ_{irr}	soil water content of irrigated croplands	$m^3\ m^{-3}$ or $m\ m^{-1}$
θ_{manure}	volumetric water content of manure	$m^3\ m^{-3}$ or $m\ m^{-1}$
θ_{rea}	reanalysis soil water content	$m^3\ m^{-3}$ or $m\ m^{-1}$
θ_{sat}	soil water content at saturation	$m^3\ m^{-3}$ or $m\ m^{-1}$
θ_{wp}	soil wilting point	$m^3\ m^{-3}$ or $m\ m^{-1}$
$\xi_{aq/gas}(\theta)$	tortuosity factors	
ρ_{air}	air density	$kg\ m^{-3}$
ρ_{faeces}	density of manure solids	$kg\ m^{-3}$
ρ_{water}	density of water	$kg\ m^{-3}$
χ	concentration of gas NH_3	$g\ m^{-3}$
χ_{atm}	concentration of atmospheric NH_3	$g\ m^{-3}$
χ_{in}	concentration of gas NH_3 in animal hosue	$g\ m^{-3}$
χ_{out}	concentration of free atmosphere NH_3 outside animal house	$g\ m^{-3}$
χ_{sfc}	concentration of gas NH_3 at the surface	$g\ m^{-3}$
$\chi(z)$	concentration of gas NH_3 at height z	$g\ m^{-3}$
$\psi_{cleaning}$	cleaning for animal house	
$\psi_{housing}$	transfer of excreta from animal house to storage unit	
ψ_{m}	stability correction function	
$\psi_{to\ land}$	stored manure used for land application	

[N]	concentration of N species	g mL^{-1}
[N(sfc)]	surface concentration of N species	g mL^{-1}
[N(soil)]	concentration of N species in soil	g mL^{-1}
[NH_3(g)]	concentration of gaseous NH_3 in soil air-filled pore space	g m^{-3}
[TAN(aq)]	concentration of aqueous TAN in soil water-filled pore space	g mL^{-1}
[TAN(s)]	concentration of exchangeable solid TAN adsorbed on soil particles	g m^{-3}
Δt	model time step	1 h
ΔT_{low}	temperature dependency for temperatures below LCT	0.5 ºC $ºC^{-1}$
Δz_{manure}	thickness of manure layer	m
Δz_{soil}	transport distance in soils	m
$\Delta\theta$	incremental change in soil moisture	m^3 m^{-3} or m m^{-1}
$\sum_{\text{NH}_3} v_i$	atomic diffusion volumes for NH_3	14.9
$\sum_{\text{air}} v_i$	atomic diffusion volumes for air	20.1

Appendix A Simulated processes in AMCLIM

A1 Hydrolysis of urea/uric acid and mineralization of organic nitrogen

A general term, K_N (s^{-1}) is used in Equation 2.7 for expressing the conversion rates of multiple nitrogen forms to TAN, e.g., urea, UA and organic nitrogen. These processes are strongly dependent on the environmental factors, such as temperature, RH, water content and the pH of soils or manure. The hydrolysis rate of urea (K_{Urea}, s^{-1}) is parameterized as follows by assuming a first order reaction according to (Sherlock and Goh, 1984):

$$\frac{\mathrm{d}M_{\mathrm{Urea}}}{\mathrm{d}t} = -K_{\mathrm{Urea}} M_{\mathrm{Urea}}, \tag{A.1}$$

$$K_{\mathrm{Urea}} = 1 - \exp\left(-k_h \cdot WFPS \cdot A_h\right), \tag{A.2}$$

$$A_h = 0.25 \exp(0.0693\,(T - 273.15)), \tag{A.3}$$

where k_h is the urea hydrolysis constant for urine (6.4×10^{-5} s^{-1} or 0.23 h^{-1}; Sherlock and Goh, (1984)) and for urea in soils (8.3×10^{-6} s^{-1} or 0.03 h^{-1}; Dutta et al. (2016)). Real urine from animals is found to have a faster decomposition rate than chemical urea fertilizer

(Sherlock and Goh, 1985; Haynes and Williams, 1993). *WFPS* is the water-filled pore space and is set to 1 for livestock urine. A_h is a temperature correction dependence, and T is the temperature in Kelvin (K).

The hydrolysis rate of uric acid (K_{UA}, s^{-1}) is calculated from the product of a series of conversion rate functions (Elliott and Collins, 1982), as follows:

$$K_{\mathrm{UA}} = 0.2 k_{pH} k_T k_{RH}, \tag{A.4}$$

where k_{pH}, k_T and k_{RH} are the functions of pH, temperature and RH influencing uric acid hydrolysis rate, respectively. The maximum estimated hydrolysis rate of uric acid is 0.2 d^{-1}. The temperature (in °C), RH and pH dependence of UA hydrolysis rate is shown by the following equations:

$$k_T = \frac{exp^{(0.149(T-273.15)+0.49)}}{exp^{(0.149(35)+0.49)}} \tag{A.5}$$

The temperature dependence follows an exponential relationship and is normalised to the maximum rate at 35 °C (Jiang et al., 2021).

$$k_{RH} = 0.0124\, RH - 0.0014 \tag{A.6}$$

The RH dependence increases linearly as RH increases, reaching the maximum rate of 1 at RH 80 % (Jiang et al., 2021). Note that the humidity level can be a key limiting factor in determining the rate of uric acid hydrolysis and subsequent TAN emissions.

$$k_{pH} = \frac{1.34(\mathrm{pH})-7.2}{1.34\,(9)-7.2} \tag{A.7}$$

A fixed pH of 8.5 is the typical value of poultry manure (Elliott and Collins, 1982; Sommer and Hutchings, 2001).

Organic N is categorised into three types: a) available organic nitrogen, b) resistant organic nitrogen and c) unavailable organic nitrogen, referring to how readily that the organic nitrogen is available to decompose to form TAN (Riddick et al., 2016). A fraction of 50 % organic nitrogen is assumed to be available organic nitrogen, 45 % is in the resistant form, and the rest of 5 % goes to the unavailable nitrogen pool (Riddick et al., 2016). The rate of mineralization of organic nitrogen is determined by the following equation:

$$K_{\mathrm{OrgN}} = B_{a,r} A_m, \tag{A.8}$$

$$A_m = t_{r1} \exp\big(t_{r2}(T - 273.15)\big), \tag{A.9}$$

where $B_{a,r}$ (B_a = 8.94×10^{-7} s^{-1}; B_r = 6.38×10^{-8} s^{-1}) are the mineralization constants for available and resistant organic N (Vigil and Kissel, 1995; Gilmour et al., 2003). A_m is a temperature correction dependence, with t_{r1} and t_{r2} are equivalent to 0.0106 K^{-1} and 0.12979 K^{-1}, respectively.

A2 Budgets of TAN and other nitrogen species in soil layers for simulating chemical fertilizer applications

The budget of TAN in each soil layer ($M_{\mathrm{TAN,\,L}}$, g N m^{-2}, given in per unit area; all masses have units of g m^{-2} if not specifically explained) varies as processes can be different. For the top soil layer (0-2 cm), the time-dependent TAN pool is expressed as:

$$\frac{\mathrm{d}M_{\mathrm{TAN,L1}}}{\mathrm{d}t} = I_{\mathrm{TAN}} + F_{\mathrm{TAN}} - F_{\mathrm{NH_3}} - F_{\mathrm{N\ runoff}} - F_{\mathrm{diffusion}} - F_{\mathrm{drainage}} - F_{\mathrm{nitrif}} \quad \text{(A.10)}$$

For soil layer 2 and 3:

$$\frac{\mathrm{d}M_{\mathrm{TAN,L2,3}}}{\mathrm{d}t} = I_{\mathrm{TAN}} + F_{\mathrm{TAN}} - F_{\mathrm{diffusion}} - F_{\mathrm{drainage\ or\ leaching}} - F_{\mathrm{nitrif}} - F_{\mathrm{uptake}} \quad \text{(A.11)}$$

The bottom soil layer acts as a boundary layer of the deeper soils where dissolved nitrogen is lost from the soil column through leaching and diffusion, where the pools and concentrations of nitrogen species are set to 0. The bottom soil layer has a thickness of 14 cm in order to define the transport distance for diffusive fluxes and also to be consistent with the layering of the reanalysis soil data used in the model.

AMCLIM also simulates urea and nitrate in soils. In the top soil layer, the time-dependent urea and nitrate pools are expresses as:

$$\frac{\mathrm{d}M_{\mathrm{urea,L1}}}{\mathrm{d}t} = I_{\mathrm{urea}} - K_{\mathrm{Urea}}M_{\mathrm{Urea}} - F_{\mathrm{urea\ runoff}} - F_{\mathrm{diffusion}} - F_{\mathrm{drainage}}, \quad \text{(A.12)}$$

$$\frac{\mathrm{d}M_{\mathrm{nitrate,L1}}}{\mathrm{d}t} = F_{\mathrm{nitrif}} - F_{\mathrm{nitrate\ runoff}} - F_{\mathrm{diffusion}} - F_{\mathrm{drainage}}. \quad \text{(A.13)}$$

For soil layer 2 and 3:

$$\frac{\mathrm{d}M_{\mathrm{urea,L2,3}}}{\mathrm{d}t} = I_{\mathrm{urea}} - K_{\mathrm{Urea}}M_{\mathrm{Urea}} - F_{\mathrm{diffusion}} - F_{\mathrm{drainage}}, \quad \text{(A.14)}$$

$$\frac{\mathrm{d}M_{\mathrm{nitrate,L2,3}}}{\mathrm{d}t} = F_{\mathrm{nitrif}} - F_{\mathrm{diffusion}} - F_{\mathrm{drainage}} - F_{\mathrm{uptake}}. \quad \text{(A.15)}$$

The fluxes have been explained in Sections 2.3 and 3.2.1 (I_{TAN} – direct input of TAN species, such as ammonium or ammonia; I_{TAN} – direct input of urea from fertilizer; F_{TAN} – TAN production through urea or UA hydrolysis and decomposition of organic N; $F_{\mathrm{NH_3}}$ – flux of NH_3 volatilization; $F_{\mathrm{TAN/urea/nitrate\ runoff}}$ – flux of surface TAN, urea or nitrate runoff; $F_{\mathrm{diffusion}}$ – diffusive fluxes; F_{drainage} – flux of drainage; F_{leaching} – flux of leaching; F_{nitrif} – nitrification; F_{uptake} – flux of N uptake by plants/crops; all N fluxes/flows have units of g N m^{-2} s^{-1} if not specifically explained).

A3 Adsorption coefficient of NH_4^+ on solid particles (soils and manure)

Soils can adsorb NH_4^+ due to cation exchange, and the adsorption of NH_4^+ on soil solids varies between different soils (Buss et al., 2004). The cation exchange capacity of soils is difficult to simulate especially on a global scale. Therefore, the partitioning coefficient K_{d} used to determine the NH_4^+ adsorption is derived from an empirical relationship depending

on the fractional soil clay content (f_{clay}) to which the soil cation exchange capacity is related (Dutta et al., 2016). The equation is expressed as:

$$K_d = 0.5\left(7.2733{f_{clay}}^3 - 11.22{f_{clay}}^2\right) + 5.7198f_{clay} + 0.0263. \quad \text{(A.16)}$$

For NH_4^+ adsorbed on manure solids, there is lack of knowledge on the K_d, so it is set to 1.0.

A4 Nitrification process

Nitrification is considered to take place in soils and solid manure systems exposed to oxygen. In contrast, for liquid systems, such as slurry system or lagoon, nitrification is considered to be absent or negligible due to the high water content that reduce the oxygen availability. In the model, nitrification is included for calculating the TAN pool in solid phase manure management simulations.

A first-order reaction is used to determine nitrification as shown in Equation 2.8. The optimum nitrification rate ($K_{Knitrif,opt}$) is set to be 10 % per day, and the nitrification rate K_{nitrif} is affected by temperature, water content, and pH as shown in Equation 3.6 (Parton et al., 1996a, 2001a). The dependence of each factor is expressed by the following equations. The temperature dependence is taken from Stange and Neue, (2009):

$$k_{nitirif,T} = \left(\frac{t_{max} - T_{gnd}}{t_{max} - t_{opt}}\right)^{a_\Sigma} \exp\left(a_\Sigma\left(\left(\frac{t_{max} - T_{gnd}}{t_{max} - t_{opt}}\right)\right)\right), \quad \text{(A.17)}$$

where T_{gnd} is the ground temperature. The maximum temperature (t_{max}) and optimum temperature (t_{opt}) for microbial activity is 313 K and 301 K, respectively. a_{Σ} is an empirical factor that equals to 2.4 for manure; optimum temperature is 303 K and a_{Σ} is 1.8 for synthetic fertilizer (Stange and Neue, 2009).

The water content and pH dependence are taken from the empirical function of Patron et al. (1996)

$$k_{\text{nitrif,WFPS}} = \left(\frac{WFPS-b}{a-b}\right)^{d\cdot\left(\frac{b-a}{a-c}\right)}\left(\frac{WFPS-c}{a-c}\right)^{d}, \quad \text{(A.18)}$$

where *WFPS* is the water-filled porosity of soil and is set to 1.0 for solid manure storage. Coefficients a, b, c and d equal to 0.60, 1.27, 0.0012 and 2.84, respectively (Parton et al., 1996a).

$$k_{\text{nitrif,pH}} = 0.56 + \frac{\tan^{-1}(0.45\pi(\text{pH}-5))}{\pi}. \quad \text{(A.19)}$$

Nitrification is found to taking place in soils at pH ranging between 5.5 to 10, with the optimum pH is around 8.5 (Parton et al., 1996a), and the processes ceases in soils under natural pH less than 5.0 (Parton et al., 1996a). In AMCLIM-Land, the pH dependence for nitrification rate is a trigonometric function from Patron et al. (1996).

A5 Nitrogen and water uptake by crops

Nitrogen uptake by plants in AMCLIM-Land is assumed to take place in soil layers 2 and 3 and is not counted in the top soil layer, which can be calculated by Equation 3.7. Crops can uptake both ammonium and nitrate from the soils, together termed as M_{Neff}, as expressed by the follows:

$$M_{\mathrm{Neff}} = M_{\mathrm{NH_4^+}} + a_{\mathrm{plant}} M_{\mathrm{NO_3^-}}, \tag{A.20}$$

where $M_{\mathrm{NH_4^+}}$ and $M_{\mathrm{NO_3^-}}$ are ammonium and nitrate pools in soils. A dimensionless parameter a_{plant} vary between 0.5 to 1.0 depending upon temperature is calculated by the following equation:

$$a_{\mathrm{plant}} = a_{20} - (a_{20} - a_{10}) \frac{(20 - T_{\mathrm{gnd}})}{(20 - 10)}, \tag{A.21}$$

where a_{20} and a_{10} are reference values at 20 and 10 °C, respectively. However, this equation is only applicable between 10 and 20 °C so is extrapolated to a broader temperature range as the following equation:

$$a_{\mathrm{plant}} = 0.25 e^{0.0693 T_{\mathrm{gnd}}}. \tag{A.22}$$

The integrated root activity parameter α_{root} is determined by the following equation:

$$\alpha_{\mathrm{root}} = \sigma_{\mathrm{N}} \sum_{i=1}^{4} v_i W_{r,i}, \tag{A.23}$$

where $W_{r,i}$ (g m^{-2}) is the root structural dry matter components, v_i is the corresponding root activity weighting parameter. σ_N (g N g^{-1} d^{-1}) is the temperature-dependent root activity parameter, which is calculated by the following equation:

$$\sigma_N = \sigma_{20} f_T, \tag{A.24}$$

σ_{20} is a reference value that equals 0.05 at 20 °C, and the temperature dependence (f_T) is identical as Equation A.22.

The combined response factor $J_{C,N}$ for substrate carbon and nitrogen is calculated by the following equation:

$$J_{C,N} = 1 + \frac{K_{CUN}}{C}\left(1 + \frac{N}{J_{NUN}}\right), \tag{A.25}$$

where K_{CUN} (0.05[C]) and J_{NUN} (0.005[N]) are constants. C (g C m^{-2}) and N (g N m^{-2}) are substrate concentration of carbon and nitrogen, respectively. As the model does not simulate plant dynamics, C and N are represented by fixed values of 40 and 4, respectively (Riedo et al., 1998). Another root activity parameter K_{Neff} is a constant of 5 g N m^{-2}.

Combining these terms, plant uptake of N (F_{uptake}) can be expressed as (Riedo et al., 1998; Thornley, 1991; Thornley and Cannell, 1992b):

$$F_{uptake} = \sigma_N \sum_{i=1}^{4} v_i W_{r,i} \frac{M_{NH_4^+} + a_{plant,nit} M_{NO_3^-}}{M_{NH_4^+} + a_{plant,nit} M_{NO_3^-} + K_{Neff}} \frac{1}{1 + \frac{K_C}{C}\left(1 + \frac{N}{K_N}\right)}. \tag{A.26}$$

There are four components in $W_{r,i}$ that represents structural dry matter of root at different stage (i.e., young and mature roots). Mature roots have larger $W_{r,i}$ values. The root activity

weighting parameter v_i changes as plant grows, i.e., larger values refer to more mature roots of the plant. AMCLIM-Land uses a set of empirical values to represent v_i, which describes the status of roots at six growing stages (Table A1). The six growing stages are evenly distributed during the growing season of a crop.

Table A1. Root activity weighting parameters at different crop growing stage.

	Stage 1	Stage 2	Stage 3	Stage 4	Stage 5	Stage 6
v_1	0.1	1.0	1.0	0.5	0.25	0.1
v_2	0.1	0.5	1.0	1.0	0.5	0.25
v_3	0.1	0.25	0.5	1.0	1.0	1.0
v_4	0.1	0.1	0.25	0.5	1.0	1.0

The water uptake by crops is represented by a simple empirical equation that is related to the soil water content (Dardanelli et al., 2004), which is expressed as follows:

$$W_{\text{uptake}} = K_{\text{uptake}}(\theta - \theta_{\text{wp}}), \tag{A.27}$$

where K_{uptake} is an empirical coefficient that equals to 0.096 d^{-1} (Dardanelli et al., 2004).

A6 Calculation of atmospheric resistances

Atmospheric resistances consist of aerodynamic (R_a) and boundary layer resistance (R_b). The value of R_a, which is dependent on the stability of air, is calculated from (Seinfeld and Pandis, 2016):

$$R_a = \frac{\left[ln\left(\frac{z}{z_0}\right) - \psi_m\left(\frac{z}{L}\right)\right]^2}{k^2 u}, \quad \text{(A.28)}$$

where u (m s^{-1}) is the wind speed measured at z (m) height above ground, z_0 (m) is the roughness length, L (m) is the Monin-Obukhov length, ψ_m is a stability correction function, and k is the von Karman constant of 0.41. The stability correction function is calculated for stable and unstable atmospheric conditions:

Stable conditions:

$$\psi_m\left(\frac{z}{L}\right) = -\frac{5z}{L}. \quad \text{(A.29)}$$

Unstable conditions:

$$\psi_m\left(\frac{z}{L}\right) = ln\left(\frac{1+X}{2}\right)^2 + ln\left(\frac{1+X^2}{2}\right) - 2tan^{-1}(X) + \frac{\pi}{2}, \quad \text{(A.30)}$$

$$X = \left(1 - 16\frac{z}{L}\right)^{\frac{1}{4}}. \quad \text{(A.31)}$$

The Monin-Obukhov length L is parameterized from:

$$L = \frac{T{u_*}^3 \rho_{\text{air}} c_p}{kgH}, \quad \text{(A.32)}$$

where T (K) is the air temperature at a reference height above ground, u_* (m s^{-1}) is the friction velocity with z_0 roughness height, ρ_{air} (kg m^{-3}) is air density, c_p (J kg^{-1} K^{-1}) is the specific heat capacity of dry air, and g (9.81; m s^{-2}) is the acceleration of gravity, and H is the sensible heat flux (J m^{-2} s^{-1}). The friction velocity is calculated from:

$$u_* = \frac{ku}{ln\left(\frac{z}{z_0}\right) - \psi_m\left(\frac{z}{L}\right)}. \quad \text{(A.33)}$$

The value of R_b depends on diffusivity through the quasi-laminar sub-layer, where the entrained transfer is described by the boundary layer Stanton number (B) and is approximately equal to 5 (Nemitz et al., 2000; Riddick et al., 2017):

$$R_b = (Bu_*)^{-1}. \quad \text{(A.34)}$$

A7 Calculation of soil resistances and manure resistances

The aqueous and gaseous diffusion of nitrogen species in soils are constrained by soil resistances, as shown in Equation 2.9. The soil resistance is determined by the following equation:

$$R_{\text{soil,aq/gas}} = \frac{\Delta z_{\text{soil}}}{\xi_{\text{aq/gas}}(\theta) D_{\text{NH}_4/\text{NH}_3}^{\text{aq/gas}}}, \quad \text{(A.35)}$$

where Δz_{soil} (m) is the transport distance in soils, which is the distance between the mid-points of each soil layer. The molecular diffusivity ($D^{\text{aq/gas}}_{\text{NH}_4/\text{NH}_3}$, $m^2\ s^{-1}$) is multiplied by the tortuosity factor, $\xi_{\text{aq/gas}}(\theta)$, to adjust for the soil water content as well as the porosity (Millington and Quirk, 1961; Móring et al., 2016; Vira et al., 2019). The molecular diffusivity and tortuosity factor are calculated by the following equations:

$$D^{\text{aq/gas}}_{\text{NH}_4/\text{NH}_3} = \begin{cases} 9.8 \times 10^{-10} \cdot 1.03^{T-273.15}, & \text{for } \text{NH}_4^+ \\ \frac{10^{-7} \cdot T^{1.75} (1/m_{\text{air}} + 1/m_{\text{NH}_3})^{0.5}}{p[(\sum_{\text{air}} v_i)^{1/3} + (\sum_{\text{NH}_3} v_i)^{1/3}]^2}, & \text{for } \text{NH}_3 \end{cases}, \quad \text{(A.36)}$$

where m_{air} and m_{NH_3} are molecular weight of air and NH_3, respectively. $\sum_{\text{air}} v_i$ (20.1) and $\sum_{\text{NH}_3} v_i$ (14.9) are atomic diffusion volumes for air and NH_3 (Perry and Green, 2008), and p is pressure in the atmosphere.

$$\xi_{\text{aq/gas}}(\theta) = \begin{cases} \frac{(\theta - \theta_{\text{sat}})^{\frac{8.5}{3}}}{\theta_{\text{sat}}^{1.7}}, & \text{for gaseous diffusion} \\ \frac{\theta^{\frac{8.5}{3}}}{\theta_{\text{sat}}^{1.7}}, & \text{for aqueous diffusion} \end{cases}, \quad \text{(A.37)}$$

where θ_{sat} is soil water content at saturation. The tortuosity factors are calibrated by site simulations using AMCLIM under GRAMINAE's conditions.

Manure is considered to be similar to soils, and the manure resistances ($R_{\text{manure,aq/gas}}$) for determining the NH_3 emission from solid manure are calculated by the same method, as expressed by follows:

$$R_{\text{manure,aq/gas}} = \frac{\Delta z_{\text{manure}}}{\xi_{\text{aq/gas}}(\theta) D^{\text{aq/gas}}_{\text{NH}_4/\text{NH}_3}}. \quad \text{(A.38)}$$

The thickness of the manure layer (Δz_{manure}) is approximated by

$$\Delta z_{\text{manure}} = \frac{M_{\text{faeces}}}{BD_{\text{manure}}}, \quad \text{(A.39)}$$

where M_{faeces} is the faeces pool, and BD_{manure} (g cm^{-3}) is the bulk density of manure which is derived from the density of manure solids (ρ_{faeces}, g cm^{-3}) and manure porosity ($\varepsilon_{\text{manure}}$) (Khater, 2015).

$$BD_{\text{manure}} = \rho_{\text{faeces}}(1 - \varepsilon_{\text{manure}}). \quad \text{(A.40)}$$

The density of manure solids is 1.46 g cm^{-3}. The manure porosity used for calculating manure bulk density and the tortuosity corrections is set to be 0.42 for all livestock (Khater, 2015). The volumetric water content of manure (θ_{manure}) is calculated by the following equations:

$$\theta_{\text{manure}} = \min\left(\varepsilon_{\text{manure}}, \frac{M_{\text{water}} BD_{\text{manure}}}{\rho_{\text{water}} M_{\text{faeces}}}\right). \quad \text{(A.41)}$$

It should be noted that the equations above for manure resistance calculations are under the assumption that the characteristic of manure is similar to soils.

A8 Concentrations of nitrogen species at surface

Volatilization and runoff take place at the land surface, which is primarily driven by the concentrations at the surface. To take into account the soil resistance and heterogeneity of the soil, the surface concentrations of nitrogen species are not calculated from dividing the mass by the volume (or the thickness over unit areas), but are solved by assuming that the upward diffusion (from the mid-point of the top soil layer to the surface) is equal to the volatilization and runoff, as expressed by Equation 3.9 and illustrated by Figure A1. Therefore, Equation 3.9 can be expanded as:

$$\frac{[\mathrm{NH_3(g)}]_{\mathrm{srf}}-\chi_{\mathrm{atm}}}{R_{\mathrm{atm}}}+q_r\cdot[\mathrm{TAN(aq)}]_{\mathrm{srf}}=\frac{[\mathrm{TAN(aq)}]_{\mathrm{L1}}-[\mathrm{TAN(aq)}]_{\mathrm{srf}}}{R_{\mathrm{L1,aq}}}+\frac{[\mathrm{NH_3(g)}]_{\mathrm{L1}}-[\mathrm{NH_3(g)}]_{\mathrm{srf}}}{R_{\mathrm{L1,gas}}}, \tag{A.42}$$

the aqueous concentration of TAN at the surface can be solved as:

$$[\mathrm{TAN(aq)}]_{\mathrm{srf}}=\frac{[\mathrm{TAN(aq)}]_{\mathrm{L1}}\cdot\left(\frac{1}{R_{\mathrm{L1,aq}}}+\frac{K_{\mathrm{NH_3}}}{R_{\mathrm{L1,gas}}}\right)+\frac{\chi_{\mathrm{atm}}}{R_{\mathrm{atm}}}}{q_{\mathrm{r}}+\frac{1}{R_{\mathrm{L1,aq}}}+K_{\mathrm{NH_3}}\cdot\left(\frac{1}{R_{\mathrm{L1,gas}}}+\frac{1}{R_{\mathrm{atm}}}\right)}, \tag{A.43}$$

and gaseous NH_3 concentration at the surface can be solved subsequently (combined with Equation 3.3).

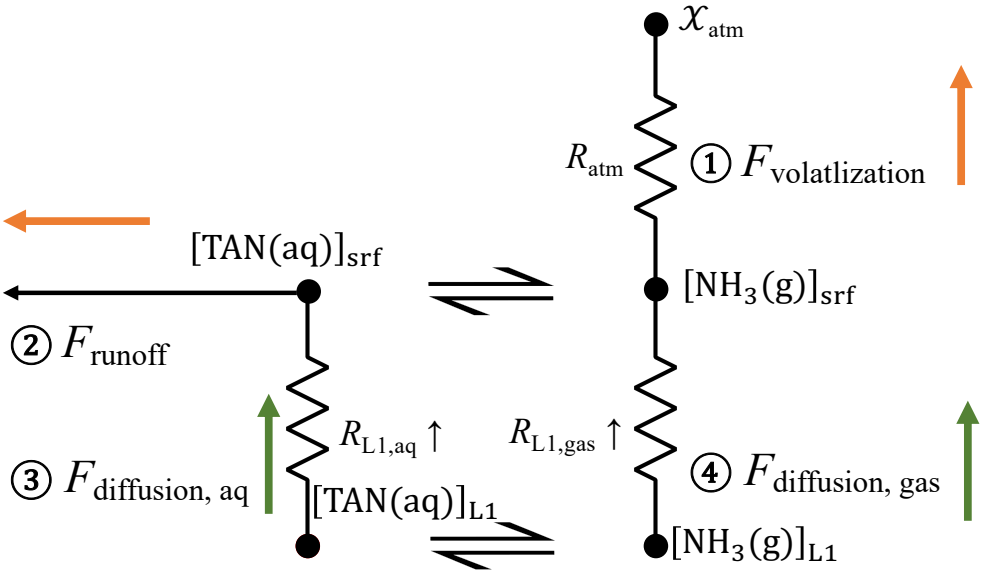

Figure A1. Sketch of the physical transport for nitrogen species (TAN as an example) in the top soil layer in AMCLIM-Land. Upward diffusions including aqueous and gaseous diffusive flux are equivalent to the surface runoff and volatilization to satisfy mass conservation (process 1+2 = 3+4; the sum of the fluxes represented by orange arrows = the sum of the fluxes represented green arrows).

For simulating NH_3 emissions from solid manure storage, the processes are similar to the land simulations. TAN is assumed to be evenly distributed in the stored manure, so the TAN concentration represents the concentration of the bulk manure ($[TAN(aq)]_{bulk}$). TAN is transferred from the manure to a source layer at the surface through diffusions. The diffusion is in aqueous phase considering the water content and is constrained by manure

resistance. Manure resistance is determined by dividing the thickness of the surface layer which has a maximum thickness of 2 cm by the aqueous diffusivity of NH_4^+. The upward diffusive fluxes are equal to the volatilization flux (as there is no runoff for housing and storage). Therefore, the TAN concentration at the manure surface can be solved by the following equation:

$$[\mathrm{TAN(aq)}]_{\mathrm{srf}} = [\mathrm{TAN(aq)}]_{\mathrm{bulk}} \cdot \frac{\left(\frac{1}{R_{\mathrm{manure,aq}}}\right)+\frac{\chi_{\mathrm{in}}}{R_{\mathrm{store}}}}{\frac{1}{R_{\mathrm{manure,aq}}}+\frac{K_{\mathrm{NH_3}}}{R_{\mathrm{store}}}}. \quad \text{(A.44)}$$

A9 Water drainage and percolation flux

Leaching of nitrogen from the soils is determined by multiplying the aqueous concentrations by the percolation flux of water. The percolation flux of water is the minimum value between the soil hydraulic conductivity and the drainage potential as shown in Equation 3.10.

The soil hydraulic conductivity (K_s) is related to the soil water content and the soil characteristics, which is calculated by the following equation (Li et al., 2019):

$$K_{\mathrm{s}} = \frac{\theta}{\theta_{\mathrm{sat}}} K_{\mathrm{sat}}, \quad \text{(A.45)}$$

$$K_{\mathrm{sat}} = 2.2 \times 10^{-7} e^{x}, \quad \text{(A.46)}$$

$$x = 7.755 + 0.0352f_{\text{silt}} - 0.967BD_{\text{soil}}{}^2 - 0.000484f_{\text{clay}}{}^2 - 0.000322f_{\text{silt}}{}^2 + \frac{0.001}{f_{\text{silt}}} - \frac{0.748}{f_{\text{som}}} - 0.643\log_e f_{\text{silt}} - 0.01398BD_{\text{soil}} \cdot f_{\text{silt}} - 0.1673BD_{\text{soil}} \cdot f_{\text{som}}, \quad \text{(A.47)}$$

where K_{sat} (m s^{-1}) is the soil hydraulic conductivity at saturation, which is dependent on the fractional soil silt (f_{silt}) and clay content (f_{clay}), bulk density of soil (BD_{soil}, g cm^{-3}) and fractional soil organic matter content (f_{som}).

The drainage potential of a soil layer is calculated by the following equation:

$$D_{\text{pot}} = \max(0, \frac{\theta - \theta_{\text{fc}}}{zt_{\text{fc}}}), \quad \text{(A.48)}$$

where t_{fc} is a reference time that soil water content reaches field capacity, which is 24 h. The field capacity of soil is determined from the bulk density (BD) (Li et al., 2019), as expressed by the following equation:

$$\theta_{\text{fc}} = 0.45 - 0.06BD_{\text{soil}}{}^2. \quad \text{(A.49)}$$

A10 Two-film model for the gas exchange across the air-liquid interface

The two-film model proposed by Liss and Slater (Liss and Slater, 1974) for estimating the gaseous flux across the air-liquid interface is used to model the NH_3 emissions from pit storage in animal houses and lagoon systems in the AMCLIM model because these systems

hold large amount of water (as mentioned in Sections 4.2.2 and 4.2.3). Figure A.2 illustrates the flux of NH_3 is transferred from the liquid to the air across the interface. The main body of the liquid is assumed to be well-mixed, so the main resistances are from the gas and liquid phase interfacial layers (gas and liquid "films"). There are two transport processes. The first process is TAN from the bulk liquid to the interface ($F_{\text{TAN to surface}}$) through molecular transfer that is driven by concentration gradients, which can be expressed as:

$$F_{\text{TAN to surface}} = k_{\text{L}}([\text{TAN (aq)}]_{\text{bulk liquid}} - [\text{TAN (aq)}]_{\text{interface}}), \quad \text{(A.50)}$$

where k_{L} (m s^{-1}) is an aqueous transfer coefficient for TAN (NH_3 and NH_4^+). The second process is NH_3 transported from the interface to the atmosphere (house atmosphere for housing simulations and free atmosphere for lagoon simulations), which can be expressed as:

$$F_{\text{NH}_3} = k_{\text{G}}([\text{NH}_3(\text{g})]_{\text{interface}} - [\text{NH}_3(\text{g})]_{\text{in/atm}}), \quad \text{(A.51)}$$

where k_{G} (m s^{-1}) is a gaseous transfer coefficient for NH_3. The aqueous TAN concentration and the gaseous NH_3 concentration at the interface is in equilibrium as shown in Equation 3.3, and it is assumed that the transfer of NH_3 across the interface is in a steady state so that the two transport processes in aqueous and gaseous phase are equivalent.

$$k_{\text{L}}\left([\text{TAN (aq)}]_{\text{bulk liquid}} - [\text{TAN (aq)}]_{\text{interface}}\right) = k_{\text{G}}([\text{NH}_3(\text{g})]_{\text{interface}} - [\text{NH}_3(\text{g})]_{\text{in/atm}}). \quad \text{(A.52)}$$

In AMCLIM, the calculations of NH_3 emissions and other transport processes such as diffusion use resistances, some of which are the reciprocals of the transfer coefficients as

shown in Equation 4.3. In addition, as NH_3 emissions take place from wet surfaces, the gaseous NH_3 concentration at the interface in the two-film model is represented by χ_{srf} in AMCLIM. By combining Equations A.49 to A.51, the NH_3 emission can be calculated by simulating the TAN concentration of the bulk liquid using the following equation (under the simplification that atmospheric indoor NH_3 concentration are 0; as expressed by Equation 4.23):

$$F_{\mathrm{NH_3}} = \frac{\chi_{\mathrm{srf}}}{R_{\mathrm{G}}} = \frac{[\mathrm{TAN\ (aq)}]}{R_{\mathrm{GL}}}, \tag{A.53}$$

where R_{GL} is a combined resistance that limits the NH_3 transfer across the gas-liquid interface, which is expressed as:

$$R_{\mathrm{GL}} = \frac{1}{k_{\mathrm{L}}} + \frac{1}{k_{\mathrm{G}} K_{\mathrm{NH_3}}}. \tag{A.54}$$

The aqueous and gaseous transfer coefficients are empirically derived (Ni, 1999), which are calculated by the following equations:

$$k_{\mathrm{L}} = 1.417 \times 10^{-12} T^4, \tag{A.55}$$

$$k_{\mathrm{G}} = 0.001 + 0.0462 u_* Sc^{0.67}, \tag{A.56}$$

where *Sc* is the Schmidt number which is calculated from the kinematic viscosity (v, $m^2\ s^{-1}$) and diffusivity of NH_3 as follows:

$$Sc = \frac{v}{D_{\mathrm{NH_3}}^{\mathrm{gas}}}, \tag{A.57}$$

$$v = 1.56 \times 10^{-5}(\frac{T+273.15}{298.15})^{\frac{3}{2}}. \quad \text{(A.58)}$$

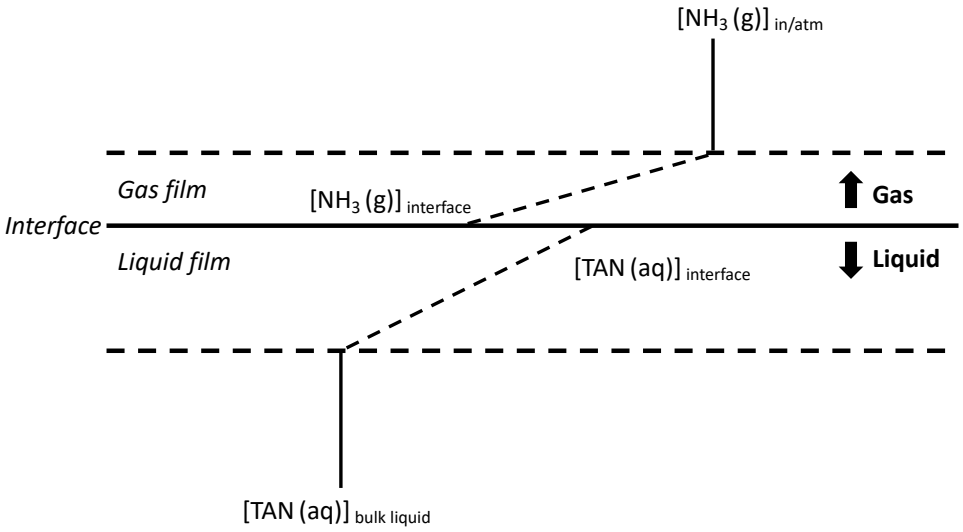

Figure A2. Sketch of the ammonia transfer processes across an air-liquid interface (adapted from Liss and Slater (1994)). In AMCLIM, $[NH3(g)]_{interface}$ in the figure is represented by χ_{srf}, and $[NH3(g)]_{in/atm}$ is represented by χ_{in} or χ_{atm}.

A11 Evaporation in animal houses

The evaporation rate in the animal houses is approximated by applying an aerodynamic method using a vapor transfer coefficient (B_{vap}, m Pa^{-1} s^{-1}) and vapor pressure deficit as follows (Chow et al., 1988):

$$F_{evap} = B_{vap}(e_s - e_a), \quad \text{(A.59)}$$

$$B_{\text{vap}} = \frac{0.622k^2\rho_{\text{air}}u}{\rho_{\text{water}}p[\ln(\frac{z}{z_0})]^2}, \quad \text{(A.60)}$$

where e_s is the saturation vapor pressure, and e_a is the actual vapor pressure at present state. ρ_{water} is the density of water, respectively. The wind speed u (m s^{-1}) is calculated from the housing ventilation at an assumed reference height of z that equals 2 m, with roughness height z_0 is assumed to be 2×10^{-3} m (2 mm).

The moisture in poultry litter and solid manure due to evaporation cannot decline further than a threshold and will eventually reach an equilibrium state to the ambient humidity, and evaporation is assumed to stop at this point. The litter moisture content exerts a vapor pressure on the adjacent air, and the ratio of this moisture vapor pressure to the saturated vapor pressure of pure water in air at the temperature of the material is called the equilibrium relative humidity (Henderson and Perry, 1976). If the air RH is higher than the equilibrium relative humidity of the material, the material will increase in moisture content. Conversely, the material will decrease in moisture content if the air RH is lower than the equilibrium. The equilibrium moisture content is calculated by the following equation (Elliott and Collins, 1982):

$$m_E = \left[\frac{-\ln(1-\frac{RH}{100})}{0.0000534\times T}\right]^{\frac{1}{1.41}}. \quad \text{(A.61)}$$

A12 Housing environments

For the enclosed houses with heating and ventilation systems for pigs, the parameterizations of housing environments are taken from Gyldenkærne (2005), as shown in Figure A3. The indoor temperature (T_{in}, ºC) is a function of outside temperature (T_{out}, ºC), as the following:

$$T_{\text{in}} = \begin{cases} T_{\text{rec}} + \Delta T_{\text{low}} \times (T_{\text{out}} - T_{\text{min}}), \text{if } T_{\text{out}} \leq T_{\text{min}} \\ T_{\text{rec}}, \text{if } T_{\text{min}} < T_{\text{out}} \leq T_{\text{max}} \\ T_{\text{rec}} + \Delta T_{\text{high}} \times (T_{\text{out}} - T_{\text{max}}), \text{if } T_{\text{max}} < T_{\text{out}} \end{cases}, \quad \text{(A.62)}$$

where T_{rec} is the recommended temperature (20 ºC), ΔT_{low} is the temperature dependency (0.5 ºC ºC^{-1}) for temperatures below T_{min} (0 ºC), ΔT_{high} is the temperature dependence (1.0 ºC ºC^{-1}) above T_{max} (12.5 ºC).

For the enclosed poultry houses, the temperature relationships are derived from the USEPA AFO dataset as the follows (as shown in Fig A3):

$$T_{\text{in}} = \begin{cases} 2.0 \times 10^{-4} {T_{\text{out}}}^3 + 1.0 \times 10^{-3} {T_{\text{out}}}^2 + 2.4 \times 10^{-2} T_{\text{out}} + 22.1, \text{for broilers} \\ 1.4 \times 10^{-4} {T_{\text{out}}}^3 + 2.3 \times 10^{-3} {T_{\text{out}}}^2 + 1.1 \times 10^{-2} T_{\text{out}} + 23.8, \text{for layers} \end{cases}. \quad \text{(A.63)}$$

The ventilation (V_{in}, m s^{-1}) of the enclosed animal houses calculated as follows (as shown in Fig A3):

$$V_{\text{in}} = \begin{cases} V_{\text{min}}, \text{if } T_{\text{out}} \leq T_{\text{min}} \\ V_{\text{min}} + T_{\text{out}} \times \left(\frac{(V_{\text{max}} - V_{\text{min}})}{(T_{\text{max}} - T_{\text{min}})}\right), \text{if } T_{\text{min}} < T_{\text{out}} \leq T_{\text{max}}, \\ V_{\text{max}}, if\ T_{\text{max}} < T_{\text{out}} \end{cases} \quad \text{(A.64)}$$

where V_{min} is the minimum ventilation (0.2 m s^{-1}), and V_{max} is the maximum ventilation rate (0.38 m s^{-1} for pigs; 0.40 m s^{-1} for poultry). It is worth noting that the unit of ventilation is expressed in meter per second, which should be distinguished from the ventilation rate used in Equation 4.2 for conceptualising the indoor NH_3 concentration of animal houses.

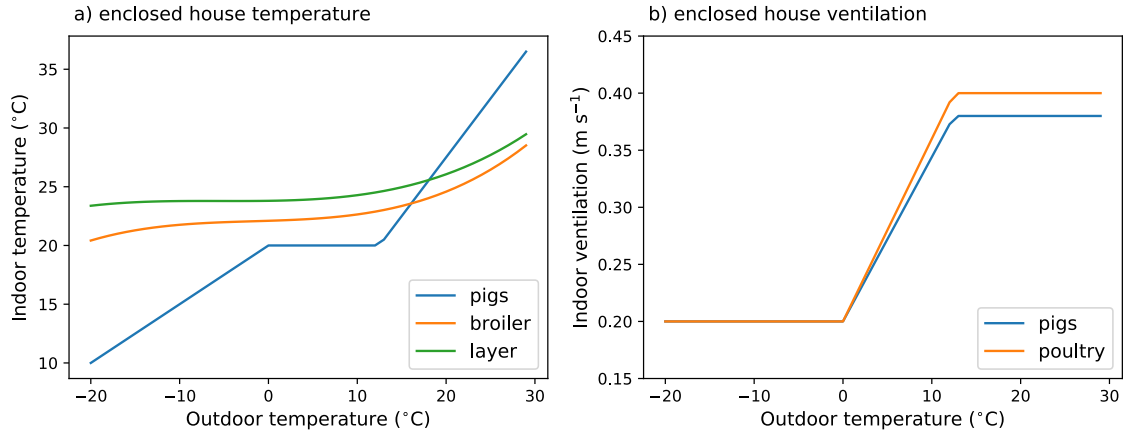

Figure A3. Modelled indoor temperature and ventilation of fully enclosed animal houses for pigs and poultry in relation to outdoor temperature.

For naturally ventilated barns where ruminants, intermediate pigs, and backyard pigs and poultry, the relationship between indoor temperature and the outdoor temperature is expressed as follows as shown in Figure A4:

$$T_{\text{in}} = T_{\text{out}} + D_{\text{temp}}, \quad \text{(A.65)}$$

$$T_{\text{floor}} = T_{\text{out}} + 0.4 \times (T_{\text{rec}} - T_{\text{out}}), \quad \text{(A.66)}$$

where D_{temp} is the temperature difference between indoor and outdoor temperature due to the warmth generated by animals (3 ºC) and T_{floor} is floor temperature.

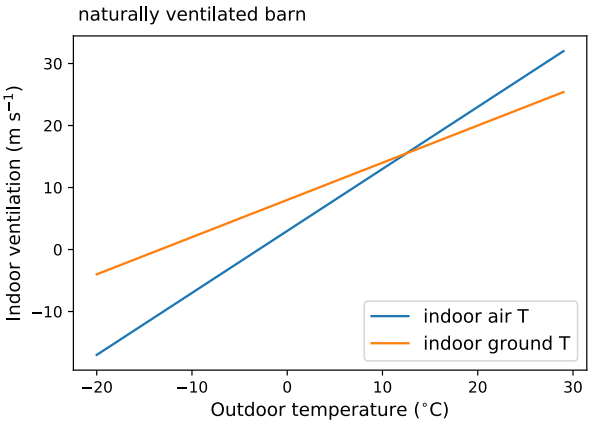

Figure A4. Modelled indoor air and ground temperature of naturally ventilated animal barns in relation to outdoor temperature.

The ventilation in the barns is related to the wind speed outside (u_{out}, m s^{-1}), which is expressed by the following equation:

$$V_{\text{in}} = \left(1 - f_{\text{blocking}}\right) u_{\text{out}}, \quad \text{(A.67)}$$

where f_{blocking} is a blocking factor due to mechanical blocking, which is larger in cold days and smaller in warm days.

$$f_{\text{blocking}} = \begin{cases} 0.2, \text{if } T_{\text{out}} > T_{\text{floor}} - D_{\text{temp}} \\ 0.8, \text{if } T_{\text{out}} \leq T_{\text{floor}} - D_{\text{temp}} \end{cases} \quad \text{(A.68)}$$

Appendix

Appendix B Supplementary information for the development and operation of AMCLIM

B1 Major crops simulated by AMCLIM-Land

The 16 major crops that are simulated by AMCLIM-Land are: 1) barley, 2) cassava, 3) cotton, 4) groundnut, 5) maize, 6) millet, 7) potato, 8) rapeseed, 9) rice, 10) rye, 11) sorghum, 12) soybean, 13) sugarbeet, 14) sunflower, 15), sugarcane and 16) wheat.

B2 Fertilizer types from IFA and disaggregation of total nitrogen rates

AMCLIM-Land uses nitrogen chemical fertilizer consumption statistics at country-level from the International Fertilizer Association. Nitrogen fertilizer types provide in the IFA dataset includes direct NH_3, ammonium phosphate (AP), ammonium sulphate (AS), ammonium nitrate (AN), calcium ammonium nitrate (CAN), NK compound fertilizer (NK), NPK compound fertilizer (NPK), nitrogen solution, other NP fertilizer (other NP), urea,

and other N straight fertilizer. It is assumed that NK compound fertilizer, NPK compound fertilizer and other NP fertilizer have equivalent amount of ammonium and nitrate. Nitrogen solution contains 75 % of ammonium and 25 % nitrate (Vira et al., 2020a). Other N straight fertilizer is treated as urea in AMCLIM-Land. The nitrogen in ammonium fertilizer, urea fertilizer and nitrate fertilizer can be calculated accordingly by the following equations:

$$Amm_{\mathrm{N}} = NH_3 + AP_{\mathrm{N}} + AS_{\mathrm{N}} + 0.5(AN_{\mathrm{N}} + CAN_{\mathrm{N}} + NK + NPK + other\ NP) + 0.75Nsolution, \quad \text{(B.1)}$$

$$Urea_{\mathrm{N}} = Urea + Other\ N\ straight, \quad \text{(B.2)}$$

$$Nit_{\mathrm{N}} = 0.5(AN_{\mathrm{N}} + CAN_{\mathrm{N}} + NK + NPK + other\ NP) + 0.25Nsolution. \quad \text{(B.3)}$$

The fraction of the major three nitrogen fertilizer groups (ammonium, urea and nitrate) is then calculated as follows:

$$f_{\mathrm{fert(j)}} = \frac{M_{\mathrm{fert(j)}}}{\sum_{\mathrm{j=1}}^{3} M_{\mathrm{fert(j)}}}. \quad \text{(B.4)}$$

The nitrogen application and fraction of three types of fertilizers in 2010 and 2018 are shown in Figure B1 and B2.

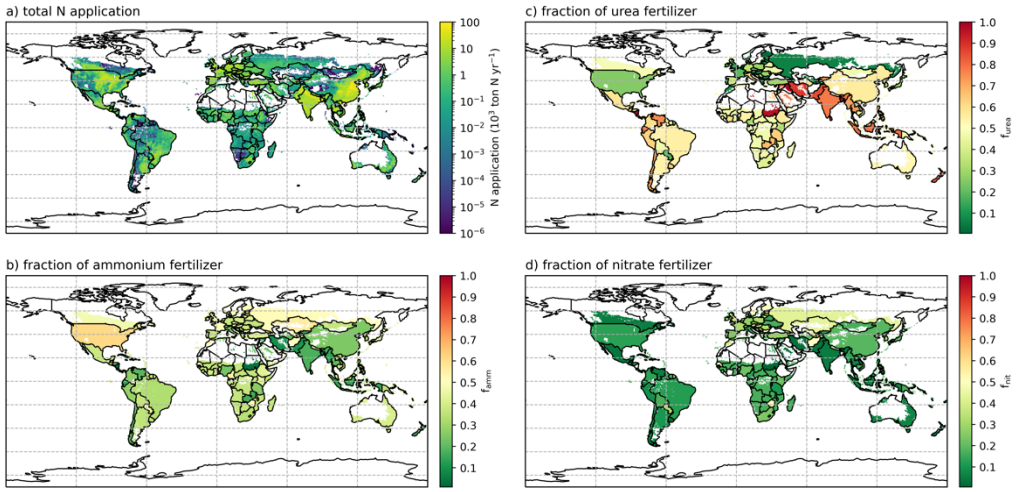

Figure B1. Fertilizer information of 2010. (a) Total nitrogen application rate. (b) Fraction of ammonium fertilizer. (c) Fraction of urea fertilizer. (d) Fraction of nitrate fertilizer.

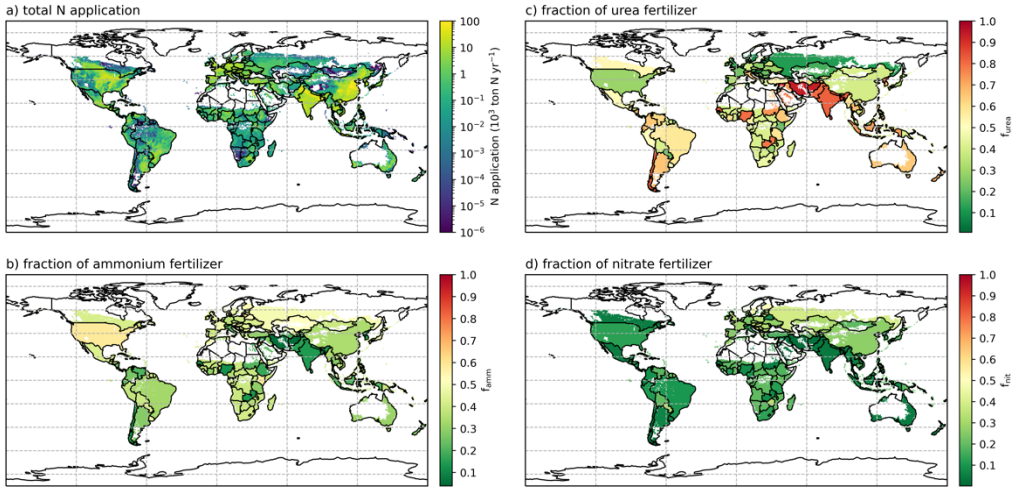

Figure B2. Same as Figure B1 but for 2018.

B3 Techniques used for chemical fertilizer application

Table B1. Fraction of techniques used for chemical fertilizer application at country-level, based on the income classification (WB, 2022).

	Broadcasting	Incorporation	Deep placement
High income	0.7	0.2	0.1
Upper middle income	0.8	0.15	0.05
Lower middle income	0.95	0.05	0
Low income	1.0	0	0

B4 Geographical regions defined in AMCLIM

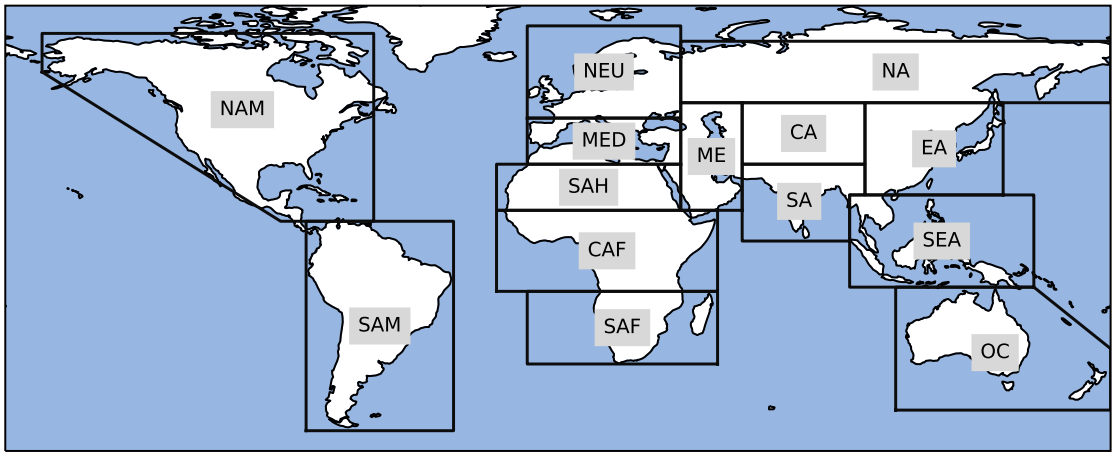

Figure B3. Geographical regions (SREX scientific region) used in AMCLIM (Seneviratne et al., 2012).

B5 Global soil pH

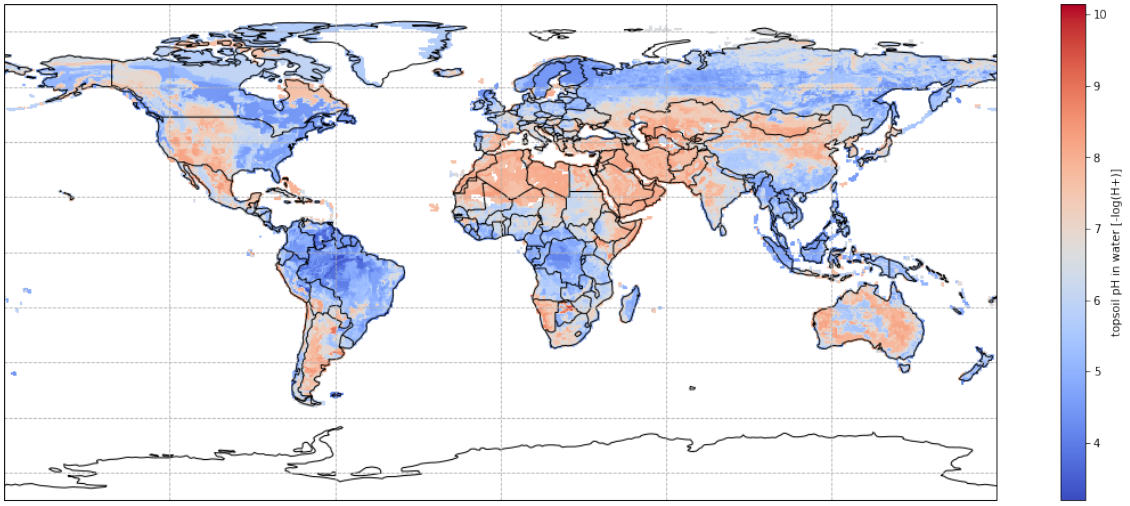

Figure B4. Global soil pH. Data from HWSD v1.2 (Wieder et al., 2014).

B6 Livestock behavioural information and excreta characteristics

Table B2. Biomaterial and characteristic information of livestock excreta (Vu et al., 2009b, a; Andersen et al., 2020; Haynes and Williams, 1993; Marsden et al., 2020; Dong et al., 2014; Waldrip et al., 2013; Nahm, 2003; Hoogendoorn et al., 2011; Choirunnisa et al., 2019; Zhao et al., 2016; Reed et al., 2015; Sommer and Hutchings, 2001; Misselbrook et al., 2016; Selbie et al., 2015).

Livestock	Urinary N : Faecal N ratio	Urinary N concentration (g N L^{-1} urine)	Faecal N content (g N kg^{-1} faeces)	Fraction of urinary N as urea	Urination (L $head^{-1}$ d^{-1}) and defecation (kg $head^{-1}$ d^{-1})	DM (g per kg excreta)	pH
Beef/Feedlot Cattle	3:2	7.2	4.85	0.75	12.0 (U) 20.9 (D)	181.5	7.8
Dairy/Other dairy	8.8:5	6.9	4.85	0.75	21.0 (U) 27.0 (D)	181.5	7.8
Sheep	2:1	8.7	6.40	0.80	2.4 (U) 1.2 (D)	155.0	8.0
Goat	1:1	12.0	6.40	0.80	2.4 (U) 1.2 (D)	155.0	8.0
Pigs	2:1	6.4	11.90	0.75	3.8 (U) 1.2 (D)	222.0	7.7
Poultry	--	--	50 (g N kg^{-1} excretion)	0.6 (excreted N as UA)	0.0 (U) 0.03 (Excretion)	574.0	8.5

UA is uric acid; U is urine; D is dung.

B7 Divisions of Manure Management Systems (MMS)

The MMS defined by the FAO GLEAM2 model and the divisions used in the AMCLIM model are summarised in Table B3 and B4, respectively. It should be noted that manure used as fuel, manure sold and thermal drying are not simulated in AMCLIM. Unmanaged manure (e.g., dumping, fishpond) are treated as nitrogen loss from the system in AMCLIM.

Table B3. Definitions of manure management systems used in GLEAM. From Uwizeye et al (2020).

Aerobic lagoon	A type of liquid uncovered manure storage with varying lengths of storage (up to a year or greater). Lagoons can both be a tank construction or an earthen basin and are characterised by natural or forced aeration.
Aerobic processing	Manure is treated through natural or forced aeration processes for oxidation of organic and nitrogenous compounds.
Burned	Manure is collected and burned, usually as (cooking) fuel.
Compost	Manure is stored and turned into compost before using it as fertilizer. Often, manure is frequently turned and mixed during composting process.
Daily spread	Manure is routinely removed from a confinement facility and applied to cropland or pasture within 24 hours of excretion.
Deep litter	An in-house system where, as manure accumulates in the stable, bedding material is continuously added to absorb moisture over a production cycle of 6 to 12 months.

Digester	Also called biogas installation, which converts liquid and solid manure into biogas. As a by-product a digestate is formed which can be used as fertilizer.
Discharge	Manure is discharged in the environment. This is done after a period of storage and activities are often not recorded as many regions do not allow for such practices.
Dry lot	A paved or unpaved open confinement without any cover and where manure is stored for several months (up to a year or more) and may be removed periodically.
Dumping	Manure is dumped in an (often nearby) river. This can be done after a period of storage and activities are often not recorded as many regions do not allow for such practices.
Fishpond	Manure is used as fertilizer to increase production of food organisms that are eaten by the fish.
Lagoon	A liquid storage system designed to combine waste stabilization and storage. Lagoons can both be a covered tank construction or an earthen basin and are characterised by the creation of an anaerobic environment.
Liquid	A system where manure as excreted (slurry) is stored in tanks or earthen ponds, sometimes with some addition of water and storage periods of usually less than a year.
Liquid crust	Same storage as ‘Liquid’, but with a naturally or artificially formed crust on the top, which reduces gas emissions.
Manure with litter (poultry)	As manure accumulates in the barn, bedding material is added to absorb the moisture over an entire production cycle. Typically used for poultry breeder flocks and meat type chickens.

Manure without litter (poultry)	Manure is dried as it accumulates and can be similar to an open confinement storage system.
Outdoor Confinement Area	Manure is allowed to lie as deposited on outdoor confinement areas and is not managed.
Pasture	Manure that is deposited on pasture and grazing land and not managed.
Pasture + paddock	Animals held on pasture and outdoor confinement areas deposit their manure and no further manure management is applied.
Pit 1, 2	Manure is collected and stored below a slatted floor in an enclosed animal confinement for 1) less than 2 months, 2) a period of 2 months or more.
Public sewage	Manure enters the public sewage system and further processed at a treatment plant.
Sold	Solid manure is sold as fertilizer or fuel, usually after a period of storage.
Solid storage	Manure is stored, typically for several months, in unconfined piles or stacks.
Thermal drying	Manure (solid) is treated through a drying process and is commonly used to remove volatile contaminants from livestock manure.

Table B4. Divisions of manure management used in AMCLIM.

Category	Solid	Liquid
A	composting, deep litter, litter (poultry)[a], pit storage (intensive layers)[a], solid storage	aerobic processing, pit storage (livestock except for intensive layers)
B	--	aerobic lagoon, liquid[b]
C	--	lagoon, liquid crust
D	daily spread (cattle, small ruminants, chickens)[c], dry lot, outdoor confinement area	daily spread (dairy cattle, pigs)[b]
Grazing	pasture, pasture + paddock	
Fuel	burned, digester (biogas)	
Unmanaged	discharge, dumping, fishpond, public sewage	
Other	sold, thermal drying	

[a] Counting as housing emissions. [b] To differentiate with "liquid crust", "liquid" is assumed to be an uncovered storage. [c] Counting as MMS emissions.

B8 Planting seasons for manure application to land

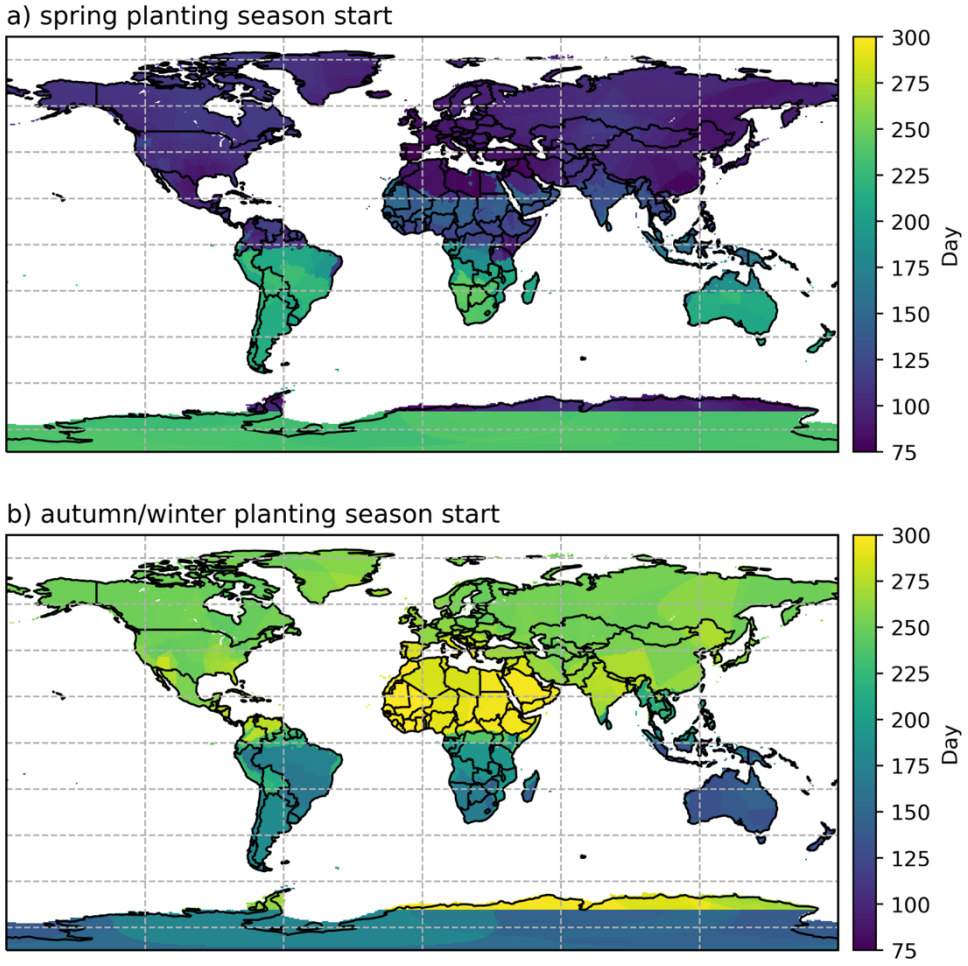

Figure B5. Planting seasons for manure application to land (a) spring (for the NH) and (b) autumn/winter (for the NH). The dates (expressed as Julian days) were derived from the mean planting seasons of 18 spring crops and 4 winter crops. If there is no difference between the spring season and autumn/winter season, it indicates that there is only one planting season.

B9 Information of US Environmental Protection Agency Animal Feeding Operations monitoring data

Site name	Location	Livestock/Production system	Number of rooms/houses monitored	Monitored period
IN3B	Carroll, Indiana	Pig	4	01 July 2007 to 31 July 2009
NC2B	Nash, North Carolina	Chicken (layer)	2	15 March 2008 to 15 March 2009
IN5B	Jasper, Indiana	Dairy	2	01 July 2007 to 31 July 2009

Appendix

Appendix C Supplementary results for Chapter 3

C1 Site simulations for NH_3 from fertilizer applications

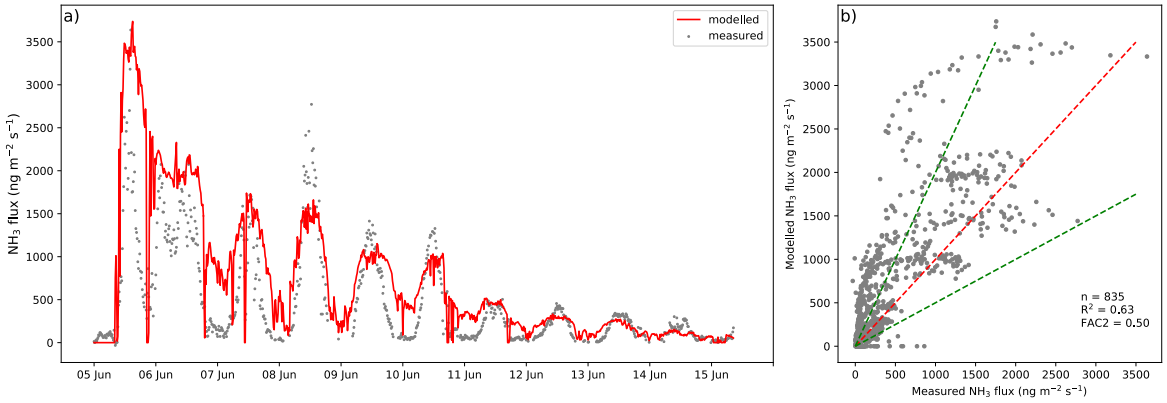

Figure C1. Modelled NH_3 emissions by AMCLIM–Land at site scale compared with measured NH_3 emissions by AGM in the GRAMINAE field experiments. (a) Modelled NH_3 emissions compared with measurements of NH_3 emissions. (b) Scatter plot of modelled NH_3 vs. measured NH_3.

C2 Crop-specific NH_3 emissions and volatilization rates

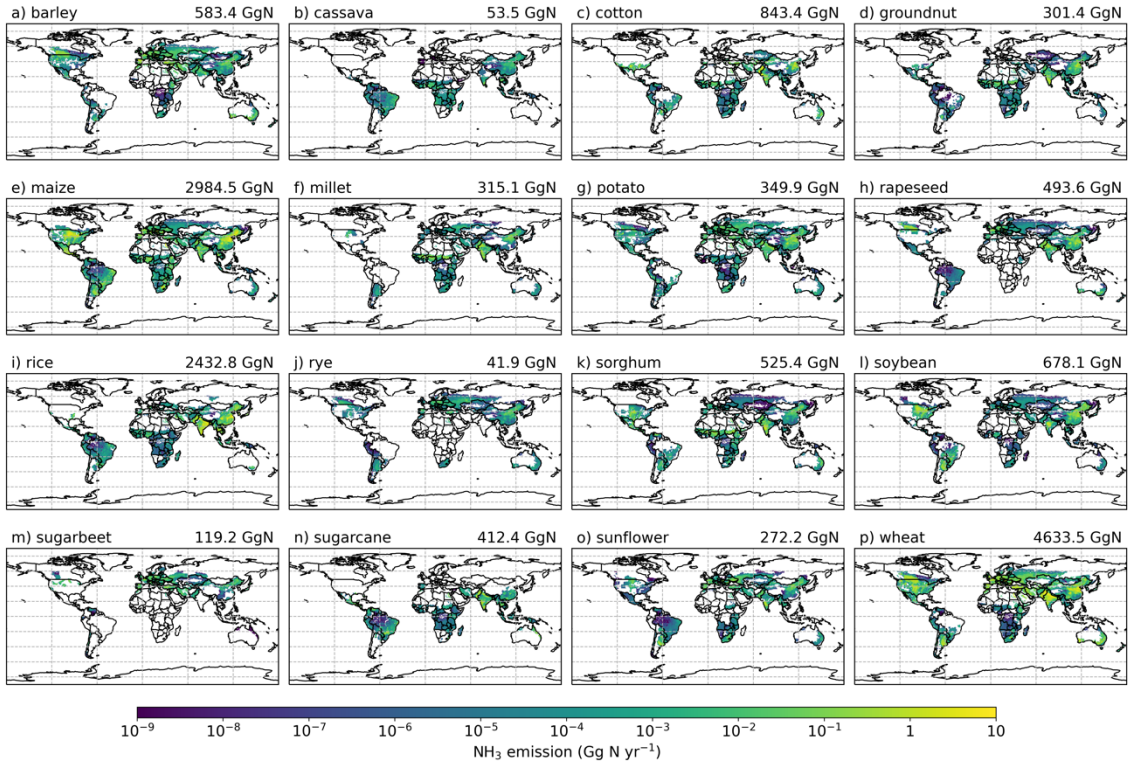

Figure C2. Ammonia emissions from 16 major crops for 2010 as simulated using AMCLIM.

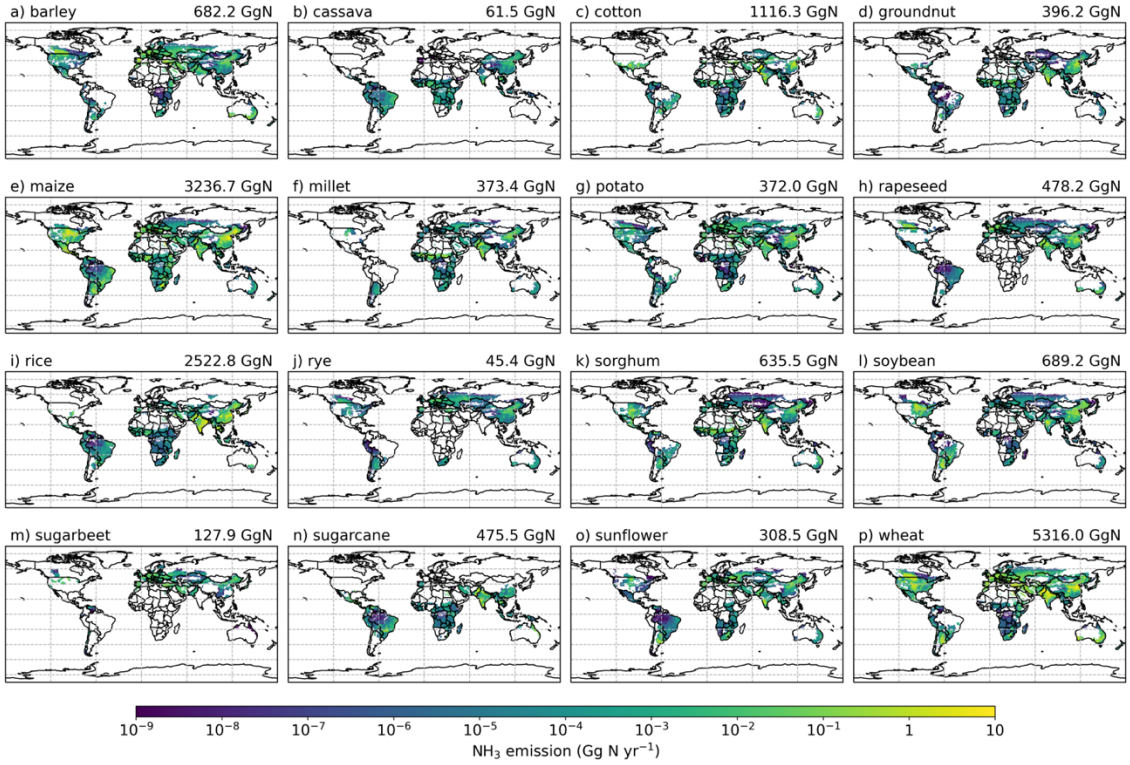

Figure C3. Same as Figure C2 but for 2018.

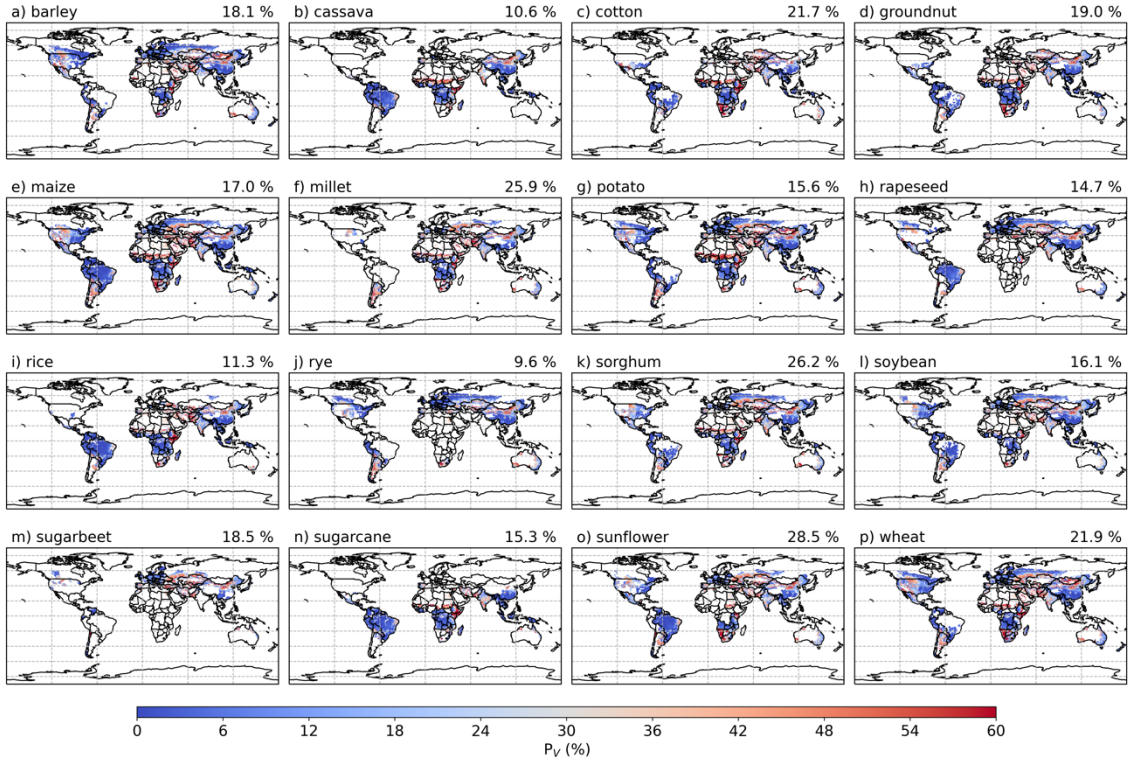

Figure C4. Percentage of applied nitrogen that volatilizes as NH_3 (P_V, %) for 16 major crops in 2010 as estimated by AMCLIM.

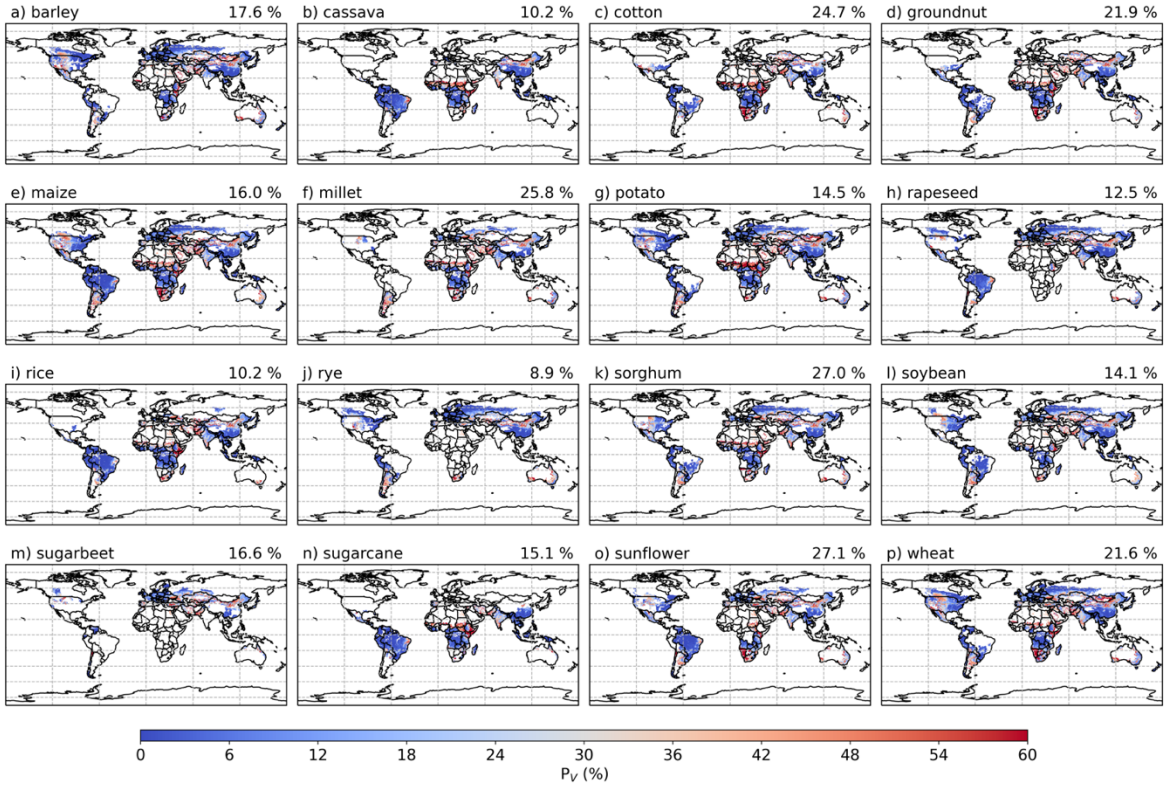

Figure C5. Same as Figure C4 but for 2018.

C3 Global fertilizer use in the 21st century

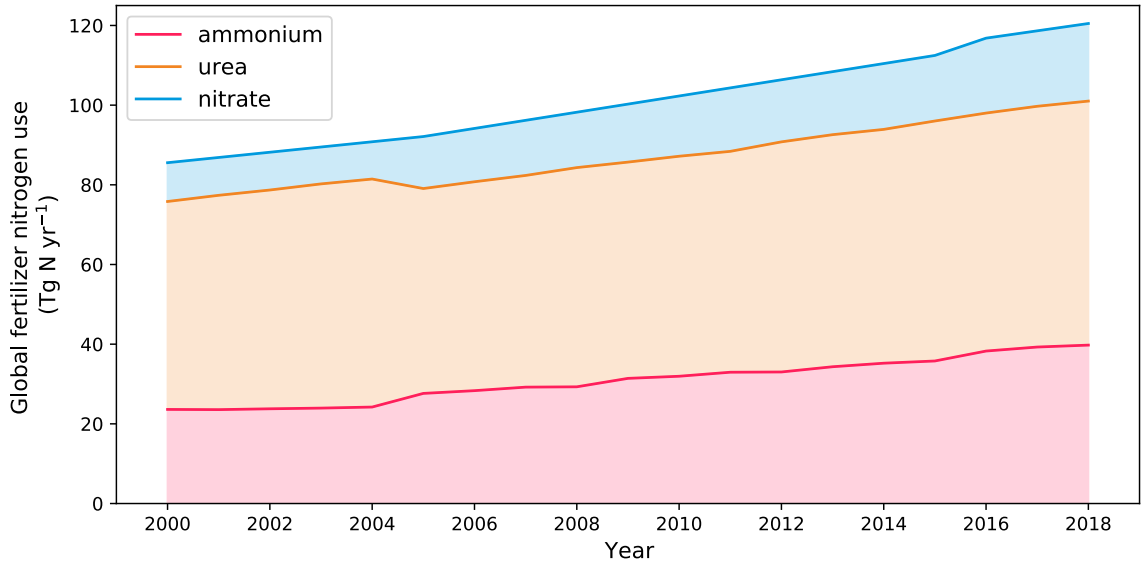

Figure C6. Global total use of three types of fertilizers in the 21st century.

Appendix D Supplementary results for Chapter 4

D1 Site simulations for NH_3 from pig housing

Appendix

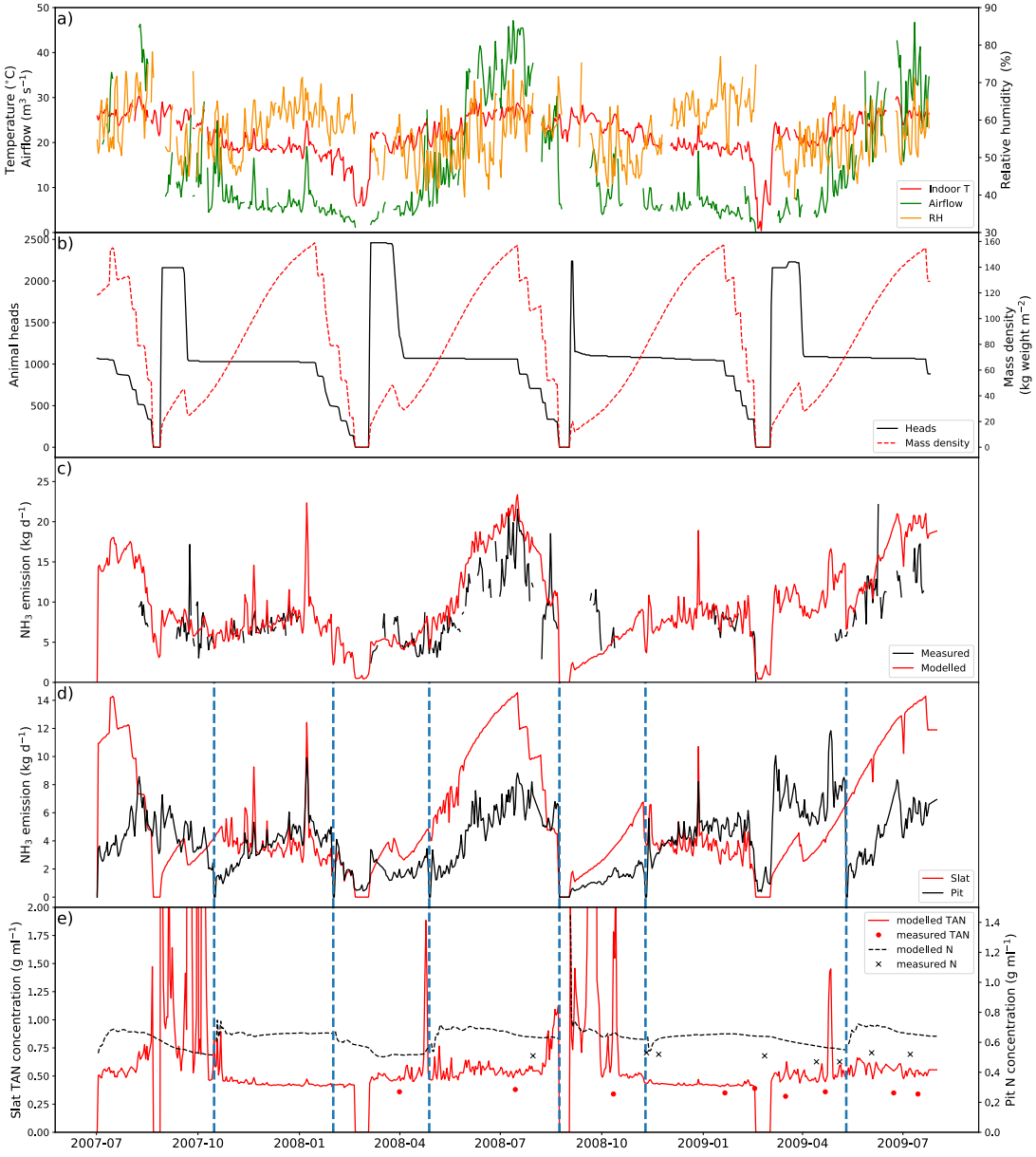
a)
Temperature (°C)
Airflow (m³ s⁻¹)
Relative humidity (%)
Indoor T
Airflow
RH
b)
Animal heads
Mass density (kg weight m⁻²)
Heads
Mass density
c)
NH3 emission (kg d⁻¹)
Measured
Modelled
d)
NH3 emission (kg d⁻¹)
Slat
Pit
e)
Slat TAN concentration (g ml⁻¹)
Pit N concentration (g ml⁻¹)
modelled TAN
measured TAN
modelled N
measured N
2007-07
2007-10
2008-01
2008-04
2008-07
2008-10
2009-01
2009-04
2009-07

Figure D1. Site simulations of House 2 in a pig farm at site IN3B, Carroll, Indiana, from 01 July 2007 to 31 July 2009. (a) Measured daily mean indoor temperature, airflow rate and relative humidity of the house. (b) Animal heads and mass density of the house. (c) Comparison between modelled NH_3 emissions and calculated NH_3 emissions from measured indoor concentrations. (d) Modelled NH_3 emissions from the slats and the pit. (e) Comparisons between measured and modelled TAN concentration of the slats and between measured and modelled nitrogen concentration of the pit. Vertical blue dashed lines refer to manure removal from the pit. (Same as Figure 4.2 but for House 2)

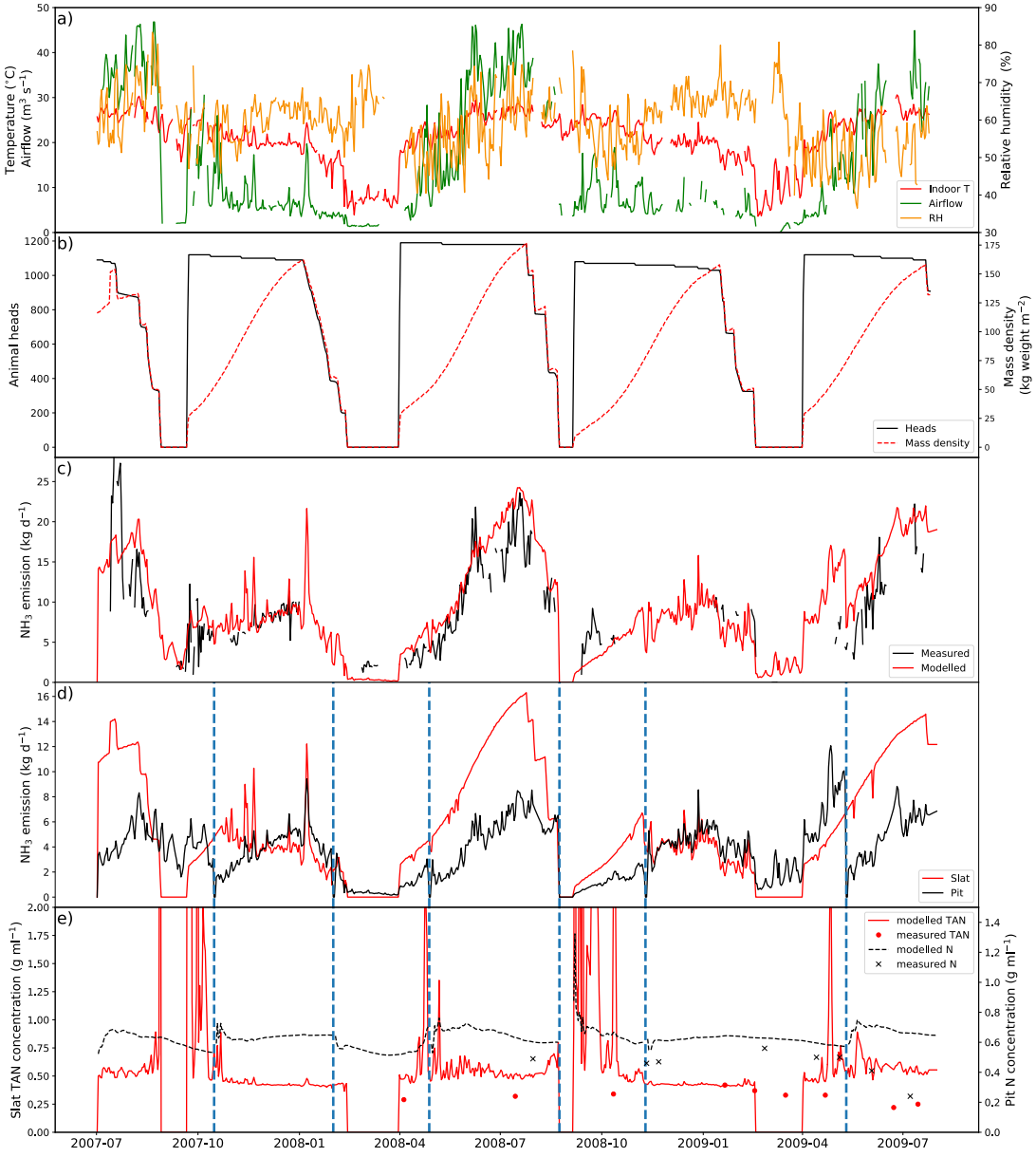

Figure D2.. Same as Figure D1 but for House 3.

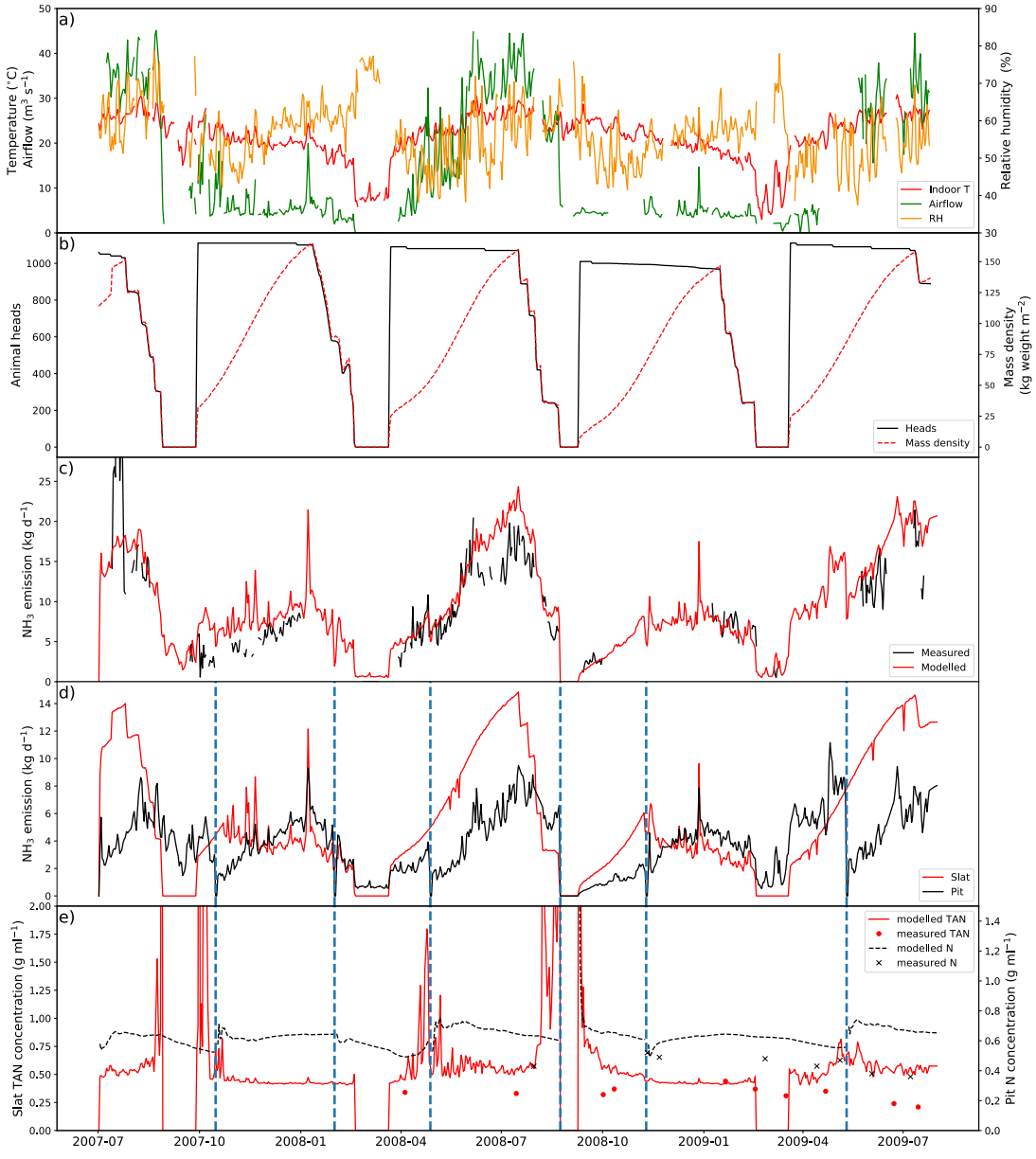

Figure D3. Same as Figure D1 but for House 4.

D2 Site simulations for NH_3 from layer chicken housing

Appendix

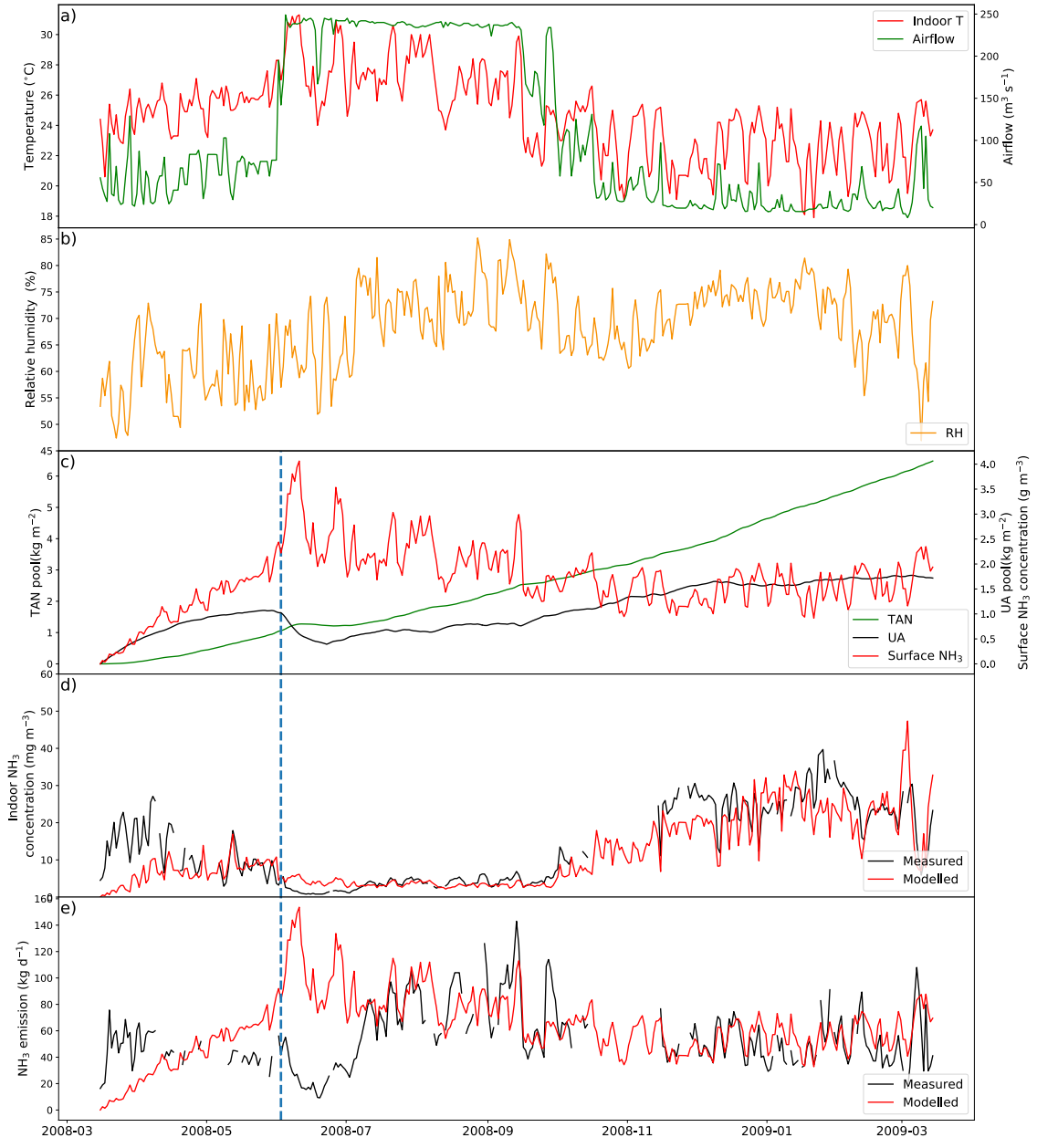
a)
Indoor T
Airflow
Temperature (°C)
Airflow (m³ s⁻¹)
b)
Relative humidity (%)
RH
c)
TAN pool(kg m⁻²)
UA pool(kg m⁻²)
Surface NH₃ concentration (g m⁻³)
TAN
UA
Surface NH₃
d)
Indoor NH₃ concentration (mg m⁻³)
Measured
Modelled
e)
NH₃ emission (kg d⁻¹)
Measured
Modelled
2008-03
2008-05
2008-07
2008-09
2008-11
2009-01
2009-03

Figure D4. Site simulations of House B in a layer farm at site NC2B, Nash, North Carolina, from 15 March 2008 to 15 March 2009. (a) Measured daily mean indoor temperature and airflow rate of the house. (b) Measured daily mean relative humidity of the house. (c) Modelled TAN pool and UA pool. (d) Comparison between measured and modelled indoor NH_3 concentrations of the house and surface NH_3 concentrations. (e) Comparison between modelled NH_3 emissions and calculated NH_3 emissions from measured indoor concentrations. Vertical blue dashed lines refer to emptying of the house. (Same as Figure 4.3 but for House B)

D3 Emissions from pig manure management

Table D1.. Global total managed nitrogen (Gg N yr^{-1}), NH_3 emissions (Gg N yr^{-1}) and volatilization rates (%) from different manure management systems for three pigs.

MMS	Year	Total managed N (Gg N yr^{-1})	NH_3 from MMS (Tg N yr^{-1})	Average P_V (%)
Indoor storage, liquid	2010	2211.6	171.6	7.7
	2018	2188.9	175.5	8.0
Outdoor storage, liquid	2010	1310.6	155.3	11.8
	2018	1283.0	158.7	12.3
Covered storage, liquid	2010	1247.9	4.5	0.3
	2018	1214.7	4.8	0.4
Lagoon	2010	42.3	7.1	16.8

	2018	42.9	7.7	17.9
Indoor storage, solid	2010	1784.4	185.2	10.3
	2018	1786.9	187.0	10.4
Left on land	2010	1767.3	478.9	27.1
	2018	1746.4	487.1	27.9
Total	2010	8364.2	1002.7	11.9
	2018	8263.0	1021.0	12.3

Appendix

Appendix E Supplementary results for Chapter 5

E1 Site simulations for NH_3 from dairy cattle barns

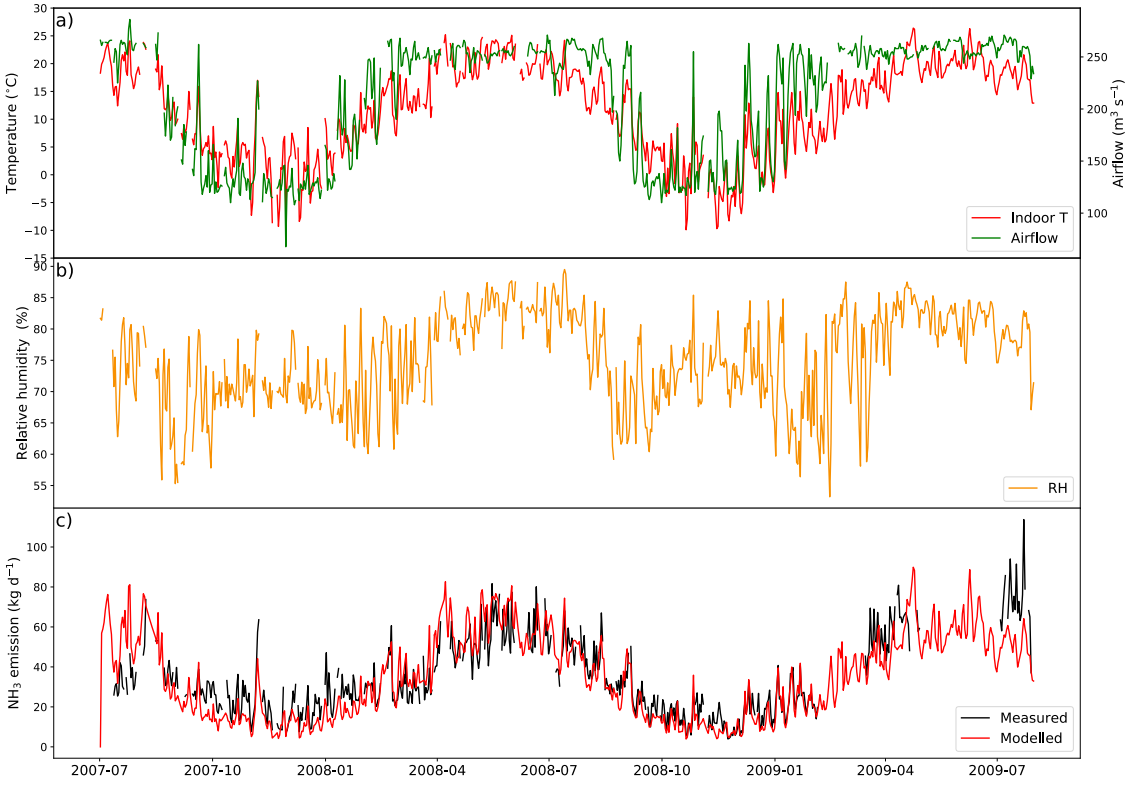

Figure E1. Site simulations of Barn 2 in a dairy farm at site IN5B, Jasper, Indiana, from 01 July 2007 to 31 July 2009. The barn is equipped with exhaust fans to facilitate ventilation. (a) Measured daily mean indoor temperature and airflow rate of the barn. (b) Measured daily mean relative humidity of the barn. (c) Comparison between modelled NH_3 emissions and calculated NH_3 emissions from measured indoor concentrations.

E2 NH_3 from different grazing schemes

Table E1. Total excreted N (Tg N yr^{-1}), NH_3 emissions (Tg N yr^{-1}) and volatilization rates (%) from each grazing scheme for cattle, sheep and goats as simulated by AMCLIM.

Ruminants	Year	Scheme	Total excreted N while grazing (Tg N yr^{-1})	NH_3 from grazing (Tg N yr^{-1})	Average P_V (%)
Cattle	2010	urine patch	21.54	5.65	26.2
		dung pat	7.49	0.22	2.9
		mixed	10.02	1.67	16.7
	2018	urine patch	22.14	4.72	21.3
		dung pat	7.69	0.25	3.3
		mixed	10.29	1.74	14.6
Sheep	2010	urine patch	2.23	0.78	35.0
		dung pat	0.62	0.01	1.6
		mixed	0.88	0.13	12.7
	2018	urine patch	2.33	0.62	26.6
		dung pat	0.65	0.02	3.1
		mixed	0.92	0.11	10.4

Goat	2010	urine patch	0.89	0.35	39.3
		dung pat	0.50	0.02	4.0
		mixed	0.60	0.12	17.1
	2018	urine patch	0.95	0.30	31.6
		dung pat	0.53	0.02	3.8
		mixed	0.64	0.11	14.5
Total	2010	urine patch	24.66	6.78	27.5
		dung pat	8.61	0.25	2.9
		mixed	11.55	1.92	19.9
	2018	urine patch	25.42	5.64	22.2
		dung pat	8.87	0.29	3.3
		mixed	11.86	1.96	14.3

Appendix

Appendix F Supplementary results for Chapter 6

F1 Dominant source of agricultural NH_3 emissions

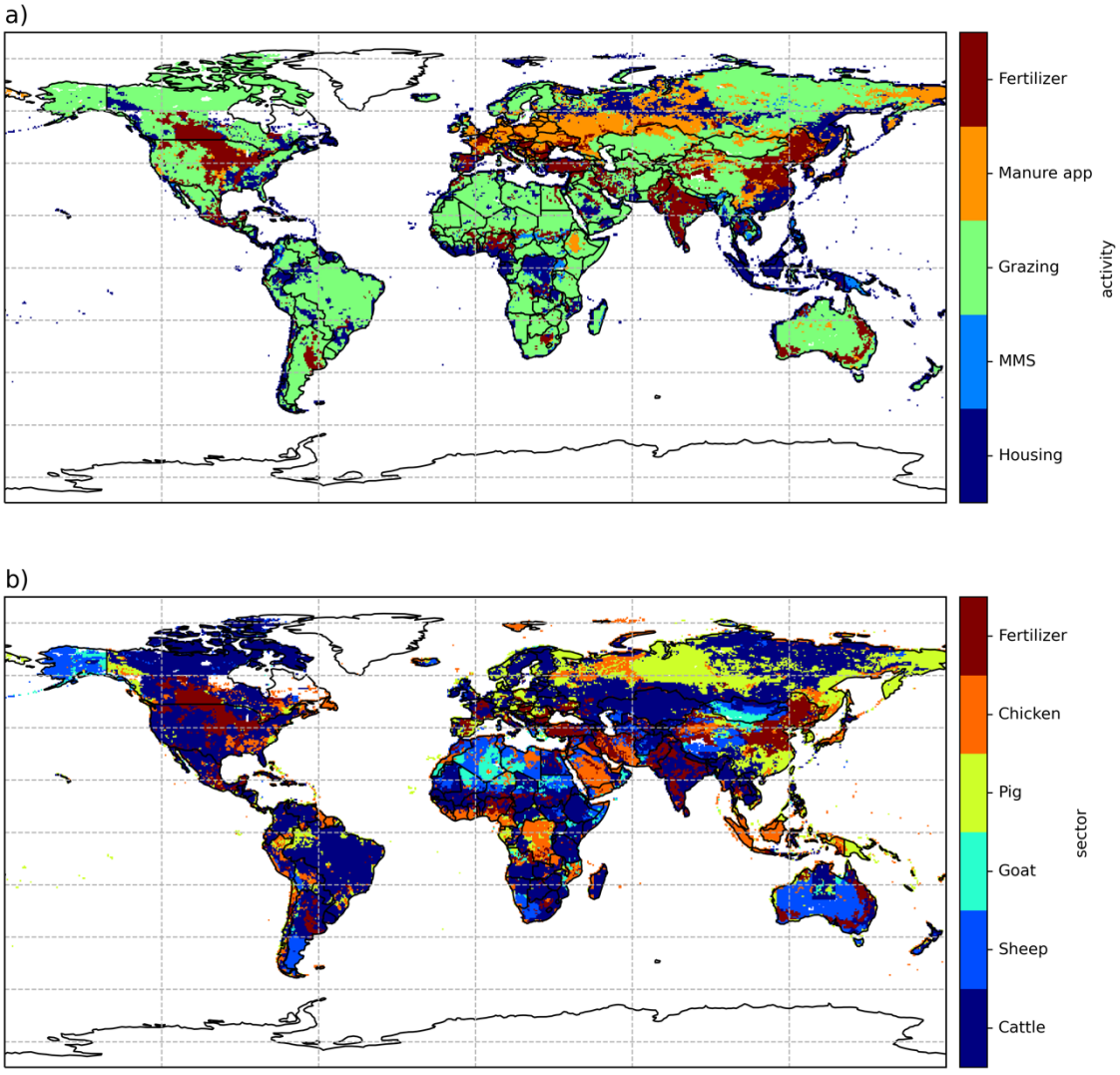

Figure F1.. Dominant source of NH_3 emissions from agricultural activities (a) and sectors (b) as estimated by AMCLIM.

F2 Volatilization of NH_3 relative to TAN

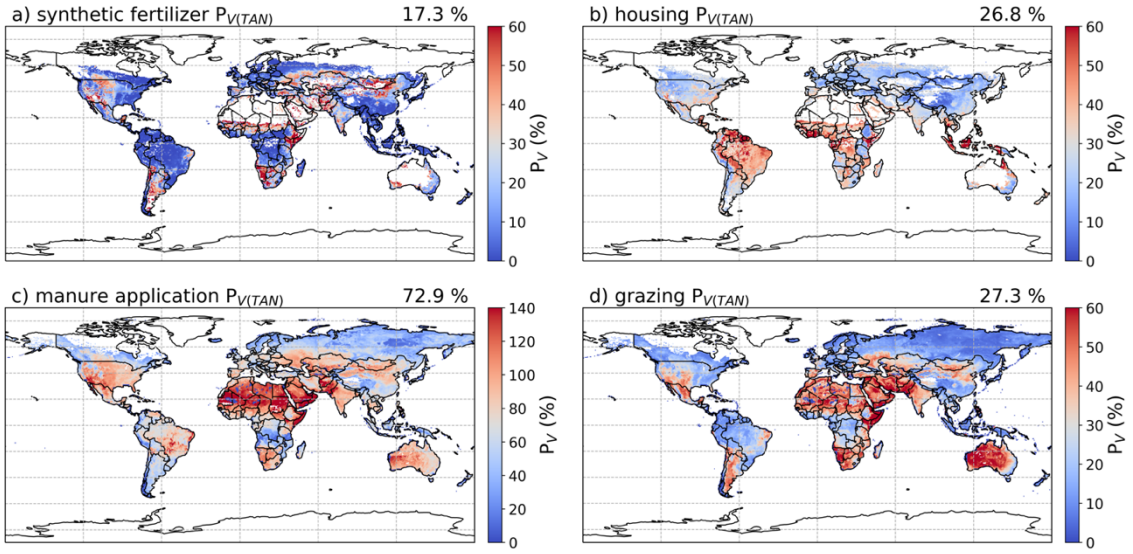

Figure F2. Percentage of TAN that volatilizes ($P_{V(TAN)}$) as NH_3 in 2010 as estimated by AMCLIM for (a) the use of ammonium and urea in synthetic fertilizer, (b) urinary N in excreta deposited in livestock houses, (c) TAN application in manure to land (note the different scale) and (d) the urine patch scheme (urinary N) of grazing.

F3 Nitrogen excreted by livestock

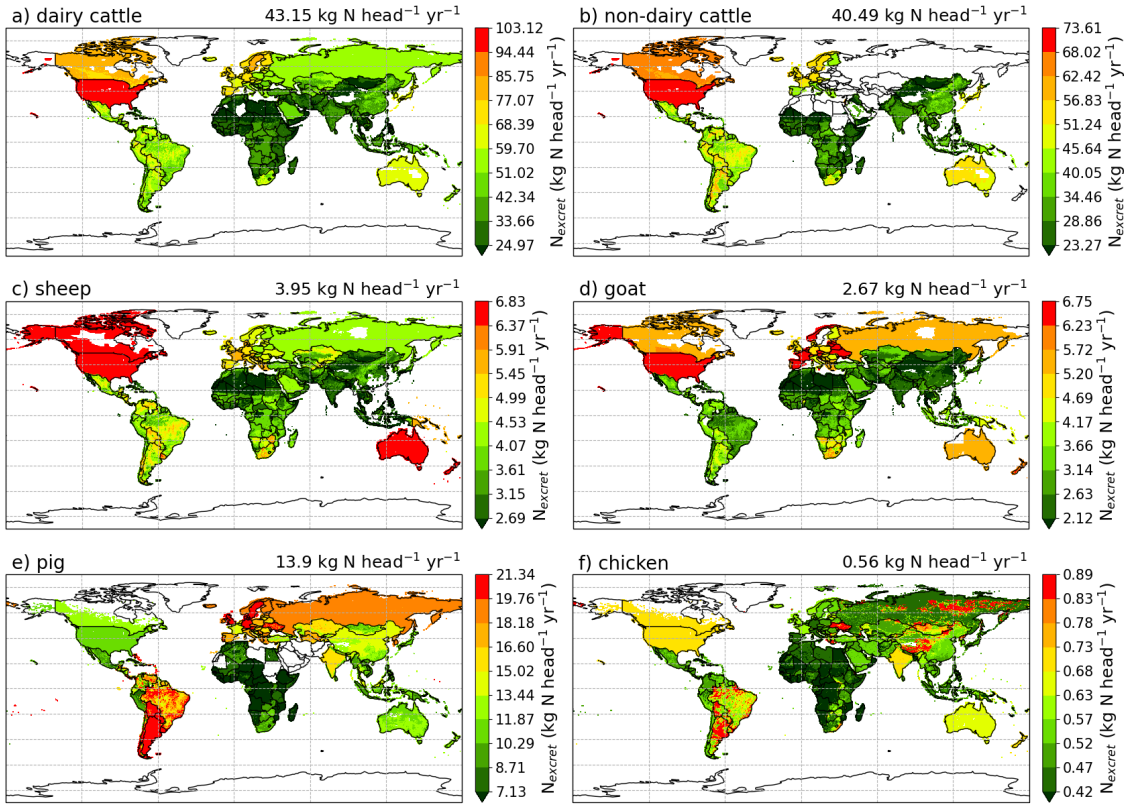

Figure F3. Annual mean excreted nitrogen (kg N head^{-1} yr^{-1}) by (a) dairy cattle, (b) non-dairy cattle, (c) sheep, (d) goat, (e) pigs and (f) chicken based on GLEAM2 for year 2010 (FAO, 2018).

F4 The impact of soil moisture on NH_3 volatilization under different temperature and soil pH conditions

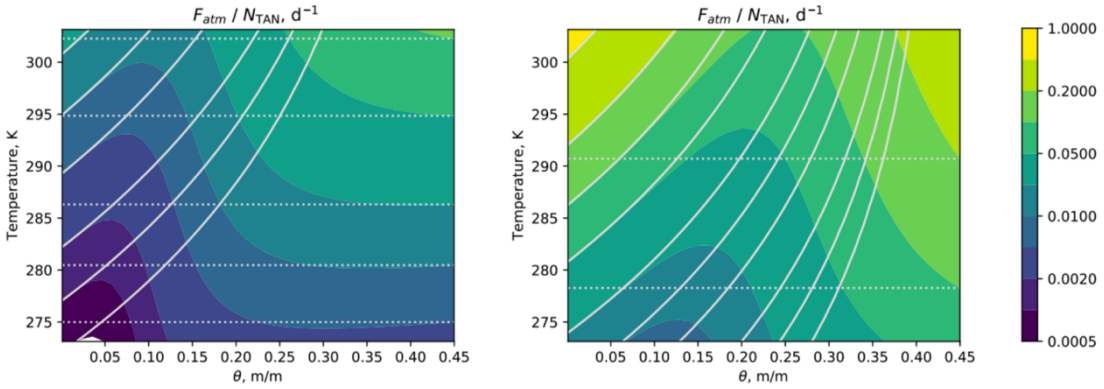

Figure F4. The fractional volatilization rates as a function of temperature and soil water content (left) soil pH = 7.0, (right) soil pH = 8.5 simulated by FANv2 (figure taken from Vira et al., 2020).

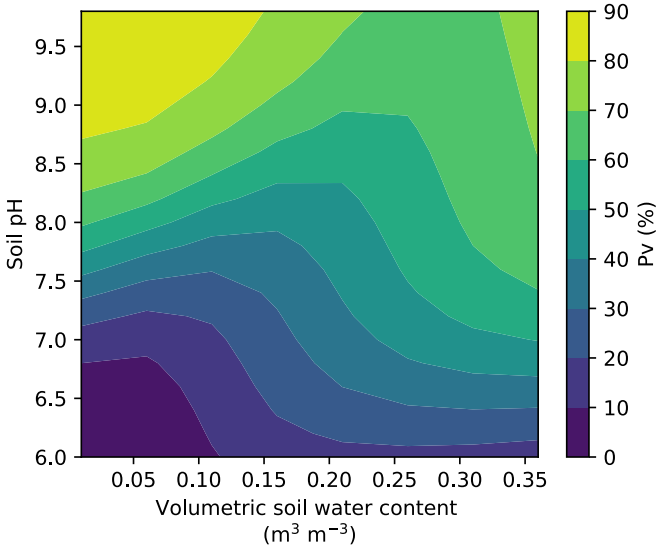

Figure F5. The percentage volatilization rates as a function of soil water content and soil pH under temperature conditions of the GRAMINAE site simulated by AMCLIM.

F5 Response of ammonia emissions due to 2 °C warming

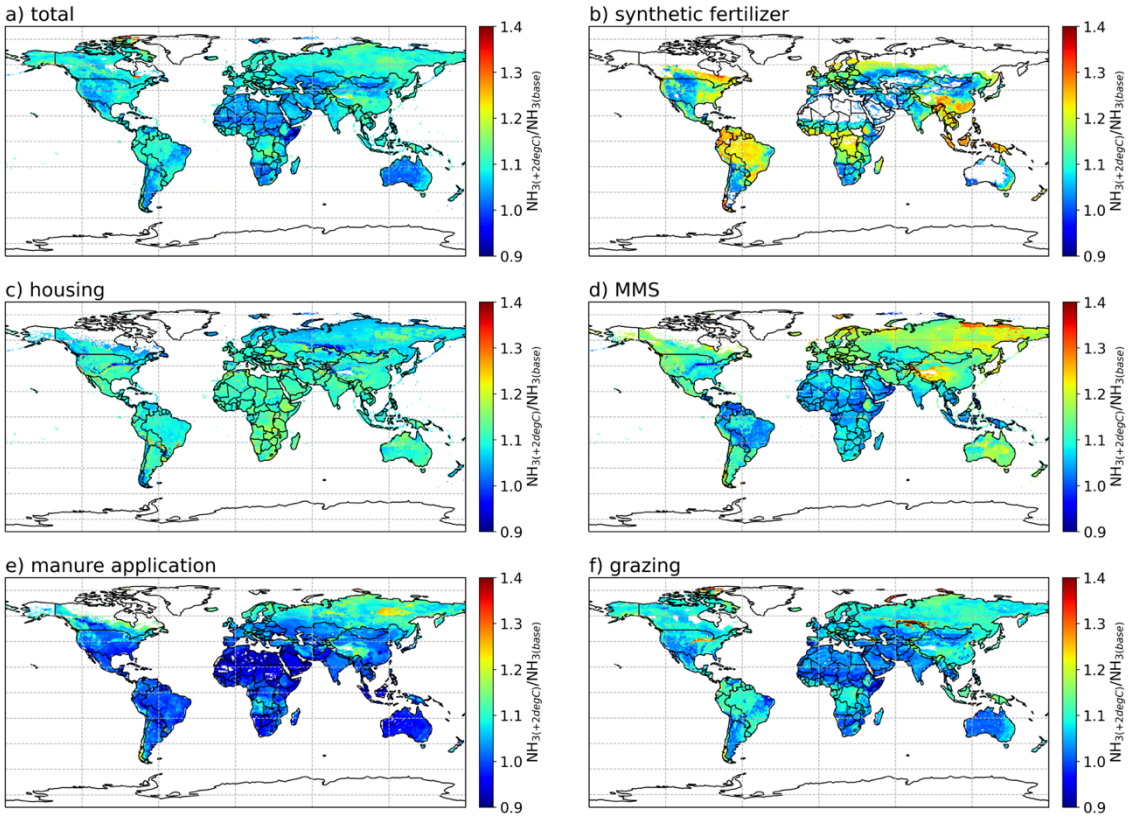

Figure F6. Ratios of NH_3 emissions due to 2 °C warming to base NH_3 emissions for (a) whole agricultural sector, (b) synthetic fertilizer use, (c) livestock housing, (d) manure management, (e) manure application and (f) grazing derived from the global temperature sensitivity tests in 2010 using AMCLIM.

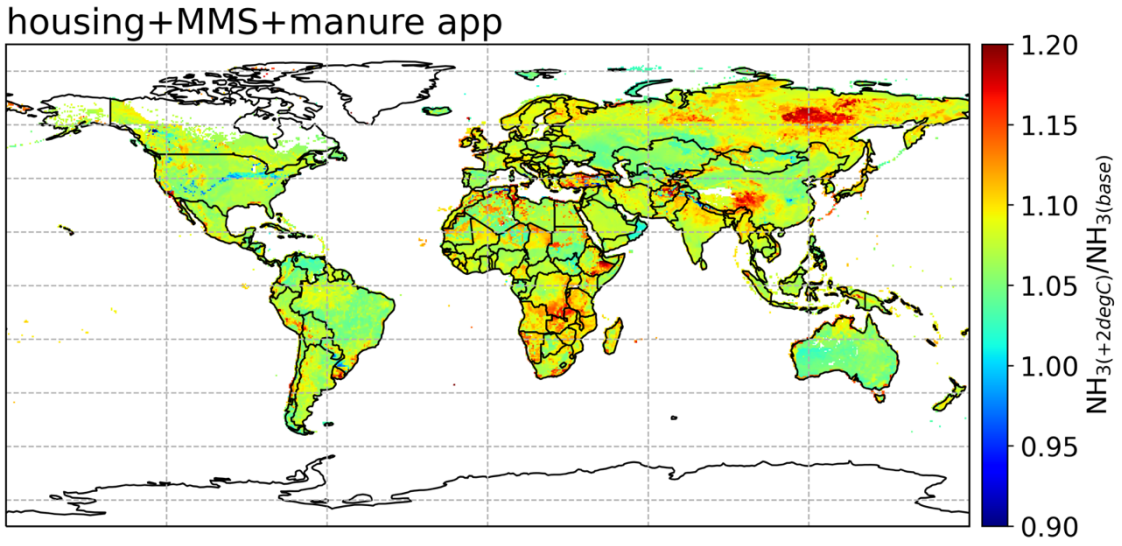

Figure F7. Same as Figure F6 but for a combined source term of livestock housing, manure management and land application of manure.

F6 Relationships between temperature sensitivity and temperature and volatilization rates

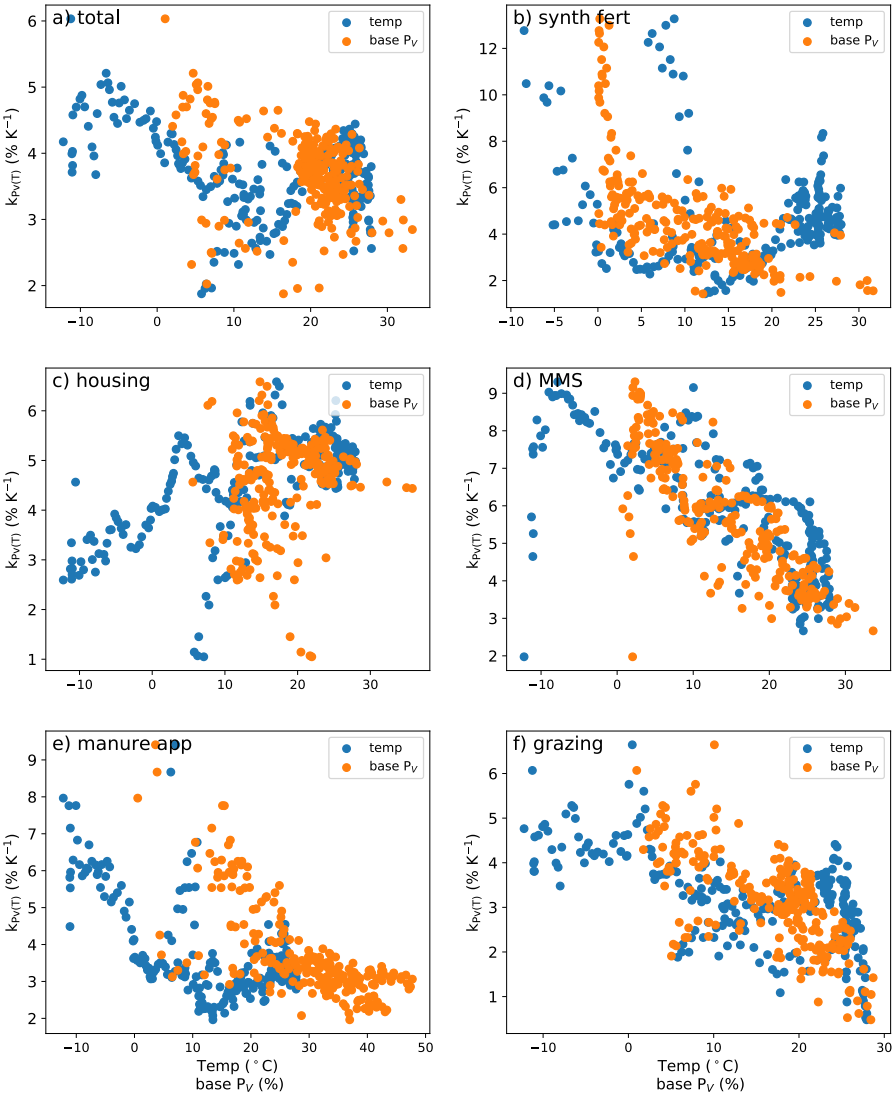

Figure F8. Simulated $k_{Pv(T)}$ of the (a) whole agricultural sector, (b) synthetic fertilizer use, (c) housing, (d) manure management, (e) manure application to land and (f) grazing plotted against air temperature at 2 m and simulated P_V from the base run.

F7 Estimates of NH_3 emission reduction

The total agricultural NH_3 emission ($F_{NH_3,agric}$) estimated by AMCLIM is the sum of emissions from synthetic fertilizer use ($F_{NH_3,syn\ fert}$) and livestock farming ($F_{NH_3,livestock}$). Livestock farming emissions consist of housing ($F_{NH_3,housing}$), manure management ($F_{NH_3,MMS}$), manure application ($F_{NH_3,manure\ app}$) and grazing ($F_{NH_3,grazing}$), as expressed by the following equations:

$$F_{NH_3,agric} = F_{NH_3,syn\ fert} + F_{NH_3,livestock}, \quad (F.1)$$

$$F_{NH_3,livestock} = F_{NH_3,housing} + F_{NH_3,MMS} + F_{NH_3,manure\ app} + F_{NH_3,grazing}. \quad (F.2)$$

The mitigation measures and corresponding impacts on volatilization have been presented in Table 6.7. The overall reduction in NH_3 emissions of the whole agricultural sector by applying all methods equals to subtracting the reduction in each component from the original emissions, which can be calculated by the following equations:

$$F_{NH_3,total\ agric'} = F_{NH_3,syn\ fert'} + F_{NH_3,housing'} + F_{NH_3,MMS'} + F_{NH_3,manure\ app'} + F_{NH_3,grazing'}, \quad (F.3)$$

$$F_{\mathrm{NH_3,total\ agric'}} = F_{\mathrm{NH_3,agric}} - (F_{\mathrm{NH_3,syn\ fert}} - F_{\mathrm{NH_3,syn\ fert_{reduction}}}) - (F_{\mathrm{NH_3,housing}} - F_{\mathrm{NH_3,housing_{reduction}}}) - (F_{\mathrm{NH_3,MMS}} - F_{\mathrm{NH_3,MMS_{reduction}}}) - (F_{\mathrm{NH_3,manure\ app}} - F_{\mathrm{NH_3,manure\ app_{reduction}}}) - (F_{\mathrm{NH_3,grazing}} - F_{\mathrm{NH_3,grazing_{reduction}}}), \quad (F.4)$$

where $F_{\mathrm{NH_3,source'}}$ represents updated NH_3 emissions of a source after applying mitigation measures, and $F_{\mathrm{NH_3,source_{reduction}}}$ represents the reduction of NH_3 emissions from a source.

The NH_3 reduction for synthetic fertilizer use ($F_{\mathrm{NH_3,syn\ fert_{reduction}}}$) is expressed as:

$$F_{\mathrm{NH_3,syn\ fert'}} = (1 - R_{\mathrm{A1}})(1 - R_{\mathrm{A2(syn\ fert)}})F_{\mathrm{NH_3,syn\ fert}}, \quad (F.5)$$

$$F_{\mathrm{NH_3,syn\ fert_{reduction}}} = F_{\mathrm{NH_3,syn\ fert}}(R_{\mathrm{A1}} + R_{\mathrm{A2(syn\ fert)}} - R_{\mathrm{A1}} \cdot R_{\mathrm{A2(syn\ fert)}}), \quad (F.6)$$

where R_{A1} to R_{D1} is the percentage reduction of NH_3 emission due to a mitigation measure.

The NH_3 reduction for housing ($F_{\mathrm{NH_3,housing_{reduction}}}$) is expressed as:

$$F_{\mathrm{NH_3,housing'}} = (1 - R_{\mathrm{B1}})(1 - R_{\mathrm{B2}})F_{\mathrm{NH_3,housing}}, \quad (F.7)$$

$$F_{\mathrm{NH_3,housing_{reduction}}} = F_{\mathrm{NH_3,housing}}(R_{\mathrm{B1}} + R_{\mathrm{B2}} - R_{\mathrm{B1}} \cdot R_{\mathrm{B2}}). \quad (F.8)$$

The NH_3 reduction for manure management ($F_{\mathrm{NH_3,MMS_{reduction}}}$) is expressed as:

$$F_{\mathrm{NH_3,MMS'}} = (1 - R_{\mathrm{C1}} - R_{\mathrm{C2}})(F_{\mathrm{NH_3,MMS}} + F_{\mathrm{NH_3,housing_{reduction}}} \cdot P_{\mathrm{V,MMS}}), \quad (F.9)$$

$$F_{\mathrm{NH_3,MMS_{reduction}}} = F_{\mathrm{NH_3,MMS}}(R_{\mathrm{C1}} + R_{\mathrm{C2}}) - (1 - R_{\mathrm{C1}} - R_{\mathrm{C2}})(R_{\mathrm{B1}} + R_{\mathrm{B2}} - R_{\mathrm{B1}}R_{\mathrm{B2}})F_{\mathrm{NH_3,housing}} \cdot P_{\mathrm{V,MMS}}. \quad (F.10)$$

Note that measure C1 and C2 are independent. Meanwhile, stored manure nitrogen increases due to less emission from housing.

The NH_3 reduction for manure application ($F_{\mathrm{NH_3,manure\ app_{reduction}}}$) is expressed as:

$$F_{\mathrm{NH_3,manure\ app}'} = (1 - R_{\mathrm{A2}})(F_{\mathrm{NH_3,manure\ app}} + F_{\mathrm{NH_3,MMS_{reduction}}} \cdot P_{\mathrm{V,manure\ app}}), \tag{F.11}$$

$$F_{\mathrm{NH_3,manure\ app_{reduction}}} = F_{\mathrm{NH_3,manure\ app}} \cdot R_{\mathrm{A2(manure)}} - \left(1 - R_{\mathrm{A2(manure)}}\right)(R_{\mathrm{C1}} + R_{\mathrm{C2}})F_{\mathrm{NH_3,MMS}} \cdot P_{\mathrm{V,manure\ app}} - (1 - R_{\mathrm{C1}} - R_{\mathrm{C2}})(R_{\mathrm{B1}} + R_{\mathrm{B2}} - R_{\mathrm{B1}}R_{\mathrm{B2}})F_{\mathrm{NH_3,housing}} \cdot P_{\mathrm{V,MMS}} \cdot P_{\mathrm{V,manure\ app}}. \tag{F.12}$$

Note that manure nitrogen that applied to land increases due to less emission from previous stages, i.e., housing and manure storage.

The NH_3 reduction for grazing ($F_{\mathrm{NH_3,grazing_{reduction}}}$) is expressed as:

$$F_{\mathrm{NH_3,grazing}'} = (1 - R_{\mathrm{A1}})(1 - R_{\mathrm{D1}})F_{\mathrm{NH_3,grazing}}, \tag{F.13}$$

$$F_{\mathrm{NH_3,grazing_{reduction}}} = F_{\mathrm{NH_3,grazing}}(R_{\mathrm{A1}} + R_{\mathrm{D1}} - R_{\mathrm{A1}}R_{\mathrm{D1}}). \tag{F.14}$$

As a result, the total reduction ($F_{\mathrm{NH_3,total\ agric_{reduction}}}$) is expressed as:

$$F_{\mathrm{NH_3,total\ agric_{reduction}}} = F_{\mathrm{NH_3,syn\ fert_{reduction}}} + F_{\mathrm{NH_3,housing_{reduction}}} + F_{\mathrm{NH_3,MMS_{reduction}}} + F_{\mathrm{NH_3,manure\ app_{reduction}}} + F_{\mathrm{NH_3,grazing_{reduction}}}, \tag{A.15}$$

$$F_{\mathrm{NH_3,total\ agric_{reduction}}} = F_{\mathrm{NH_3,syn\ fert}}\left(R_{\mathrm{A1}} + R_{\mathrm{A2(syn\ fert)}} - R_{\mathrm{A1}} \cdot R_{\mathrm{A2(syn\ fert)}}\right) + F_{\mathrm{NH_3,housing}}(R_{\mathrm{B1}} + R_{\mathrm{B2}} - R_{\mathrm{B1}} \cdot R_{\mathrm{B2}}) + \left(F_{\mathrm{NH_3,MMS}}(R_{\mathrm{C1}} + R_{\mathrm{C2}}) - (1 - R_{\mathrm{C1}} - R_{\mathrm{C2}})(R_{\mathrm{B1}} + R_{\mathrm{B2}} - R_{\mathrm{B1}}R_{\mathrm{B2}})F_{\mathrm{NH_3,housing}} \cdot P_{\mathrm{V,MMS}}\right) + (F_{\mathrm{NH_3,manure\ app}} \cdot R_{\mathrm{A2(manure)}} - \left(1 - R_{\mathrm{A2(manure)}}\right)(R_{\mathrm{C1}} + R_{\mathrm{C2}})F_{\mathrm{NH_3,MMS}} \cdot P_{\mathrm{V,manure\ app}} - (1 - R_{\mathrm{C1}} - R_{\mathrm{C2}})(R_{\mathrm{B1}} + R_{\mathrm{B2}} - R_{\mathrm{B1}}R_{\mathrm{B2}})F_{\mathrm{NH_3,housing}} \cdot P_{\mathrm{V,MMS}} \cdot P_{\mathrm{V,manure\ app}}) + F_{\mathrm{NH_3,grazing}}(R_{\mathrm{A1}} + R_{\mathrm{D1}} - R_{\mathrm{A1}}R_{\mathrm{D1}}). \quad \text{(F.15)}$$

It is worth noting that this is an approximating estimation of NH_3 emissions at the global scale.

F8 Change in temperature and NH_3 emissions under different SSPs

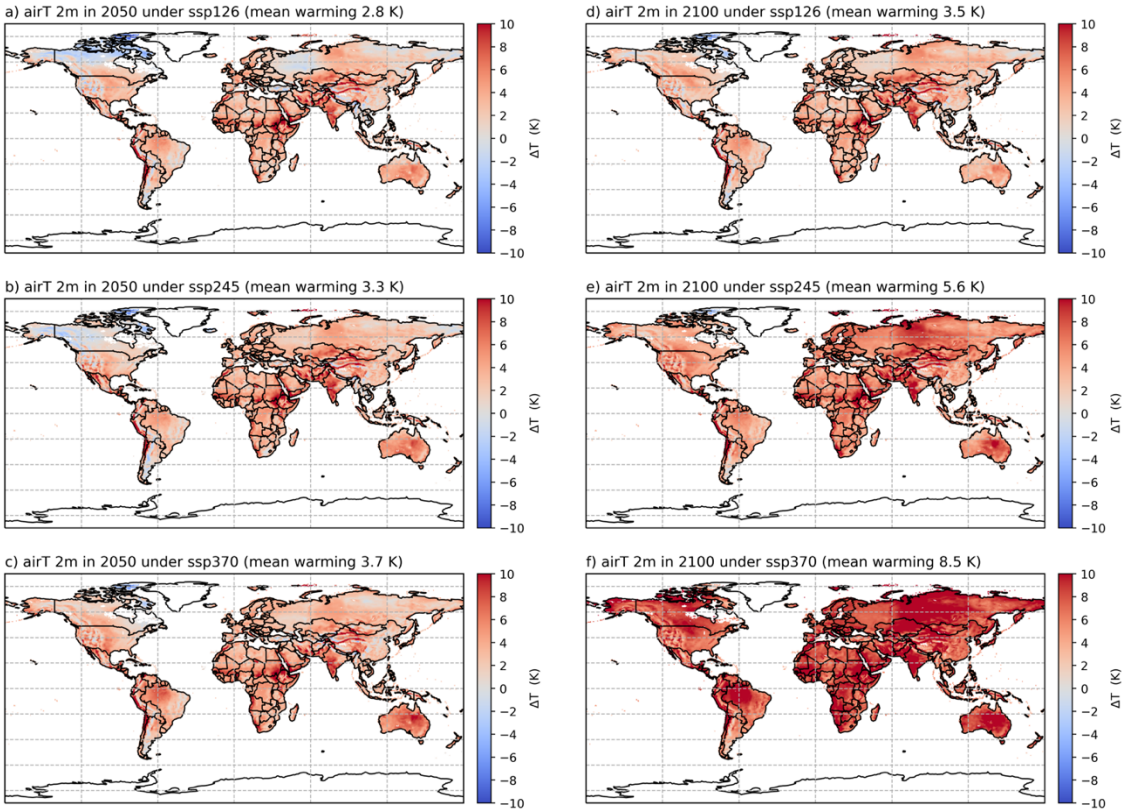

Figure F9. Projected change in air temperate at 2 m in 2050 (a, b, c) and in 2100 (d, e, f) relative to 2010 under three SSPs: SSP126 (a, d), SSP245 (b, e) and SSP370 (c, f).

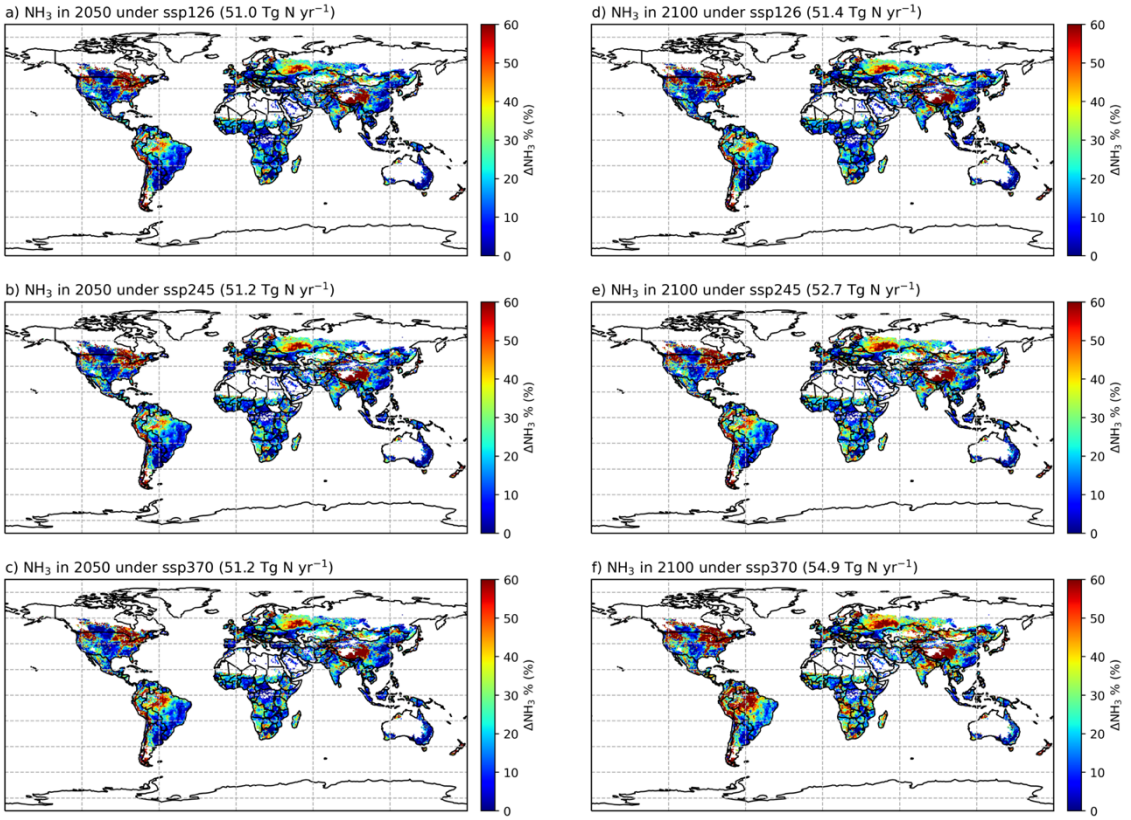

Figure F10. Projected change in agricultural NH_3 emissions in 2050 (a, b, c) and in 2100 (d, e, f) relative to 2018 under three SSPs: SSP126 (a, d), SSP245 (b, e) and SSP370 (c, f). The projections only consider the temperature effect and use the same activity data in 2018.

Reference

Aarnink, A. J. A., Swierstra, D., van den Berg, A. J., and Speelman, L.: Effect of Type of Slatted Floor and Degree of Fouling of Solid Floor on Ammonia Emission Rates from Fattening Piggeries, Journal of Agricultural Engineering Research, 66, 93–102, https://doi.org/10.1006/jaer.1996.0121, 1997.

Allott, T. E. H., Curtis, C. J., Hall, J., Harriman, R., and Battarbee, R. W.: The impact of nitrogen deposition on upland surface waters in Great Britain: A regional assessment of nitrate leaching, Water Air Soil Pollut, 85, 297–302, https://doi.org/10.1007/BF00476845, 1995.

Andersen, H. M.-L., Kongsted, A. G., and Jakobsen, M.: Pig elimination behavior—A review, Applied Animal Behaviour Science, 222, 104888, https://doi.org/10.1016/j.applanim.2019.104888, 2020.

Aneja, V., Bunton, B., Walker, J. T., and Malik, B. P.: Measurement and analysis of atmospheric ammonia emissions from anaerobic lagoons, Atmospheric Environment, 35, 1949–1958, https://doi.org/10.1016/S1352-2310(00)00547-1, 2001.

Aneja, V. P., Schlesinger, W. H., Erisman, J. W., Behera, S. N., Sharma, M., and Battye, W.: Reactive nitrogen emissions from crop and livestock farming in India, Atmospheric Environment, 47, 92–103, https://doi.org/10.1016/j.atmosenv.2011.11.026, 2012.

Aneja, V. P., Schlesinger, W. H., Li, Q., Nahas, A., and Battye, W. H.: Characterization of the Global Sources of Atmospheric Ammonia from Agricultural Soils, J. Geophys. Res. Atmos., 125, https://doi.org/10.1029/2019JD031684, 2020.

Ball, R., Keeney, D. R., Thoebald, P. W., and Nes, P.: Nitrogen Balance in Urine-affected Areas of a New Zealand Pasture [1], Agronomy Journal, 71, 309–314, https://doi.org/10.2134/agronj1979.00021962007100020022x, 1979.

Bash, J. O., Cooter, E. J., Dennis, R. L., Walker, J. T., and Pleim, J. E.: Evaluation of a regional air-quality model with bidirectional NH_3 exchange coupled to an agroecosystem model, Biogeosciences, 10, 1635–1645, https://doi.org/10.5194/bg-10-1635-2013, 2013.

Bateman, E. J. and Baggs, E. M.: Contributions of nitrification and denitrification to N2O emissions from soils at different water-filled pore space, Biol Fertil Soils, 41, 379–388, https://doi.org/10.1007/s00374-005-0858-3, 2005.

Beaudor, M., Vuichard, N., Lathière, J., Evangeliou, N., Van Damme, M., Clarisse, L., and Hauglustaine, D.: Global agricultural ammonia emissions simulated with the ORCHIDEE land surface model, Geosci. Model Dev., 16, 1053–1081, https://doi.org/10.5194/gmd-16-1053-2023, 2023.

Behera, S. N., Sharma, M., Aneja, V. P., and Balasubramanian, R.: Ammonia in the atmosphere: a review on emission sources, atmospheric chemistry and deposition on terrestrial bodies, Environ Sci Pollut Res, 20, 8092–8131, https://doi.org/10.1007/s11356-013-2051-9, 2013.

Bell, M., Flechard, C., Fauvel, Y., Häni, C., Sintermann, J., Jocher, M., Menzi, H., Hensen, A., and Neftel, A.: Ammonia emissions from a grazed field estimated by miniDOAS measurements and inverse dispersion modelling, Atmos. Meas. Tech., 10, 1875–1892, https://doi.org/10.5194/amt-10-1875-2017, 2017.

Beusen, A. H. W., Bouwman, A. F., Heuberger, P. S. C., Van Drecht, G., and Van Der Hoek, K. W.: Bottom-up uncertainty estimates of global ammonia emissions from global agricultural production systems, Atmospheric Environment, 42, 6067–6077, https://doi.org/10.1016/j.atmosenv.2008.03.044, 2008.

Bian, H., Chin, M., Hauglustaine, D. A., Schulz, M., Myhre, G., Bauer, S. E., Lund, M. T., Karydis, V. A., Kucsera, T. L., Pan, X., Pozzer, A., Skeie, R. B., Steenrod, S. D., Sudo, K., Tsigaridis, K., Tsimpidi, A. P., and Tsyro, S. G.: Investigation of global particulate nitrate from the AeroCom phase III experiment, Atmos. Chem. Phys., 17, 12911–12940, https://doi.org/10.5194/acp-17-12911-2017, 2017.

Billen, G., Silvestre, M., Grizzetti, B., Leip, A., Garnier, J., Voss, M., Howarth, R., Bouraoui, F., Lepistö, A., Kortelainen, P., Johnes, P., Curtis, C., Humborg, C., Smedberg, E., Kaste, Ø., Ganeshram, R., Beusen, A., and Lancelot, C.: Nitrogen flows from European regional watersheds to coastal marine waters, in: The European Nitrogen Assessment, edited by: Sutton, M. A., Howard, C. M., Erisman, J. W., Billen, G., Bleeker, A., Grennfelt, P., Van Grinsven, H., and Grizzetti, B., Cambridge University Press, 271–297, https://doi.org/10.1017/CBO9780511976988.016, 2011.

Bittman, S., Dedina, M., Howard, C. M. (Clare), Oenema, O., and Sutton, M. A.: Options for ammonia mitigation: guidance from the UNECE Task Force on Reactive Nitrogen, Centre for Ecology & Hydrology, on behalf of Task Force on Reactive Nitrogen, of the UNECE Convention on Long Range transboundary Air Pollution, Edinburgh, 2014.

Bouwman, A. F., Lee, D. S., Asman, W. A. H., Dentener, F. J., Van Der Hoek, K. W., and Olivier, J. G. J.: A global high-resolution emission inventory for ammonia, Global Biogeochem. Cycles, 11, 561–587, https://doi.org/10.1029/97GB02266, 1997a.

Bouwman, A. F., Lee, D. S., Asman, W. A. H., Dentener, F. J., Van Der Hoek, K. W., and Olivier, J. G. J.: A global high-resolution emission inventory for ammonia, Global Biogeochem. Cycles, 11, 561–587, https://doi.org/10.1029/97GB02266, 1997b.

Bouwman, A. F., Boumans, L. J. M., and Batjes, N. H.: Estimation of global NH_3 volatilization loss from synthetic fertilizers and animal manure applied to arable lands and grasslands: AMMONIA EMISSION FROM FERTILIZERS, Global Biogeochem. Cycles, 16, 8-1-8–14, https://doi.org/10.1029/2000GB001389, 2002.

Brunekreef, B. and Holgate, S. T.: Air pollution and health, The Lancet, 360, 1233–1242, https://doi.org/10.1016/S0140-6736(02)11274-8, 2002.

Buss, S. R., Herbert, A. W., Morgan, P., Thornton, S. F., and Smith, J. W. N.: A review of ammonium attenuation in soil and groundwater, QJEGH, 37, 347–359, https://doi.org/10.1144/1470-9236/04-005, 2004.

Bussink, D. W.: Ammonia volatilization from grassland receiving nitrogen fertilizer and rotationally grazed by dairy cattle, Fertilizer Research, 33, 257–265, https://doi.org/10.1007/BF01050881, 1992.

Bussink, D. W. and Oenema, O.: Ammonia volatilization from dairy farming systems in temperate areas: a review, 15, n.d.

Butterbach-Bahl, K., Gundersen, P., Ambus, P., Augustin, J., Beier, C., Boeckx, P., Dannenmann, M., Gimeno, B. S., Ibrom, A., Kiese, R., Kitzler, B., Rees, R. M., Smith, K. A., Stevens, C., Vesala, T., and Zechmeister-Boltenstern, S.: Nitrogen processes in terrestrial ecosystems, in: The European Nitrogen Assessment, edited by: Sutton, M. A., Howard, C. M., Erisman, J. W., Billen, G., Bleeker, A., Grennfelt, P., van Grinsven, H., and Grizzetti, B.,

Cambridge University Press, Cambridge, 99–125, https://doi.org/10.1017/CBO9780511976988.009, 2011a.

Butterbach-Bahl, K., Gundersen, P., Ambus, P., Augustin, J., Beier, C., Boeckx, P., Dannenmann, M., Gimeno, B. S., Ibrom, A., Kiese, R., Kitzler, B., Rees, R. M., Smith, K. A., Stevens, C., Vesala, T., and Zechmeister-Boltenstern, S.: Nitrogen processes in terrestrial ecosystems, in: The European Nitrogen Assessment, vol. Chapter 6, Cambridge University Press, 99–125, 2011b.

Cabrera, M. L., Kissel, D. E., and Bock, B. R.: Urea hydrolysis in soil: Effects of urea concentration and soil pH, Soil Biology and Biochemistry, 23, 1121–1124, https://doi.org/10.1016/0038-0717(91)90023-D, 1991.

Carran, R. A., Ball, P. R., Theobald, P. W., and Collins, M. E. G.: Soil nitrogen balances in urine-affected areas under two moisture regimes in Southland, New Zealand Journal of Experimental Agriculture, 10, 377–381, https://doi.org/10.1080/03015521.1982.10427902, 1982.

Chantigny, M. H., Rochette, P., Angers, D. A., Massé, D., and Côté, D.: Ammonia Volatilization and Selected Soil Characteristics Following Application of Anaerobically Digested Pig Slurry, Soil Sci. Soc. Am. J., 68, 306–312, https://doi.org/10.2136/sssaj2004.3060, 2004.

Chen, Y., Shen, H., Kaiser, J., Hu, Y., Capps, S. L., Zhao, S., Hakami, A., Shih, J.-S., Pavur, G. K., Turner, M. D., Henze, D. K., Resler, J., Nenes, A., Napelenok, S. L., Bash, J. O., Fahey, K. M., Carmichael, G. R., Chai, T., Clarisse, L., Coheur, P.-F., Van Damme, M., and Russell, A. G.: High-resolution hybrid inversion of IASI ammonia columns to constrain US ammonia emissions using the CMAQ adjoint model, Atmos. Chem. Phys., 21, 2067–2082, https://doi.org/10.5194/acp-21-2067-2021, 2021.

Choirunnisa, R., Luthfi, N., Prima, A., Restitrisnani, V., Subagyo, W., Arifin, M., Rianto, E., and Purnomoadi, A.: Comparison of N excretion between Goat and Sheep, IOP Conf. Ser.: Earth Environ. Sci., 247, 012018, https://doi.org/10.1088/1755-1315/247/1/012018, 2019.

Chow, V. T., Maidment, D. R., and Mays, L. W.: Applied hydrology, [Nachdr.]., internat. ed. 1988., McGraw-Hill, New York, 572 pp., 1988.

Corre, M. D., Brumme, R., Veldkamp, E., and Beese, F. O.: Changes in nitrogen cycling and retention processes in soils under spruce forests along a nitrogen enrichment gradient in Germany, Global Change Biol, 13, 1509–1527, https://doi.org/10.1111/j.1365-2486.2007.01371.x, 2007.

Cortus, E. L., Lin, X.-J., Zhang, R., and Heber, A. J.: National Air Emissions Monitoring Study: Emissions Data from Two Broiler Chicken Houses in California - Site CA1B. Final Report, Purdue University, 2010a.

Cortus, E. L., Lin, X.-J., Zhang, R., and Heber, A. J.: National Air Emissions Monitoring Study: Emissions Data from Two Layer Houses in California - Site CA2B. Final Report, Purdue University, 2010b.

Crippa, M., Guizzardi, D., Muntean, M., Schaaf, E., Dentener, F., van Aardenne, J. A., Monni, S., Doering, U., Olivier, J. G. J., Pagliari, V., and Janssens-Maenhout, G.: Gridded emissions of air pollutants for the period 1970–2012 within EDGAR v4.3.2, Earth Syst. Sci. Data, 10, 1987–2013, https://doi.org/10.5194/essd-10-1987-2018, 2018.

Curtin, D., Peterson, M. E., Qiu, W., and Fraser, P. M.: Predicting soil pH changes in response to application of urea and sheep urine, J. environ. qual., 49, 1445–1452, https://doi.org/10.1002/jeq2.20130, 2020.

Danish Ministry of Climate, Energy and Utilities: Denmark's Integrated National Energy and Climate Plan under the REGULATION OF THE EUROPEAN PARLIAMENT AND OF THE COUNCIL on the Governance of the Energy Union and Climate Action, Denmark, 2019.

Dardanelli, J. L., Ritchie, J. T., Calmon, M., Andriani, J. M., and Collino, D. J.: An empirical model for root water uptake, Field Crops Research, 87, 59–71, https://doi.org/10.1016/j.fcr.2003.09.008, 2004.

Dawar, K., Zaman, M., Rowarth, J. S., Blennerhassett, J., and Turnbull, M. H.: Urea hydrolysis and lateral and vertical movement in the soil: effects of urease inhibitor and irrigation, Biol Fertil Soils, 47, 139–146, https://doi.org/10.1007/s00374-010-0515-3, 2011.

DEFRA: Clean Air Strategy, UK, 2019.

Dentener, F. J. and Crutzen, P. J.: A three-dimensional model of the global ammonia cycle, J Atmos Chem, 19, 331–369, https://doi.org/10.1007/BF00694492, 1994.

Dise, N. B., Rothwell, J. J., Gauci, V., van der Salm, C., and de Vries, W.: Predicting dissolved inorganic nitrogen leaching in European forests using two independent databases, Science of The Total Environment, 407, 1798–1808, https://doi.org/10.1016/j.scitotenv.2008.11.003, 2009.

Dise, N. B., Ashmore, M., Belyazid, S., Bleeker, A., Bobbink, R., de Vries, W., Erisman, J. W., Spranger, T., Stevens, C. J., and van den Berg, L.: Nitrogen as a threat to European terrestrial biodiversity, in: The European Nitrogen Assessment, edited by: Sutton, M. A., Howard, C. M., Erisman, J. W., Billen, G., Bleeker, A., Grennfelt, P., van Grinsven, H., and Grizzetti, B., Cambridge University Press, Cambridge, 463–494, https://doi.org/10.1017/CBO9780511976988.023, 2011.

Dong, R. L., Zhao, G. Y., Chai, L. L., and Beauchemin, K. A.: Prediction of urinary and fecal nitrogen excretion by beef cattle, Journal of Animal Science, 92, 4669–4681, https://doi.org/10.2527/jas.2014-8000, 2014.

Durand, P., Breuer, L., Johnes, P. J., Billen, G., Butturini, A., Pinay, G., van Grinsven, H., Garnier, J., Rivett, M., Reay, D. S., Curtis, C., Siemens, J., Maberly, S., Kaste, Ø., Humborg, C., Loeb, R., de Klein, J., Hejzlar, J., Skoulikidis, N., Kortelainen, P., Lepistö, A., and Wright, R.: Nitrogen processes in aquatic ecosystems, in: The European Nitrogen Assessment, edited by: Sutton, M. A., Howard, C. M., Erisman, J. W., Billen, G., Bleeker, A., Grennfelt, P., van Grinsven, H., and Grizzetti, B., Cambridge University Press, Cambridge, 126–146, https://doi.org/10.1017/CBO9780511976988.010, 2011.

Dutta, B., Congreves, K. A., Smith, W. N., Grant, B. B., Rochette, P., Chantigny, M. H., and Desjardins, R. L.: Improving DNDC model to estimate ammonia loss from urea fertilizer application in temperate agroecosystems, Nutr Cycl Agroecosyst, 106, 275–292, https://doi.org/10.1007/s10705-016-9804-z, 2016.

EDGAR: Emissions Database for Global Atmospheric Research v6.1, available at: http://edgar.jrc.ec.europa.eu/ (last access: 21 May 2023), 2022.

Elliott, H. A. and Collins, N. E.: Factors Affecting Ammonia Release in Broiler Houses, Transactions of the ASAE, 25, 0413–0418, https://doi.org/10.13031/2013.33545, 1982.

Erisman, J. W., Sutton, M. A., Galloway, J., Klimont, Z., and Winiwarter, W.: How a century of ammonia synthesis changed the world, nature geoscience, 1, 2008.

FAO: Global Livestock Environmental Assessment Model, 121, 2018a.

FAO: Nitrogren inputs to agricultural soils from livestock manure: new statistics, Food and Agriculture Organization of the United Nations, Rome, 2018b.

Farquhar, G. D., Firth, P. M., Wetselaar, R., and Weir, B.: On the Gaseous Exchange of Ammonia between Leaves and the Environment: Determination of the Ammonia Compensation Point, Plant Physiol., 66, 710–714, https://doi.org/10.1104/pp.66.4.710, 1980.

Fischer, K., Burchill, W., Lanigan, G. J., Kaupenjohann, M., Chambers, B. J., Richards, K. G., and Forrestal, P. J.: Ammonia emissions from cattle dung, urine and urine with dicyandiamide in a temperate grassland, Soil Use Manage, 32, 83–91, https://doi.org/10.1111/sum.12203, 2016.

Flechard, C. R., Massad, R.-S., Loubet, B., Personne, E., Simpson, D., Bash, J. O., Cooter, E. J., Nemitz, E., and Sutton, M. A.: Advances in understanding, models and parameterizations of biosphere-atmosphere ammonia exchange, Biogeosciences, 10, 5183–5225, https://doi.org/10.5194/bg-10-5183-2013, 2013.

Fowler, D., Coyle, M., Skiba, U., Sutton, M. A., Cape, J. N., Reis, S., Sheppard, L. J., Jenkins, A., Grizzetti, B., Galloway, J. N., Vitousek, P., Leach, A., Bouwman, A. F., Butterbach-Bahl, K., Dentener, F., Stevenson, D., Amann, M., and Voss, M.: The global nitrogen cycle in the twenty-first century, Phil. Trans. R. Soc. B, 368, 20130164, https://doi.org/10.1098/rstb.2013.0164, 2013.

Frank, D. A. and Zhang, Y.: Ammonia volatilization from a seasonally and spatially variable grazed grassland: Yellowstone National Park, Biogeochemistry, 36, 1997.

Fu, X., Wang, S. X., Ran, L. M., Pleim, J. E., Cooter, E., Bash, J. O., Benson, V., and Hao, J. M.: Estimating NH₃ emissions from agricultural fertilizer application in China using the bi-directional CMAQ model coupled to an agro-ecosystem model, Atmos. Chem. Phys., 15, 6637–6649, https://doi.org/10.5194/acp-15-6637-2015, 2015.

Galloway, J. N., Aber, J. D., Erisman, J. W., Seitzinger, S. P., Howarth, R. W., Cowling, E. B., and Cosby, B. J.: The Nitrogen Cascade, BioScience, 53, 341, https://doi.org/10.1641/0006-3568(2003)053[0341:TNC]2.0.CO;2, 2003a.

Galloway, JamesN., Aber, J. D., Erisman, J. W., Seitzinger, S. P., Howarth, R. W., Cowling, E. B., and Cosby, B. J.: The Nitrogen Cascade, BioScience, 53, 341, https://doi.org/10.1641/0006-3568(2003)053[0341:TNC]2.0.CO;2, 2003b.

Ge, Y., Vieno, M., Stevenson, D. S., Wind, P., and Heal, M. R.: A new assessment of global and regional budgets, fluxes, and lifetimes of atmospheric reactive N and S gases and aerosols, Atmos. Chem. Phys., 22, 8343–8368, https://doi.org/10.5194/acp-22-8343-2022, 2022.

Ge, Y., Vieno, M., Stevenson, D. S., Wind, P., and Heal, M. R.: Global sensitivities of reactive N and S gas and particle concentrations and deposition to precursor emissions reductions, Atmos. Chem. Phys., 23, 6083–6112, https://doi.org/10.5194/acp-23-6083-2023, 2023.

Gilmour, J. T.: The Effects of Soil Properties on Nitrification and Nitrification Inhibition, 1984.

Gilmour, J. T., Cogger, C. G., Jacobs, L. W., Evanylo, G. K., and Sullivan, D. M.: Decomposition and Plant-Available Nitrogen in Biosolids, Journal of Environment Quality, 32, 1498, https://doi.org/10.2134/jeq2003.1498, 2003.

Glendining, M. J., Powlson, D. S., Poulton, P. R., Bradbury, N. J., Palazzo, D., and Ll, X.: The effects of long-term applications of inorganic nitrogen fertilizer on soil nitrogen in the Broadbalk Wheat Experiment, J. Agric. Sci., 127, 347–363, https://doi.org/10.1017/S0021859600078527, 1996.

Gruber, N. and Galloway, J. N.: An Earth-system perspective of the global nitrogen cycle, Nature, 451, 293–296, https://doi.org/10.1038/nature06592, 2008.

Gu, B., Zhang, L., Van Dingenen, R., Vieno, M., Van Grinsven, H. J., Zhang, X., Zhang, S., Chen, Y., Wang, S., Ren, C., Rao, S., Holland, M., Winiwarter, W., Chen, D., Xu, J., and Sutton, M. A.: Abating ammonia is more cost-effective than nitrogen oxides for mitigating $PM_{2.5}$ air pollution, Science, 374, 758–762, https://doi.org/10.1126/science.abf8623, 2021.

Gundersen, P., Callesen, I., and De Vries, W.: Nitrate leaching in forest ecosystems is related to forest floor C/N ratios, in: Nitrogen, the Confer-N-s, Elsevier, 403–407, https://doi.org/10.1016/B978-0-08-043201-4.50058-7, 1998.

Gyldenkærne, S.: A dynamical ammonia emission parameterization for use in air pollution models, J. Geophys. Res., 110, D07108, https://doi.org/10.1029/2004JD005459, 2005a.

Gyldenkærne, S.: A dynamical ammonia emission parameterization for use in air pollution models, J. Geophys. Res., 110, D07108, https://doi.org/10.1029/2004JD005459, 2005b.

Haynes, R. J. and Williams, P. H.: Nutrient cycling and soil fertilizer in the grazed pasture ecosystem, Advances in Agronomy, 1993.

Henderson, S. M. and Perry, R. L.: Agricultural process engineering, 3d ed., Avi Pub. Co, Westport, Conn, 442 pp., 1976.

Hersbach, H., Bell, B., Berrisford, P., Hirahara, S., Horányi, A., Muñoz-Sabater, J., Nicolas, J., Peubey, C., Radu, R., Schepers, D., Simmons, A., Soci, C., Abdalla, S., Abellan, X., Balsamo, G., Bechtold, P., Biavati, G., Bidlot, J., Bonavita, M., Chiara, G., Dahlgren, P., Dee, D., Diamantakis, M., Dragani, R., Flemming, J., Forbes, R., Fuentes, M., Geer, A., Haimberger, L., Healy, S., Hogan, R. J., Hólm, E., Janisková, M., Keeley, S., Laloyaux, P., Lopez, P., Lupu, C., Radnoti, G., Rosnay, P., Rozum, I., Vamborg, F., Villaume, S., and Thépaut, J.: The ERA5 global reanalysis, Q.J.R. Meteorol. Soc., 146, 1999–2049, https://doi.org/10.1002/qj.3803, 2020.

Hertel, O., Reis, S., Skjøth, C. A., Bleeker, A., Harrison, R., Cape, J. N., Fowler, D., Skiba, U., Simpson, D., Jickells, T., Baker, A., Kulmala, M., Gyldenkærne, S., Sørensen, L. L., and Erisman, J. W.: Nitrogen processes in the atmosphere, in: The European Nitrogen Assessment, edited by: Sutton, M. A., Howard, C. M., Erisman, J. W., Billen, G., Bleeker, A., Grennfelt, P., van Grinsven, H., and Grizzetti, B., Cambridge University Press, 177–208, https://doi.org/10.1017/CBO9780511976988.012, 2011.

Hoogendoorn, C. J., Betteridge, K., Ledgard, S. F., Costall, D. A., Park, Z. A., and Theobald, P. W.: Nitrogen leaching from sheep-, cattle- and deer-grazed pastures in the Lake Taupo catchment in New Zealand, Anim. Prod. Sci., 51, 416, https://doi.org/10.1071/AN10179, 2011.

Hurtt, G. C., Chini, L., Sahajpal, R., Frolking, S., Bodirsky, B. L., Calvin, K., Doelman, J. C., Fisk, J., Fujimori, S., Klein Goldewijk, K., Hasegawa, T., Havlik, P., Heinimann, A., Humpenöder, F., Jungclaus, J., Kaplan, J. O., Kennedy, J., Krisztin, T., Lawrence, D., Lawrence, P., Ma, L., Mertz, O., Pongratz, J., Popp, A., Poulter, B., Riahi, K., Shevliakova, E., Stehfest, E., Thornton, P., Tubiello, F. N., van Vuuren, D. P., and Zhang, X.: Harmonization of global land use change and management for the period 850–2100 (LUH2) for CMIP6, Geosci. Model Dev., 13, 5425–5464, https://doi.org/10.5194/gmd-13-5425-2020, 2020.

Hutchings, N. J., Sommer, S. G., and Jarvis, S. C.: A model of ammonia volatilization from a grazing livestock farm, Atmospheric Environment, 30, 589–599, https://doi.org/10.1016/1352-2310(95)00315-0, 1996.

Intergovernmental Panel On Climate Change: Climate Change 2021 – The Physical Science Basis: Working Group I Contribution to the Sixth Assessment Report of the Intergovernmental Panel on Climate Change, 1st ed., Cambridge University Press, https://doi.org/10.1017/9781009157896, 2023.

Isaksen, I. S. A., Granier, C., Myhre, G., Berntsen, T. K., Dalsøren, S. B., Gauss, M., Klimont, Z., Benestad, R., Bousquet, P., Collins, W., Cox, T., Eyring, V., Fowler, D., Fuzzi, S., Jöckel, P., Laj, P., Lohmann, U., Maione, M., Monks, P., Prevot, A. S. H., Raes, F., Richter, A., Rognerud, B., Schulz, M., Shindell, D., Stevenson, D. S., Storelvmo, T., Wang, W.-C., Van Weele, M., Wild, M., and Wuebbles, D.: Atmospheric composition change: Climate–Chemistry interactions, Atmospheric Environment, 43, 5138–5192, https://doi.org/10.1016/j.atmosenv.2009.08.003, 2009.

Jacob, D. J.: Introduction to Atmospheric Chemistry, Princeton University Press, https://doi.org/10.1515/9781400841547, 2000.

Jägermeyr, J., Müller, C., Ruane, A. C., Elliott, J., Balkovic, J., Castillo, O., Faye, B., Foster, I., Folberth, C., Franke, J. A., Fuchs, K., Guarin, J. R., Heinke, J., Hoogenboom, G., Iizumi, T., Jain, A. K., Kelly, D., Khabarov, N., Lange, S., Lin, T.-S., Liu, W., Mialyk, O., Minoli, S., Moyer, E. J., Okada, M., Phillips, M., Porter, C., Rabin, S. S., Scheer, C., Schneider, J. M., Schyns, J. F., Skalsky, R., Smerald, A., Stella, T., Stephens, H., Webber, H., Zabel, F., and Rosenzweig, C.: Climate impacts on global agriculture emerge earlier in new generation of climate and crop models, Nat Food, 2, 873–885, https://doi.org/10.1038/s43016-021-00400-y, 2021.

Jarvis, S. C., Hatch, D. J., and Lockyer, D. R.: Ammonia fluxes from grazed grassland: annual losses from cattle production systems and their relation to nitrogen inputs, J. Agric. Sci., 113, 99–108, https://doi.org/10.1017/S0021859600084677, 1989a.

Jarvis, S. C., Hatch, D. J., and Roberts, D. H.: The effects of grassland management on nitrogen losses from grazed swards through ammonia volatilization; the relationship to excretal N returns from cattle, J. Agric. Sci., 112, 205–216, https://doi.org/10.1017/S0021859600085117, 1989b.

Jarvis, S. C., Hatch, D. J., Orr, R. J., and Reynolds, S. E.: Micrometeorological studies of ammonia emission from sheep grazed swards, J. Agric. Sci., 117, 101–109, https://doi.org/10.1017/S0021859600079028, 1991.

Jiang, J., Stevenson, D. S., Uwizeye, A., Tempio, G., and Sutton, M. A.: A climate-dependent global model of ammonia emissions from chicken farming, Biogeosciences, 18, 135–158, https://doi.org/10.5194/bg-18-135-2021, 2021.

Jørgensen, H., Prapaspongsa, T., Vu, V. T. K., and Poulsen, H. D.: Models to quantify excretion of dry matter, nitrogen, phosphorus and carbon in growing pigs fed regional diets, J Animal Sci Biotechnol, 4, 42, https://doi.org/10.1186/2049-1891-4-42, 2013.

Kang, Y., Liu, M., Song, Y., Huang, X., Yao, H., Cai, X., Zhang, H., Kang, L., Liu, X., Yan, X., He, H., Zhang, Q., Shao, M., and Zhu, T.: High-resolution ammonia emissions inventories in China from 1980 to 2012, Atmos. Chem. Phys., 16, 2043–2058, https://doi.org/10.5194/acp-16-2043-2016, 2016.

Khater, E. S. G.: Some Physical and Chemical Properties of Compost, Int J Waste Resources, 05, https://doi.org/10.4172/2252-5211.1000172, 2015.

Krupa, S. V.: Effects of atmospheric ammonia (NH3) on terrestrial vegetation: a review, Environmental Pollution, 124, 179–221, https://doi.org/10.1016/S0269-7491(02)00434-7, 2003.

Kurokawa, J., Ohara, T., Morikawa, T., Hanayama, S., Janssens-Maenhout, G., Fukui, T., Kawashima, K., and Akimoto, H.: Emissions of air pollutants and greenhouse gases over Asian regions during 2000–2008: Regional Emission inventory in ASia (REAS) version 2, Atmos. Chem. Phys., 13, 11019–11058, https://doi.org/10.5194/acp-13-11019-2013, 2013.

Laubach, J., Taghizadeh-Toosi, A., Sherlock, R. R., and Kelliher, F. M.: Measuring and modelling ammonia emissions from a regular pattern of cattle urine patches, Agricultural and Forest Meteorology, 156, 1–17, https://doi.org/10.1016/j.agrformet.2011.12.007, 2012.

Laubach, J., Taghizadeh-Toosi, A., Gibbs, S. J., Sherlock, R. R., Kelliher, F. M., and Grover, S. P. P.: Ammonia emissions from cattle urine and dung excreted on pasture, Biogeosciences, 10, 327–338, https://doi.org/10.5194/bg-10-327-2013, 2013.

Li, S., Zheng, X., Zhang, W., Han, S., Deng, J., Wang, K., Wang, R., Yao, Z., and Liu, C.: Modeling ammonia volatilization following the application of synthetic fertilizers to cultivated uplands with calcareous soils using an improved DNDC biogeochemistry model, Science of The Total Environment, 660, 931–946, https://doi.org/10.1016/j.scitotenv.2018.12.379, 2019.

Lim, T. T., Chen, L., Jin, Y., Ha, C., Ni, J.-Q., Bogan, B. W., Ramirez, J. C., Diehl, C., Xiao, C., and Heber, A. J.: National Air Emissions Monitoring Study: Emissions Data from Four Swine Finishing Rooms - Site IN3B. Final Report, Purdue University, 2010a.

Lim, T. T., Jin, Y., Ha, J. H., and Heber, A. J.: National Air Emissions Monitoring Study: Emissions Data from Two Freestall Barns and a Milking Center at a Dairy Farm in Indiana - Site IN5B, Purdue University, 2010b.

Liss, P. S.: Processes of gas exchange across an air-water interface, Deep-sea Research, 20, 221–238, 1973.

Liss, P. S. and Slater, P. G.: Flux of Gases across the Air-Sea Interface, Nature, 247, 181–184, https://doi.org/10.1038/247181a0, 1974.

Liu, Z., Rieder, H. E., Schmidt, C., Mayer, M., Guo, Y., Winiwarter, W., and Zhang, L.: Optimal reactive nitrogen control pathways identified for cost-effective PM2.5 mitigation in Europe, Nat Commun, 14, 4246, https://doi.org/10.1038/s41467-023-39900-9, 2023.

Lockyer, D. R. and Whitehead, D. C.: Volatilization of ammonia from cattle urine applied to grassland, Soil Biology and Biochemistry, 22, 1137–1142, https://doi.org/10.1016/0038-0717(90)90040-7, 1990.

Lu, C. and Tian, H.: Global nitrogen and phosphorus fertilizer use for agriculture production in the past half century: shifted hot spots and nutrient imbalance, 2017.

Malhi, S. S. and McGill, W. B.: Nitrification in three Alberta soils: Effect of temperature, moisture and substrate concentration, Soil Biology and Biochemistry, 14, 393–399, https://doi.org/10.1016/0038-0717(82)90011-6, 1982.

Marsden, K. A., Lush, L., Holmberg, Jon. A., Whelan, M. J., King, A. J., Wilson, R. P., Charteris, A. F., Cardenas, L. M., Jones, D. L., and Chadwick, D. R.: Sheep urination frequency, volume, N excretion and chemical composition: Implications for subsequent agricultural N losses, Agriculture, Ecosystems & Environment, 302, 107073, https://doi.org/10.1016/j.agee.2020.107073, 2020.

Millington, R. J. and Quirk, J. P.: Permeability of porous solids, Trans. Faraday Soc., 57, 1200, https://doi.org/10.1039/tf9615701200, 1961.

Misselbrook, T., Fleming, H., Camp, V., Umstatter, C., Duthie, C.-A., Nicoll, L., and Waterhouse, T.: Automated monitoring of urination events from grazing cattle, Agriculture, Ecosystems & Environment, 230, 191–198, https://doi.org/10.1016/j.agee.2016.06.006, 2016.

Misselbrook, T. H. and Powell, J. M.: Influence of Bedding Material on Ammonia Emissions from Cattle Excreta, Journal of Dairy Science, 88, 4304–4312, https://doi.org/10.3168/jds.S0022-0302(05)73116-7, 2005.

Misselbrook, T. H., Nicholson, F. A., and Chambers, B. J.: Predicting ammonia losses following the application of livestock manure to land, Bioresource Technology, 96, 159–168, https://doi.org/10.1016/j.biortech.2004.05.004, 2005.

Misselbrook, T. H., Scholefield, D., and Parkinson, R.: Using time domain reflectometry to characterize cattle and pig slurry infiltration into soil, Soil Use and Management, 21, 167–172, https://doi.org/10.1111/j.1475-2743.2005.tb00121.x, 2006.

Monfreda, C., Ramankutty, N., and Foley, J. A.: Farming the planet: 2. Geographic distribution of crop areas, yields, physiological types, and net primary production in the year 2000: GLOBAL CROP AREAS AND YIELDS IN 2000, Global Biogeochem. Cycles, 22, n/a-n/a, https://doi.org/10.1029/2007GB002947, 2008.

Móring, A., Vieno, M., Doherty, R. M., Laubach, J., Taghizadeh-Toosi, A., and Sutton, M. A.: A process-based model for ammonia emission from urine patches, GAG (Generation of

Ammonia from Grazing): description and sensitivity analysis, Biogeosciences, 13, 1837–1861, https://doi.org/10.5194/bg-13-1837-2016, 2016.

Móring, A., Vieno, M., Doherty, R. M., Milford, C., Nemitz, E., Twigg, M. M., Horváth, L., and Sutton, M. A.: Process-based modelling of NH_3 exchange with grazed grasslands, Biogeosciences, 14, 4161–4193, https://doi.org/10.5194/bg-14-4161-2017, 2017.

Mueller, N. D., Gerber, J. S., Johnston, M., Ray, D. K., Ramankutty, N., and Foley, J. A.: Closing yield gaps through nutrient and water management, Nature, 490, 254–257, https://doi.org/10.1038/nature11420, 2012.

Murdoch, P. S. and Stoddard, J. L.: The role of nitrate in the acidification of streams in the Catskill Mountains of New York, Water Resour. Res., 28, 2707–2720, https://doi.org/10.1029/92WR00953, 1992.

Nahm, K. H.: Evaluation of the nitrogen content in poultry manure, World's Poultry Science Journal, 59, 77–88, https://doi.org/10.1079/WPS20030004, 2003.

Nemitz, E., Sutton, M. A., Schjoerring, J. K., Husted, S., and Paul Wyers, G.: Resistance modelling of ammonia exchange over oilseed rape, Agricultural and Forest Meteorology, 105, 405–425, https://doi.org/10.1016/S0168-1923(00)00206-9, 2000.

Nemitz, E., Milford, C., and Sutton, M. A.: A two-layer canopy compensation point model for describing bi-directional biosphere-atmosphere exchange of ammonia, Q.J Royal Met. Soc., 127, 815–833, https://doi.org/10.1002/qj.49712757306, 2001.

Ni, J.: Mechanistic Models of Ammonia Release from Liquid Manure: a Review, Journal of Agricultural Engineering Research, 72, 1–17, https://doi.org/10.1006/jaer.1998.0342, 1999.

Norton, J. M. and Stark, J. M.: Regulation and Measurement of Nitrification in Terrestrial Systems, in: Methods in Enzymology, vol. 486, Elsevier, 343–368, https://doi.org/10.1016/B978-0-12-381294-0.00015-8, 2011.

Parton, W. J., Mosier, A. R., Ojima, D. S., Valentine, D. W., Schimel, D. S., Weier, K., and Kulmala, A. E.: Generalized model for N_2 and N_2O production from nitrification and denitrification, Global Biogeochem. Cycles, 10, 401–412, https://doi.org/10.1029/96GB01455, 1996a.

Parton, W. J., Mosier, A. R., Ojima, D. S., Valentine, D. W., Schimel, D. S., Weier, K., and Kulmala, A. E.: Generalized model for N_2 and N_2O production from nitrification and denitrification, Global Biogeochem. Cycles, 10, 401–412, https://doi.org/10.1029/96GB01455, 1996b.

Parton, W. J., Holland, E. A., Del Grosso, S. J., Hartman, M. D., Martin, R. E., Mosier, A. R., Ojima, D. S., and Schimel, D. S.: Generalized model for NO_x and N_2O emissions from soils, J. Geophys. Res., 106, 17403–17419, https://doi.org/10.1029/2001JD900101, 2001a.

Parton, W. J., Holland, E. A., Del Grosso, S. J., Hartman, M. D., Martin, R. E., Mosier, A. R., Ojima, D. S., and Schimel, D. S.: Generalized model for NO_x and N_2O emissions from soils, J. Geophys. Res., 106, 17403–17419, https://doi.org/10.1029/2001JD900101, 2001b.

Paulot, F., Jacob, D. J., Pinder, R. W., Bash, J. O., Travis, K., and Henze, D. K.: Ammonia emissions in the United States, European Union, and China derived by high-resolution inversion of ammonium wet deposition data: Interpretation with a new agricultural emissions inventory (MASAGE_NH3), J. Geophys. Res. Atmos., 119, 4343–4364, https://doi.org/10.1002/2013JD021130, 2014.

Paulot, F., Ginoux, P., Cooke, W. F., Donner, L. J., Fan, S., Lin, M.-Y., Mao, J., Naik, V., and Horowitz, L. W.: Sensitivity of nitrate aerosols to ammonia emissions and to nitrate chemistry: implications for present and future nitrate optical depth, Atmos. Chem. Phys., 16, 1459–1477, https://doi.org/10.5194/acp-16-1459-2016, 2016.

Perry, R. H. and Green, D. W. (Eds.): Perry's chemical engineers' handbook, 8th ed., McGraw-Hill, New York, 1 pp., 2008.

Personne, E., Loubet, B., Herrmann, B., Mattsson, M., Schjoerring, J. K., Nemitz, E., Sutton, M. A., and Cellier, P.: SURFATM-NH3: a model combining the surface energy balance and bi-directional exchanges of ammonia applied at the field scale, 2009.

Pinder, R. W., Pekney, N. J., Davidson, C. I., and Adams, P. J.: A process-based model of ammonia emissions from dairy cows: improved temporal and spatial resolution, Atmospheric Environment, 38, 1357–1365, https://doi.org/10.1016/j.atmosenv.2003.11.024, 2004.

Pinder, R. W., Adams, P. J., and Pandis, S. N.: Ammonia Emission Controls as a Cost-Effective Strategy for Reducing Atmospheric Particulate Matter in the Eastern United States, Environ. Sci. Technol., 41, 380–386, https://doi.org/10.1021/es060379a, 2007.

Ramanantenasoa, M. M. J., Génermont, S., Gilliot, J.-M., Bedos, C., and Makowski, D.: Meta-modeling methods for estimating ammonia volatilization from nitrogen fertilizer and manure applications, Journal of Environmental Management, 236, 195–205, https://doi.org/10.1016/j.jenvman.2019.01.066, 2019.

Reed, K. F., Moraes, L. E., Casper, D. P., and Kebreab, E.: Predicting nitrogen excretion from cattle, Journal of Dairy Science, 98, 3025–3035, https://doi.org/10.3168/jds.2014-8397, 2015.

Ren, C., Huang, X., Liu, T., Song, Y., Wen, Z., Liu, X., Ding, A., and Zhu, T.: A dynamic ammonia emission model and the online coupling with WRF–Chem (WRF–SoilN–Chem v1.0): development and regional evaluation in China, Geosci. Model Dev., 16, 1641–1659, https://doi.org/10.5194/gmd-16-1641-2023, 2023.

Riddick, S., Ward, D., Hess, P., Mahowald, N., Massad, R., and Holland, E.: Estimate of changes in agricultural terrestrial nitrogen pathways and ammonia emissions from 1850 to present in the Community Earth System Model, Biogeosciences, 13, 3397–3426, https://doi.org/10.5194/bg-13-3397-2016, 2016.

Riddick, S. N., Blackall, T. D., Dragosits, U., Tang, Y. S., Moring, A., Daunt, F., Wanless, S., Hamer, K. C., and Sutton, M. A.: High temporal resolution modelling of environmentally-dependent seabird ammonia emissions: Description and testing of the GUANO model, Atmospheric Environment, 161, 48–60, https://doi.org/10.1016/j.atmosenv.2017.04.020, 2017a.

Riddick, S. N., Blackall, T. D., Dragosits, U., Tang, Y. S., Moring, A., Daunt, F., Wanless, S., Hamer, K. C., and Sutton, M. A.: High temporal resolution modelling of environmentally-dependent seabird ammonia emissions: Description and testing of the GUANO model, Atmospheric Environment, 161, 48–60, https://doi.org/10.1016/j.atmosenv.2017.04.020, 2017b.

Riedo, M., Grub, A., Rosset, M., and Fuhrer, J.: A pasture simulation model for dry matter production, and fluxes of carbon, nitrogen, water and energy, Ecological Modelling, 105, 141–183, https://doi.org/10.1016/S0304-3800(97)00110-5, 1998.

Riedo, M., Milford, C., Schmid, M., and Sutton, M. A.: Coupling soil-plant-atmosphere exchange of ammonia with ecosystem functioning in grasslands, Ecological Modelling, 2002.

Rodríguez, S. B., Alonso-Gaite, A., and Álvarez-Benedí, J.: Characterization of Nitrogen Transformations, Sorption and Volatilization Processes In Urea Fertilized Soils, Vadose Zone Journal, 4, 329–336, https://doi.org/10.2136/vzj2004.0102, 2005.

Ryden, J. C., Whitehead, D. C., Lockyer, D. R., Thompson, R. B., Skinner, J. H., and Garwood, E. A.: Ammonia emission from grassland and livestock production systems in the UK, Environmental Pollution, 48, 173–184, https://doi.org/10.1016/0269-7491(87)90032-7, 1987.

Saarijärvi, K. and Virkajärvi, P.: Nitrogen dynamics of cattle dung and urine patches on intensively managed boreal pasture, J. Agric. Sci., 147, 479–491, https://doi.org/10.1017/S0021859609008727, 2009.

Saarijärvi, K., Mattila, P. K., and Virkajärvi, P.: Ammonia volatilization from artificial dung and urine patches measured by the equilibrium concentration technique (JTI method), Atmospheric Environment, 40, 5137–5145, https://doi.org/10.1016/j.atmosenv.2006.03.052, 2006.

Seedorf, J., Hartung, J., Schröder, M., Linkert, K. H., Pedersen, S., Takai, H., Johnsen, J. O., Metz, J. H. M., Groot Koerkamp, P. W. G., Uenk, G. H., Phillips, V. R., Holden, M. R., Sneath, R. W., Short, J. L. L., White, R. P., and Wathes, C. M.: A Survey of Ventilation Rates in Livestock Buildings in Northern Europe, Journal of Agricultural Engineering Research, 70, 39–47, https://doi.org/10.1006/jaer.1997.0274, 1998a.

Seedorf, J., Hartung, J., Schröder, M., Linkert, K. H., Pedersen, S., Takai, H., Johnsen, J. O., Metz, J. H. M., Groot Koerkamp, P. W. G., Uenk, G. H., Phillips, V. R., Holden, M. R., Sneath, R. W., Short, J. L. L., White, R. P., and Wathes, C. M.: A Survey of Ventilation Rates in Livestock Buildings in Northern Europe, Journal of Agricultural Engineering Research, 70, 39–47, https://doi.org/10.1006/jaer.1997.0274, 1998b.

Seinfeld, J. H. and Pandis, S. N.: Atmospheric chemistry and physics: from air pollution to climate change, Third edition., John Wiley & Sons, Hoboken, New Jersey, 1 pp., 2016.

Selbie, D. R., Buckthought, L. E., and Shepherd, M. A.: The Challenge of the Urine Patch for Managing Nitrogen in Grazed Pasture Systems, in: Advances in Agronomy, vol. 129, Elsevier, 229–292, https://doi.org/10.1016/bs.agron.2014.09.004, 2015.

Seneviratne, S. I., Nicholls, N., Easterling, D., Goodess, C. M., Kanae, S., Kossin, J., Luo, Y., Marengo, J., McInnes, K., Rahimi, M., Reichstein, M., Sorteberg, A., Vera, C., Zhang, X., Rusticucci, M., Semenov, V., Alexander, L. V., Allen, S., Benito, G., Cavazos, T., Clague, J., Conway, D., Della-Marta, P. M., Gerber, M., Gong, S., Goswami, B. N., Hemer, M., Huggel, C., Van Den Hurk, B., Kharin, V. V., Kitoh, A., Tank, A. M. G. K., Li, G., Mason, S., McGuire, W., Van Oldenborgh, G. J., Orlowsky, B., Smith, S., Thiaw, W., Velegrakis, A., Yiou, P., Zhang, T., Zhou, T., and Zwiers, F. W.: Changes in Climate Extremes and their Impacts on the Natural Physical Environment, in: Managing the Risks of Extreme Events and Disasters to Advance Climate Change Adaptation, edited by: Field, C. B., Barros, V., Stocker, T. F., and Dahe, Q., Cambridge University Press, 109–230, https://doi.org/10.1017/CBO9781139177245.006, 2012.

Senior, C. A., Jones, C. G., Wood, R. A., Sellar, A., Belcher, S., Klein-Tank, A., Sutton, R., Walton, J., Lawrence, B., Andrews, T., and Mulcahy, J. P.: U.K. Community Earth System Modeling for CMIP6, J Adv Model Earth Syst, 12, https://doi.org/10.1029/2019MS002004, 2020.

Sherlock, R. and Goh, K.: Dynamics of ammonia volatilization from simulated urine patches and aqueous urea applied to pasture I. Field experiments, Fertilizer Research, 5, 181–195, https://doi.org/10.1007/BF01052715, 1984.

Sherlock, R. and Goh, K.: Dynamics of ammonia volatilization from simulated urine patches and aqueous urea applied to pasture. II. Theoretical derivation of a simplified model, Fertilizer Research, 6, 3–22, https://doi.org/10.1007/BF01058161, 1985.

Sleutel, S., Neve, S., and Hofman, G.: Estimates of carbon stock changes in Belgian cropland, Soil Use and Management, 19, 166–171, https://doi.org/10.1111/j.1475-2743.2003.tb00299.x, 2003.

Sommer, S. G. and Hutchings, N. J.: Ammonia emission from field applied manure and its reduction—invited paper, European Journal of Agronomy, 15, 1–15, https://doi.org/10.1016/S1161-0301(01)00112-5, 2001.

Sommer, S. G., Zhang, G. Q., Bannink, A., Chadwick, D., Misselbrook, T., Harrison, R., Hutchings, N. J., Menzi, H., Monteny, G. J., Ni, J. Q., Oenema, O., and Webb, J.: Algorithms Determining Ammonia Emission from Buildings Housing Cattle and Pigs and from Manure Stores, in: Advances in Agronomy, vol. 89, Elsevier, 261–335, https://doi.org/10.1016/S0065-2113(05)89006-6, 2006.

Stange, C. F. and Neue, H.-U.: Measuring and modelling seasonal variation of gross nitrification rates in response to long-term fertilisation, Biogeosciences, 6, 2181–2192, https://doi.org/10.5194/bg-6-2181-2009, 2009.

Stelson, A. W. and Seinfeld, J. H.: Thermodynamic prediction of the water activity, NH4NO3 dissociation constant, density and refractive index for the NH4NO3-(NH4)2SO4-H2O system at 25°C, Atmospheric Environment (1967), 16, 2507–2514, https://doi.org/10.1016/0004-6981(82)90142-1, 1982.

Stelson, A. W., Friedlander, S. K., and Seinfeld, J. H.: A note on the equilibrium relationship between ammonia and nitric acid and particulate ammonium nitrate, Atmospheric Environment (1967), 13, 369–371, https://doi.org/10.1016/0004-6981(79)90293-2, 1979.

Sutton, M. A., Schjørring, J. K., and Wyers, G. P.: Plant-atmosphere exchange of ammonia, Phil. Trans. R. Soc. Lond. A, 351, 261–278, https://doi.org/10.1098/rsta.1995.0033, 1995.

Sutton, M. A., Dragosits, U., Tang, Y. S., and Fowler, D.: Ammonia emissions from non-agricultural sources in the UK, Atmospheric Environment, 34, 855–869, https://doi.org/10.1016/S1352-2310(99)00362-3, 2000.

Sutton, M. A., Nemitz, E., Theobald, M. R., Milford, C., Dorsey, J. R., Gallagher, M. W., Hensen, A., Jongejan, P. A. C., Erisman, J. W., Mattsson, M., Schjoerring, J. K., Cellier, P., Loubet, B., Roche, R., Neftel, A., Hermann, B., Jones, S. K., Lehman, B. E., Horvath, L., Weidinger, T., Rajkai, K., Burkhardt, J., Lopmeier, F. J., and Daemmgen, U.: Dynamics of ammonia exchange with cut grassland: strategy and implementation of the GRAMINAE Integrated Experiment, 2009a.

Sutton, M. A., Nemitz, E., Milford, C., Campbell, C., Erisman, J. W., Hensen, A., Cellier, P., David, M., Loubet, B., Personne, E., Schjoerring, J. K., Mattsson, M., Dorsey, J. R., Gallagher, M. W., Horvath, L., Weidinger, T., Meszaros, R., Dammgen, U., Neftel, A., Herrmann, B., Lehman, B. E., Flechard, C., and Burkhardt, J.: Dynamics of ammonia exchange with cut

grassland: synthesis of results and conclusions of the GRAMINAE Integrated Experiment, 2009b.

Sutton, M. A., Grinsven, H. Van, Billen, G., Bleeker, A., Bouwman, A. F., Bull, K., Erisman, J. W., Grennfelt, P., Grizzetti, B., Howard, C. M., Oenema, O., and Spranger, T.: Summary for policy makers Main messages Too much nitrogen harms the environment, The European Nitrogen Assessment, 2011a.

Sutton, M. A., Howard, C. M., Erisman, J. W., Billen, G., Bleeker, A., Grennfelt, P., Van Grinsven, H., and Grizzetti, B. (Eds.): The European Nitrogen Assessment: Sources, Effects and Policy Perspectives, 1st ed., Cambridge University Press, https://doi.org/10.1017/CBO9780511976988, 2011b.

Sutton, M. A., Oenema, O., Erisman, J. W., Leip, A., van Grinsven, H., and Winiwarter, W.: Too much of a good thing, Nature, 472, 159–161, https://doi.org/10.1038/472159a, 2011c.

Sutton, M. A., Reis, S., Riddick, S. N., Dragosits, U., Nemitz, E., Theobald, M. R., Tang, Y. S., Braban, C. F., Vieno, M., Dore, A. J., Mitchell, R. F., Wanless, S., Daunt, F., Fowler, D., Blackall, T. D., Milford, C., Flechard, C. R., Loubet, B., Massad, R., Cellier, P., Personne, E., Coheur, P. F., Clarisse, L., Van Damme, M., Ngadi, Y., Clerbaux, C., Skjøth, C. A., Geels, C., Hertel, O., Wichink Kruit, R. J., Pinder, R. W., Bash, J. O., Walker, J. T., Simpson, D., Horváth, L., Misselbrook, T. H., Bleeker, A., Dentener, F., and de Vries, W.: Towards a climate-dependent paradigm of ammonia emission and deposition, Phil. Trans. R. Soc. B, 368, 20130166, https://doi.org/10.1098/rstb.2013.0166, 2013.

Sutton, M. A., Van Dijk, N., Levy, P. E., Jones, M. R., Leith, I. D., Sheppard, L. J., Leeson, S., Sim Tang, Y., Stephens, A., Braban, C. F., Dragosits, U., Howard, C. M., Vieno, M., Fowler, D., Corbett, P., Naikoo, M. I., Munzi, S., Ellis, C. J., Chatterjee, S., Steadman, C. E., Móring, A., and Wolseley, P. A.: Alkaline air: changing perspectives on nitrogen and air pollution in an ammonia-rich world, Phil. Trans. R. Soc. A., 378, 20190315, https://doi.org/10.1098/rsta.2019.0315, 2020.

Sutton, M. A., Howard, C. M., Mason, K. E., Brownlie, W., and Cordovil, C.: Nitrogen Opportunities for Agriculture, Food & Environment: UNECE Guidance Document on Integrated Sustainable Nitrogen Management, 2022.

Thornley, J. H. M.: A Transport-resistance Model of Forest Growth and Partitioning, Annals of Botany, 68, 211–226, https://doi.org/10.1093/oxfordjournals.aob.a088246, 1991.

Thornley, J. H. M. and Cannell, M. G. R.: Nitrogen Relations in a Forest Plantation—Soil Organic Matter Ecosystem Model, Annals of Botany, 70, 137–151, https://doi.org/10.1093/oxfordjournals.aob.a088450, 1992a.

Thornley, J. H. M. and Cannell, M. G. R.: Nitrogen Relations in a Forest Plantation—Soil Organic Matter Ecosystem Model, Annals of Botany, 70, 137–151, https://doi.org/10.1093/oxfordjournals.aob.a088450, 1992b.

Thornley, J. H. M. and Verberne, E. L. J.: A model of nitrogen flows in grassland, Plant Cell Environ, 12, 863–886, https://doi.org/10.1111/j.1365-3040.1989.tb01967.x, 1989.

UNECE: Draft decision on amending the text of and annexes II to IX to the Gothenburg protocol to abate acidification, eutrophication and ground-level ozone and addition of new annexes X and XI., 2012.

UNECE: Guidance document on preventing and abating ammonia emissions from agricultural sources, 2014.

UNECE: United Nations Economic Commission for Europe Framework Code for Good Agricultural Practice for Reducing Ammonia Emissions, 2015.

UNEP: Colombo Declaration on Sustainable Nitrogen Management. Final text agreed by fourteen associating countries. Launch of United Nations Global Campaign on Sustainable Nitrogen Management, Colombo, Sri Lanka, 2019.

UNEP: Resolution adopted by the United Nations Environment Assembly on 2 March 2022 5/2. Sustainable nitrogen management., 2022.

USEPA: Clean Air Act, US, 2021.

Uwizeye, A., de Boer, I. J. M., Opio, C. I., Schulte, R. P. O., Falcucci, A., Tempio, G., Teillard, F., Casu, F., Rulli, M., Galloway, J. N., Leip, A., Erisman, J. W., Robinson, T. P., Steinfeld, H., and Gerber, P. J.: Nitrogen emissions along global livestock supply chains, Nat Food, 1, 437–446, https://doi.org/10.1038/s43016-020-0113-y, 2020.

Vallis, I., Harper, L., Catchpoole, V., and Weier, K.: Volatilization of ammonia from urine patches in a subtropical pasture, Aust. J. Agric. Res., 33, 97, https://doi.org/10.1071/AR9820097, 1982.

Vallis, I., Peake, D., Jones, R., and McCown, R.: Fate of urea-nitrogen from cattle urine in a pasture-crop sequence in a seasonally dry tropical environment, Aust. J. Agric. Res., 36, 809, https://doi.org/10.1071/AR9850809, 1985.

Van Aardenne, J. A., Dentener, F. J., Olivier, J. G. J., Goldewijk, C. G. M. K., and Lelieveld, J.: A 1°×1° resolution data set of historical anthropogenic trace gas emissions for the period 1890-1990, Global Biogeochem. Cycles, 15, 909–928, https://doi.org/10.1029/2000GB001265, 2001.

Van Vuuren, D. P., Riahi, K., Calvin, K., Dellink, R., Emmerling, J., Fujimori, S., Kc, S., Kriegler, E., and O'Neill, B.: The Shared Socio-economic Pathways: Trajectories for human development and global environmental change, Global Environmental Change, 42, 148–152, https://doi.org/10.1016/j.gloenvcha.2016.10.009, 2017.

Vigil, M. F. and Kissel, D. E.: Rate of Nitrogen Mineralized from Incorporated Crop Residues as Influenced by Temperature, Soil Science Society of America Journal, 59, 1636–1644, https://doi.org/10.2136/sssaj1995.03615995005900060019x, 1995.

Vira, J., Hess, P., Melkonian, J., and Wieder, W. R.: An improved mechanistic model for ammonia volatilization in Earth system models: Flow of Agricultural Nitrogen, version 2 (FANv2), Biogeosciences, https://doi.org/10.5194/gmd-2019-233, 2019.

Vira, J., Hess, P., Melkonian, J., and Wieder, W. R.: An improved mechanistic model for ammonia volatilization in Earth system models: Flow of Agricultural Nitrogen version 2 (FANv2), Geosci. Model Dev., 13, 4459–4490, https://doi.org/10.5194/gmd-13-4459-2020, 2020a.

Vira, J., Hess, P., Melkonian, J., and Wieder, W. R.: An improved mechanistic model for ammonia volatilization in Earth system models: Flow of Agricultural Nitrogen version 2 (FANv2), Geosci. Model Dev., 13, 4459–4490, https://doi.org/10.5194/gmd-13-4459-2020, 2020b.

Vitousek, P. M., Aber, J. D., Howarth, R. W., Likens, G. E., Matson, P. A., Schindler, D. W., Schlesinger, W. H., and Tilman, D. G.: Technical Report: Human Alteration of the Global Nitrogen Cycle: Sources and Consequences, Ecological Applications, 7, 737, https://doi.org/10.2307/2269431, 1997.

Voglmeier, K., Jocher, M., Häni, C., and Ammann, C.: Ammonia emission measurements of an intensively grazed pasture, Biogeosciences, 15, 4593–4608, https://doi.org/10.5194/bg-15-4593-2018, 2018.

de Vries, W., van der Salm, C., Reinds, G. J., and Erisman, J. W.: Element fluxes through European forest ecosystems and their relationships with stand and site characteristics, Environmental Pollution, 148, 501–513, https://doi.org/10.1016/j.envpol.2006.12.001, 2007.

Vu, T. K. V., Sommer, G. S., Vu, C. C., and Jørgensen, H.: Assessing Nitrogen and Phosphorus in Excreta from Grower-finisher Pigs Fed Prevalent Rations in Vietnam, Asian Australas. J. Anim. Sci, 23, 279–286, https://doi.org/10.5713/ajas.2010.90340, 2009a.

Vu, V. T. K., Prapaspongsa, T., Poulsen, H. D., and Jørgensen, H.: Prediction of manure nitrogen and carbon output from grower-finisher pigs, Animal Feed Science and Technology, 151, 97–110, https://doi.org/10.1016/j.anifeedsci.2008.10.008, 2009b.

Waldrip, H. M., Todd, R. W., and Cole, N. A.: Prediction of nitrogen excretion by beef cattle: A meta-analysis1,2,3, Journal of Animal Science, 91, 4290–4302, https://doi.org/10.2527/jas.2012-5818, 2013.

Wang, K., Kilic, K. I., Li, Q., Wang, L., Bogan, W. L., Ni, J.-Q., Chai, L., and Heber, A. J.: National Air Emissions Monitoring Study: Emissions Data from Two Tunnel-Ventilated Layer Houses in North Carolina - Site NC2B. Final Report, Purdue University, 2010.

Whitehead, D. C.: Atmospheric ammonia in relation to grassland agriculture and livestock production, Soil Use & Management, 6, 63–65, https://doi.org/10.1111/j.1475-2743.1990.tb00802.x, 1990.

Wieder, W. R., Boehnert, J., and Bonan, G. B.: Evaluating soil biogeochemistry parameterizations in Earth system models with observations: Soil Biogeochemistry in ESMs, Global Biogeochem. Cycles, 28, 211–222, https://doi.org/10.1002/2013GB004665, 2014.

Wright, R. F., Alewell, C., Cullen, J. M., Evans, C. D., Marchetto, A., Moldan, F., Prechtel, A., and Rogora, M.: Trends in nitrogen deposition and leaching in acid-sensitive streams in Europe, Hydrol. Earth Syst. Sci., 5, 299–310, https://doi.org/10.5194/hess-5-299-2001, 2001.

Wyer, K. E., Kelleghan, D. B., Blanes-Vidal, V., Schauberger, G., and Curran, T. P.: Ammonia emissions from agriculture and their contribution to fine particulate matter: A review of implications for human health, Journal of Environmental Management, 323, 116285, https://doi.org/10.1016/j.jenvman.2022.116285, 2022.

Xu, L. and Penner, J. E.: Global simulations of nitrate and ammonium aerosols and their radiative effects, Atmos. Chem. Phys., 12, 9479–9504, https://doi.org/10.5194/acp-12-9479-2012, 2012.

Xu, R., Tian, H., Pan, S., Prior, S. A., Feng, Y., Batchelor, W. D., Chen, J., and Yang, J.: Global ammonia emissions from synthetic nitrogen fertilizer applications in agricultural systems: Empirical and process-based estimates and uncertainty, Glob Change Biol, 25, 314–326, https://doi.org/10.1111/gcb.14499, 2019a.

Xu, R., Tian, H., Pan, S., Prior, S. A., Feng, Y., Batchelor, W. D., Chen, J., and Yang, J.: Global ammonia emissions from synthetic nitrogen fertilizer applications in agricultural systems: Empirical and process-based estimates and uncertainty, Glob Change Biol, 25, 314–326, https://doi.org/10.1111/gcb.14499, 2019b.

Xu, R. T., Pan, S. F., Chen, J., Chen, G. S., Yang, J., Dangal, S. R. S., Shepard, J. P., and Tian, H. Q.: Half-Century Ammonia Emissions From Agricultural Systems in Southern Asia: Magnitude, Spatiotemporal Patterns, and Implications for Human Health, GeoHealth, 2, 40–53, https://doi.org/10.1002/2017GH000098, 2018.

Xu, W., Zhao, Y., Wen, Z., Chang, Y., Pan, Y., Sun, Y., Ma, X., Sha, Z., Li, Z., Kang, J., Liu, L., Tang, A., Wang, K., Zhang, Y., Guo, Y., Zhang, L., Sheng, L., Zhang, X., Gu, B., Song, Y., Van Damme, M., Clarisse, L., Coheur, P.-F., Collett, J. L., Goulding, K., Zhang, F., He, K., and Liu, X.: Increasing importance of ammonia emission abatement in PM2.5 pollution control, Science Bulletin, 67, 1745–1749, https://doi.org/10.1016/j.scib.2022.07.021, 2022.

Yang, Y., Liu, L., Bai, Z., Xu, W., Zhang, F., Zhang, X., Liu, X., and Xie, Y.: Comprehensive quantification of global cropland ammonia emissions and potential abatement, Science of The Total Environment, 812, 151450, https://doi.org/10.1016/j.scitotenv.2021.151450, 2022.

Yang, Y., Liu, L., Liu, P., Ding, J., Xu, H., and Liu, S.: Improved global agricultural crop- and animal-specific ammonia emissions during 1961–2018, Agriculture, Ecosystems & Environment, 344, 108289, https://doi.org/10.1016/j.agee.2022.108289, 2023.

Zhan, X., Adalibieke, W., Cui, X., Winiwarter, W., Reis, S., Zhang, L., Bai, Z., Wang, Q., Huang, W., and Zhou, F.: Improved Estimates of Ammonia Emissions from Global Croplands, Environ. Sci. Technol., 55, 1329–1338, https://doi.org/10.1021/acs.est.0c05149, 2021.

Zhang, C., Song, X., Zhang, Y., Wang, D., Rees, R. M., and Ju, X.: Using nitrification inhibitors and deep placement to tackle the trade-offs between NH_3 and N_2O emissions in global croplands, Global Change Biology, 28, 4409–4422, https://doi.org/10.1111/gcb.16198, 2022.

Zhang, L., Chen, Y., Zhao, Y., Henze, D. K., Zhu, L., Song, Y., Paulot, F., Liu, X., Pan, Y., Lin, Y., and Huang, B.: Agricultural ammonia emissions in China: reconciling bottom-up and top-down estimates, Atmos. Chem. Phys., 18, 339–355, https://doi.org/10.5194/acp-18-339-2018, 2018.

Zhang, X., Wu, Y., Liu, X., Reis, S., Jin, J., Dragosits, U., Van Damme, M., Clarisse, L., Whitburn, S., Coheur, P.-F., and Gu, B.: Ammonia Emissions May Be Substantially Underestimated in China, Environ. Sci. Technol., 51, 12089–12096, https://doi.org/10.1021/acs.est.7b02171, 2017.

Zhao, Y. G., Gordon, A. W., O'Connell, N. E., and Yan, T.: Nitrogen utilization efficiency and prediction of nitrogen excretion in sheep offered fresh perennial ryegrass (Lolium perenne)1, Journal of Animal Science, 94, 5321–5331, https://doi.org/10.2527/jas.2016-0541, 2016.